Molecular and cellular analysis of the interaction between soluble CD23 and CD11/CD18 integrins

Brodie Belinda Daniels

Submitted in partial fulfillment of the requirements for the degree

Philosophiae Doctor

in the Faculty of Science

at the Nelson Mandela Metropolitan University

Promoter: Prof Vaughan Oosthuizen

Co-Promoter: Prof Maryna van de Venter

Declaration

I hereby declare that this thesis is my own unaided work. It is being submitted for the PhD degree in Science at the Nelson Mandela Metropolitan University, Port Elizabeth, South Africa. It has not been submitted before for any degree or examination at any other University.

_____

B Daniels

On this _____ day of _____, 2010

ACKNOWLEDGEMENTS

I would like to extend my sincere thanks and appreciation to all who made the present study possible, but especially to:

My Creator, for strength and faith.

Professor Vaughan Oosthuizen for his support, guidance and motivation, as well as his enthusiasm for immunology and his assistance in the preparation of this manuscript.

Professor Maryna van de Venter for her advice, ideas, support, immense cell biology knowledge and her assistance in the preparation of this manuscript. Thanks also for always being able to make me laugh at myself.

All staff and postgraduate students in the Department of Biochemistry and Microbiology, Nelson Mandela Metropolitan University, for their continual help, support and friendship over the years. You are all the reason I kept coming to the lab even when I ran out of enthusiasm.

Addgene, for the donation of the CD11 clones.

Dr Sang-Uk Nham, for the donation of the CD11 I domain vectors.

Dr Fritz Tiedt for his infinite patience and guidance in teaching me insect cell culture.

CSBE for the use of their BIAcore T100 instrument, and Dr Sarah Martin for technical expertise, assistance with experiments, and data analysis.

The National Research Foundation and Nelson Mandela Metropolitan University for their financial support.

The Medical Research Council for funding the project.

To my several special friends; you know who you are. You carried me through the rough times, and for that I am ever grateful. Thank you.

My brother Ryan, you are so much more of an inspiration than you think you are. When I grow up, I want to be just like you.

My mother and father, Belinda and Donald. You made me what I am today. Thank you for many years of support, love and understanding and always pointing me in the right direction.

To Rob, your constant enthusiasm and dogged determination to get me through this is much appreciated! Thank you for always believing in me and putting up with me when I was impossible (I realise how often this was)! Thanks for being my number one supporter.

Abstract

The low affinity IgE receptor, CD23, is expressed by a wide variety of cells and cleaved from its original 45 kDa size to several smaller soluble CD23 proteins. Soluble CD23 function depends on the form of the protein and its interaction with various ligands. CD23 is believed to play an important role in regulating allergic responses and in inflammation, amongst others. β_2 integrins are important in a variety of cell-adhesion reactions during immune-inflammatory mechanisms and the binding of their natural ligands generates outside-in cellular signalling, leading to cell activation. Although the binding of CD23 to β_2 integrins contributes to this signalling in monocytes, the interaction site for CD23 is unknown. This study focused on the interaction of three soluble CD23 proteins with the β_2 integrins CD11b/CD18 and CD11c/CD18. Differentiated HL60, THP1 and U937 monocytic cells were used to demonstrate the binding of three recombinant CD23 constructs (corresponding to 16, 25 and 33 kDa human soluble CD23) to upregulated CD11b/CD18 and CD11c/CD18. This binding was partially blocked by an antibody specific for the CD11b/CD18 αI domain, demonstrating that αI domains are involved in binding to CD23. Recombinant αI domain proteins of CD11b and CD11c were demonstrated to bind CD23 using ELISA and in surface plasmon resonance spectroscopy. The dissociation constants for CD23-CD11b/CD18 and CD23-CD11c/CD18 are comparable to other integrin ligands. This study has shown that CD23 interacts directly with the αI domains of β_2 integrins and that the interaction surface likely spans the lectin domain as well as either the stalk and/or C-terminal tail of CD23. This study also looked at the effect that soluble CD23 proteins had on monocyte biology. It appears that

sCD23 proteins have little effect on the phagocytic or chemotactic ability of monocytes, while an increase in oxidative burst was shown with the 16 kDa and 25 kDa CD23 proteins. Signalling pathways for the production of reactive oxygen species were investigated and it appears that the CD23 proteins signal mainly through the phosphoinositide-3 kinase pathway, although the mitogen activated protein kinase and Src kinase pathways may also play a role. These data suggest that sCD23 proteins induce outside-in signalling of β_2 integrins and are able to change the activation state of CD11b/CD11c by stimulating oxidative burst. This needs to be further investigated by determining how the three sCD23 proteins are binding the CD11 proteins and investigating further leukocyte function and inflammatory responses by the cells.

Table of Contents

List of Figures

List of Tables

List of Abbreviations

ε : epsilon

α: alpha

δ: delta

γ: gamma

μ: mu

μl: microliter

°C: degrees Celsius

Ab: antibody

AcNPV: *Autographa californica* nuclear polyhedrosis virus

Ag: antigen

AMPK: AMP-kinase

AP-1: activator protein 1

APC: antigen-presenting cell

B-CLL: B-chronic lymphocytic leukemia

BCR: B-cell receptor

BSA: bovine serum albumin

cAMP: cyclic adenosine monophosphate

CFSE: carboxyfluorescein diacetate, succinimidyl ester

cGMP: cyclic guanosine monophosphate

CMV: cytomegalovirus

CR2: complement receptor 2

CR3: complement receptor 3

CR4: complement receptor 4

CTLD: C-type lectin-like domain

DCF-DA: 2’7’-dichlorofluorescin diacetate

ddH_2O: distilled deionized water

DAF-DA: 4,5,-diaminofluorescein-diacetate

DAF-2T: triazolofluorescein

DAG: diacylglycerol

DMSO: dimethyl sulfoxide

DNA: deoxyribonucleic acid

dNTP’s: deoxynucleoside triphosphates

DTNB: 5, 5’-dithiobis (2-nitrobenzoic acid)

EAE: Experimental autoimmune encephalomyelitis

EBV: Epstein-Barr Virus

EDTA: ethylenediaminetetraacetic acid tetrasodium salt

ELISA: enzyme linked immunosorbent assay

eNOS: endothelial NOS

ERK: extracellular regulated kinases

EU: endotoxin units

Fab: Ag-binding fragment

FAK: focal adhesion kinase

FcεRI: high affinity IgE receptor

FcεRII: low affinity receptor for IgE

Fc: crystallizable fragment

FcR: Fc receptor

FCS: foetal calf serum

FDCs: follicular dendritic cells

FITC: fluorescein 5'-isothiocyanate

fMLP: formyl-methionyl-leucyl-phenylalanine

FPLC: fast protein liquid chromatography

Gdn-HCl: guanidinium hydrochloride

GM-CSF: granulocyte-macrophage colony stimulating factor

GPI: glycosylphosphatidylinositol

GSH: L-glutathione

GST: glutathione S-transferase

HBSS: Hanks buffered saline solution

HEPES: piperazineethanesulfonic acid

HIES: hyper-IgE syndrome

HI-FBS: heat-inactivated foetal bovine serum

HRP: horseradish peroxidase

I: inserted

IB's: inclusion bodies

ICAMs: intercellular-leukocyte adhesion molecules

Ie1: immediate early promoter 1

IFN: interferon

Ig: immunoglobulin

IKK: IκB kinase

IL: interleukin

ILK: integrin-linked kinase

IMF-1: integrin modulating factor 1

iNOS: inducible nitric oxide synthase

IP_3: inisitol triphosphate

IPTG: isopropyl-β-D-thiogalactopyranoside

ITAM: immunoreceptor tyrosine-based activation motifs

JNK: c-Jun N-terminal kinase

kDa: kilo Dalton

L: liter

LAD: leukocyte adhesion deficiency

LAL: limulus amoebocyte lysate

LB: Luria Bertani

LDAO: N, N–dimethyldodecylamine N-oxide

LFA-1: lymphocyte function-associated antigen 1

LIC: ligation independent cloning

LPS: lipopolysaccharide

M: molar

mAbs: monoclonal antibodies

MACS: magnetic activated cell sorting

MAPK: mitogen activated protein kinase

mCD23: membrane CD23

MCP: monocyte chemotactic protein

MCS: multiple cloning site

MHC II: major histocompatibility complex class two

MIDAS: metal ion-dependent adhesion site

MIP-1α: macrophage inflammatory protein 1α

MPO: myeloperoxidase

mRNA: messenger ribonucleic acid

MRP14: myeloid-related protein 14

MW: molecular weight

NADPH: nicotinamide adenine dinucleotide phosphate

NEMO: NF-κB essential modulator

NFκB: nuclear factor κB

NIK: NF-κB inducing kinase

NK: natural killer

nNOS: neuronal NOS

NOS: nitric oxide synthase

NO: nitric oxide

NOX: NADPH oxidase

NTA: nitrolotriacetic acid

PBMCs: peripheral blood mononuclear cells

PBS: phosphate buffered saline

PBS-T: PBS-Tween 20

PCR: polymerase chain reaction

PE: phycoerythrin

PI3K: phosphoinositide-3 kinase

PLC: phospholipase C

PMA: phorbol 12-myristate 13-acetate

PMN: polymorphonuclear leukocyte

pp: pages

PP2: 4-Amino-5-(4-chlorophenyl)-7-(*t*-butyl) pyrazolo[3,4-*d*]pyrimidine

PP2A: protein phosphatase 2A

PS: phosphatidyl serine

PTK: phosphorylation of tyrosine kinase

QCM-D: quartz crystal microbalance with dissipation

RA: retinoic acid

RANTES: regulated upon activation, normal T cell expressed and secreted

ROS: reactive oxygen species

rpm: revolutions per minute

RU: resonance units

SAPKs: stress activated protein kinases

sCD21: soluble CD21

sCD23: soluble CD23

SCR's: short consensus repeats

SDS-PAGE: sodium dodecylsulfate-polyacrylamide gel electrophoresis

sFcεRII: soluble FcεRII fragment

SFK: Src-family kinases

SOB: Hanahan's broth

SOD: superoxide dismutase

SPR: surface plasmon resonance

TAE: tris-acetate-EDTA

Tc cells or CTLs: cytotoxic T lymphocytes

T_H: T helper lymphocytes

T_H2: type 2 helper lymphocytes

TM: transmembrane domain

TMB: 3,3',5,5'-tetramethylbenzidine

TNB: 2-nitro-5-thiobenzoic acid

TNFα: tumour necrosis factor α

TNFR-1: receptor for tumour necrosis factor

uPAR: urokinase-type plasminogen activated receptor

UV: ultra violet

VCAM-1: vascular cell adhesion molecule 1

X-gal: 5-bromo-4-chloro-3-indolyl-β-D-galactopyranoside

ZAP-70: Zeta-chain-associated protein kinase-70

Chapter 1: Literature review

1.1 Introduction

Immunity is the ability of an organism to protect itself from disease by producing a complex series of defensive actions widely distributed throughout the host body; this is termed an immune response. The innate immune system is an organism's first line of defense against attack and is mediated, amongst others, by phagocytic cells which do not require prior exposure to the foreign agent [known as an antigen (Ag)]. The adaptive immune system is driven by lymphocytes, which are able to recognise a specific foreign agent and result in its elimination. Lymphocytes are then able to recognize these pathogens on subsequent infections and provide increased protection (Janeway *et al.*, 2001). Once a foreign agent has penetrated the epithelial barriers of the body, the cells of the innate immune system recognize them via cell surface receptors and engulf them. These phagocytic macrophages are then able to release cytokines (proteins released by cells that influence the behaviour of other cells which bear their receptors) and chemokines (proteins which attract other cells that possess their receptor). The production of cytokines and chemokines results in inflammation and also stimulates the adaptive immune response. The presence of inflammation causes the movement of cells to the site of inflammation. Neutrophils are the first cells at the site of inflammation and possess surface receptors, generally called pattern recognition receptors, which enable them to recognise common bacterial constituents (pathogen-associated molecular patterns) engulf and destroy them. Monocytes are also recruited to sites of inflammation, where they differentiate into macrophages (Janeway *et al. 2001).*

This inflammatory response by the innate immune system contributes to the activation of the adaptive immune response by increasing the flow of antigen-bearing cells into lymphoid tissue and providing signals that synergise the activation of lymphocytes (Janeway *et al.*, 2001). The elimination of the Ag can only occur by direct destruction of the Ag by the lymphocyte or by the formation of specialized proteins that either disrupt the Ag's function or target the Ag for destruction by other cells. These specialized glycoproteins are called antibodies (Ab).

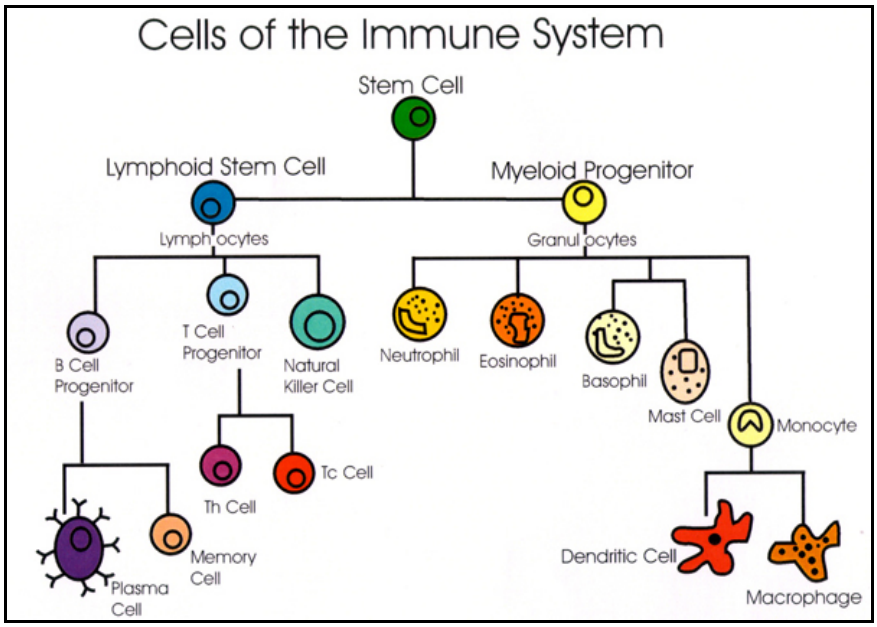

Figure 1.1: Origin and differentiation of cells of the immune system (Todar, 2008).

Both the innate and adaptive immune systems make use of a wide range of cell types (Figure 1.1). B lymphocytes develop into antibody-secreting plasma cells after stimulation by foreign antigens of bacteria, viruses and tumour cells. T lymphocytes are divided into two major subsets that are functionally and phenotypically different. T helper (T_H) cells, also referred to as $CD4^+$ T cells, are responsible for the coordination and regulation of immunological responses. They mediate responses by the secretion of cytokines that stimulate other cells involved in the immune response.

Cytotoxic T lymphocytes (Tc cells or CTLs) or $CD8^+$ T cells are involved in directly killing certain tumour cells, virus-infected cells, transplant cells, and sometimes eukaryotic parasites (reviewed in Todar, 2008). These are also important in the down-regulation of immune responses. Natural killer cells (NK cells**)**, are similar to CTLs. They are able to directly kill certain tumours such as melanomas, lymphomas and virus-infected cells, most notably herpes and cytomegalovirus-infected cells. However they are able to destroy their target cells without need for recognition of antigen in association with major histocompatibility complex (MHC) molecules. Macrophages are important in the regulation of immune responses by being involved in phagocytosis and functioning as antigen-presenting cells (APCs). Stimulated macrophages show increased levels of phagocytosis and are also able to secrete cytokines that modulate immune responses. Dendritic cells originate in the bone marrow and function as APCs (Todar, 2008).

Plasma cells are fully differentiated cells that are derived from B-cells and are able to synthesize Ab's, also called immunoglobulins (Ig's) in response to Ag's. Ab's are a group of glycoproteins present in the blood serum and tissue fluid, and can be separated according to their charge in an electric field. Ab's have more than one Ag-combining site. The basic structure of Ig's is four polypeptide chains that are connected to each other by disulfide bonds. There are two light chains and two heavy chains. The heavy and light chains are made up of two regions; a constant region (which does not vary significantly between Ab's of the same subclass) and a variable region (with varying sequences between Ab's). These four chains are arranged in the form of a Y with a hinge region that allows the Ab to form a T shape. The stalk of this Y is called the crystallizable fragment (Fc) and contains the site at which the Ab molecule can bind a cell via Fc receptors (FcR). The arms of the Y are made of two

Ag-binding fragments (Fab) that are able to bind compatible antigenic determinant sites. There are five subclasses of human heavy chains called gamma (γ), alpha (α), mu (μ), delta (δ) and epsilon (ε). It is the properties of these heavy chains that determine the five Ig classes – IgG, IgA, IgM, IgD and IgE, respectively. Each class of Ig differs in its half-life, distribution in the body and interaction with the other components of the host's defense system (Prescott *et al.*, 1996).

When an Ab comes into contact with an Ag, the Fab region binds the Ag, while the Fc region mediates the binding to the host tissue, or cells of the immune system or the first component of the complement system. The binding of the Ab to Ag serves to mark the Ag as a target for immunologic attack (Prescott *et al.*, 1996). IgG is the major Ab found in human serum and accounts for between 70-75% of the serum Ab pool. It acts against bacteria and viruses by activating molecules such as complement and Fc receptors. IgM makes up 10% of the serum Ab pool and is also found in the gastrointestinal tract, upper and lower respiratory tracts and the genitourinary system. It is involved in the immunity necessary at secretory mucosal surfaces and prevents the adherence of the pathogen to the mucosal surfaces and subsequent invasion of the host tissues. IgA is present in the body in three soluble forms (monomeric, dimeric and secretory IgA) and defends the body against microorganisms using specific Fc receptors. IgD is present in trace amounts in the serum. It is abundant on the surface of B-cells and binds Ag's, causing the B-cell to begin Ab production. IgE makes up 0.00005% of the serum Ab pool. This class is made up of the classic skin-sensitizing and anaphylactic Ab's. These Ab's have four constant region domains (Cε1, Cε2, Cε3 and Cε4) and two light chains. The Fc portion of the Cε4 chain is able to bind special Fcε receptors on mast cells and basophils. When two IgE molecules on the surface of these cells are cross-linked by binding to the same Ag an acute

inflammatory reaction is initiated which causes cells to degranulate, releasing histamine and other mediators of anaphylaxis (Prescott *et al.*, 1996; Delves *et al.*, 2006).

Cells that can be stimulated by the Ag-Ab complexes are triggered by surface receptors that are able to bind the Fc region of the Ig's. When this binding occurs, the Ab confers on these cells their specificity for their Ag. The release of mediators by the degranulation of Fc receptor-bearing cells or by the synthesis of newly formed bioactive molecules is an essential component of many Ab-dependant reactions that are involved in pathogen defense or in allergic disorders. IgE only exerts its biological function through its interaction with cell surface receptors that are specific for its Fc region. The resulting dramatic release of a number of potent proinflammatory mediators triggered by Fc receptor aggregation is recognized in anaphylaxis and allergic disease (Dessaint *et al.*, 1990).

There are two types of IgE binding proteins; the high affinity IgE receptor (FcεRI), which is found on mast cells and basophils and the low affinity receptor for IgE (FcεRII or CD23). FcεRI binds with such high affinity to IgE that it is permanently coated with IgE and therefore sensitized for rapid activation should it be challenged with an allergen (Sutton *et al.*, 2000). FcεRI has a binding affinity with IgE of ~1 x 10^{10} M^{-1}, while CD23 only has a binding affinity of ~6 x 10^{7} M^{-1} (Shi *et al.*, 1997). This activation can be triggered by as few as two receptor molecules by multivalent allergens and causes the release of molecules that promote an immediate inflammatory response (Sutton *et al.*, 2000). FcεRI mediates IgE-antigen complex-induced degranulation of mast cells and basophils, causing the release of histamine, leukotrienes, interleukin-4 (IL-4), IL-5 and IL-6 (Richards and Katz, 1991). CD23 is

found on a variety of cell types, such as human peripheral blood B- lymphocytes, B-lymphoblastoid cell lines, mast cells and basophils. It is also found on a variety of haematopoietic cell lines (Conrad, 1990). The IgE response is regulated by its low affinity receptor, CD23, but the effector mechanisms involved are not known. However, direct B-cell signaling, Ag presentation and increased follicular localization are some possibilities (Heyman, 2000). In addition to the ability of CD23 to regulate IgE, it is also able to bind several other ligands, thereby enhancing Ag processing and presentation, and influencing the production of Ag-specific IgG, IgM and IgE (Conrad *et al.*, 2007).

1.2 The CD23 protein

1.2.1 Structure of CD23

Of the many Fc receptors that bind immunoglobulins, CD23 is the only type II membrane and non-Ig superfamily protein. This means that it has a cytoplasmic N-terminus and an extracellular C-terminus and that it also lacks the Ig fold structure (Kijimoto-Ochiai, 2002). There is much evidence to support this theory of CD23's orientation. Firstly, there is no signal sequence for CD23. Its proposed hydrophobic transmembrane region (residues 24-44) is preceded by an N-terminal hydrophilic stretch of 21 amino acids with a cluster of basic residues (residues 14-20, Arg-Arg-Arg-Cys-Cys-Arg-Arg) which might act as a stop-transfer sequence. The N-linked carbohydrate-addition site is located on the C-terminal side of the proposed transmembrane region. The N-terminal amino acid sequences of the three peptide fragments of soluble CD23 were detected on the C-terminal side of the proposed

transmembrane region. Lastly, the sequence of CD23 is highly homologous to that of chicken hepatic lectin, which has a similar orientation (Kikutani *et al.*, 1986).

The human CD23 exists in two forms (CD23a and CD23b) that differ in the N-terminal cytoplasmic regions. The two forms are generated through the use of different transcription initiation sites and alternative RNA splicing. This causes differences in the 5' untranslated regions and the first 6 amino acids in the predicted amino acid sequence. The CD23a form is found only on B-lymphocytes and follicular dendritic cells, while CD23b is found exclusively on monocytes, eosinophils and human T-cell lymphotrophic virus-1-infected T-cell lines (Conrad, 1990; Chen *et al.*, 2002).

Human CD23 is a single chain glycoprotein of 321 amino acids and is 45 kDa in size. It is encoded by a single-copy gene that contains 11 exons and spans 13 kb found on chromosome 19 (Conrad, 1990). It is a member of the C-type (Ca^{2+}-dependent) animal lectin family and has six main structural features. These are the C-type lectin domain, the a and b forms of the protein that differ in their amino acid sequences at the N-terminal region, the leucine-zipper structure, the protease cleavage sites, the reverse-RGD sequence near the C-terminus and the "RGD-binding inhibition peptide" at the root of the N-linked carbohydrate chain (Figure 1.2) (Kijimoto-Ochiai, 2002).

The leucine-zipper sequence is found near the transmembrane domain of the extracellular region. This sequence mediates the formation of trimers by forming an α-helical coiled-coil stalk. This coiled stalk provides the protein with an easier way to form a polymer than with a disulphide bridge (Kijimoto-Ochiai, 2002).

CD23 contains three disulphide bridges between cysteine residues 163 and 282, 174 and 273 and 191 and 259 (Ludin *et al.*, 1987). It also has twenty hydrophobic amino acids located from position 24-44 forming the transmembrane region (Mossalayi *et al.*, 1997). It has an N-linked carbohydrate at position 64, an O-linked carbohydrate and sialic acid residues (Richards and Katz, 1991). The presence of the N-linked carbohydrate is shown to enhance the stability of the receptor (Conrad, 1990).

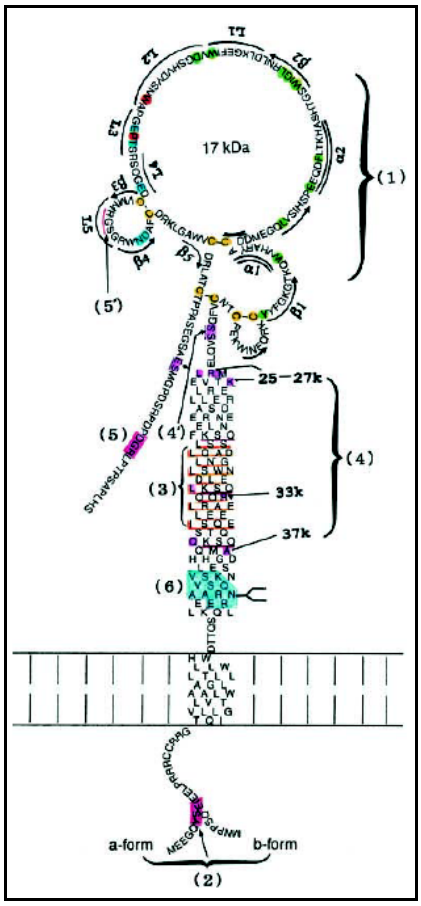

Figure 1.2: A two dimensional representation of the structure of CD23. 1) IgE-binding lectin domain; 2) the a and b form of CD23; 3) leucine-zipper sequence; 4) protease cleavage sites giving rise to the soluble forms of CD23; 5) reverse-RGD sequence and 6) RGD-binding inhibition peptide. Arrows indicate β sheet, lines indicate loops and double lines indicate α helix. The sizes of the released soluble molecules are indicated and the cleavage sites are coloured pink (Kijimoto-Ochiai, 2002).

The RGD sequence of CD23 is read from the C-terminus as opposed to being read from the N-terminus, and is therefore inverted. This sequence is known as a cell-adhesion sequence in integrin ligands, while in the cellular disintegrin family it plays a role in both cell adhesion and information signalling. However, the function of this sequence in CD23 is unknown. Human CD23 also has a reversed RGD-binding inhibitory peptide around the N-sugar chain. The function that this peptide performs is also unknown (Kijimoto-Ochiai, 2002).

CD23 is a labile protein in that soluble CD23 fragments (sCD23) are released from the cell in human and murine systems. The human CD23 has four cleavage sites that release soluble forms of the protein, approximately 25, 27-29, 33 and 37 kDa in size (as seen in Figure 1.2). The initial human sCD23 fragment released (37 kDa) is known from cloning studies to be derived from the carboxy terminal portion of the molecule (position 81 in the amino acid sequence). sCD23 does not have any N-linked carbohydrates. It degrades into 33, 25, 16 and finally a 12 kDa species, which with the exception of the 12 kDa species, bind IgE. The murine sCD23 does not bind IgE. The site of sCD23 production is most likely the cell surface, but CD23 fragmentation can also occur inside the cell (Conrad, 1990). The 33 kDa protein is cleaved by a membrane-bound metalloprotease. Members of the disintegrin/metalloproteinase family (ADAM-8, -10, -15 and -28) are able to cleave CD23 (Lemieux *et al.*, 2007; Charrier-Hisamuddin *et al.*, 2008; Fourie *et al.*, 2003). CD23 is also cleaved by the cysteine protease *Der pI*, which is a house dust mite allergen, yielding a 16 kDa fragment. Due to the upregulation of sCD23 production by various other molecules, it is possible that other molecules are also able to cause this cleavage (Kijimoto-Ochiai, 2002). The lectin head of CD23 can self-associate

independently of the stalk region, giving rise to oligomers of sCD23 and trimers of mCD23 on the cell surface (Beavil *et al.*, 1995).

1.2.2 The functions of CD23

1.2.2.1 Membrane CD23 functions

The function of CD23 depends on which cell type is expressing the molecule (Paul-Eugene *et al.*, 1992). CD23 plays a role in T cell-dependent IgE production, B-cell proliferation, thymocyte maturation, myelopoiesis, Ag presentation and rescue of germinal center B cells from apoptosis (Texido *et al.*, 1994).

Membrane CD23 (mCD23) is found in the cell membrane as a mixture of a 45 kDa CD23 monomer and a trimer. The formation of trimers leads to a 10-fold greater affinity for IgE (Gould *et al.*, 2003).

CD23a on B-cells mediates endocytosis, while CD23b on monocytes mediates phagocytosis. The function of CD23 on B-cells is the enhancement of IgE-dependent antigen presentation to T cells. For this to occur, CD23 must bind Ag-IgE complexes, internalize these complexes and transport them to compartments of the endosomal network containing proteolytic enzymes and MHC II proteins. After proteolysis of the Ag, restricted peptides are loaded onto MHC II proteins and returned to cell surfaces for T cell presentation (Karagiannis *et al.*, 2001).

CD23a signalling involves the triggering of two main pathways. Firstly, it involves association with a pertussis toxin-insensitive G protein and the *Src*-related kinase Fyn

that results in phospholipase C (PLC) activation. This is the main pathway and involves the release of serotonin and tumour necrosis factor α (TNFα). The second pathway is the generation of cAMP (Sancho *et al.*, 2000). CD23 ligation by some epitopes provides a progression signal to human B-cells (Mossalayi *et al.*, 1997). G-proteins may couple mCD23 to a phospholipase C in human B cells (Mossalayi, *et al.*, 1997).

CD23b-mediated functions are dependent on CD23 cross-linking by IgE immune complexes. A relatively high density of surface CD23b on B-cells is necessary for optimal signalling. Cross-linking of CD23b on all other human cells has little, if any effect on calcium influx and the phosphoinositide pathway. Intracellular accumulation of cyclic guanosine monophosphate (cGMP) is observed during the first minutes of CD23-ligation, reaching a maximum level at 5-10 minutes before decreasing. cAMP accumulation appears several minutes later and may therefore be a result of phosphodiesterase diminution by excess cGMP. CD23 ligation leads to the activation of nuclear factor-κB (NF-κB) transcription factor and the modulation of proto-oncogene expression in U937 promonocytic cells. TNFα mRNA was detected as early as 6 hours after CD23 ligation. The addition of inhibitors of cAMP and nitric oxide (NO) abolishes the above modifications in target cells, therefore indicating the importance of NO and cyclic nucleotides in membrane CD23 signal transduction (Mossalayi *et al.*, 1997). NF-κB was found to be the main transcription factor involved in CD23 signal transduction in monocytes and promonocytic U937 cells (Ten *et al.*, 1999a). CD23 crosslinking in monocytes induces the activation of tyrosine kinase, which in turn activates IκB kinase, which phosphorylates IκBα, resulting in its degradation and therefore NF-κB activation and gene transcription (Ten *et al.*, 1999b).

CD23 on macrophages, eosinophils and platelets mediates IgE-dependent cytotoxicity and promotes the phagocytosis of IgE-coated particles (Conrad, 1990). In eosinophils and platelets, the CD23 of each of these two cell types binds IgE-coated particles causing their phagocytosis and the release of cytokines. In this role, CD23 acts in conjunction with the complement receptor CD11b/CD18 for both adherence of the particles and the resulting cytotoxicity. Both receptors are required for the IgE-dependent effector function of eosinophils. The IgE-Ag- mediated activation of the effector cells causes the release of inflammatory mediators such as leukotrienes (Richards and Katz, 1991).

On monocytes and macrophages, CD23 controls the IgE-dependent inflammatory processes, especially during allergic manifestations (Richards and Katz, 1991). Binding of IgE to CD23 on monocytes induces the release of IL-13 and TNFα (Soussi *et al.*, 1998). CD23 interacts with the α chain of integrins CD11b/CD18 and CD11c/CD18 on monocytes, stimulating the production of pro-inflammatory mediators IL-1β, TNFα, IL-6 and nitrite oxidative products (Lecoanet-Henchoz *et al.*, 1995; Karagiannis *et al.*, 2001). Ligation of CD23 on monocytes results in cAMP increase, but via a different mechanism to B-cell cAMP increase, because different CD23-associated proteins may contribute to transduction of the signal (Paul-Eugene *et al.*, 1992).

1.2.2.2 Soluble CD23 functions

Most activities of sCD23 are pleiotropic and IgE independent. This includes costimulation with IL-1 of prothymocyte maturation, myeloid precursor cell growth,

T-cell precursor growth, mast-cell activation, prevention of apoptosis of germinal center B-cells and increase of histamine release by human basophils. IL-4 and IL-13 are potent inducers of mCD23 and sCD23 in B-cells (Armant *et al.*, 1994; Soussi *et al.*, 1998).

On monocytes, interferon gamma (IFNγ) induces sCD23 release. sCD23 in turn costimulates IL-2 or IL-2-induced IFNγ production and directly triggers TNFα, IL-1α, IL-1β and IL-6 release by human peripheral blood mononuclear cells (PBMCs) (Daniels *et al.*, 2005; Armant *et al.*, 1994). IFNγ expression is limited to T and NK cells. IFNγ and TNFα play important roles in macrophage-mediated host defense against intracellular pathogens (Armant *et al.*, 1994).

sCD23 together with IL-4 is a major regulator of IgE biosynthesis (section 1.2.4.1) and in conjunction with IL-1 is also a differentiation factor for pre-T cells and other haematopoietic precursor cells (Kolb *et al.*, 1993).

1.2.3 The regulation of CD23

The exposure of CD23-positive cells to high concentrations of IgE has been associated with an increase in cellular density of CD23. However, IgE does not appear to enhance CD23 at the mRNA or protein levels in B-cells; nor does it stimulate CD23 synthesis in monocytes, eosinophils, or T-cell lines. T-cells are required for B-cells to continuously express CD23 *in vivo* and *in vitro*. IL-4 enhances the expression of CD23 on normal human B-cells and has been reported to stimulate the release of sCD23 from these cells. This is most likely a direct result of increased cell surface expression of CD23 and its subsequent shedding. The accumulation of

CD23 mRNA and protein is enhanced up to 5-fold by IL-4. CD23 expression and sCD23 production by B-lymphocytes is profoundly inhibited by IFNγ, in the presence or absence of IL-4. IFNα similarly suppresses CD23 expression and sCD23 release, and both interferons have been shown to act at the transcription and/or biosynthesis levels (Richards and Katz, 1991).

IL-3, IL-4 and granulocyte-macrophage colony stimulating factor (GM-CSF) have been shown to increase mCD23 and sCD23 on human monocytes. IL-4, IFNγ and GM-CSF increase surface and soluble CD23 expression by U937 premonocytic cells (Alderson *et al.*, 1992). Stimulation by TNFα, IL-1 and other cytokines activates p38 and the downstream kinases within thirty minutes. p38 Mitogen activated protein kinase (MAPK) plays a role in CD23 regulation as p38 MAPK inhibitors down-regulate CD23 formation in monocytes (Marshall *et al.*, 1998).

In addition to the a and b transcripts of CD23, shorter transcripts which lack the third exon have been found on the human B-cell line RPMI 8866 as well as PBMCs and other haematopoietic cell lines. These transcripts could be regulatory elements for the expression of full length CD23 protein through a novel mechanism. The skipping of exon three could convert full length CD23 mRNA into unstable transcripts and this could decrease the expression of the full length protein. Another possibility is that full-length mRNA stabilities are negatively correlated with those of truncated ones through competition for a common degradation pathway. It is possible that CD23 is regulated through multiple mechanisms including alternative mRNA splicing as well as proteolytic cleavage of the extracellular portion of the intact surface molecule (Matsui *et al.*, 1993).

1.2.4 The interaction of CD23 with its ligands

1.2.4.1 CD23 and IgE

IgE-secreting B-cells are abundant in lungs, skin and gut which are the main sites of parasitic invasion. This causes a range of cellular responses to antigens resulting in physiological and anatomical changes to exclude parasites from the body, such as inflammation, coughing, itching, lacramation, bronchoconstriction, mucous secretion, vomiting and diarrhea. Allergy is caused by an overproduction of IgE, which is present in much smaller quantities than the other antibodies (50-300 ng/ml of IgE in blood compared to 10 mg/ml IgG). Its action is amplified by the activities of the receptors to which it binds, the high affinity FcεRI being responsible for the immediate hypersensitivity reactions (Corry and Kheradm, 1999).

Activation of inflammatory cells by products of mast-cell degranulation induces CD23 expression. This mediates phagocytosis of immune complexes by monocytes *in vitro*. On the surface of B-cells it plays a role in IgE-dependent antigen presentation to T cells and in adhesion of B-cells to each other (Figure 1.3). It is also expressed on follicular dendritic cells and therefore could be involved in the homing of B-cells to the germinal centers of secondary follicles in the lymph nodes and spleen (Sutton and Gould, 1993).

CD23 has an unusual metabolic pathway. When it arrives at the cell surface, and possibly internally, it is cleaved and the majority of the C terminus is released. The initial fragment is not N-glycosylated and is further broken down into the size limit of 12-16 kDa. CD23 is regulated by the same cytokines that induce IgE; therefore, these

cytokines may be involved in the induction of isotype switching to IgE and induce a regulator for IgE (Cho *et al.*, 1997).

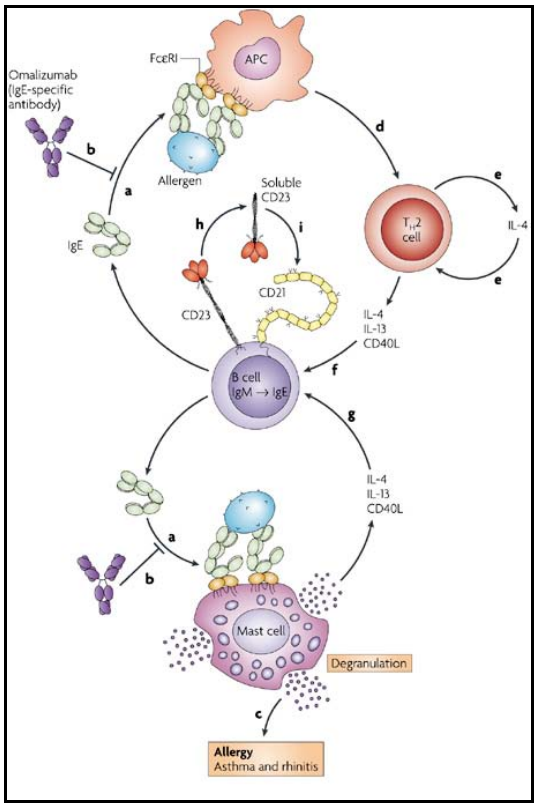

Figure 1.3: IgE is produced and secreted by B cells that have undergone class switching from IgM to IgE. IgE secreted from the B cell binds to FcεRI on mast cells and antigen-presenting cells (APCs) (a) and sensitizes these cells to allergens. The binding of IgE to FcεRI on mast cells and APCs is blocked by Omalizumab (b). Binding of allergen to IgE triggers mast-cell degranulation therefore causing an allergic response (c). Binding of the allergen to the APC leads to the presentation of allergenic peptides to T helper 2 (T_H2) cells (d). The activated T_H2 cells secrete interleukin-4 (IL-4) (e) to maintain the T_H2-cell lineage and recruit more T_H cells into this lineage (e). T_H2 cells also secrete IL-13 and express CD40 ligand (CD40L), which stimulates heavy-chain class switching to IgE together with IL-4 (f). The activated mast cells contribute to the production of IL-4 and IL-13 (and express CD40L), which could stimulate heavy-chain class switching to IgE (g). IL-4, IL-13 and CD40L also stimulate the expression of CD23 and the release of soluble CD23 (h). Soluble trimeric CD23 upregulates IgE synthesis and secretion through interaction with CD21 (i). Thus, allergen acts in pump priming of the allergic response (Gould and Sutton, 2008).

IgE interacts with human CD23 and its 37, 33 and 25 kDa soluble fragments. The glycosylation of CD23 is not necessary for IgE binding because the truncated products of human CD23 have no N-glycosylation sites. The peptide region that interacts with IgE has been shown to be the lectin domain of CD23, supported by evidence that binding is calcium dependent. Mutations in the lectin domain of CD23 change its IgE binding ability, further supporting the theory that the interaction site with IgE is in the lectin cassette (Cho *et al.*, 1997; Hibbert *et al.*, 2005). It could be that CD23 interacts with the protein backbone of IgE. CD23 binds enzymatically deglycosylated IgE and oligosaccharide-free IgE peptides. It has also been shown that the interaction between IgE and CD23 isolated from murine B-cells is not inhibited by high concentration of mono- or disaccharides. Therefore, despite the localization of the IgE-binding epitope within the lectin domain of CD23, carbohydrate does not appear to be required for binding. Monoclonal antibody epitope mapping studies of the CD23 binding site on IgE have shown that both human and murine CD23 interact with the Cε3 domain of their respective IgE ligands (Sayers *et al.*, 2004). IgE peptides that lacked Cε2 bound less efficiently to CD23 and if the Cε4 domains were absent, no binding resulted (Richards and Katz, 1991; Hibbert *et al.*, 2005). CD23 has also been shown to require calcium for binding to IgE (Wurzburg, *et al.*, 2006).

CD23 has been shown to be involved in the regulation of IgE synthesis on B-lymphocytes *in vivo*. When CD23 is not occupied by IgE, it is cleaved to release soluble CD23 fragments that upregulate IgE synthesis in an autocrine fashion (Figure 1.4). The binding of IgE to CD23 protects the receptor against proteolytic cleavage, but also allows membrane CD23 to deliver a negative IgE regulatory signal to the B-lymphocyte (Schulz *et al.*, 1997).

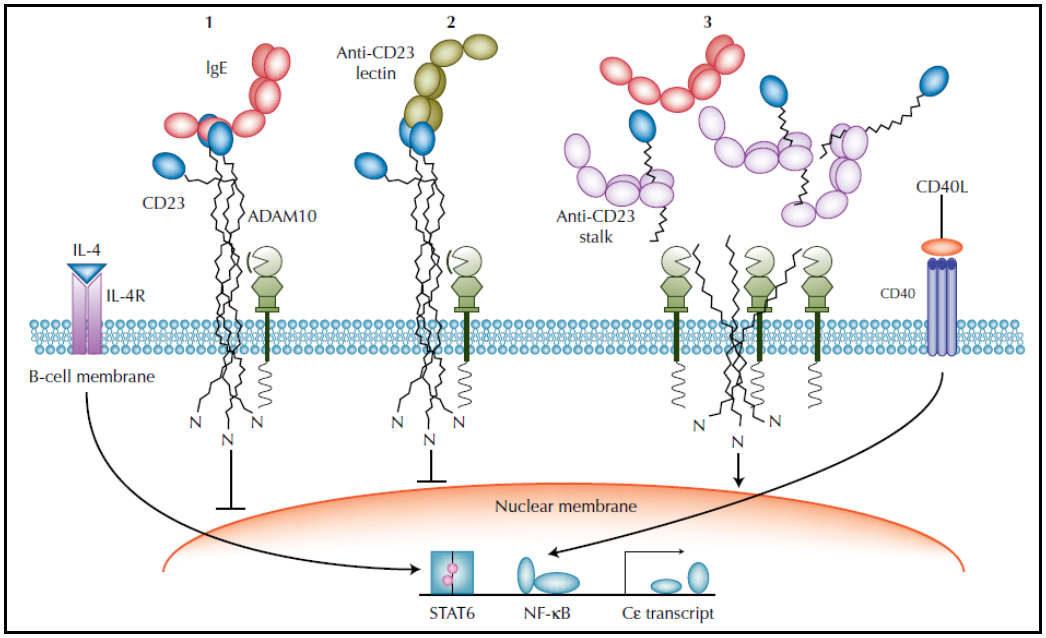

Figure 1.4: Model illustrating the influence of CD23 on the production of IgE. This figure illustrates two of the primary signals for IgE synthesis, IL-4 and CD40 ligation. In schemes 1 and 2, either high concentrations of IgE or anti-CD23 lectin result in CD23 trimer stabilization and modulation of IgE synthesis. In scheme 3, anti-stalk (as a model for proteases in allergens) destabilizes the CD23 stalk, resulting in ADAM10 cleavage and increased IgE synthesis (Conrad *et al.*, 2007).

The protective effect of IgE on initial cleavage of CD23 (through the binding of the lectin domain), results from stabilizing the integrity of the coiled coil structure which contains the cleavage site. Unraveling of the coiled coil domain via the leucine zipper region of CD23 when IgE is not bound induces cleavage of the receptor. It is thought that any exogenous agent able to interact with the leucine zipper domain of CD23 would disrupt the IgE inhibitory mechanism thereby leading to enhanced IgE synthesis. Expression of CD23 is increased in allergic disorders, in terms of membrane expression on B-cells as well as sCD23 production. sCD23 fragments larger than 25 kDa that retain a part of the stalk region promote continuing IgE production by at least two mechanisms: 1) sCD23 directly stimulates IgE production

possibly through triggering of CD21; 2) sCD23 by its ability to trap IgE in the medium prevents negative feedback through membrane CD23 (Tsicopoulos and Joseph, 2000).

In the prevention of the allergic response, it is important to maintain low serum levels of IgE. This is achieved by a feedback mechanism that suppresses further IgE production by B-cells (Nissim *et al.*, 1993; McCloskey *et al.*, 2007). It is thought that CD23 plays a key role in the suppression of IgE production (Sarfati *et al.*, 1992); therefore immunotherapy directed towards CD23 could be effective in the prevention of IgE-related disease (Nissim *et al.*, 1993; McCloskey *et al.*, 2007).

1.2.4.2 CD23 and CD21

CD21 is a 140 kDa membrane glycoprotein found on B lymphocytes, a subpopulation of T lymphocytes, follicular dendritic cells and pharyngeal epithelial cells. It is a receptor for the C3d, g and iC3b proteins of the complement system and is a receptor for the gp350/220 envelope glycoprotein of the Epstein-Barr Virus (EBV). It is also a receptor for IFN-γ. CD23 is also a CD21 ligand. The CD21 protein is composed of an extracellular domain of 15-16 repetitive units of 60-75 amino acids (short consensus repeats or SCR's) followed by a transmembrane domain (24 amino acids) and an intracytoplasmic region of 34 amino acids. The amino acid sequence of CD21 has potential sites for N-linked glycosylation. The binding site for CD23 is located on SCR's 5-8, but an accessory site is located on SCR's 1 and 2 (Aubry *et al.*, 1994).

Soluble CD21 (sCD21) and sCD23 form biologically active complexes (Fremeaux-Bacchi *et al.*, 1998). CD21 seems to mediate two important cytokine activities

ascribed to CD23; the upregulation of IgE synthesis and the rescue of germinal center B-cells from apoptosis. IgE also closes a negative feedback loop by switching off its own synthesis, through interaction with CD23. B-cell signalling is, however, controversial; sCD23 is able to increase spontaneous *in vitro* synthesis of IgE by *in vivo* pre-activated B-cells from allergic donors, but lower molecular weight sCD23 seems to inhibit IgE release. It is not known what ligand is involved here, but it could possibly be CD21. This is because CD21 clearly delivers co-stimulatory signals to B-cells, sub-optimally achieved with various physiologic pathways (Mossalayi *et al.*, 1997).

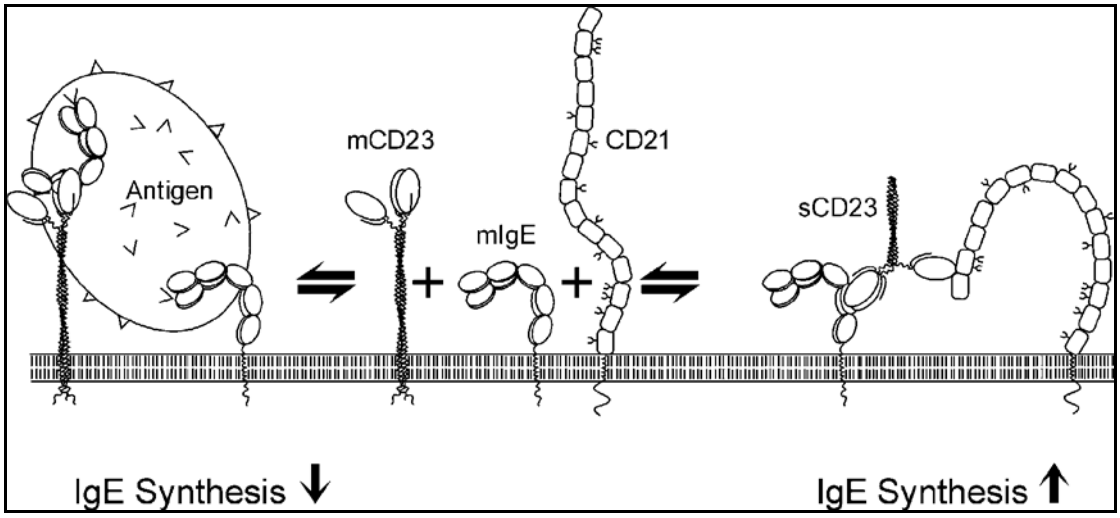

Figure 1.5: Competition between CD23 and CD21 for membrane IgE on the B cell surface. Co-cross-linking of membrane CD23 and membrane IgE by an allergen–IgE complex leads to down-regulation of IgE synthesis (left). Trimeric soluble CD23 co-cross-linking of membrane IgE and CD21 leads to up-regulation (right). IgE binding to membrane CD23 also protects the latter against proteolysis and prevents formation of soluble CD23 (Hibbert *et al.*, 2005).

The attachment of sCD23 to CD21 on peripheral B cells before their differentiation into IgE-secreting plasma cells enhances IgE synthesis (Figure 1.5). B cells express membrane IgE and CD21 before differentiation and CD23 may therefore upregulate

the synthesis of IgE by co-ligation of the mIgE and CD21 on these cells, causing selective proliferation and therefore higher levels of IgE synthesis. The binding sites for mIgE and CD21 are distinct and both ligands can bind CD23 simultaneously, supporting this cross-linking theory. mCD23 is associated with IgE downregulation. The cross-linking of mCD23 on B cells by IgE inhibits B cell proliferation and IgE production. This binding also inhibits CD23 cleavage and the release of soluble CD23 fragments that are able to stimulate IgE synthesis (Hibbert *et al.*, 2005).

In T cells, CD23 and sCD23 have been shown to play an accessory role in the T cell response to mitogens and allogenic or autologous B-cells. CD23 mRNA has been found in the outer cortex of the thymus, which is a region known to contain very early thymocytes. The differentiating effect of sCD23 seems to be due to its ability to downregulate apoptosis of early thymic precursor cells. T cell and thymocytes ligate sCD23, in part through CD21, expressed on the thymic precursor cells. This enables them to mediate CD21-related signal transduction (Mossalayi *et al.*, 1997).

The interaction between CD23 and CD21 requires glycosylation of CD21. This interaction involves the C-type lectin domain of CD23 and these two molecules are regarded as a pair of adhesion molecules (White *et al.*, 1997).

1.2.4.3 The β_2 integrins

The integrin family of proteins is made up of heterodimeric membrane-bound glycoproteins that mediate homotypic and heterotypic cell-to-cell adhesion and cell-matrix interactions in a broad range of biological functions (Rezzonico *et al.*, 2000). Integrins have been organized into 8 distinct subfamilies based on their β subunit

associations (Figure 1.6). The β_2 subfamily are cell surface glycoproteins that have four distinct α subunits (CD11a, b, c and d) which associate with the β_2 subunit (Mazzone and Ricevuti, 1995).

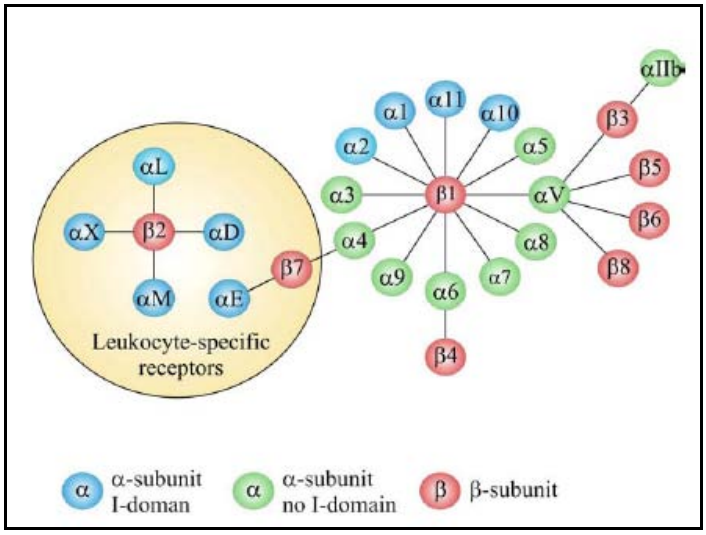

Figure 1.6: The integrin family. Integrins can be subdivided according to their β chains (Gahmberg *et al.*, 2009).

Integrins are composed of type I transmembrane α and β subunits, each with a large extracellular domain, a single-pass transmembrane domain and a small tail or cytoplasmic domain. Src-family protein tyrosine kinases are required for integrin-mediated cellular responses and result in numerous aspects of adhesive signalling (Ginsberg *et al.*, 2005).

Integrins are important in a variety of cell-adhesion reactions during immune-inflammatory mechanisms, but the engagement of β_2 integrins by natural ligands (like CD23) and certain monoclonal antibodies (mAbs) also generates outside-in cellular signalling, leading to cell activation. In monocytes, this activation causes the induction of procoagulant activity, production of inflammatory cytokines (TNFα, IL-

1β, IL-6), generation of nitric oxide and upregulation of cell-surface molecule expression (Rezzonico *et al.*, 2000).

The α subunit of integrins has a long extracellular domain and a short cytoplasmic domain. The α subunits of integrin heterodimers contain a β propeller structure formed by 7 repeating elements. Nine of the 18 α subunits, including the 4 that combine with β_2, contain an inserted (I) domain between the second and third blades of the β propeller. The αI domain is important for ligand binding. αI domains belong to the VWA domain family. The fold resembles that of small G proteins and assume a dinucleotide binding/Rossmann fold with a central hydrophobic 6-stranded β sheet surrounded by 6 or 7 amphipathic α helices. A metal ion-dependent adhesion site (MIDAS) is located at the upper surface of the αI domain. An Mg^{2+} ion is ligated at a MIDAS at the ligand-binding 'top' face of the domain, at the C-terminal ends of the parallel β strands. At the opposite end of the domain, the N and C termini of the αI domain connect to the β-propeller domain (Vorup-Jensen *et al.*, 2003). Two conformations of the αI domain have been found; open and closed. Only an open conformation can allow ligand binding (Walters, 2005). There are 5 exposed loops surrounding the MIDAS, which undergo conformational changes to bind ligands (Choi and Nham, 2002). The β_2 subunit has a highly conserved cysteine-rich region which gives it a rigid tertiary structure. Calcium and magnesium cations are essential for the stability and function of the αβ complex. The primary structure comparison of the α and β_2 subunits of leukocyte adhesion receptors with extracellular matrix receptors shows strong homologies. All have heterodimeric α-β structure and recognize the RGD (argininyl-glycinyl-aspartic acid) sequence in adhesive proteins (Mazzone and Ricevuti, 1995).

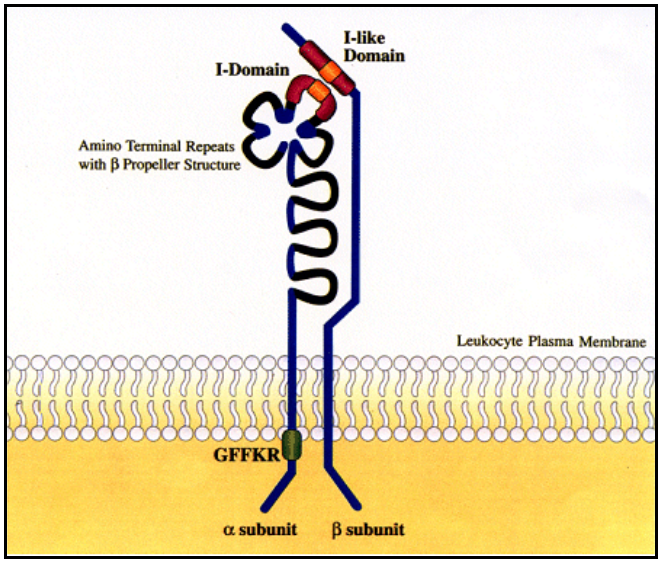

Figure 1.7: The structure of integrin α and β subunits (Harris *et al*., 2000).

The N-terminal portions of the α and β subunits fold into the globular headpiece which is connected by the α and β tailpiece domains to the membrane (Figure 1.7). The α subunit β-propeller domain and the β-subunit I-like domain form the integrin head, a ligand-binding structure in the headpiece. The I domain is located at the top of the integrin head. The α subunit I domains and β subunit I-like domains form an α/β fold with the MIDAS on the "top" of the domain, while C and N terminal connections are on the distal "bottom" face (Shimaoka and Springer, 2004).

The α and β subunits of β_2 integrins are synthesized as precursors that are cotranslationally glycosylated with N-linked high mannose carbohydrate groups. After α and β subunit association, (occurring 1-2 hours after synthesis) most of the high mannose groups are converted to complex-type carbohydrates in the Golgi apparatus and subunits increase slightly in molecular weight. Mature glycoproteins are then transported to the cell surface or to storage sites (Anderson and Springer, 1987). The molecular weights of the three distinct a, b and c subunits are 177 kDa, 165 kDa and 150 kDa, respectively. They are products of three separate genes. The

gene for the β_2 subunit is on chromosome 21 band 21q22. All three α subunits are localized to bands p11-p13.1 on chromosome 16 (Mazzone and Ricevuti, 1995). CD11b has eighteen N-glycosylation sites while CD11c has ten (Figure 1.8) (Arnoat *et al.*, 1988).

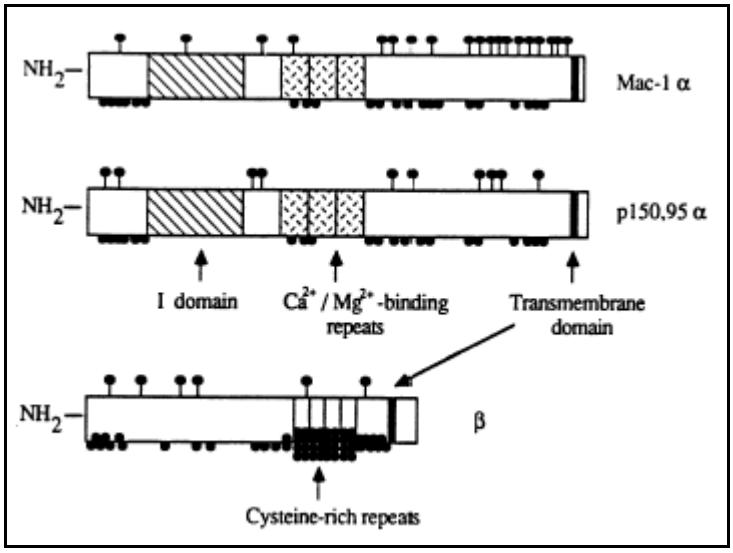

Figure 1.8: Schematic representation of primary structure of Mac-1α (CD11b) and p150, 95 (CD11c) α subunits and common β subunit. Black lollipops and circles represent N-linked glycosylation and cysteines, respectively (Kishimoto *et al.*, 1987).

There are two major pathways of activation for integrins. Leukocyte adhesion activation by increased affinity of individual integrin molecules for their ligands or by increasing the avidity of adhesion. The former is caused by conformational changes occurring in the integrins while the latter is caused by the increase in number /clustering of integrins in the plane of membranes, therefore increasing the adhesion by high local concentration of molecules (Ginsberg *et al.*, 2005).

1.2.4.3.1 CD11b/CD18

CD11b is found on macrophages, blood monocytes, in small amounts on granulocytes and NK cells, and is absent on lymphocytes and nonhaematopoietic cells (Ho and Springer, 1983; Rezzonico *et al.*, 2000). CD11b can be upregulated several fold from intracellular pools by chemotactic factors [C5a, IL-8, platelet activating factor, formyl methionyl leucyl phenylalanine (fMLP) and others] (Mazzone and Ricevuti, 1995). More than thirty protein and non-protein molecules are reported to bind CD11b/CD18. These include intracellular adhesion molecule 1, complement C3 fragment iC3b, junctional adhesive molecule c, fibrinogen, heparin, neutrophil elastase, neutrophil inhibitory factor, complement factor H, glycoprotein Ibα. uPAR, E-selectin and extracellular matrix proteins laminin, collagens, vitronectin, Cyr61 and connective tissue growth factor. In neutrophils, CD11b/CD18 is present in secondary granules under resting conditions where, upon activation, it is translocated to the plasma membrane (Zen, *et al*., 2004). Neutrophil engagement of fibrin(ogen) with CD11b causes cellular changes *in vitro* including calcium mobilisation, NF-κB activation, increased phosphorylation events, increased migration and decreased apoptosis (Flick *et al.*, 2004).

CD11b also acts as a pattern recognition receptor of innate immunity by interacting with LPS and other microbial glycoconjugates. This is done both in cooperation with CD14 and independently. CD14 is the main signal-transducing receptor in this relationship while CD11b is the main LPS-binding molecule. However, there is a CD14-independent pathway of LPS-stimulation that is mediated by CD11b. This pathway leads to upregulation of inducible nitric oxide synthase (iNOS) and increased nitric oxide production (Ehlers, 2000).

The activation signals which trigger the high affinity binding state of CD11b (inside-out signalling) and CD11b-mediated phagocyte activation (outside-in signalling) are still poorly understood. Outside-in signalling pathways by integrins are better understood than the reverse process and several of the signalling pathways have been clarified. The full activation of neutrophils and monocytes to enable their phagocytic, adhesive and chemotactic abilities is critically dependent on CD11b-mediated activation. However, the activation of leukocyte effector functions is dependent on the prior activation of CD11b. This is achieved by one of two mechanisms. The first is dependent on receptor clustering and most likely is achieved by ligation of coreceptors such as FcγR or selectins, and requires cytoskeleton rearrangement. The second mechanism is induced by the ligation of G protein-coupled receptors by classical chemoattractants (like fMLP, platelet-activating factor and chemokines) and does not require actin reorganisation. The receptor-clustering pathway has been shown to signal via phosphoinositide-3 kinase (PI3K), while the G protein pathway is PI3K independent. Other endogenous activators of CD11b have been elucidated. Oleic acid, usually released after bone injury, causes a rapid increase in cell surface expression of CD11b and its affinity state, promotes neutrophil aggregation and adherence to cultured endothelial cells. Myeloid-related protein 14 (MRP-14) is a prominent cytosolic protein in myeloid cells and directly induces the CD11b high-affinity state without activating other neutrophil functions and appears to do so via a specific G protein-coupled receptor. β-glucans are microbial polysaccharides which have also been shown to prime neutrophils and NK cell CD11b for phagocytosis of iC3b-opsonised particles. However the β-glucan-primed CD11b does not display a high affinity epitope necessary for efficient adhesion to substrates. This evidence

suggests that there are several pathways which cause CD11b activation as well as there being more than one activation state for CD11b (Ehlers, 2000).

Phosphorylation of the CD11b/CD18 α subunit, interaction of integrin cytoplasmic tails with cytoskeletal proteins, divalent cations or involvement of RhoA (a small guanosine triphosphate binding protein) may be crucial for inside-out signalling which leads to its activation. Integrin modulating factor 1 (IMF-1) is a small anionic lipid mediator which was discovered after neutrophil stimulation by phorbol 12-myristate 13-acetate (PMA), fMLP or TNF-α. IMF-1 was found to enhance β_2 integrin-dependent neutrophil adhesion as well as ligand binding activity of the isolated CD11b/CD18 (Klugewitz *et al.*, 1997).

CD11b/CD18 mediates the binding of neutrophils to their environment so that they can move to sites of inflammation. Enhancement of this ligand binding is induced by cellular activation, leading to expression of new epitopes on CD11b. This is a prerequisite for adhesion as CD11b on resting neutrophils exerts poor ligand-binding activity (Klugewitz *et al.*, 1997). It also plays a role in regulating the movement of PMN through tissues.

IL-1β is produced mostly by monocytes and macrophages and plays a vital role in immuno-inflammatory processes that cause tissue destruction in chronic diseases. sCD23 plays a role in inflammatory mechanisms and has been shown to induce IL-1β production through the activation of macrophages via its CD11b and CD11c interaction (Rezzonico *et al.*, 2000; Sato *et al.*, 1997).

1.2.4.3.2 CD11c/CD18

CD11c is found on monocytes, macrophages, granulocytes, some T and B lymphocytes and dendritic cells. CD11c binds iC3b, fibrinogen, LPS and CD23 (Rezzonico *et al.*, 2000; Ingalls and Golenbock, 1995). Antibodies to CD11c blocked monocyte migration, chemotaxis, adherence to plastic and endothelial cells and phagocytosis of latex beads. CD11c mediates the adherence of TNFα-stimulated neutrophils and activated B-cells to fibrinogen. CD11c also stimulates respiratory burst in neutrophils. Its expression on cytotoxic cells is shown to be essential for target cell destruction (Noti and Reinemann, 1995).

CD11c/CD18 is less susceptible to activation compared with other β_2 integrins. This was shown by stronger stimulation required to permit CD11c/CD18 ligand binding in U937 and alveolar macrophage cells than CD11b/CD18. Src kinase activity is required for CD11c-mediated adhesion of cultured monocytes to fibrinogen, and plays a role in regulating CD11c avidity (Georgakopoulos *et al.*, 2008). Monocyte chemotactic protein 1 (MCP-1), macrophage inflammatory protein (MIP)-1α, MIP-1β and RANTES (regulated upon activation, normal T cell expressed and secreted) have been shown to increase surface expression of CD11c and CD11b on monocytes (Rezzonico *et al*., 1997).

sCD23 binding to β_2 integrins causes NO production and IL-1β, IL-6 and TNF-α in monocytes. Engagement of CD11b or CD11c on monocytes by antibodies induces nuclear translocation of NF-κB and the subsequent production of MIP-1α and MIP-1β, which in turn play a role in the recruitment of inflammatory cells during an inflammatory response (Rezzonico *et al*., 2001).

1.3 Diseases associated with CD23

Allergic disease is caused primarily by the formation of IgE antibodies against environmental antigens. The formation of immune complexes made up of IgE and allergens induces the release of inflammatory mediators, proteases and cytokines from mast cells and basophils, leading to an allergic reaction within a few minutes. Immediate allergy is therefore mediated by IgE and a Th2 cell process (Valenta *et al.*, 2008). CD23 is increased in atopic disease where it has been implicated in excessive IgE production. Dexamethazone (a corticosteroid) is a potent downregulator of CD23; acting directly on normal human B lymphocytes or B lymphoblastoid cell lines (Kaufmanpaterson *et al.*, 1994) and it is widely used as an anti-inflammatory and to treat autoimmune diseases. CD23 is also implicated in cancer, although its role is poorly defined. High levels of sCD23 and L-selectin are found in the serum of patients with B-chronic lymphocytic leukemia (B-CLL). Lower levels of sCD23 and L-selectin are also found in B-cell immunocytomas and low-grade non-Hodgkin's lymphomas, while only small amounts of these soluble molecules are found in the sera of normal patients. This suggests that sCD23 and L-selectin in B-CLL are derived from the circulating pool of lymphocytes and there is some evidence that sCD23 levels may reflect disease activity and be a prognostic indicator of B-CLL (Gu *et al.*, 1998). Elevated levels of sCD23 have also been found in clinical conditions like rheumatoid arthritis. The prevalence of asthma, hayfever and IgE-mediated diseases has increased drastically in industrialised countries in the last few decades. The rate of asthma in the USA has increased by 75% between 1980 and 1994 and approximately 20% of British children under the age of 14 suffer from asthma (Hamelmann *et al.*, 2002).

1.4 Diseases associated with β_2 Integrins

Deficiency of CD11/CD18 results in congenital defects of chemotaxis and phagocytosis and therefore increased bacterial infections. Neutrophils have a decreased phagocytic response to bacteria and yeast and a reduced ability to adhere to various substrates and migrate to infected sites. Deficiency or absence of leukocyte integrins causes a clinical syndrome called leukocyte adhesion deficiency (LAD), which is characterized by diminished pus formation, abnormal wound healing, and susceptibility to pyrogenic infections (Diamond *et al.*, 1991). The most important clinical effect in LAD patients is the inability of circulating neutrophils and monocytes to bind to endothelial cells at sites of inflammation and migrate to the inflamed tissue. CD11c/CD18 is the most important of the three in monocyte adhesion and chemotaxis while CD11b/CD18 is the most important with neutrophils. Monocyte extravasation and differentiation into tissue macrophages is accompanied by an increase in CD11c/CD18 expression, as is differentiation of myelomonocytic precursor cells *in vitro.* LAD patients suffer from recurrent necrotic and indolent infections of the soft tissue, mainly involving skin, mucous membranes and intestinal tract. They are plagued by small, non-pustulating skin lesions which often progress to large, well-demarcated, ulcerative craters which heal slowly. Perirectal abcesses or cellulitis leading to peritonitis and/or septicaemia is also common. Recurrent otitis media is also common with occasional progression to mastoiditis and facial nerve paralysis. Patients suffer from bacterial respiratory infections, recurrent pneumonitis or sinusitis. Severe gingivitis and/or periodontitis are major features. Recurrent necrotic soft tissue infections indicate impaired leukocyte mobility to inflamed sites and abnormalities in tissue leukocyte infiltration (Anderson, 1987).

Increased CD11b/CD18 on circulating leukocytes causes several inflammatory disorders associated with neutrophil activation, eg. sepsis, burns, hemodialysis, systemic lupus erythmatosis, diabetes mellitus and coronary artery disease (Mazzone and Ricevuti, 1995). CD11c plays an important role in the progression of the inflammatory events leading to demyelination and paralysis during experimental autoimmune encephalomyelitis (EAE) and it is believed that β_2 integrin proteins are involved in demyelinating diseases (Bullard *et al.*, 2007).

1.5 Aims of the study

CD23 has been shown to play a role in the growth and differentiation of T and B cells, apoptotic rescue of B cells, cellular adhesion, IgE regulation, release of inflammatory mediators and in the resistance to certain bacteria, fungi and parasites. It is clear that CD23 plays an important role in normal immune responses, as well as immune diseases. The CD11b and CD11c β_2 integrins play a role in inflammation, phagocytosis, cellular migration, chemotaxis and cellular activation. These integrins are known to bind CD23 and it is this relationship between CD23 and the β_2 integrins that required further investigation.

The aim of this study was to investigate the immune regulatory functions of soluble CD23 together with its integrin ligands CD11b and CD11c. This was done in the hope of elucidating the effect of sCD23 interactions with β_2 integrins in monocytes and assisting in our understanding of what might be occurring in cells when the sCD23 proteins are upregulated in the immune system. This information could then assist in the understanding of allergic and inflammatory disease and therefore the development of more specific interventions for allergic and inflammatory conditions.

The study encompassed two approaches. We firstly wanted to investigate the *in vitro* interaction between sCD23 and the β_2 integrin proteins. This involved producing recombinant sCD23 in a bacterial host, *Escherichia coli*. We produced recombinant homologs of the three major soluble CD23 proteins naturally found in human serum, namely 16 kDa derCD23, 25 kDa and 33 kDa sCD23, termed CD23M150 and CD23M79, respectively in this study. Recombinant CD11b and CD11c α subunits were to be produced by baculoviral expression from insect cells as secreted proteins, while recombinant CD11b and CD11c αI domains were produced in *E. coli*. Another protein interaction that we wanted to investigate was the binding of sCD23 proteins to cells which had been differentiated to increase the surface expression of β_2 integrin proteins.

The second approach used the recombinant sCD23 proteins in various cell based experiments. CD11-producing monocytic cell lines were used to investigate the effect that sCD23 has on these cell lines. In cell based experiments, we wanted to investigate the production of inflammatory cytokines, the effect of sCD23 on the cells' normal functions (such as phagocytosis and chemotaxis), the signalling pathways induced, as well as the induction of oxidative stress to indicate whether the cells are stimulated by sCD23 or not.

Chapter 2: Recombinant Protein Production

2.1 Introduction

The number of proteins being produced using recombinant techniques is increasing on a daily basis due to advances in genomics, proteomics and bioinformatics. Many expression hosts have been developed to express these proteins, such as *Escherichia coli*, *Saccharomyces cerevisiae*, *Pichia pastoris* as well as insect and mammalian cell lines (Arnau *et al.*, 2006).

Two of these expression host systems were used to attempt the expression and purification of human recombinant CD23 and CD11b/c. The bacterial *E. coli* expression system was used to express and purify recombinant human CD23 and recombinant human CD11b and CD11c αI domain proteins, while an insect cell system was used to try to express and purify full-length human CD11b and CD11c α subunits.

2.1.1 Insect cell expression

Baculovirus-mediated insect cell expression is a very popular method of producing large quantities of recombinant proteins for structural and functional studies of therapeutic biomolecules. Since this is a eukaryotic-based system, it offers protein modification and processing patterns similar to higher eukaryotes. In most baculovirus systems the gene of interest is cloned into a transfer vector which contains the sequences that flank the polyhedrin gene in the baculovirus genome. The transfer vector and the viral genome are then co-transfected into the insect cell and the

gene is inserted into the virus genome via homologous recombination under the strong late viral polyhedrin promoter. However, homologous recombination is never perfectly efficient, producing a mixture of recombinant and parental virus, therefore requiring plaque purification of recombinant progeny before expression studies can continue. This is labour intensive and technically demanding (Loomis *et al.* 2005).

However, there are vectors available which can be used for the expression of recombinant protein in bacterial, baculovirus and mammalian systems. This removes the need to generate specific expression plasmids for each expression system, for every construct of protein that is required. Novagen has produced the InsectDirect system that incorporates these features. The InsectDirect system uses pIEx and pTriEx vectors that allow for the expression of protein by transient transfection of *Spodoptera*-derived insect cells in the case of pIEx vectors and bacterial, insect and mammalian cells in the case of pTriEx vectors (Loomis *et al.* 2005).

pIEx vectors drive gene expression in insect cells using the *Autographa californica* nuclear polyhedrosis virus (AcNPV) homologous region 5 (hr5) enhancer and the AcNPV immediate early promoter (ie1) transcription elements derived from AcNPV baculovirus (Rodem and Friesen, 1993; Pullen and Friesen, 1995). This promoter/enhancer combination uses the cells' endogenous cell transcription machinery to express protein, which eliminates the need to use baculovirus itself. The vectors also have a high-copy pUC replicon to facilitate the preparation of high-quality plasmid DNA for transfection. The pIEx-10 vector has an N-terminal Strep II tag and a mouse IgM signal sequence to facilitate expression, secretion and purification of recombinant proteins (Loomis *et al.* 2005).

The pTriEx expression plasmids have cytomegalovirus (CMV), T7 *lac* and p10 promoters (Pp10) and a single multiple cloning site (MCS) for mammalian, bacterial and baculovirus-mediated expression, respectively. The pTriEx-7 vector has a T7 *lac* promoter, a ribosome binding site and the pUC replication origin for high plasmid yields to facilitate bacterial expression. For insect cell expression they contain the *lef*2/603 and ORF1629 sites for recombination into the baculovirus genome and have a p10 baculovirus promoter. They also have a CMV promoter, along with a CMV immediate early enhancer and rabbit β-globin polyadenylation signal to drive human cell expression. pTriEx-7 vectors have an N-terminal Strep II tag and a mouse IgM signal sequence as well (Novagen User Manual TB250, 2006). These vectors were designed by Novagen as part of their ligation independent cloning (LIC) range. Ek/LIC vectors are designed for the rapid cloning and expression of genes in multiple expression systems. This method allows for the directional cloning of PCR products without the need for restriction enzyme or ligation reactions. These vectors all have the same Ek/LIC cloning site so that any Ek/LIC-prepared insert can be annealed into any of the Ek/LIC vectors in a 5 minute reaction. This method utilises the 3' to 5' exonuclease activity of T4 DNA polymerase to create a specific 13- or 14-base overhang in the Ek/LIC vector. PCR products are then designed with complementary overhangs by building appropriate 5' extensions into the primers. Purified PCR products are treated with LIC-quality T4 DNA polymerase in the presence of dATP to produce the necessary vector-compatible overhangs (Figure 2.1). Covalent bonds form at the vector-insert junctions within the *E. coli* cell to yield circular DNA that is used to transform bacteria, insect or mammalian cells (Loomis *et al.* 2005).

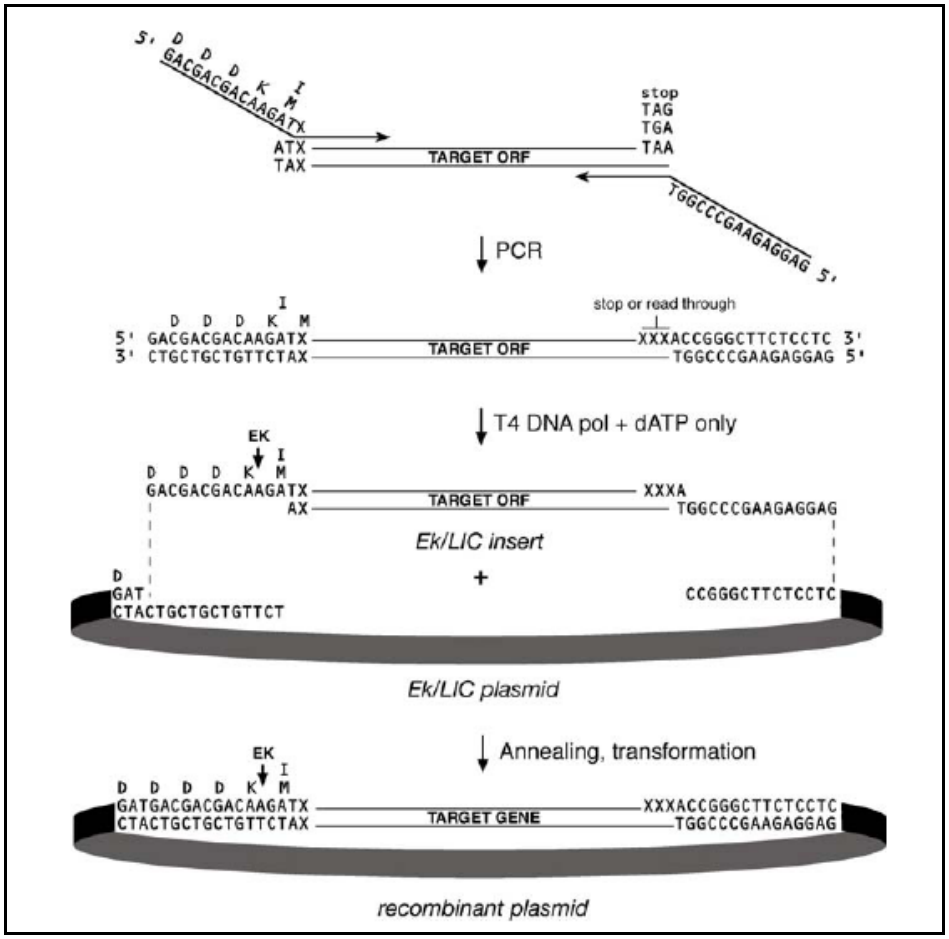

Figure 2.1: The Ek/LIC cloning strategy. After amplification with primers that produce complementary 5'overhangs, the insert is treated with T4 DNA polymerase and dATP and annealed to the plasmid before transformation of the desired cells (Novagen User Protocol TB163, 2004).

Streptag II, an affinity tag found in the pIEx and pTriEx systems, is a streptavidin-recognising octapeptide (WSHPQFEK) selected for its improved affinity. The expressed proteins containing Streptag II are purified using an affinity matrix with a modified streptavidin and eluted with a biotin analog (Arnau *et al.*, 2006). This allows for an easy one-step isolation and purification of proteins.

Sf21 cells originate from IPLBSF-21 cells derived from *Spodoptera frugiperda* pupal ovarian tissue. These insect cells are commonly used for insect cell expression of recombinant proteins. However, insect cells have a different N-glycosylation

pathway to mammalian cells. They are unable to produce complex binary N-linked oligosaccharide side chains containing penultimate galactose and terminal sialic acid residues (Hunt, 2005).

The full length CD11b and CD11c have only successfully been expressed by transforming human cells with both the α subunit and the common β subunit (CD18). In this study, the InsectDirect system was investigated as an alternative method to express only the α subunit of CD11b and CD11c.

2.1.2 Bacterial cell expression

The development of bacterial expression systems, especially those in *E. coli*, enables scientists to produce large amounts of recombinant proteins from cloned genes. Recombinant DNA technology has already facilitated the production of therapeutic-grade proteins, like growth hormone, interferon and insulin (Middleton, 2002). One disadvantage of using *E. coli* for recombinant protein expression is the possibility that the desired protein will be expressed into insoluble and inactive aggregates called inclusion bodies (IB's). These are dense, amorphous protein deposits that can be found in the cytoplasmic and periplasmic space of bacteria. The proteins in these aggregates then have to be renatured and purified. IB's are formed intracellularly either due to the aggregation characteristics of the protein or due to the inability of the cellular processes to correctly solubilise or fold the protein (Middleton, 2002).

There are, however, advantages in the production of recombinant proteins in this manner. Often the recombinant protein is unstable if produced in the *E. coli* cytoplasm due to proteolysis and may also prove toxic to the host cell, thereby

affecting the expression levels of the protein. Under the appropriate conditions, it is possible for the recombinant protein in the inclusion bodies to amount to approximately 50 % or more of the total cellular protein. The relatively high density of the inclusion bodies also facilitates their isolation from the other cellular proteins by centrifugation (Clark, 2001; Lilie *et al.*, 1998; Misawa and Kumagai, 1999).

The main task after the high level expression of the recombinant protein into IB's is the conversion of inactive and misfolded IB proteins into soluble, biologically active products. The first step in achieving this task is the purification of the inclusion bodies from impurities by washing with a detergent. Triton X-100, deoxycholate or low molar concentration of chaotrophs are usually used for this purpose (Clark, 2001; Lilie *et al.*, 1998; Misawa and Kumagai, 1999).

The purified IB's must then be solubilised using a strong denaturant, usually 6 M guanidinium hydrochloride (Gdn-HCl) or 8 M urea. Gdn-HCl is usually preferred for this purpose, firstly because it is a strong chaotroph that might allow solubilisation of extremely aggregated IB's, where urea may not solubilise the aggregates. Secondly, urea solutions often contain isocyanate which causes the carbamylation of free amino groups of the polypeptide. The addition of thiol agents, such as L-glutathione (GSH), cysteine or β-mercaptoethanol, allow the reduction of the disulphide bonds by thio-disulphide exchange and facilitates the solubilisation of cysteine-containing proteins. After solubilisation of the IB's the excess denaturants and thiol reagents must be removed and the reduced proteins transferred to oxidizing conditions to allow for the formation of correctly folded proteins. For the renaturing to be efficient there has to be competition between the correct folding and aggregation. To slow down the formation of aggregates, the refolding process is usually performed at low protein

concentrations of 10–100 μg/mL. The condition under which this renaturation takes place has to be optimized with regard to external parameters such as temperature, pH and ionic strength (De Bernadez and Clark, 2001; Lilie *et al.*, 1998; Misawa and Kumagai, 1999).

If the target protein contains disulfide bonds, the renaturation buffer has to be supplemented with a redox system. The addition of a mixture of reduced and oxidized forms of low molecular weight thiol reagents (such as glutathione, cysteine and cysteamine) in molar ratios between 5:1 and 10:1 provides the appropriate redox potential to allow the formation of thiol bonds. This thiol-disulphide exchange is accelerated by keeping the pH of the renaturation buffer at the upper limit which still allows renaturation of the protein (De Bernadez and Clark, 2001; Lilie *et al.*, 1998; Misawa and Kumagai, 1999).

The presence of low molecular weight compounds in the renaturation buffer may also have an effect on the yield of renatured protein. Nondenaturing conditions of chaotrophs are often efficient refolding enhancers. L-arginine is a popular additive in this regard, although the reason for its renaturation support is unknown. It is thought, however, that it is due to its increased solubilisation of folding intermediates (Clark, 2001; Lilie *et al.*, 1998; Misawa and Kumagai, 1999).

In this study we used Novagen's pET system for the expression of recombinant proteins in *E. coli*. Target genes are cloned into pET plasmids which are under the control of strong bacteriophage T7 transcription and translation signals. Expression is induced by providing a source of T7 RNA polymerase in the host cell which, when fully induced, converts almost all of the cells' resources to target gene expression. It

is usually suggested that target genes are first cloned into hosts that do not have the T7 RNA polymerase gene, thereby eliminating the instability of the plasmid due to the production of potentially toxic proteins. The plasmid is then transferred into an expression host containing a chromosomal copy of the T7 RNA polymerase gene under *lac UV5* control. Expression can then be induced by the addition of isopropyl-β-D-thiogalactopyranoside (IPTG) or lactose. By adding IPTG, the T7 RNA polymerase is induced, which results in the transcription of the target DNA in the plasmid. There are two categories of pET vectors; transcription and translation vectors. Transcription vectors were designed to express target genes carrying their own prokaryotic ribosome binding site and AUG start codon [such as pET-21(+), pET-24(+) and pET-23(+)]. Translation vectors are distinguished by the addition of a letter suffix following the name, which indicates the reading frame relative to the *BamH1* cloning recognition sequence GGATCC. Vectors having an 'a' suffix express from the GGA triplet while those with a 'b' express from the GAT triplet and so on. All pET translation vectors possess translation stop codons in all three reading frames following the MCS, as well as a downstream T7 transcription terminator. pET vectors often carry an antibiotic resistance gene to assist with positive identification of transformed host cells (Novagen User Manual TB055, 2006).

The use of affinity tags to purify these recombinant proteins enables us to use the same chromatographic purification systems to purify a wide range of proteins. Not only does the use of affinity tags decrease the number of chromatographic isolation steps, but it usually results in a higher yield of pure protein, decreased proteolysis, increased solubility and protection of the antigenicity of the recombinant protein. Tags can, however, change the protein conformation, lower protein yields, inhibit enzyme activity, alter biological activity and cause toxicity. Polyhistidine (His) tags

are the most widely used affinity tags because they are small and most often do not interfere with folding of the desired protein. It also shows very strong reversible binding to chelated metals, therefore making the purification process faster (Hunt, 2005). An alternative affinity tag is glutathione S-transferase (GST) of *Schistosoma japonicum* first cloned into an *E. coli* expression vector in 1988 (Smith and Johnson, 1988). This enabled fusion proteins to be purified by affinity chromatography on immobilised glutathione. Bound fusion proteins are then eluted using 10 mM reduced glutathione under non-denaturing conditions (Terpe, 2003). GST tags are large (26 kDa) and have slow binding kinetics to glutathione-Sepharose resin.

This study made use of the *E. coli* recombinant protein expression system using pET vectors for the expression and purification of recombinant human CD23 proteins and pGEX vectors with a GST tag for the expression and purification of CD11b and CD11c αI domain proteins.

2.2 Methods

2.2.1 Materials

The EconoTaq DNA polymerase and 10x buffer were from Lucigen (Wisconsin, USA); alkaline phosphatase, dNTP's, T4 DNA ligase, lysozyme, PVDF membrane, ethidium bromide, IPTG and bovine serum albumin were from Roche (Mannheim, Germany); Generuler DNA marker, *NdeI*, *XhoI*, *BstXI* and *PstI* were from MBI Fermentas (Germany); Wizard SV gel and PCR cleanup System was from Promega (Wisconsin, USA); KOD HiFi DNA polymerase kit, Novablue Gigasingles cells, Insect Genejuice, X-gal solution, *E. coli* BL21 (DE3), pET23a(+) and pET28b(+)

vectors were from Novagen (Madison, Wisconsin); GSH, GSSG, Fluka Salmon testis DNA, 6-(biotinamidocaproylamido) caproic acid succinamide ester, anti-goat IgG peroxidase conjugate, 3,3',5,5'-tetramethylbenzidine (TMB) and Bradford reagent were from Sigma Aldrich (St. Louis, Missouri, USA); GSTrap columns and Superdex 75 26/60 FPLC column were from Amersham Pharmacia Biosciences AB (Uppsala, Sweden); Endosafe LAL test kit was from Charles River (Wilmington, Massachusetts); electrophoresis grade agarose from Hispanager (Spain); EndoFree Plasmid Maxi Kit from QIAgen (Hilden, Germany); peqGOLD protein marker II was from PEQLAB (Erlangen, Germany); Gibco TC100 medium and Gibco FCS were from Invitrogen (California, USA); penicillin-streptomycin was from Lonza (Basel, Switzerland); and anti-CD11b (CRBM1/5) antibody was from eBioscience (San Diego, USA). All standard laboratory chemicals used were of the highest analytical grade available.

2.2.2 Vectors

2.2.2.1 CD11b and CD11c vectors

The α subunits of CD11b (Corbi *et al.* (1988)) and CD11c (Corbi *et al.* (1987)) have been cloned into a pCMD8 vector. These two vectors were used to transfect COS (derived from the cells being **C**V-1 (simian) in **O**rigin, and carrying the **S**V40 genetic material) cells together with a clone for CD18 in a pEYFP NI vector (Kim *et al.*, 2003). These vectors were kindly donated to our laboratory by ADDGENE (USA), and were received in transformed *E. coli* MC106/P3 cells on agar slants. Figure A.1 in Appendix A shows the vector maps for pCDM1 (CD11b) and pCDP1 (CD11c) that

were received (Figure A.1). These vectors were used as template DNA for the cloning of full length CD11b and CD11c α subunits into pIEx and pTriEx vectors.

Dr Sang-Uk Nham (Kangwon National University, South Korea) donated two vectors to our laboratory that contained the coding regions of CD11b and CD11c αI domains (Fig A.2, Appendix A). CD11b αI domain was cloned into a pGEX (Amersham Biosciences) vector backbone and called pGEXhCD11bI and is predicted to be 5609 bp in size. CD11c was also cloned into a pGEX vector backbone and called pEXCD11cI and is predicted to be 5604 bp in size. The pGEX vector has a GST tag for affinity purification and it has an ampicillin resistance marker. It is known that a large majority of CD11b and CD11c's ligands bind via their αI domain, and therefore it was decided to express and purify these proteins for use in experiments.

2.2.2.2 CD23 vectors

The ectodomain of CD23 was amplified from a λ-phage complementary DNA library, prepared from buffy coat, and ligated into pET22b by Dr Peter Sondermann at the Structural Research Department at the Max-Planck Institute for Biochemistry, Martinsried, Germany. This construct was called pET22b.CD23 and was used to amplify the three different coding regions of CD23 produced in this thesis (Figure A.3, Appendix A).

2.2.3 DNA amplification and primers

Two different DNA polymerases were used for experiments. When EconoTaq was used, the PCR reaction mixture was conducted with 2 µl of template DNA that was denatured by heating to 95 ºC for two minutes with a heating block, 2 U EconoTaq DNA polymerase, 2.5 µl 10x polymerase buffer, 2.5 µl of 2.5 mM dNTP's and 1 µl each of the forward and reverse primers (at 100 ρmols/µl). The reaction volume was made up to 25 µl with nuclease free H_2O. When the KOD HiFi DNA polymerase was used, 2 µl of template DNA was then used in a PCR reaction with 2.5 µl each of forward primer and reverse primer, 5 µl KOD PCR Reaction buffer, 4 µl of 25 mM $MgCl_2$, 5 µl of dNTP's (2.5 mM stock of each), 2.5 U KOD HiFi Polymerase and made up to 50 µl with sterile ddH_2O. A negative control was run with every PCR experiment, which was exactly the same as the samples being amplified, but with sterile ddH_2O substituted for the template DNA.

The PCR conditions used in all experiments were one cycle of denaturation at 95 ºC for 2 minutes, followed with 25-30 cycles of denaturing, annealing and elongation. The denaturing was conducted at 95 ºC for 45 seconds, annealing at 55 ºC or 60ºC for 1 minute and elongation at 72 ºC for 3 minutes. These 25 cycles were followed by another elongation cycle at 72 ºC for 15 minutes. The PCR reactions were conducted using a Bio-Rad iCycler.

Table 2.1 shows the PCR primers used for amplification or sequencing of the full-length CD11b and CD11c as well as the CD23 proteins.

Table 2.1: Table of PCR primers used for sequencing or amplification of β_2 integrin DNA and CD23 DNA. Underlined sequences represent restriction enzyme sites.

Name	Sequence	Target
Vector sequence primers		
pGEX5	5'GGGCTGGCAAGCCACGTTTGGTG-3'	pGEX vector
pGEX3	5'CCGGGAGCTGCATGTGTCAGAGG-3'	pGEX vector
T7	5'TAATACGACTCACTATAGGG-3'	pET vectors
T7TERM	5'GCTAGTTATTGCTCAGCGG-3'	pET vectors
IEProm	5'TGGATATTGTTTCAGTTGCAAG-3'	pIEx vector
IETerm	5'CAACAACGGCCCCTCGATA-3'	pIEx vector
TriExUP	5'GGTTATTGTGCTGTCTCATCA-3'	pTriEx vector
TriExDOWN	5'TCGATCTCAGTGGTATTTGTG-3'	pTriEx vector
EGFP-N	5'CGTCGCCGTCCAGCTCGACCAG-3'	pCDM8
EFGP-C	5'CATGGTCCTGCTGGAGTTCGTG-3'	pCDM8
BGH-REV	5'TAGAAGGCACAGTCGAGG-3'	pCDM8
pCDM8-REV	5'AACTGGTAGGTATGGAAGATCC	pCDM8
CD11 Gene specific primers		pCDM8
CD11bBDF	5'(GAC)3AAGATGTTCAACTTGGAC-3'	CD11b
CD11bBDR	5'(GAG)2AAGCCCGGTATCAATGGTAATGGGTTGGGGAC-3'	CD11b
CD11cBDR	5'(GAG)2AAGCCCGGTATCAATGGAGTTGGGTTGTGGAC-3'	CD11c
CD23 Primers		
GB16F3	5'TAGTGTCCATGGGCTTTGTGTGC-3'	CD23(der)
GB16R3	5'TGTCAAGCTTACTCCGCAGAACC-3'	CD23(der)
sCD23-IBF	5'(A)7CATATGGAGTTGCAGG-3'	CD23(M150)
3CD23	5'TGGCTGGATCCATGCTCAAG-3'	CD23 (M150 and M79)
5CD23tri	5'(A)7CATATGGCGCAGAAATCC-3'	CD23(M79)

Amplified PCR products were then electrophoresed with an appropriate DNA size marker on a 1% (w/v) agarose gel in Tris acetate ethylenediaminetetraacetic acid (EDTA) [TAE (40 mM Tris, 1.14 mL/L acetic acid, and 2 mM EDTA)] containing 5 μg/ml ethidium bromide at 120V and 60 mA for 45 minutes and visualised on an AlphaImager 3400 transilluminator (Alpha Innotech).

2.2.4 Chemically competent cells

Chemically competent cells were prepared using the calcium chloride method described by Sambrook *et al*. (1989). Competent cells were transformed with DNA by gently thawing 20 μl of competent cells on ice and adding 2 μl of ligation mix

before gently swirling them and incubating them on ice for fifteen minutes. The mixture was incubated at 42 ºC for thirty seconds before incubating on ice for two minutes. Cells were incubated at 37ºC with 100 µL of Luria Bertani [LB (10 g Tryptone, 10 g NaCl, 5 g Yeast extract)] broth for one hour. The transformed cells (100 µl) were plated onto LB agar plates (LB broth with 15 g/L bacteriological agar) containing the appropriate antibiotic and incubated overnight at 37 ºC.

2.2.5 Electrocompetent cells

Electrocompetent cells were produced for *E. coli* Bl21 (DE3) cells by streaking the cells onto LB plates. The plates were incubated overnight at 37 °C. A single colony was inoculated into 50 ml of SOB medium (50g Bactotryptone, 12.5g Yeast extract, 1.46g NaCl, 0.465g KCl, 2.5 L ddH_2O), which was grown overnight at 37 °C at 160 revolutions per minute (rpm) on an orbital shaker. Five ml of the overnight culture was used to inoculate 4 x 1L of SOB media and grown to mid-log phase (OD_{600nm} approximately 0.8, measured on an Ultraspec 2000 from Pharmacia Biotech) at 37 °C and 160 rpm. The cells were immediately chilled on ice. The cultures were decanted into chilled, sterile centrifuge bottles, pre-rinsed with wash buffer [10% (v/v) ultrapure glycerol]. These cultures were centrifuged at 3000 x g for 15 minutes at 4 °C using an Avanti JA25 centrifuge (Beckman). The cells were loosened and resuspended in wash buffer before being centrifuged as before. Washing was repeated twice. The cells were loosened and resuspended in approximately 4 ml of wash buffer (on ice). Ninety µl of cells were aliquoted into sterile Eppendorfs and frozen immediately in liquid nitrogen, before storing at –80 °C. The resulting electrocompetent cells were used for transformation using a GenePulser Xcell (Bio-Rad). This was done by adding 2 µl of plasmid DNA to 40 µl of chilled

electrocompetent cells in a chilled Eppendorf tube. This was mixed by pipetting up and down a few times and transferred to a chilled 1 mm gap electroporation cuvette (Eppendorf). Cells were electroporated using the pre-set *E. coli* Bacteria 1 protocol on the GenePulser Xcell (1800 V; 200 Ohms; 25 μF) before adding 1 ml of warm LB broth. The cuvettes were incubated for 1 hour at 37˚C, before plating 100 μl onto LB plates with the appropriate antibiotic and incubated overnight at 37 ºC.

2.2.6 Protein Quantification

A quick, simple and sensitive method for protein determination is vital to any biochemistry laboratory. In addition to having all these qualities, the Bradford method of protein determination is also subject to less interference by common reagents and non-protein components of samples than other methods of protein determination (Bradford, 1976). Bradford reagent contains Coomassie blue G250 which is anionic, binds to protein, and has an absorbance maximum of 590 nm. Thus the quantity of protein can be estimated by measuring the absorbance of the solution at 595 nm (Kruger, 1994).

Bovine serum albumin (BSA) was used to construct a standard curve in the same buffer as the sample being measured, starting at a concentration of 2.5 mg/mL with two-fold dilutions. Briefly, 10 μl of sample (or BSA standard) was added to a 96-well plate in triplicate. One hundred μl of Bradford reagent (Sigma) was added and the plate incubated at room temperature for a minute before reading at 595 nm. Sample readings were compared to a standard curve and protein levels determined.

2.2.7 SDS-PAGE and protein sequencing

SDS-PAGE was performed in a buffer system according to the method of Laemmli (1970). The gel contained 15% acrylamide and was stained using Coomassie Brilliant Blue (0.2% Coomassie blue; 7.5% acetic acid; 50% ethanol) and destained using methanol, glacial acetic acid and water in a ratio of 40:10:50 (v/v), respectively. For protein sequencing, a duplicate, unstained gel was used to transfer protein to polyvinyldifluoride (PVDF) membranes for sequencing of the protein. To transfer the protein, the gel was first equilibrated in 500 mL of chilled transfer buffer (48 mM Tris, 39 mM glycine, 20% methanol) for 15 minutes. The transfer membrane and filter paper were also soaked for 5-10 minutes in the transfer buffer. The above components were assembled in the order; filter, transfer membrane, gel above it and another filter. The transfer was achieved using a constant voltage (25 V) at 200 mA for 90 minutes using a Bio-Rad Trans-Blot SD Semidry Electrophoretic transfer cell. The membrane was stained using Coomassie Blue and destained as previously mentioned, before being sent for sequencing. N-terminal amino acid sequencing was performed by Dr Koji Muramoto (Graduate School of Life Sciences, Tohoku University, Sendai, Japan) on a Shimadzu PSQ-1 gas-phase protein sequencer using the FITC-PITC double coupling method of Muramoto *et al*. (1993).

2.2.8 Routine Insect cell culture

Sf21 insect cells were a kind gift from Dr Fritz Tiedt (University of Cape Town, SA). Cells were routinely maintained in 25 cm^2 flasks (Greiner) in TC100 medium with 5% foetal calf serum (FCS) and 1% (v/v) each of penicillin and streptomycin. The cells

were grown at 28 ºC in an incubator. Cells were seeded at 1-2 x 10^6 cells/mL, and allowed to attach to the flask for at least one hour. Thereafter, the unattached cells were discarded with the medium and 5 mL of fresh medium was added. Cells were allowed to grow until almost confluent before being dislodged mechanically and removing 4 mL of the 5mL cell suspension. Medium was made up to 5 mL again. Cells were serum starved for at least two subcultures before being used for transfection.

2.2.9 Recombinant β2 integrin proteins

2.2.9.1 Insect cell expression of β_2 integrins

2.2.9.1.1 Molecular cloning of β_2 integrin vectors for insect cell expression

The pCDM1 (CD11b) and pCDP1 (CD11c) plasmids carry both ampicillin and tetracycline resistance. The slants received from ADDGENE were streaked onto LB agar plates with the appropriate antibiotics added (12.5 μg/mL ampicillin and 15 μg/mL tetracycline). Five mL overnight cultures in LB broth (and the appropriate antibiotics) were inoculated and plasmids isolated using the QIAGEN plasmid mini kit.

PCR using vector-specific sequencing primers was used to confirm that the desired plasmids were isolated. T7 and pCDM8 primers (Table 2.1) were used to amplify DNA (as per the method in Section 2.2.3 using EconoTaq). PCR products were elecrophoresed as mentioned in Section 2.2.3.

Once the pCDM1 (CD11b) and pCDP1 (CD11c) plasmids were confirmed, the isolated plasmids were used as template DNA to produce DNA inserts for Ek/LIC vectors. Table 2.1 shows the primer sequences used for PCR amplification of these DNA inserts as per the method described for KOD HiFi DNA polymerase in Section 2.2.3. PCR products were elecrophoresed as mentioned in Section 2.2.3.

The PCR products that were in the expected size range were extracted from the agarose gel using a Wizard SV Gel and PCR cleanup system according to manufacturer's instructions. Purified PCR products (0.2 pmol in T low E buffer) were prepared for annealing into Ek/LIC vectors by polymerase activity according to manufacturer's instructions (Novagen). Briefly, PCR products were treated with T4 DNA polymerase (2 µl PCR product, 2 µl 10x T4 DNA polymerase buffer, 2 µl 25 mM dATP, 1 µl 100 mM DTT, 0.4 µl T4 DNA polymerase and 12.6 µl sterile ddH_2O) for 30 minutes at 22 ºC before inactivation at 75 ºC for 20 minutes. An Ek/LIC -galactosidase control insert was included in the kit and was treated in the same way as the CD11 PCR fragments to verify the system's annealing, transformation and transfection performance. The PCR products were used for annealing into the desired Ek/LIC vectors. This was done by incubating 2 µl of the polymerase-treated PCR reaction mixture with 1 µl of Ek/LIC vector for 5 minutes at 22ºC. One µl of 25 mM EDTA was added and mixed before further incubation for 1 hour at 22 ºC. The annealed plasmids were used to transform Novablue Gigasingle cells. The cells were thawed on ice before gently flicking twice for even resuspension. One µl of the annealing reaction was added and gently mixed with the pipette before incubating on ice for 5 minutes. Samples were incubated at 42 ºC for 30 seconds in an Eppendorf Thermomixer, before being incubated on ice for 2 minutes. SOC medium (250 µl) was added to the transformed cells before being incubated at 37 ºC at 250 rpm for 1

hour in an Eppendorf Thermomixer. Transformed cells (100 µl) were plated onto agar plates containing the appropriate antibiotics (50 µg/ml ampicillin and 30 µg/ml kanamycin) and incubated overnight at 37 ºC.

Positive transformants were then used to prepare overnight cultures for plasmid isolations using the EndoFree Plasmid Maxi kit as per manufacturer's instructions. Plasmids were digested with *Pst*I restriction enzyme to investigate the digestion profile and presence of desired DNA in the plasmids. This was done using 1 µl of *Pst*I, 3 µl of plasmid DNA, 1 µl of restriction enzyme buffer and 5 µl of sterile ddH_2O for 1 hour at 37 ºC. Plasmids and restricted plasmids were analysed by electrophoresis on a 1% agarose gel in TAE buffer. Plasmids were sent for sequencing at the DNA sequencing facility of the University of Stellenbosch to determine whether the inserted DNA was correct while the DNA was used for the transfection of insect cells.

2.2.9.1.2 Transfection of insect cells with pIEx vectors

Vectors that had been annealed and sent for sequencing were used to transfect insect cells while the vectors were being sequenced. The transfection system was first tested on a smaller scale in 24-well plates (Nunc). Insect cells that were in exponential growth phase were seeded at $2x10^4$ cells/well and left for one hour. For each well that was transfected, 0.4 µg of DNA was diluted with 20 µl of serum-free medium. Two µl of Insect GeneJuice was also diluted with 20 µl of serum-free medium. The diluted DNA was added dropwise to the diluted Insect GeneJuice transfection reagent and mixed gently. The transfection mixture was incubated for 15 minutes at room temperature, before adding 160 µl serum-free medium. The medium was aspirated

from the cells that had been incubated for an hour and the transfection mixture was added to cells. The 24-well plate was incubated in a closed container containing a damp paper towel for moisture. After 4 hours, the transfection mixture was removed from the cells and complete growth medium was added. Cells were incubated at 28°C for 48 hours prior to testing for positive transfection and harvesting cells and supernatants for analysis.

The insect cells transfected with control β-galactosidase vector were tested with X-gal solution (5-bromo-4-chloro-3-indolyl-β-D-galactopyranoside) to determine whether the transfection system was successful. The X-gal substrate is a chromogenic stain for β-galalactosidase activity. Cell supernatants of the β-galactosidase transfected cells were aspirated before adding X-gal solution (diluted to 1 mg/ml in PBS). Cells were incubated overnight and inspected visually for a colour change.

Once a functional transfection system had been confirmed, the experiment was scaled up. The procedure followed was as previously described, but conducted in 25 cm^2 flasks, seeded at $5x10^6$ cells/flask. Ten µg of DNA was used, diluted in 500 µl of serum-free medium. Fifty µl of Insect GeneJuice was used, diluted in 500 µl of serum-free medium and 2 mL of serum-free medium was added after incubation of the DNA and GeneJuice reagent. After 4 hours the transfection reagent was removed and cells incubated for 48 hours as above before cell culture supernatants and cells were collected for analysis. Cell culture supernatants were analysed on a 15% acrylamide SDS-PAGE gel to ascertain whether any protein was produced. Cell culture supernatants were also used to isolate protein using a Strep·Tactin kit (Novagen) according to manufacturer's instructions.

2.2.9.2 Production of β2 integrin αI domains

2.2.9.2.1 Expression of CD11 αI domain proteins

The DNA of both CD11 αI domain expression vectors was used to transform *E. coli* BL21(DE3) electrocompetent cells as described in Section 2.2.5. Transformed cells were plated onto LB agar plates containing 100 µg/mL ampicillin. Positive transformants were used to inoculate 5 mL overnight cultures grown at 37 ºC. After overnight incubation, the cultures were used to inoculate 1 L of LB broth containing 100 µg/mL ampicillin. The culture was grown to OD_{600nm} of 0.4 to 0.6 before being induced to express CD11b or CD11c αI domains by adding IPTG to a concentration of 1 mM. Expression was allowed to take place for four hours before harvesting the cells by centrifugation at 5 000 x g for thirty minutes at 4 ºC using a Beckman Avanti JA25 centrifuge. Harvested cells were resuspended in I domain isolation buffer (20 mM Tris/HCl pH 7.5, 10 mM EDTA) before being frozen at -80 ºC. Frozen cells were thawed the following day and sonicated with a Sonopuls Sonicator (Bandelin) for 3 minutes at 40% power. Sonicated cells were centrifuged for 30 minutes at 4500x g at 4 ºC using an Eppendorf 5804R centrifuge. The supernatant was removed and filtered with a 0.45 µm filter. The filtered supernatant was applied to a GSTrap column (Amersham Biosciences) for purification.

2.2.9.2.2 Purification of CD11 αI domains

GSTrap columns (2 mL) were washed with 5 column volumes of equilibration buffer (20 mM Tris/HCl, pH 8.0) at 2 mL/min, before the sample was injected. It has previously been shown that the interaction between GST and the glutathione-

Sepharose of the column is slow. The flow rate was decreased to 0.5 mL/min while the sample was being injected. The column was washed with 5 column volumes of equilibration buffer to remove any unbound protein. The GST-tagged bound protein was eluted with I domain elution buffer (15 mM reduced glutathione in 20 mM Tris/HCl, pH 8.0). The fractions containing the eluted protein were collected and dialysed using 3 500 Da molecular weight cutoff Snake skin pleated dialysis tubing (Pierce) against two changes of PBS for at least 12 hours to remove any glutathione. The dialysed protein was concentrated using Amicon Ultra 15 Centrifugal Filters and stored at -20 ºC.

2.2.10 Production of recombinant human CD23 proteins

Due to the different soluble forms of human CD23 found to be cleaved from mCD23, it was decided to use three CD23 constructs of different lengths for experiments. Plasmids containing the coding DNA of 16 kDa, 25 kDa and 33 kDa CD23 (without a purification tag) had previously been designed and used in the Fc Receptor Laboratory at NMMU. The 16 kDa (Boukes, 2005), 25 kDa (Daniels, 2003) and 33 kDa (Askew, 2006) constructs were used to express, refold and purify recombinant protein. The 16, 25, and 33 kDa sCD23 proteins are herein after referred to as derCD23, CD23M150, and CD23M79, respectively. The constructs that were decided best for this work correspond to the 16 kDa, 25 kDa and 33 kDa biological proteins which are cleaved from mCD23 (Figure 2.2).

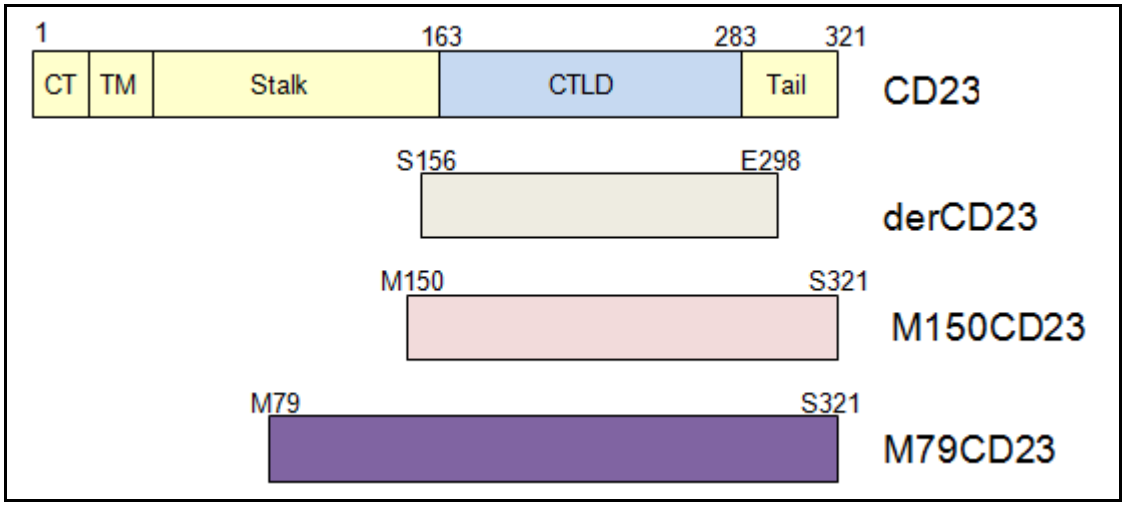

Figure 2.2: Schematic of CD23 protein variants. The CD23 variants encode M79CD23$^{79 - 321}$, M150CD23$^{150 - 321}$ and derCD23$^{156 - 298}$. CT, N-terminal cytoplasmic domain; TM, transmembrane domain; Stalk, α-helical coiled coil; CTLD, C-type lectin-like domain; Tail, C-terminal tail region.

2.2.10. 1 Preparative expression of CD23 proteins

A single colony of transformed *E. coli* was used to inoculate cultures of LB medium containing ampicillin (100 µg/mL) in the case of clones p23aCD23M150 and p23aCD23M79 or kanamycin (15 µg/mL) with the p28bderCD23 clone. This was grown at 37 ºC and 160 rpm until the OD_{600nm} reached 0.7 – 0.9. Two cultures of 50 ml LB broth (with the appropriate antibiotic) were then inoculated with 100 µl of the starter culture and grown overnight at 37 ºC and 160 rpm. The cells were harvested by centrifugation at 4000 x g for ten minutes at 4 ºC. The cells were gently resuspended in 50 ml fresh LB. Two 1 L cultures were inoculated with 5 ml of the resuspended cells and the appropriate antibiotic. These cultures were grown at 37 ºC and 160 rpm until an OD_{600nm} of 0.7 – 0.9 was reached, keeping 0.5 ml aliquots of cells at this time point. The expression of protein was induced by adding IPTG to a concentration of 1 mM and the OD_{600nm} was monitored every hour for the induction time chosen. Aliquots of cells were kept from each of these time points, for analysis

using sodium dodecyl sulfate polyacrylamide gel electrophoresis (SDS-PAGE). The cells were harvested by centrifugation at 5 000 x g for thirty minutes at 4 ºC using a Beckman Avanti JA25 centrifuge. The cells were resuspended in 10 ml of sonication buffer (50 mM Tris-HCl, pH 7.8, containing 0.3 M NaCl, 0.2 % NaN_3) and stored at – 80 ºC.

2.2.10.2 Inclusion body isolation

The cells harvested from expressions were thawed and sonication buffer was added if necessary to dilute. Lysozyme (0.01g) was added and incubated at room temperature for 30 minutes, mixing end-over-end. The cells were chilled and transferred to a prechilled Rosette vial, kept on ice. The cells were sonicated for six bursts of three minutes, pulsing at 50% duty cycle and 40% power with a Bandelin Sonopuls HD2200 sonicator. The cells were centrifuged at 32 795 x g for 40 minutes at 4 ºC using a Beckman Avanti JA25 centrifuge. The pellet was resuspended in approximately 15 ml of inclusion body wash buffer (50 mM Tris-HCl, pH 7.8, containing 0.3 M NaCl, 0.5 % N, N–dimethyldodecylamine N-oxide (LDAO), 0.2 % NaN_3). A Potter-Elvejham homogeniser was used to resuspend the inclusion bodies, with 5 – 6 strokes on ice. The washes were pooled and centrifuged as before, keeping an aliquot of the wash supernatant for analysis. The inclusion bodies were continuously washed until most of the *E. coli* proteins were removed. The washed inclusion bodies were resuspended in 4-5 ml of sonication buffer and stored at 4 ºC.

2.2.10.3 Refolding using rapid dilution technique

A protein stock was prepared from the IB preparation by diluting 1:2 with inclusion body dissolving buffer (20 mM Tris-HCl, pH 8.0, 6 M guanidinium hydrochloride). β-mercaptoethanol was added to a final concentration of 100 mM. The protein stock was added to the refolding buffer (1.5 M arginine, 100 mM Tris, 150 mM NaCl and 10 mM $CaCl_2$ to which GSH and GSSG are added to final concentrations of 5 and 0.5 mM, respectively) by very slow dropwise additions at 4 ºC, with stirring of the refolding buffer, such that the protein stock is diluted 1:100 in the refolding buffer by volume (i.e. a 5 mL protein stock is added to 500 mL refolding buffer). The redox potential was monitored (Section 2.2.10.4) until it was below 1 mM (approximately 70-80 hours), with continuous stirring of the refolding mixture at 4 ºC. The refolding buffer was removed by overnight dialysis at 4 °C against phosphate buffered saline [PBS (8g of NaCl, 0.2g of KCl, 1.44g of Na_2HPO_4 and 0.24g of KH_2PO_4 / L, pH 7.4)]. The protein solution was concentrated using an Amicon stirred ultrafiltration cell (Millipore) with a Millipore 5 kDa molecular weight limit regenerated cellulose ultrafiltration disc.

2.2.10.4 Measurement of redox potential

Ellman's reagent was first used for the estimation of free thiol groups in 1959. This method is based on the reaction of the thiol with 5, 5'-dithiobis (2-nitrobenzoic acid) (DTNB) to give the mixed disulphide and 2-nitro-5-thiobenzoic acid (TNB) that can be quantified by absorbance at 412 nm (Aitken and Learmonth, 1996).

The redox potential of the refolding buffer was monitored using Ellman's reagent. In this method, 25 µl of 1M Tris (pH 8) was mixed with 2 µl 100 mM DTNB (in ethanol) and 1-5 µl of the refolding buffer and made up to 500 µl with ddH_2O. The optical density was then measured at 412 nm using an Ultrospec 2000 (Pharmacia Biotech). The optical density obtained is then used to calculate the redox potential, using a molar extinction coefficient of 13 600 $cm^{-1}M^{-1}$ for TNB (Ellman, 1959).

2.2.10.5 Purification of recombinant human CD23

The concentrated protein solutions after refolding were passed through a Superdex 75 (26/60) gel filtration chromatography column using an ÄKTA FPLC (Amersham Pharmacia Biotech). This was done by injecting a 2 mL sample of the protein with a flow rate of 2 mL per minute with PBS pH 7.4 as eluent. The fractions collected were 5 mL in volume and the relevant peaks were pooled together and concentrated using ultrafiltration as described in 2.2.10.3. The protein level was determined using the Bradford assay.

2.2.10.6 Endotoxin determination

One of the toxins produced by *E. coli* is an endotoxin called lipopolysaccharide (LPS). This endotoxin can have a dramatic effect on human cells, resulting in the activation of many signalling pathways and inflammatory cascades. It was therefore important to determine what the level of LPS in purified protein samples were. The most specific and sensitive method available to detect LPS is the Limulus amebocyte lysate (LAL) test (Petsch *et al.*, 1998). This test makes use of the blood corpuscle of

Limulus horseshoe crabs and is based on the formation of a firm gel after the reaction of endotoxin with various endotoxin-sensitive clotting factors in the LAL enzymatic cascade (Haishima *et al.*, 2003). The endotoxin concentration is proportional to the gel clotting reaction, which allows for detection and quantification of the endotoxin. A synthetic substrate has been added to the LAL reagent which releases a chromophore at the end of the endotoxin-induced coagulation cascade, allowing for the colourimetric determination of the amount of endotoxin present.

The Endosafe LAL kit was used to determine the concentration of LPS present in samples. It is a simple end point chromogenic test where endotoxin levels can be quantitatively determined against a standard curve. LPS levels in purified protein were determined as endotoxin units (EU) as per manufacturer instructions. It has been reported that 1 EU is the equivalent of 1 ng of LPS (Webb *et al*, 1998).

2.2.11 Binding studies

It is well known that β_2 integrins have many ligands that they bind to, as described in Chapter 1. Many of these binding relationships have been investigated and characterised and the αI domains of CD11/CD18 integrins contain the recognition sites for most ligands of leukocyte integrins (Ihanas *et al.*, 2003). However while there is data available proving that CD11b and CD11c bind to CD23 (Lecoanet-Henchoz *et al.*, 1995), there is no data available to show that the αI domains are involved in this binding. We hypothesized that it is therefore very likely that this will be the site for binding of CD23 molecules and accordingly investigated this using CD11 expressing cells as well as with purified αI domain proteins.

2.2.11.1 Binding of CD11-upregulated cells to recombinant human soluble CD23

Carboxyfluorescein diacetate, succinimidyl ester (CFSE) is a dye that was used to label human cells for the binding experiments. This dye diffuses passively into cells. It is colourless and non-fluorescent until intracellular esterases cleave its acetate groups to yield highly fluorescent carboxyfluorescein succinimidyl ester. This ester group reacts with intracellular amines, resulting in fluorescent conjugates. Any excess unconjugated reagents and by-products passively diffuse into the extracellular medium and are washed away (Lyons and Parish, 1994). This dye is commonly used to track the proliferation of cells over several days since the amount of dye each cell takes up is divided exactly equally between its two daughter cells when it divides and the same occurs with the dye in the daughter cells in subsequent cell divisions. However, CFSE labels cells regardless of what stage of the cell cycle they are in (Asquith *et al.*, 2006). Due to the dye's ability to label cells so efficiently and since the experiment is conducted in less than two hours, therefore allowing very little time for cell division to occur and therefore skew results, this dye was used to quantify the differences in cell binding to CD23 proteins by measuring CFSE fluorescence.

Three human cell lines were used to investigate whether CD11-upregulated cells would bind to the three different recombinant CD23 proteins. This was done by differentiating HL60, U937 and THP-1 cells. The methods used to culture and differentiate these cells will be discussed in Chapter 4. For the binding assay, 1 µg/mL of each recombinant CD23 protein in PBS as well as the same concentration of fibrinogen as a positive control was used to coat a black 96-well plate overnight at 4 ºC. Negative control wells contained PBS only. Plates were washed three times with PBS, before being blocked for 1 hour at room temperature with 2% (w/v) BSA.

PBS was used to wash plates three times again. While the plate was being blocked, differentiated cells were stained with CFSE (Molecular Probes) according to manufacturer's instructions. Briefly, cells were resuspended in PBS/0.1% BSA at $1x10^6$ cells/mL. Two µl of a 5 mM CFSE stock was added per mL of cells to give a 10 µM final concentration. Cells were incubated in the dark for 10 minutes at 37 ºC before the reaction was stopped by adding 5 volumes of ice cold cell culture medium to the cells. Cells were further incubated on ice for 5 minutes before being centrifuged at 1000 rpm for 5 minutes using an Eppendorf centrifuge. Cells were washed with PBS and centrifuged twice before being resuspended in binding buffer [Hanks buffered saline solution (HBSS), 10 mM 4-(2-hydroxyethyl)-1-piperazineethanesulfonic acid (HEPES), 1 mM $CaCl_2$, pH 7.3]. Once the cells were in binding buffer, 100 µl of cells was aliquoted into each well of a CD23-coated 96-well plate and the plate was incubated in the dark for one hour. The cells were gently removed and washed twice with PBS to remove any unbound cells. One hundred µl of PBS was added to each well and the fluorescence produced by bound cells was measured using a Fluoroscan Ascent FL microtiter plate reader (Thermo Labsystems) with the excitation wavelength set at 488 nm and the emission wavelength set at 518 nm.

To investigate whether this binding was due to CD11/CD18 integrins, a blocking antibody was preincubated with differentiated cells for 30 minutes at 37 ºC at a concentration of 5 µg/mL before being washed and used in the above experiment. The blocking antibody used was CBRM1/5 monoclonal antibody and reacts with an activation specific epitope of human CD11b. The epitope recognised by this mAb is the αI domain of CD11b. CBRM1/5 blocks CD11b-dependent adhesion to fibrinogen and ICAM1 (Diamond and Springer, 1993; Oxvig *et al*., 1999). Data was analysed

with a one way ANOVA with Tukeys Multiple Comparison post-test using Graphpad Prism 5 software.

2.2.11.2 ELISA of CD11 αI domain binding to recombinant human sCD23

The ability of CD11b and CD11c αI domains to bind recombinant human CD23 was tested using an enzyme linked immunosorbent assay (ELISA). Fibrinogen was used as a positive control, since it is known that it binds CD11b and CD11c at their αI domains (Choi and Nham, 2002). CD23 proteins and fibrinogen were used to coat a 96-well plate (50 µl of a 20 µg/mL concentration in PBS). Plates were incubated overnight at 4 ºC. Plates were washed three times with PBS-Tween (0.05%) (PBS-T) before being blocked with 100 µl 1% salmon testis DNA in PBS for one hour at room temperature. Plates were washed three times with PBS-T, before varying concentrations of CD11b αI domain or CD11c αI domain (0 - 1000 µg/mL) were added in 50 µl aliquots in binding buffer and incubated for one hour at room temperature. PBS-T was used to wash the plates three times before adding 100 µl of a 1:10 000 dilution of a polyclonal goat anti-schistosomal GST antibody diluted in PBS-T. The plate was incubated for 1 hour before washing three times with PBS-T. An anti-goat IgG secondary antibody conjugated to peroxidase was used to detect the primary antibody at a concentration of 1:20 000 in PBS-T for one hour at room temperature. This was washed thrice with PBS-T before adding 100 µl of 3,3',5,5'-tetramethylbenzidine (TMB) substrate. Once a blue colour had developed, the reaction was stopped using 50 µl of a 1 N solution of sulphuric acid before reading at 450 nm using a Multiscan MS microplate reader (Labsytsems). The amount of binding was plotted using GraphPad Prism software and binding curves were fitted to the data using a one-site specific binding nonlinear fit model.

2.2.11.3 Surface plasmon resonance spectroscopy

Surface plasmon resonance (SPR) spectroscopy was used to measure binding between CD11b and CD11c αI domains and sCD23 at the Centre for Systems Biology at Edinburgh. All experiments were performed at 25°C on a Biacore T100 instrument. Biotinylation of proteins was achieved by mixing with 6-(biotinamidocaproylamido) caproic acid succinamide ester at a molar ratio of 1:13, followed by gel filtration to remove excess biotin. A specific binding surface was prepared by coupling biotinylated CD23 fragments (CD23M79 and derCD23) to a stable streptavidin capture system (SA chip). Coupling densities of 110 and 56 resonance units (RUs) were used for CD23M79 and derCD23, respectively. CD11c αI domain was injected over the sensor chip at 10 µl/min with a 270 second association phase followed by a 240 second dissociation phase using HBS [10 mM Hepes, pH 7.4, 150 mM NaCl, and 0.05% (v/v) Tween 20] containing 1 mM $MgCl_2$ as running buffer. When necessary, regeneration of the sensor surface was performed using 2 pulses of HBS containing 10 mM EDTA (20 s per pulse). Injections included a zero concentration (i.e. buffer only) and duplicates of specific concentrations of CD11c. Standard double reference data subtraction methods were used before analysis of kinetic binding. Curve fit and other data analyses were performed using BiaEvaluation Version 2.02 software (Biacore).

2.3. Results and discussion

2.3.1 Production of β2 integrins CD11b and CD11c

2.3.1.1 Molecular cloning of β2 integrin vectors for insect cell expression

Full-length β_2 integrins have only successfully been expressed by transfecting human cells with both the α subunit and the common β subunit (CD18) (Larson *et al.,* 1990). In this study, the InsectDirect expression system was investigated as an alternative method to express only the α subunits of CD11b and CD11c.

The pCDM1 and pCDP1 plasmids received from ADDGENE (USA) were isolated from the *E. coli* MC106/P3 cells as shown in Figure 2.3. The plasmids show two bands of DNA, one above the marker range and one that is approximately 6000 bp in size (lane 2 and 3). PCR was used to confirm that the plasmids contained inserted CD11b and CD11c DNA. The T7 forward primer and pCDM8 reverse primer were used and the PCR reaction produced the expected bands of approximately 4200 bp and 4500 bp for CD11b and CD11c, respectively (Figure 2.4).

The pCDM1 and pCDP1 plasmids were used to amplify the α subunits with Ek/LIC vector-compatible overhangs for annealing into the pIEx-10 vector. Figure 2.5 shows the agarose gel of these PCR amplicons at two different annealing temperatures (Lane 2 – Lane 5). The AlphaImager 3400 software used to analyse the bands in the agarose gels measured the bands at approximately 3400 bp, which was the expected size of the desired fragment. Smaller bands were also produced, possibly due to non-specific annealing of the primers to template DNA or due to slippage of the polymerase. The 3.4 kb bands were purified and used to anneal into the pIEx-10 vector.

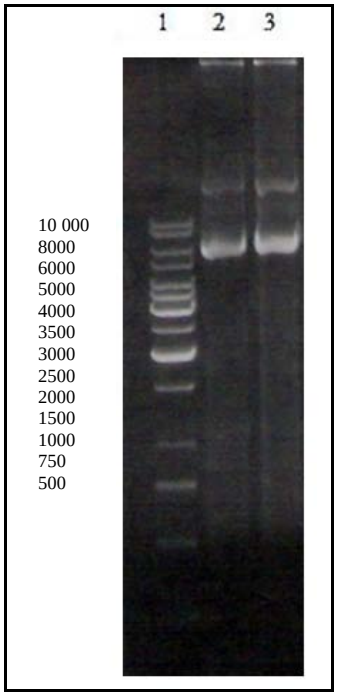

Figure 2.3: Agarose gel analysis of pCDM1 (CD11b) and pCDP1 (CD11c) plasmid isolations. Lane 1, 1kb DNA ladder; Lane 2, pCDM1 (CD11b) plasmid isolation; Lane 3pCDP1 (CD11c) plasmid isolation.

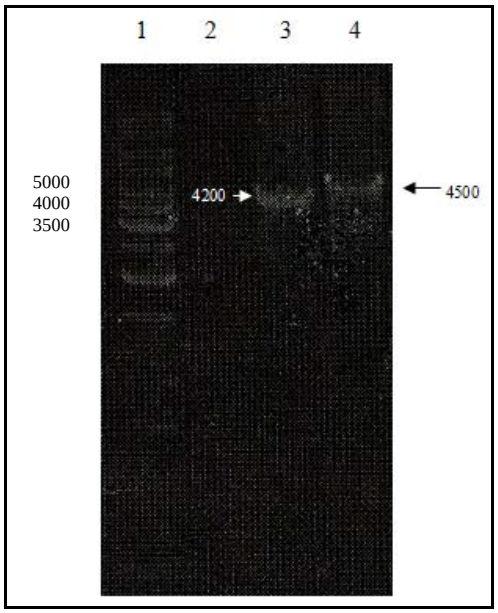

Figure 2.4: Agarose gel analysis of PCR amplification of pCDM1 (CD11b) and pCDP1 (CD11c) plasmid isolations using the T7 forward primer and pCDM8 reverse primer. Lane 1, 1kb DNA ladder; Lane 3, pCDM1 amplification, Lane 4, pCDP1 amplification.

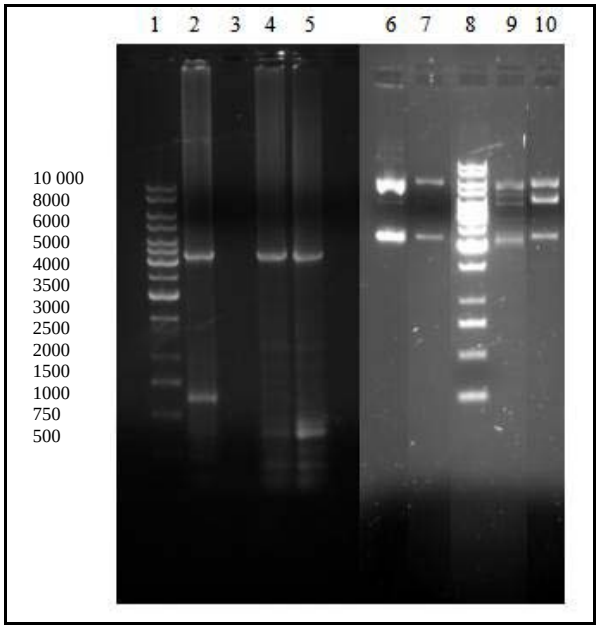

Figure 2.5: Agarose gel analysis of PCR amplification of CD11b and CD11c using LIC primers and pIEx plasmid isolations and *PstI* digestion. Lane 1, 1 kb DNA ladder; Lane 2, CD11b annealing at 55 ºC; Lane 3, CD11b annealing at 60 ºC; Lane 4, CD11c annealing at 55 ºC; Lane 5, CD11c annealing at 60 ºC. Lane 6, undigested CD11b pIEx vector; Lane 7, undigested CD11c pIEx vector, Lane 8, 1 kb DNA ladder; Lane 9, *Pst*I digested CD11b pIEx vector; Lane 10, *PstI* digested CD11c pIEx vector.

Once annealed, the plasmids were used to transform Novablue Gigasingles and plasmid isolations were performed on positive colonies. These plasmids were digested with *Pst*I (Figure 2.5 Lane 6 – Lane 10).

As can be seen in Figure 2.5, two bands are visible for the undigested plasmids isolated, one of approximately 6500 to 6600 bp and one of approximately 2900 bp. These bands are the open circle plasmid DNA and the supercoiled plasmid DNA. The expected size of ligated pIEx vectors is approximately 7000 bp, while empty vector is expected to be 3801 bp. The digestion of the CD11b pIEx vector should yield two bands of 4681 and 2357 bp. The gel shows several bands, approximately 6500, 5400, 4700, 3700 and 2600 bp in size. The largest band is the open circle plasmid DNA as seen in the plasmid isolation. The middle (4700 bp) band is the expected band of

insert DNA, while the lower band (2600 bp) is possibly the supercoiled plasmid DNA (also seen in the plasmid isolation). The other bands could be due to partial digestion of the plasmid DNA, as it appears that *PstI* did not cleave the plasmid DNA entirely, or they could be digested fragments that could not be separated from the supercoiled DNA. The digestion of CD11c pIEx vector should yield three bands of approximately 4700, 1500 and 845 bp. The digestion profile shows three bands of approximately 6300, 4900 and 2800 bp in size. The top band is open circle plasmid DNA and the bottom band is the supercoiled plasmid DNA, both observed in the plasmid isolation. The band that is approximately 4900 bp in size appears to be the expected band. However, there should be two smaller bands of 1500 and 845 bp in size. These are perhaps not visible due to incomplete digestion by *PstI*.

Since the restriction digestion of these plasmids did not yield results as expected, the plasmids were sent for sequencing. While awaiting the sequencing results, the plasmid DNA was used to test the InsectDirect system.

2.3.1.2 Transfection of insect cells with pIEx vectors

Insect cells in exponential growth phase were transfected with CD11b pIEx, CD11c pIEx and β-galactosidase pIEx control vector as described in section 2.2.9.1.2. β-galactosidase was used as described to test whether the transfection system was functioning properly. Figure 2.6 shows untransfected insect cells compared with cells transfected with the positive control vector. The formation of a blue colour indicates a positive result and therefore a properly functioning transfection and expression of β-galactosidase.

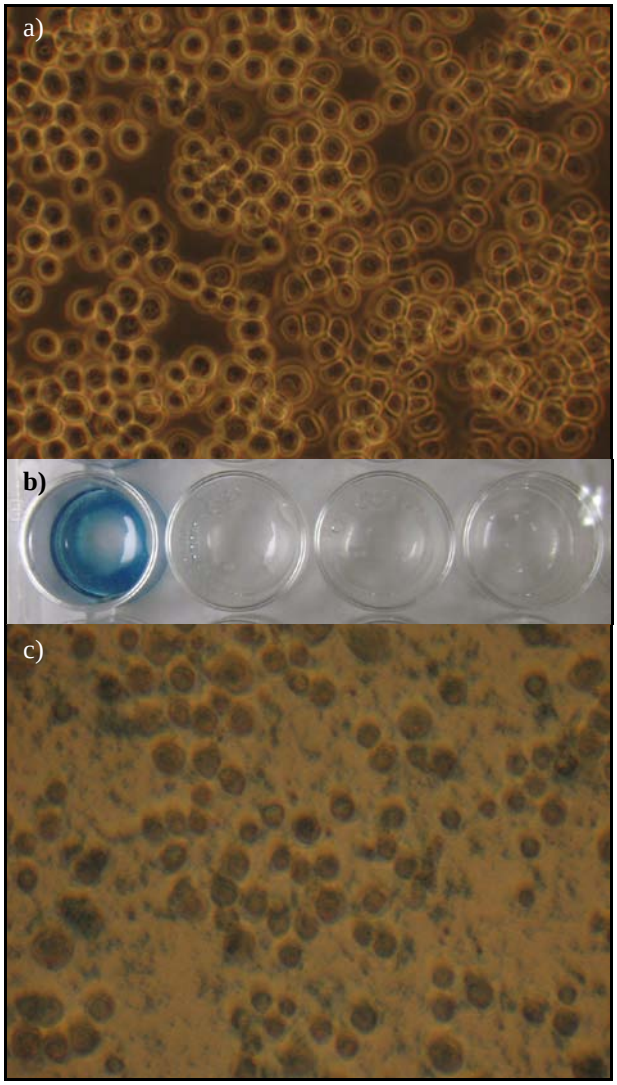

Figure 2.6: Untransfected *Sf21* insect cells and cells transfected with the β-galactosidase encoding positive control vector. a) Control untransfected cells (40x mag); b) test transfection in 24-well plate, where first well is transfected with positive control DNA while the other three wells contain untransfected cells; c) cells transfected with positive control (40x mag).

This experiment was scaled-up to 25 cm^2 flasks and *Sf21* insect cells transfected with CD11b- and CD11c-encoding pIEx DNA. Cell culture supernatant was isolated and applied to a Streptactin column to isolate any CD11b or CD11c that had been produced by the cells. However, no protein was isolated from the cell culture supernatants using these columns and SDS-PAGE gels confirmed that no CD11b or CD11c proteins were produced prior or subsequent to Streptactin column isolation

(data not shown). The DNA sequences of the CD11b and CD11c pIEx vectors verified the restriction digestion data, since it was shown that the vectors contained incomplete CD11 sequences (data not shown). Due to the DNA sequence results indicating that the vectors were not viable to use for further transfections and since the CD11b and CD11c αI domain vectors were donated to our laboratory, it was decided to continue the investigation of binding to CD23 proteins with the I domain proteins.

2.3.2 Production of purified recombinant proteins

2.3.2.1 Expression and purification of CD11 αI domain proteins

Vectors for CD11b and CD11c αI domains were used to transform *E. coli* BL21(DE3) cells. These transformed cells were used to express the recombinant αI domain proteins. Figure 2.7 shows the SDS-PAGE gel of the expression of CD11b and CD11c αI domains. In this figure, there is clearly upregulation of a band of protein at approximately 50 kDa. This band contains the GST-tagged αI domain proteins. The αI domain proteins were then extracted from the bacteria by sonication and concentrated before isolation and purification using a GSTrap column.

Isolated GST-tagged αI domain proteins were injected onto a GSTrap column for purification. Figure 2.8 shows the elution profiles of CD11b and CD11c αI domains. The fall-through peak (first peak) contains contaminating *E. coli* proteins. The contaminating proteins were washed off the column with equilibration buffer and the second peak which contains the GST-tagged αI domain protein was eluted using 10 mM GSH. The corresponding tubes were collected, pooled, dialysed against PBS and analysed with SDS-PAGE to check their purity (inset of Figure 2.8 A and B). On

average, between 4 and 7 mg of pure protein was isolated from 1L of bacterial culture.

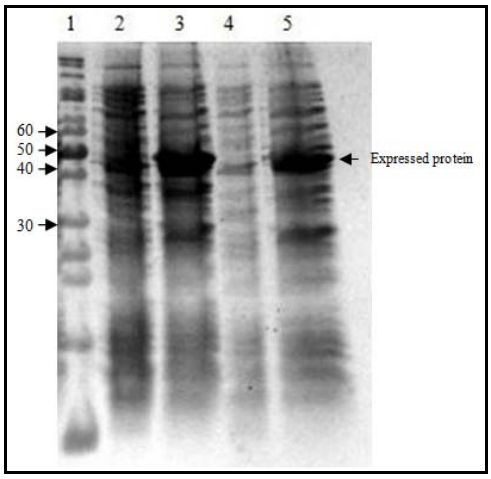

Figure 2.7: SDS-PAGE gel analysis of expression of CD11b and CD11c αI domain proteins (total protein extracts). Lane 1, Molecular weight marker (kDa on left); Lane 2, CD11b pre-induction; Lane 3, CD11b post-induction; Lane 4, CD11c pre-induction; Lane 5, CD11c post-induction. An arrow indicates the bands of interest.

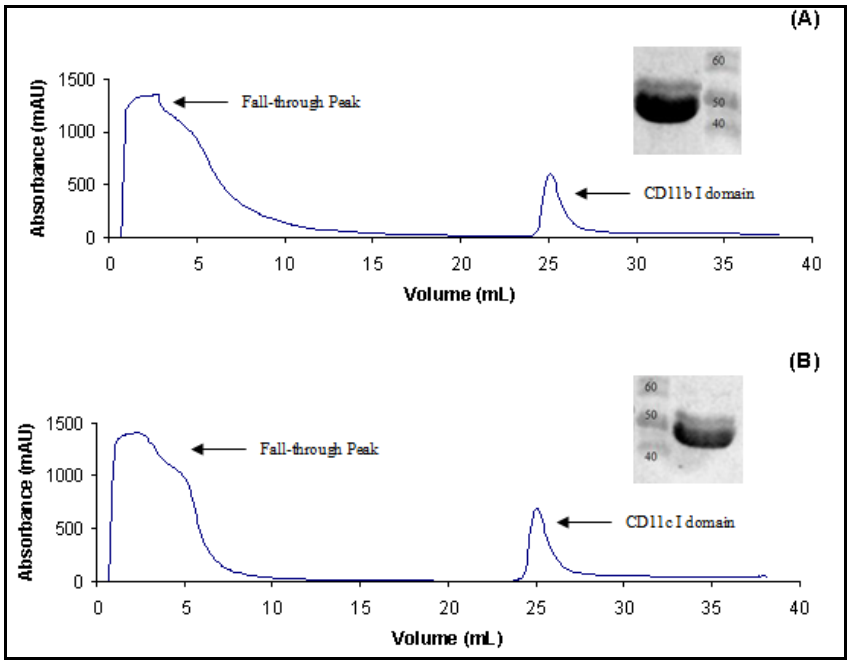

Figure 2.8: Chromatogram of CD11 αI domain protein purification using a glutathione sepharose column. A) CD11b αI domain and B) CD11c αI domain. The columns were equilibrated with 5

column volumes of equilibration buffer at 2 mL/minute, before adding the protein sample at 0.5 mL/minute. The column was washed with 5 column volumes of equilibration buffer, before the GST-tagged protein was eluted with elution buffer at 2 mL/minute. Each chromatogram has an SDS-PAGE inset showing the purified band of protein isolated.

2.3.2.2 Purification of CD23 proteins

2.3.2.2.1 CD23 expression, refolding and purification

All three clones of CD23 protein were expressed using the same method (Daniels *et al.*, 2005). After the induction of protein expression, the *E. coli* were incubated for four hours before being harvested. Figure 2.9 shows the expression, IB washing and washed IB isolation of CD23M150. The expression and purification methods for the CD23 proteins were identical and therefore the SDS-PAGE gel patterns look the same, except for the size at which the protein is expressed and purified. Therefore this figure is representative of the other two proteins. In Figure 2.9 it is clear that the proteins expression is strongly upregulated after four hours (as can be seen by the darker bands at the 25 kDa molecular weight marker in Lanes 2-5) and that the majority of IB protein is the desired 25 kDa CD23 protein, after washing (Lane 13).

Once IB's of each protein were washed, they were solubilised, refolded and concentrated for further purification by chromatography.

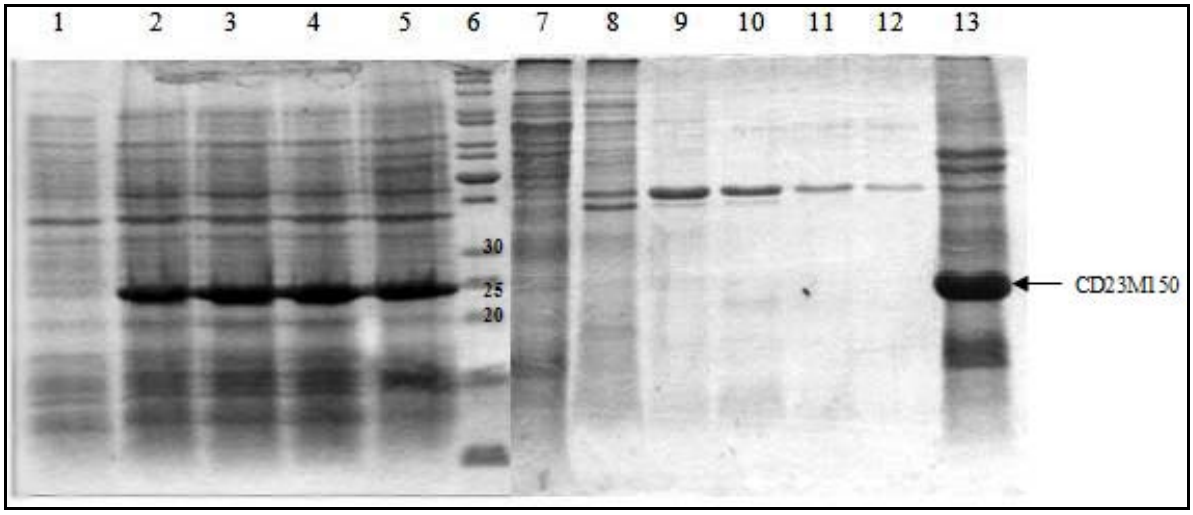

Figure 2.9: SDS-PAGE gel (15% acrylamide) analysis of CD23M150 expression by *E. coli* BL21 (DE3) cells and isolation of inclusion bodies. Lane 1, pre-induction; Lane 2, 1 hour post-induction; Lane 3, 2 hours post-induction; Lane 4, 3 hours post-induction; Lane 5, 4 hours post-induction; Lane 6, peqGOLD protein marker II; Lanes 7 to 12, supernatants from inclusion body washes; Lane 13, purified inclusion bodies. Arrow indicates CD23M150.

2.3.2.2.2 Superdex gel filtration of CD23 proteins

The three FPLC elution profiles (Figure 2.10 A to C) show the purification of the three CD23 proteins using Superdex 75 gel filtration chromatography. The smaller of the three proteins, derCD23 [Figure 2.10 (A)] is eluted from the column later, with its peak at 198 mL. Figure 2.10 (B) shows the CD23M150 protein that is eluted at approximately 170 mL. The largest of the proteins, CD23M79 is eluted first at 153 mL [Figure 2.10(C)]. All profiles also show the elution of the redox couple from the refolding buffer.

The appropriate collection tubes were pooled together and the purified proteins were concentrated before being checked for purity on a SDS-PAGE gel (Figure 2.11). This method of protein purification yielded approximately 1 mg of pure protein per 2L of

E. coli culture. Sequence alignments of the recombinant sCD23 proteins compared to human CD23 can be seen in Figure A.4 in Appendix A.

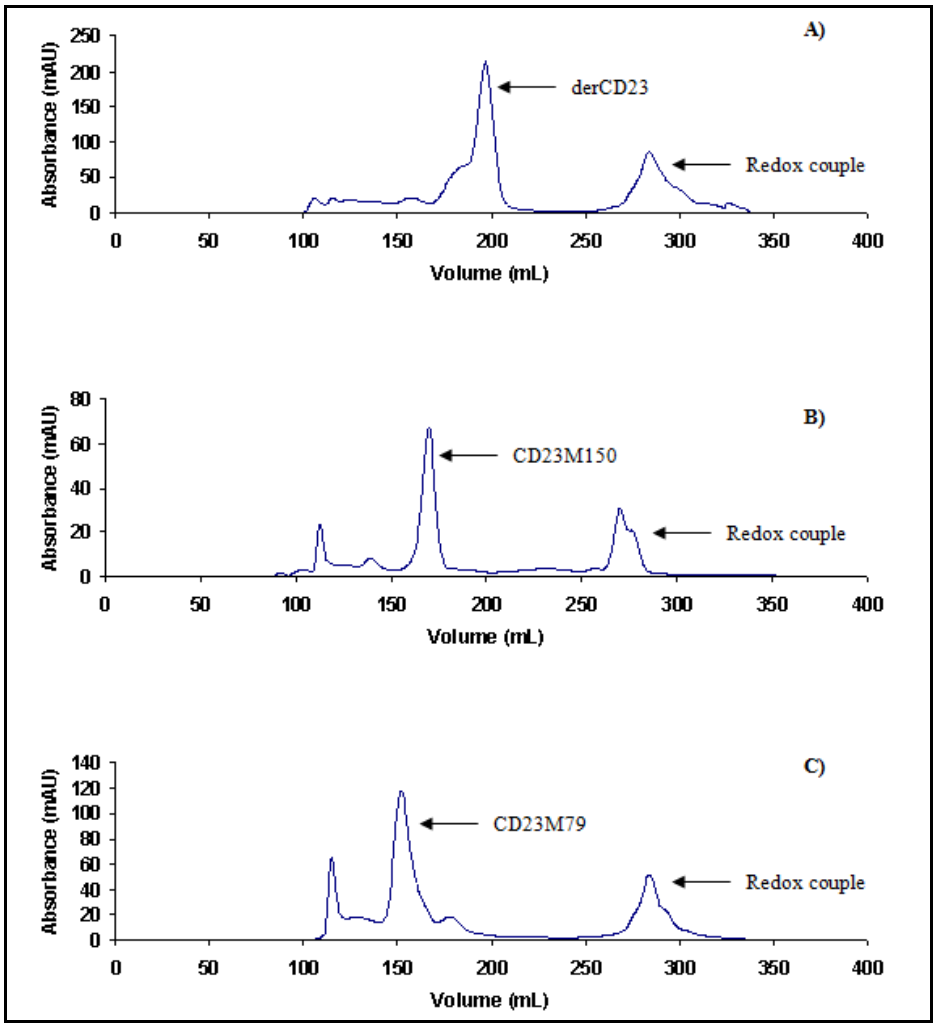

Figure 2.10: Chromatograms obtained from gel filtration chromatography of recombinant CD23. A) derCD23; B) CD23M150 and C) CD23M79. Gel filtration was performed using a Superdex 75 26/60 column with PBS (pH 7.4) as developing buffer at a flow rate of 2 mL/minute.

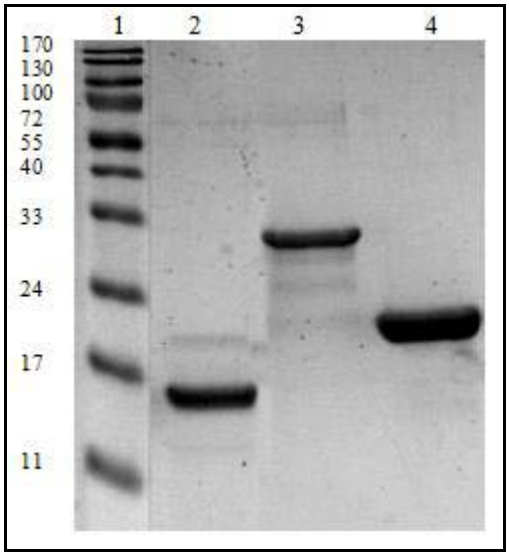

Figure 2.11: SDS-PAGE gel (15% acrylamide) analysis of purified recombinant CD23 proteins. Lane 1, Sigma LMW marker; Lane 2, derCD23; Lane 3, CD23M79; Lane 4, CD23M150.

2.3.2.2.3 Endotoxin determination

As the recombinant proteins were going to be used in cell culture experiments, it was vital to ensure that very low levels of endotoxin were present. The LAL test kit was used for these determinations. The standard curve constructed using control standard endotoxin supplied with the assay kit can be seen in Figure A.5 in Appendix A.

When producing recombinant proteins using *E. coli*, there is always the possibility that the bacterium will produce a large amount of endotoxin which will contaminate the recombinant protein. This becomes a problem when the recombinant protein is to be used in cell culture experiments, as the endotoxin can affect many cell types [for example, it can increase the production of inflammatory cytokines and, more specifically to this study, it is known to bind β_2 integrins (Wright *et al.*, 1989)], resulting in false results. Table 2.2 shows the levels of endotoxin present in the recombinant CD23 proteins purified, as well as the maximum amount of LPS added

to cell culture experiments during an experiment. It is clear from this table that very low levels of LPS were added to the cell culture experiments; although an accepted level of 1 ng/ml of LPS for immunological studies has been previously published (Pollock *et al.*, 2003). We discovered that by using high quality water during our expression and purification of recombinant proteins, we managed to decrease the levels of endotoxin present in the purified proteins. This eliminated the need to remove the endotoxins using Detoxi-gel columns (Pierce) as has been done previously in our laboratory. Use of Detoxi-gel columns usually resulted in a substantial loss of recombinant protein (sometimes up to half the protein), and the elimination of this step is therefore very useful. The purified, recombinant CD23 proteins were filter-sterilised and stored in aliquots at -20 ºC until required.

Table 2.2: Endotoxin levels in recombinant CD23 proteins.

Protein	EU/ml	ng LPS/ml	ng LPS/mg protein	LPS added to cell culture (ng)
derCD23	1.34	0.13	0.12	0.012
CD23M150	3.60	0.36	0.36	0.036
CD23M79	2.95	0.30	0.06	0.006

2.3.3 Binding studies

2.3.3.1 Binding of CD11-upregulated cells to recombinant human soluble CD23

CD11/CD18 was upregulated on three cell lines by differentiation with vitamin D_3. The ability of these cells to bind to recombinant human soluble CD23 of different lengths was determined. Figure 2.12 shows the binding of HL60, THP1 and U937 cells to fibrinogen and the three constructs of CD23 compared to the BSA control. Data is expressed as a percentage of the control, with the control set to 100%.

Graphpad Prism software was used for statistical analysis. The figure shows that differentiated HL60 cells are able to bind to fibrinogen as well as all three CD23 proteins in a statistically significant manner. While the CD23M150 and CD23M79 show similar binding levels in all experiments, the derCD23 shows a lower level of binding, although still significantly higher than the control. The THP1 cell line, although differentiated (and showing upregulation of CD11b) was not able to significantly bind fibrinogen or CD23 as seen in Figure 2.12. Although a slightly higher percentage of cells binding to the ligands was observed, no significant differences in the binding of the cells to fibrinogen or CD23 was seen. As was seen with the HL60 cells, U937 cells bound the CD23 proteins significantly, with the CD23M150 and CD23M79 having similar levels of binding and the derCD23 having lower, but still significant binding to the cells when compared with the control.

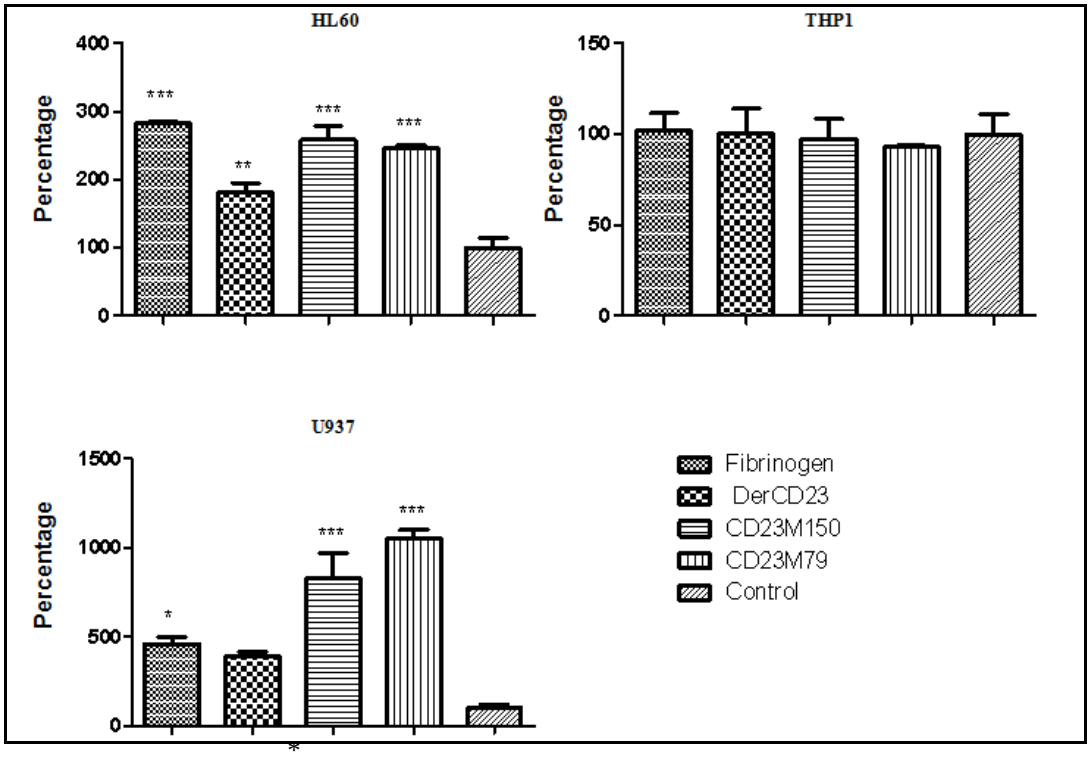

Figure 2.12: Binding of differentiated HL60, THP1 and U937 cells to CD23 and fibrinogen. Differentiated cells were labelled with CFSE before being incubated for 1 hour in a 96-well plate, precoated with CD23 proteins, fibrinogen or BSA as control. Unbound cells were removed with

washing and the fluorescence of remaining cells measured on a fluorimeter. Each graph is a representative graph of three experiments done in triplicate, showing similar results. Error bars represent SEM values. Asterisks represent significant difference compared to BSA where (*) represents $P<0.05$, (**) $P<0.005$ and (***) $P<0.0005$.

The cell binding studies were repeated in the presence of a blocking antibody (CBRM1/5) to prove that differentiated cells bound recombinant sCD23 proteins through interaction with CD11b. CBRM1/5 blocks CD11b-dependent adhesion to fibrinogen and ICAM1 (Diamond and Springer, 1993; Oxvig *et al.*1999).

Figure 2.13 shows the binding experiments repeated in the same manner, but with the CBRM1/5 blocking antibody preincubated with the cells for each ligand in addition to the unblocked cells. The HL60 graph shows that the CD11b αI domain blocking antibody is able to inhibit binding of the cells to the CD23 proteins, although the antibody does not completely inhibit binding. The antibody also appeared to decrease the level of binding of THP1 cells to the three CD23 proteins, but as with the previous THP1 binding studies, no significant difference was seen. The same experiment with U937 cells shows that although the binding of the proteins is blocked by the addition of the antibody (significantly in the case of the CD23M150 and CD23M79) it is not completely blocked, indicating that the cells are possibly binding with another ligand in addition to CD11b.

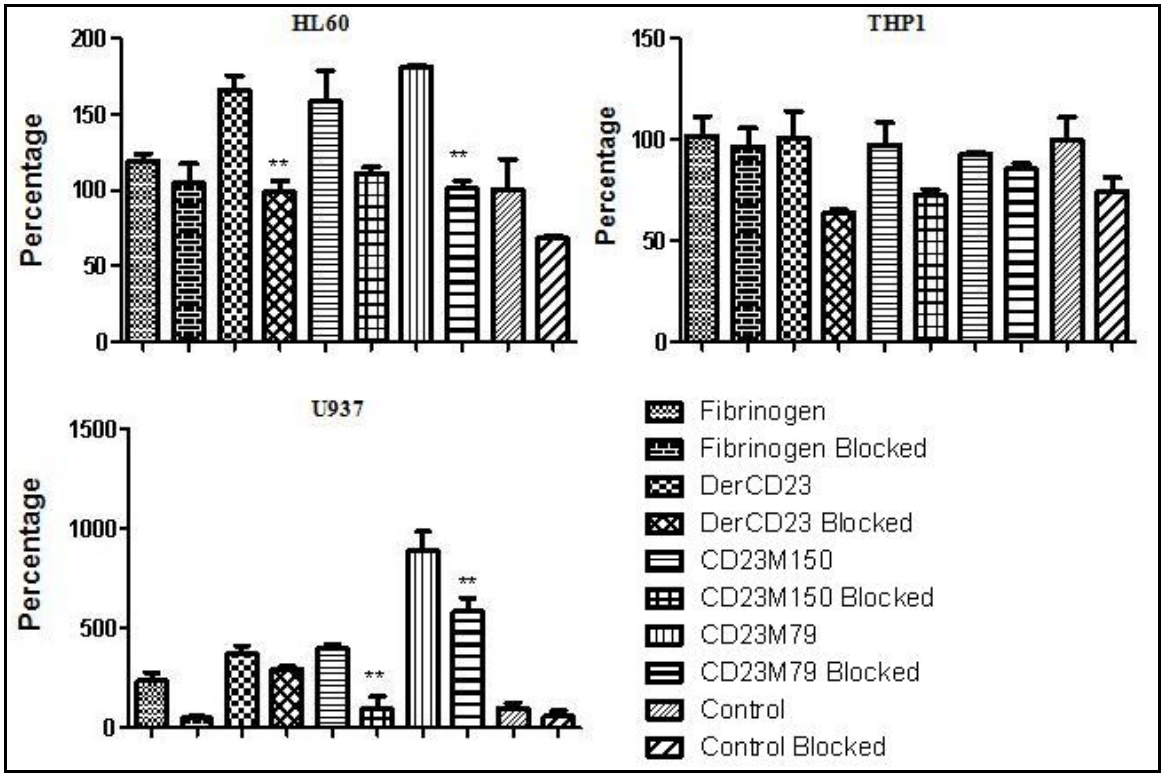

Figure 2.13: Inhibition of binding of differentiated HL60, THP1 and U937 cells to CD23 and fibrinogen. Differentiated cells were labelled with CFSE before being incubated for 1 hour in a 96-well plate, precoated with CD23 proteins, fibrinogen or BSA as control. Half of the cells were preincubated with an anti-CD11b antibody for 30 minutes before being used in the experiment. Unbound cells were removed with washing and the fluorescence of remaining cells measured on a fluorimeter. Each graph is a representative experiment of two experiments done in triplicate, both showing similar results. Error bars represent SEM values. Asterisks represent significance compared to unblocked control cells where (*) represents $P<0.05$, (**) $P<0.005$ and (***) $P<0.0005$.

These experiments demonstrated that CD11-upregulated cells are able to bind both fibrinogen and CD23 proteins in a cell-specific manner. They also demonstrated that the binding of these cells is partially blocked by inhibiting binding to the αI domain of CD11b. Since CBRM1/5 recognizes an epitope on the CD11b αI domain, we conclude that sCD23 binds CD11b/CD18 and possibly also CD11c/CD18 through the αI domain.

2.3.3.2 ELISA of CD11 αI domain binding to recombinant human sCD23

Due to cell binding results, and the problems encountered with producing full length CD11 proteins, it was decided to do ELISA binding experiments with purified CD11 αI domains. Binding of GST-tagged CD11b and CD11c αI domains to CD23 proteins was therefore investigated. This was done by ELISA and the data was used to produce binding curves using a one site binding model in Graphpad Prism 5 software.

An example of a binding curve seen in these experiments is shown in Figure A.6 in Appendix A. Table 2.3 shows the binding affinities during separate experiments of the CD11b and CD11c αI domain proteins for CD23 proteins and fibrinogen.

Table 2.3: Equilibrium dissociation constants for CD11b/c αI domain interaction with CD23 and fibrinogen. K_D (in μM) is determined from three experiments done in triplicate for CD11b and two experiments done in triplicate for CD11c.

Protein	CD11b αI domain	CD11c αI domain
Fibrinogen	0.44 ± 0.13	0.33 ± 0.09
derCD23	0.27 ± 0.07	0.46 ± 0.13
CD23M150	0.32 ± 0.06	0.28 ± 0.08
CD23M79	0.25 ± 0.06	0.29 ± 0.07

These data confirm the cell data that shows an interaction between CD23 and CD11b/CD11c occurs through the αI domain of the integrins. The CD11b αI domain appeared to have very little difference in its affinity for the CD23 proteins (K_D of 0.27 ± 0.07 μM for derCD23, 0.32 ± 0.06 μM for CD23M150 and 0.25 ± 0.06 μM for CD23M79), although these affinities seemed slightly higher than what was seen for fibrinogen (K_D 0.44 ± 0.13 μM). The affinity of CD11c αI domain for CD23M150

and CD23M79 were very similar (K_D of 0.28 ± 0.08 μM and 0.29 ± 0.07 μM, respectively), while the affinity for derCD23 was lower (K_D 0.46 ± 0.13 μM). Fibrinogen had a dissociation constant of 0.33 ± 0.09 μM for CD11c αI domain. It is well known that binding affinities derived from ELISA binding experiments are not as sensitive as using surface plasmon resonance (SPR) spectroscopy. However, it does show that the binding occurring between CD23 and CD11b/CD11c is able to take place in the αI domain of the integrins. To obtain more sensitive binding data and attempt kinetic constants of on- and off-rates, the binding of CD11b/c αI domains with CD23 was investigated using SPR spectroscopy next.

2.3.3.3 SPR spectroscopy analysis of CD11 αI domain interaction with recombinant human sCD23

Although the ELISA binding data showed the binding of β_2 integrin αI domains, a more sensitive method of measuring the binding was required. This was attempted with SPR spectroscopy at the Centre for Systems Biology at Edinburgh.

On travelling, the β_2 integrin αI domain proteins aggregated in the storage buffer and therefore the protein concentrations are lower than expected during the experiment. The CD23M150 protein also failed to remain stable during transportation and failed to immobilize onto the chip. Therefore only the derCD23 and CD23M79 proteins were used for this experiment. The CD11c αI domain protein was used as an analyte first, but was found to bind non-specifically to the reference chip (data not shown), and therefore the CD11b αI domain protein could not be investigated.

Figure 2.14 shows the kinetic binding curves of CD11c αI domain to derCD23 using a Langmuir 1:1 binding fit. This experiment was designed to yield a 100 RU response upon saturation of binding. This did not occur due to the lower than expected CD11 αI domain concentration as well as the subtraction of non-specific binding that was seen throughout the experiment. Despite these challenges, the K_D was still determined from this binding data to be 0.17 µM.

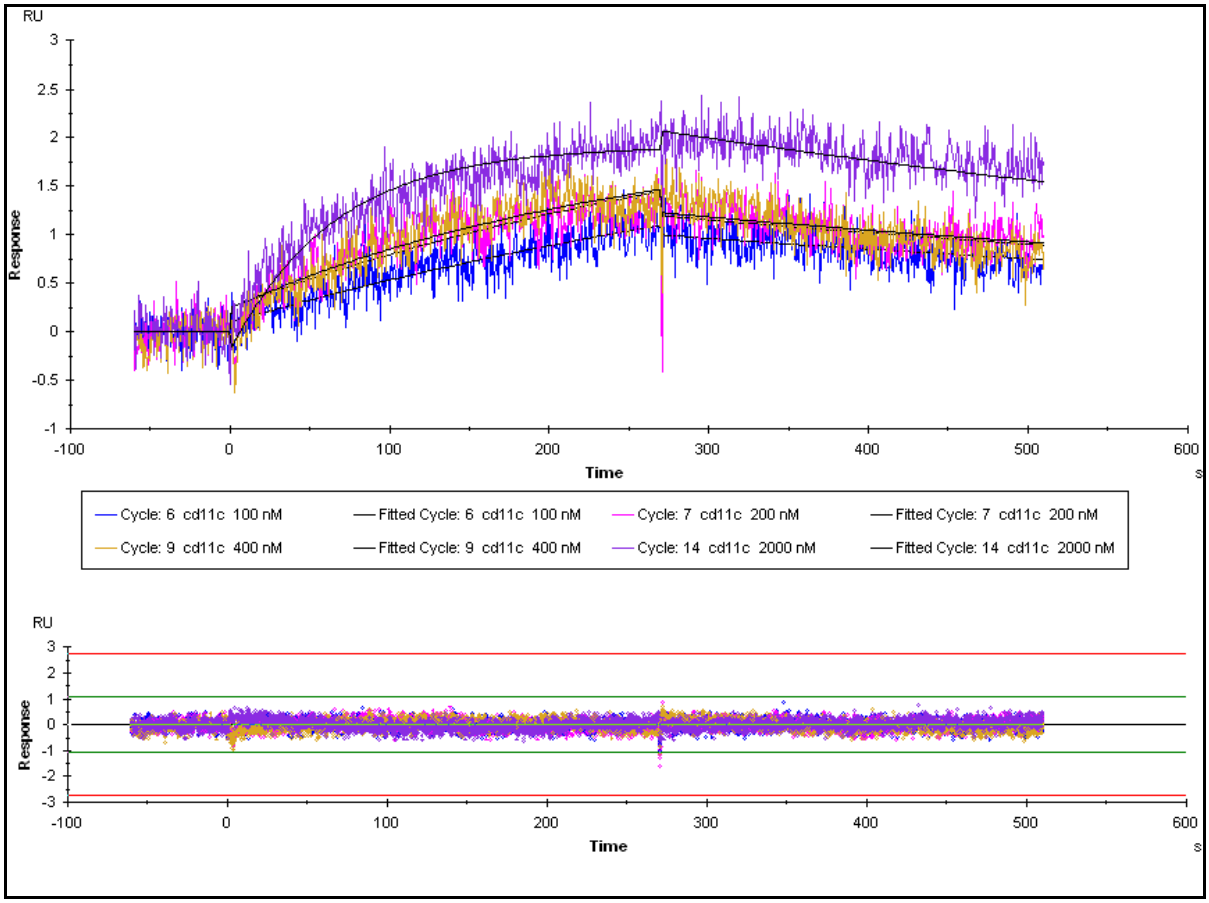

Figure 2.14: Sensorgram showing the Langmuir fit of derCD23 binding to varying concentrations of CD11c αI domain.

The binding of CD23M79 to CD11c αI domain is shown in Figure 2.15. The same 1:1 binding fit was applied to this experiment and the K_D of the binding was determined to be 0.13 µM.

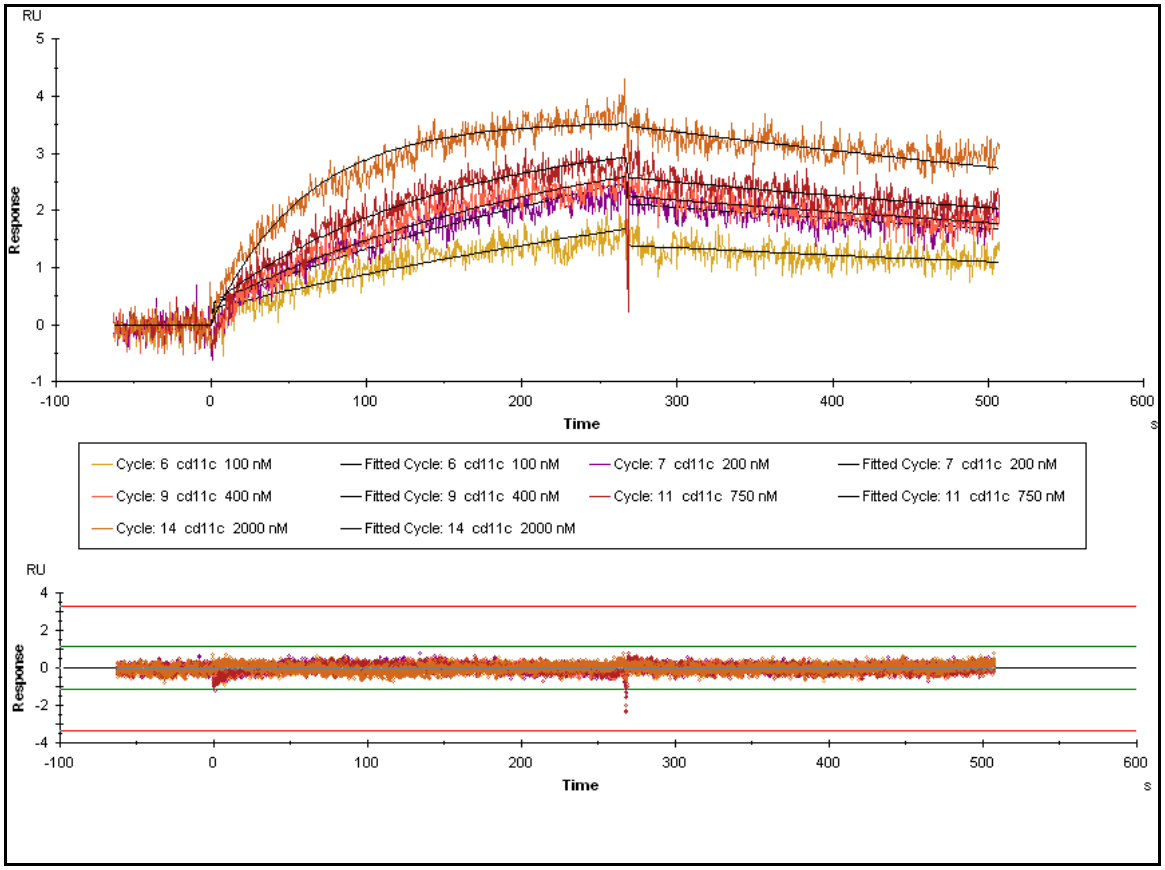

Figure 2.15: Sensorgram showing the Langmuir fit of CD23M79 binding to varying concentrations of CD11c αI domain.

The SPR experiments involved overseas travel, the hiring of equipment from another lab and limited access time on the instrument. This is why they could not be repeated and why troubleshooting could not be used to resolve nonspecific binding events (for example, the addition of dextran to running buffer). However, they did confirm our ELISA data in that they show specific binding of CD11c αI domains to CD23 proteins.

2.4 Conclusions

The aims of recombinant protein production were to express and purify three constructs of CD23 for use in cell-based experiments as well as using them to investigate their interaction with CD11b and CD11c. It was therefore also necessary to produce recombinant CD11 proteins.

CD23, in a wide variety of constructs, has been produced in our laboratory and their expression and purification has been optimised some time ago (Daniels *et al.*, 2005). Due to the purification methods for CD23 being optimised prior to this project, these same methods were used to express and purify three soluble CD23 proteins

The production of full length CD11b and CD11c proteins was not successful. This could be due to several reasons. A β-galactosidase insert provided in the Ek/LIC kit was used as a positive control and treated in the same way as the CD11 insert DNA. This positive control was successful in transfecting insect cells and expressing the desired β-galactosidase (Figure 2.6). Since this control was run with every transfection, this eliminates the possibility that the transfection process itself was unsuccessful. Therefore there is a possibility that the proteins were not expressed properly or that there was a problem with the CD11-encoding DNA used to transfect the cells. The sequencing results of the vectors showed that the DNA inserted into the pIEx vectors was not complete for the expected CD11 coding regions. The sequencing results showed sequences at the start of the coding regions were as expected, however, there were regions thereafter in the same DNA sequence that had a background signal, were poorly resolved and showed possible sequence slippage by the polymerase during amplification. This could be caused by a number of problems,

such as the contamination of reagents, a partially failed sequence reaction, non-specific primer binding, long runs of mononucleotide bases (typically G and C repeats) which causes the DNA polymerase to 'slip' on the template, poor quality DNA (usually due to plasmid preparations and excess salt used in the sequencing reaction). However, a clear band of the right size was seen after PCR and this was inserted into the vector. At this stage it is important to note that the target DNA insert was very large in size (3300 bp) which often complicates the PCR reaction. The primers that are used for these reactions have to be designed to have a 13 or 14 base pair overhang complementary to the pIEx vector in addition to an extra section that is complementary to the target DNA. This results in a very long primer. Unfortunately, due to the sequence of the desired protein, the primers had poly-G regions which is also not desirable for primers.

Due to the lack of success of full-length integrin production, and because literature states that most CD11b and CD11c ligands bind to their αI domain, it was decided to continue work with the αI domain vectors received as a donation. These GST-tagged proteins demonstrated the ease of purification when isolating a fusion-tagged protein by affinity chromatography. These recombinant proteins were easily purified and used in binding experiments.

The cells used in the binding experiments were differentiated by vitamin D_3. The HL60 and U937 cells are differentiated into monocytic cells while the THP-1 cells are differentiated into a macrophage-like cell. This differentiation is marked by an upregulation in surface expression of CD11b and CD11c. These binding assays showed that the differentiated cells were able to bind the three different CD23 proteins significantly in HL60 and U937 cells. The binding of these cells to the CD23

proteins was also almost completely blocked by the addition of an antibody that blocks the αI domain of CD11b. This indicates that the binding to CD23 proteins was definitely in part due to their ability to bind the αI domain of CD11b. It is possible that the residual binding shown that could not be blocked by the antibody was caused by the binding of the CD23 proteins to the αI domain of CD11c. There is also the possibility, however, that the CD23 was also able to bind other ligands on the cells, such as the vitronectin receptor. It was also interesting to note that the CD23M150 and CD23M79 proteins had very similar levels of binding to the two αI domains. The derCD23 protein, although it still showed significant binding, demonstrated a lower level of binding. This could be explained by its shorter length compared to the other two CD23 proteins. This could indicate that the lectin domain of CD23 is involved in binding to the αI domains of integrins, but that the larger proteins may have a region of CD23 that is useful for binding these αI domains, in addition to the lectin domain, perhaps in the stalk or C-terminal tail.

The THP1 cell line on the other hand showed no significant binding compared to the control. This could be because it was differentiated into a different cell type compared to the HL60 and U937 cell lines and that other up-regulated cell surface markers play a role in how the cells respond. Although the binding of THP1 cells to CD23 was not significant, the use of the blocking antibody was able to lower this binding, demonstrating some influence of CD11b αI domain in the binding. It is interesting to note, however, that when differentiated, the HL60 and U937 cells show a greater upregulation of CD11b compared to undifferentiated cells than that seen with CD11c (results shown in chapter 3). The THP1 cells show the opposite effect, where differentiated cells show a greater upregulation of CD11c compared to naïve cells than that seen with CD11b. This could indicate that the adhesion of these

differentiated cells to other cells or surfaces is mediated by CD11b rather than CD11c. This has been demonstrated in neutrophils with the urokinase-type plasminogen activator receptor (uPAR) which binds both CD11b and CD11c. During neutrophil chemotaxis, uPAR binds CD11b first, before polarising to the leading edge of the migrating cell where it then associates with CD11c (Porter and Hogg, 1998). Georgakopoulos *et al.* (2008) also showed that CD11c is less susceptible to activation than CD11b, due to the stronger stimulation necessary to allow ligand binding in U937 and alveolar macrophage cells than CD11b.

There are several ligands for CD11 integrins and in many cases their ligand affinities have been elucidated. Thy-1 is a membrane protein involved in cell adhesion and signalling regulation in neurons and T-cells and it binds CD11b and CD11c. Thy-1 binds CD11c I domain with a K_D of 1.16 ± 0.14 μM, which is approximately 2-fold higher than its binding to CD11b I domain (K_D 2.4 ± 0.46 μM) (Choi *et al.*, 2005). CD11b binds iC3b with a K_D of 12.5 nM and the I domain alone binds at 300 nM. The hookworm-derived neutrophil inhibitory factor (NIF) binds to the I domain with a K_D of 1 nM and this binding is activation independent (Li and Arnaout, 1999). CD11b has also been shown to bind fibrinogen with a K_D of 0.22 ± 0.06 μM (Zhou *et al.*, 1994). The affinity that integrin αI domains in our experiments bind to fibrinogen is similar to that seen in published data (Zhou *et al.*, 1994) as well as having similar affinities as other ligands of these I domains.

The *in vitro* ELISA results with GST-tagged αI domain proteins confirm the cell-binding results that CD23 recombinant proteins of varying sizes are able to bind the αI domains of CD11b and CD11c. Using an ELISA to obtain binding kinetics is not a very sensitive method to use; however, it was able to confirm that the binding is

occurring as we predicted. Since the binding affinities of CD11 αI domains to fibrinogen that we observed are very similar to those obtained in literature, it can be said that the binding results for the CD23 proteins give us an estimation of the binding affinities for the experiments conducted using SPR spectroscopy. Although there were several complications with the SPR experiments, the binding curves obtained were able to support our ELISA results showing that CD23 proteins are able to bind CD11b and CD11c through their αI domains. The binding kinetics obtained were not accurate for SPR since the protein aggregated during travel, however it also implies binding in the μM range, as did the ELISA data. The SPR data also showed that derCD23 had a lower binding affinity to CD11c αI domain than CD23M79, as was found with the ELISA data. However, the SPR experiments should be repeated since they have not been replicated sufficiently. The SPR experiments should also be replicated with a GST control as a negative control, since the αI domain proteins are tagged with GST for purification purposes.

However, integrins occur as heterodimers of α and β subunits *in vivo*, and the use of the I domain of the α subunit alone for binding experiments is not desirable. Although the binding of sCD23 proteins to heterodimeric integrins expressed on cells was demonstrated and then subsequently blocked with an antibody blocking the αI domain of the CD11 proteins, the binding of sCD23 proteins to the full length α domain integrins themselves in addition to this I domain binding would provide a more thorough investigation into the binding interactions of these integrins with sCD23 proteins.

It should be noted that all three of the CD23 proteins produced in our laboratory have the RKC motif shown to be the site of CD23 binding for the integrin $\alpha_v\beta_5$ by Borland

et al. (2007). This motif is found from amino acids 172-174 in all three variants of the sCD23 protein. Therefore it is possible that this motif is also a binding site for the CD11b and CD11c αI domains. However, the cell binding data shows that the binding of derCD23 to the I domains is much weaker than the other two CD23 proteins, indicating further interaction sites in either the stalk or C-terminal tail. Figure 2.16 demonstrates the proposed binding sites for IgE, CD21 and the $\alpha_v\beta_5$ integrin. Further study into the interaction between these proteins using more sensitive binding analysis methods could further elucidate their interaction sites. Site directed mutagenesis of the CD23 proteins would also be useful to elucidate which parts of the CD23 proteins are binding the CD11b and CD11c integrins. Nevertheless, this study is the first time that it has been shown that sCD23 proteins bind CD11b and CD11c through their αI domains.

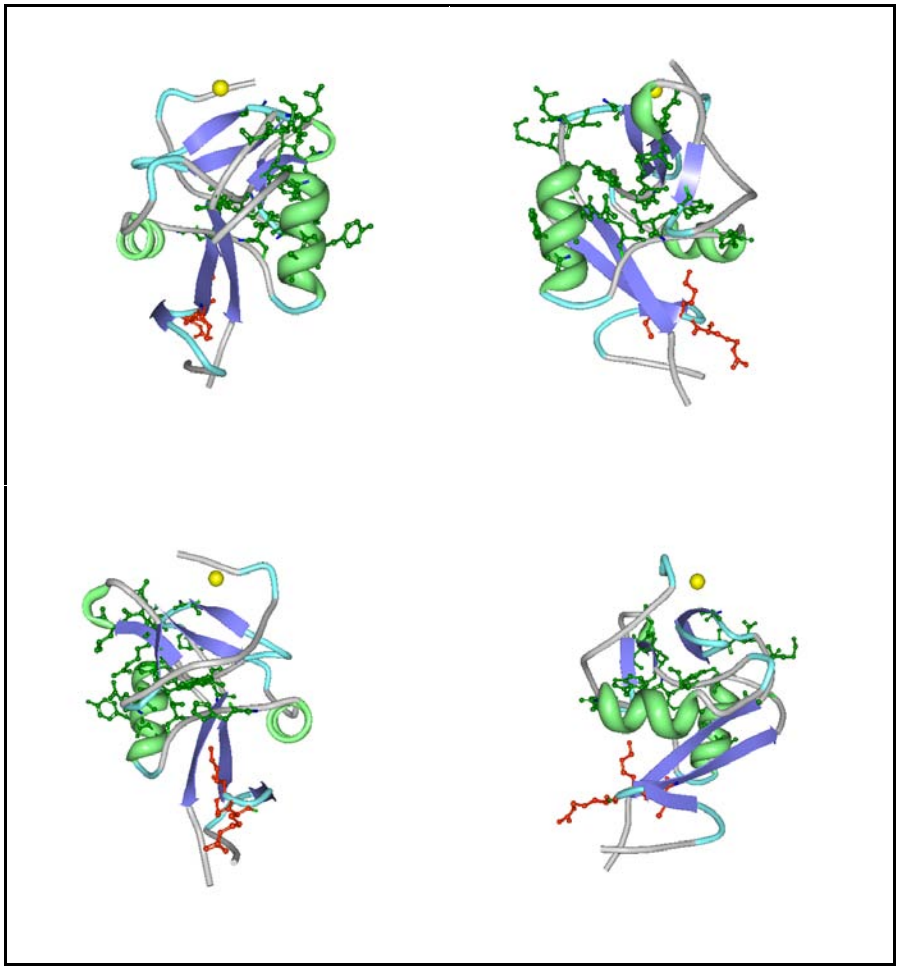

Figure 2.16: Structure of sCD23 showing ligand interaction sites. Ribbon representation of CD23 X-ray crystal structure 2H2T (Wurzburg *et al.*, 2006) showing the proposed interaction sites for IgE (residues shown as ball-and-stick representation in green), CD21 (blue) and $\alpha_V\beta_5$ integrin (red), and the calcium ion (yellow).

Chapter 3: Effect of CD23 proteins on monocytes

3.1 Introduction

3.1.1. Monocytes

Both CD11b and CD11c are expressed primarily on monocytes and neutrophils. Mononuclear phagocytes share many properties with neutrophils, despite having many distinctive morphological and functional properties, depending on their state of differentiation. Monocytes are able to differentiate into macrophages and dendritic cells (Dale *et al.*, 2008). Granule-associated proteins are similar between the two cell types; however monocytes are able to augment the production of granule proteins through new protein synthesis, while neutrophils are not. There are also differences in their chemotactic and metabolic burst responses. Monocytes accumulate more slowly at inflammatory sites, but persist for longer. They have a less extreme metabolic burst than neutrophils; however they have a more diverse capacity to kill. Mononuclear phagocytes have three major functions in the immune system; they are responsible for antigen presentation, phagocytosis and immunomodulation. They internalise material either to eliminate waste or to kill microbes. Activated monocytes produce IL-1β, IL-6, TNFα and IFN-α/β and are subject to immune modulation (Dale *et al.*, 2008).

3.1.2 Cellular functions of integrins

Integrins regulate the complex sequence of events that lead to leukocyte activation and recruitment to sites of inflammation. β_2 integrins are upregulated during inflammation and play a role in leukocyte adhesion and functional responses during

infiltration. CD11b was found to be crucial for cytoskeletal changes and formation of actin foci, indicating a contribution by CD11b and CD11c in the integrin-mediated responses of monocytes (Georgakopoulos *et al.*, 2008). β_2 integrins are present in an inactive state on circulating leukocytes. However, on neutrophils, the stimulation of β_2 integrins with various cytokines, a G-protein coupled receptor agonist and high valency ligands causes a conformational change resulting in their activation. These activated β_2 integrins mediate leukocyte adhesion and transmigration across the endothelium, through their interaction with ICAM-1. CD11b and CD11c also promote phagocytosis of microbes into phagosomes, an intracellular compartment containing various proteinases and into which nicotinamide adenine dinucleotide phosphate (NADPH) oxidase-derived ROS are directed (Mayadas *et al.*, 2005).

Integrins have a two-way activation signalling (outside-in signalling and inside-out signalling). The activation signals which trigger the high affinity binding state of CD11b (inside-out signalling) and CD11b-mediated phagocyte activation (outside-in signalling) are still poorly understood.

Outside-in signalling pathways by integrins are better understood than the reverse process and several of the signalling pathways have been clarified. Full activation of monocytes and neutrophils (which includes the ability to phagocytose, adhere, migrate and degranulate) is dependent on CD11b-mediated activation. The activation of leukocyte effector functions is dependent in turn on prior activation of CD11b itself (Ehlers, 2000). This is achieved via one of two mechanisms. The first is dependent on receptor clustering and most likely is achieved by ligation of coreceptors such as FcγR or selectins, and requires actin reorganisation. The second is induced by ligation of G-protein coupled receptors (GPCR) for the classical chemoattractants

(fMLP, platelet-activating factor and chemokines) and is independent of actin reorganisation. The receptor-clustering pathway has been shown to signal via PI3 kinase, while the G-protein dependent pathway is PI3K independent (Ehlers, 2000).

The complement system is made up of a major group of recognition molecules, activated by several pathways, following direct or indirect contact with microbes. CD11b primarily binds iC3b (a complement activation product) on a particle surface, but also cooperates with complement receptor (CR) 1, which binds C3b and converts it to iC3b via intrinsic factor/cofactor activity. It is thought that simple binding of CR3 (ie CD11b) to iC3b in a particle is not sufficient to trigger phagocytosis, but that receptor activation is necessary. An alternative possibility is the cooperation of a second phagocytic receptor. FcγRIII cooperates with CD11b to stimulate respiratory burst and facilitate antibody dependent phagocytosis (Ehlers, 2000). Other endogenous activators of CD11b have been elucidated. Oleic acid, usually released after bone injury, causes a rapid increase in cell surface expression of CD11b as well as an increase in its affinity state and promotes neutrophil aggregation and adherence to cultured endothelial cells. Myeloid-related protein 14 (MRP-14) is a prominent cytosolic protein in myeloid cells and directly induces the CD11b high-affinity state without activating other neutrophil functions and appears to do so via a specific GPCR. β-glucans are microbial polysaccharides which have also been shown to prime neutrophils and NK cell CD11b for phagocytosis of iC3b-opsonised particles. However the β-glucan-primed CD11b does not display a high affinity epitope necessary for efficient adhesion to substrates. This evidence suggests that there are several pathways which cause CD11b activation as well as more than one activation state for CD11b (Ehlers, 2000).

Inside-out signalling of integrins is mediated by the phosphorylation of the α subunit, interaction of integrin cytoplasmic tails with cytoskeletal proteins, divalent cations or involvement of guanosine triphosphate-binding protein RhoA. Cytohesin-1 upregulates β_2 integrin-mediated binding by interacting with the intracellular domain of the β subunit, CD18. IMF1 is a small ionic lipid mediator that enhances integrin-dependent neutrophil adhesion and ligand binding activity of CD11b, stimulated by fMLP, TNFα or PMA (Klugewitz *et al.*, 1997).

Phagocytosis is considered a special case of cell spreading and therefore the signalling molecules and cytoskeleton rearrangements that determine cell shape and motility have been investigated. The importance of the Rho family of small GTPases (Rho, Rac and Cdc42) in regulating cytoskeletal rearrangements and the role that integrins play in their activation has been established (Ehlers, 2000). Cdc42 induces filopodia, Rac induces lamellipodia and Rho induces focal adhesion/stress fibers. The activation of particular Rho GTPases may therefore relate to receptor-specific forms of phagocytosis. CD11b-mediated phagocytosis results in a tight-fitting, zippered phagosome, while FcR-mediated phagocytosis results in a more spacious phagosome. CD11b-mediated phagocytosis has been shown to be dependent on Rho activity, while Cdc42 and Rac mediate FcR-mediated phagocytosis. These differences may explain the observed differences in the cellular events following the two phagocytic mechanisms, such as absent respiratory burst and failure to elicit proinflammatory signals during CD11b-dependent phagocytosis (Ehlers, 2000).

Most phagocytic receptors can perform phagocytosis constitutively. However, CD11b requires extracellular signals, like cytokines (TNF) and bacterial products, to do this. Rap1 (a Ras-family small GTP-binding protein) is activated by these stimuli

and its accumulation is necessary to activate CD11b binding and phagocytosis in macrophages (Dupuy and Caron, 2008). Serrander *et al.* (1999) found that particles coated with antibodies to phagocytic receptors on neutrophil cells bound and activated the cells, but were not ingested. This is thought to be due to three possible reasons. Firstly, it may be necessary for other surface molecules to be activated. Secondly, a special epitope may need to be bound simultaneously for uptake. Lastly and more likely, the density or affinity of the ligand was not sufficient to induce the conformational changes necessary for uptake.

It is believed that tyrosine kinases play an essential role in integrin signalling, leading to cytoskeleton rearrangements, cell growth and survival, and motility. Tyrosine kinase inhibitors have been shown to block integrin-dependent PMN spreading and reactive oxygen intermediate generation. Integrin ligation has been shown to activate the MAPK cascade, primarily ERK1 and ERK2 (Berton and Lowell, 1999). Evidence shows that Src family kinases play a central role in integrin signalling. β_2 integrin-elicited stimulation of Rap1 requires Src tyrosine kinases, but they are not necessary for activation of Rap2. PI3K is also involved in adhesion-dependent activation of Rap1 but not Rap2. PI3K and Src tyrosine kinases are thought to regulate Rap1 via a linear pathway. PI3K is the downstream target of Src tyrosine kinases in the β_2 integrin signalling pathway. Protein kinase C (PKC) and calcium signalling, however, are also involved in β_2 integrin activation of Rap1 (Jenei *et al.*, 2006). Src kinase activity has been shown to be necessary for CD11b and CD11c mediated adhesion of cultured monocytes to fibrinogen, and Src kinase activity plays a role in regulating CD11c avidity (Georgakopoulos *et al.*, 2008). One of the initial events in integrin signalling is, therefore, the activation of Src tyrosine kinase and PI3K (Dib *et al*., 2008).

It is useful to note the effects of β_2 integrin interactions with their other ligands. CD11b interacts with LPS and other microbial glycoconjugates. CD11b seems to contribute to host recognition and the response to LPS. This is done both in cooperation with CD14 as well as independently. CD14 is the main signal-transducing receptor in this relationship while CD11b is the main LPS-binding molecule. However, there is a CD14-independent pathway of LPS-stimulation that is mediated by CD11b. This pathway leads to upregulation of inducible nitric oxide synthase (iNOS) and increased nitric oxide (NO) production. Fibrinogen is also involved in inflammatory responses, regulating the accumulation of leukocytes. Fibrinogen has also been shown to activate NF-κB transcription via CD11b/CD18 signalling in U937 cells (Rezzonico *et al.*, 2001). Neutrophil engagement of fibrin(ogen) with CD11b causes cellular changes *in vitro* including Ca^{2+} mobilisation, NK-κB activation, increased phosphorylation events, increased migration and decreased apoptosis (Flick *et al.*, 2004).

CD11c/CD18 is less susceptible to activation, suggesting tighter regulation than CD11b/CD18. This was shown by the stronger stimulation necessary to permit CD11c/CD18 ligand binding in U937 and alveolar macrophage cells than that of CD11b/CD18. PI3K has also been implicated in integrin-mediated adhesion by CD11c. PBMCs expressing both CD11b and CD11c used CD11b exclusively to mediate fibrinogen binding while monocytes cultured in human serum showed a shift in participation of integrins, with both being involved in fibrinogen adhesion. Src family tyrosine kinase activity was required for the adhesion of monocytes by regulating integrin activity (Georgakopoulos *et al.*, 2008).

3.1.3 CD23's involvement in cell functions and signalling

CD23 (both membrane-bound and soluble) has been shown to have a wide effect on different cell types. However, since the literature review covered these effects, this section will just recap on how sCD23 affects cell signalling pathways pertinent to β_2 integrin-linked cell functions and pathways.

sCD23 has been shown to activate the nitric oxide synthase (NOS) pathway in monocytes (with mRNA upregulation after 16 hours and NOS after 24 hours) and induces a rapid increase in cGMP and calcium production. This is thought to be through CD11b and CD11c (Aubry *et al.*, 1997). Rezzonico *et al.* (2001) demonstrated that sCD23 binding to β_2 integrins caused NO production and IL-1β, IL-6 and TNF-α in isolated monocytes, while the same inflammatory cytokines were produced in the SMS-SB cell line (White *et al.*, 1997). sCD23-induced cGMP production was abrogated in the presence of calcium chelator or calcium calmodulin inhibitors. CD23 has also been shown to activate the constitutive NOS (cNOS) pathway (Aubry *et al.*, 1997).

3.1.3 Reactive oxygen species, nitric oxide and cell signalling pathways

3.1.3.1 Reactive oxygen species

All aerobic organisms require molecular oxygen for survival. Aerobic metabolism depends on oxidative phosphorylation, a process whereby the oxidoreduction energy of mitochondrial electron transport is converted to the high-energy phosphate bond of ATP via a multicomponent NADH dehydrogenase enzymatic complex. O_2 is the final

electron acceptor for cytochrome c oxidase, which is the final enzymatic component of the mitochondrial enzyme complex, which catalyses the four-electron reduction of O_2 to H_2O. Highly reactive and partially reduced O_2 metabolites may be formed during these reductions, as well as other electron transfer reactions. These include the superoxide anion and hydrogen peroxide (one and two electron reductions). However, in the presence of transition metals, a hydroxyl radical may form ($OH\cdot$) which is more reactive. These metabolites are called reactive oxygen species (ROS) due to their higher reactivities in relation to molecular oxygen (Turrens, 2003). ROS are implicated in a wide range of biological processes, from embryogenesis to aging, from normal tissue homeostasis to human disease. ROS regulate critical steps in signal transduction cascades and important cellular events such as protein phosphorylation, gene expression, transcription factor activation, DNA synthesis and cellular proliferation. Due to aerobic metabolism, all aerobic organisms are subjected to a certain level of oxidative stress as ROS are continually being produced in a number of biological processes (Hoidal, 2001). These ROS from mitochondria were always considered toxic by-products of metabolism that could potentially cause damage to lipids, DNA and proteins. Cells can protect themselves from ROS by several antioxidant enzymes such as superoxide dismutase, catalase and glutathione peroxidase (Thannickal and Fanburg, 2000). An imbalance between oxidant production and antioxidant capacity of the cell is called oxidative stress, and it has been implicated in many diseases (atherosclerosis, arthritis, ischemia/reperfusion injury, stroke, sepsis, pulmonary fibrosis, cancer, neurodegenerative disease and aging) (Thannickal and Fanburg, 2000; Tang *et al.*, 2007). After much research, ROS are understood to be mediators of human disease, and have been shown to play a role in the pathogenesis of pulmonary diseases such as acute respiratory distress

syndrome, chronic obstructive pulmonary disease, asthma and interstitial pulmonary fibrosis (Hoidal, 2001).

Cellular ROS is produced by enzymatic and nonenzymatic sources. Due to high concentrations of superoxide dismutase (SOD), the intramitochondrial concentrations of O_2^- are usually kept at low steady-state levels. H_2O_2 is capable of diffusing across the mitochondrial membrane into the cytoplasm, while mitochondrial O_2^- is unlikely to escape the mitochondria. Evidence suggests that TNFα and IL-1 induced apoptosis may involve mitochondrial-derived ROS. Mitochondria may also act as O_2 sensors to mediate hypoxia-induced gene transcription. Plasma membrane-associated oxidases are thought to be the sources of most growth factor- and/or cytokine-stimulated oxidant production, although the enzymatic sources are not fully elucidated (Thannickal and Fanburg, 2000). Superoxide is the product of a one-electron reduction of oxygen and is the precursor to most ROS and a mediator in oxidative chain reactions. SOD mediates the dismutation of O_2^- to hydrogen peroxide, which may be reduced to water or to a hydroxyl radical, which is a strong oxidant. The formation of $OH^{\bullet}$ is catalysed by reduced transition metals, which may then be re-reduced by O_2^-. Superoxide may also react with other radicals, including nitric oxide in a reaction controlled by the rate of diffusion of both radicals. The by-product is peroxynitrite, a powerful oxidant. Superoxide is produced both enzymatically and non-enzymatically *in vivo*. NADPH oxidases and cytochrome P_{450}-dependent oxygenases enzymatically produce O_2^-. Non-enzymatic production occurs when a single electron is directly transferred to oxygen by reduced coenzymes or prosthetic groups or by xenobiotics previously reduced by certain enzymes (Turrens, 2003).

If not generated in too high concentrations, ROS act as second messengers in signal transduction and gene regulation in several cell types and under various biological conditions such as growth factor, cytokine and hormone treatments, ion transport, transcription, neuromodulation and apoptosis. H_2O_2 is the main ROS mediating cellular signalling due to its ability to inhibit tyrosine phosphatases through the oxidation of cysteine residues in their catalytic domain, which then activates tyrosine kinases and downstream signalling. Different redox-sensitive transcription factors are activated depending on the level of ROS. Low oxidative stress triggers *Nfr2*, a transcription factor implicated in the transactivation of genes coding for antioxidant enzymes. Intermediate levels of ROS trigger inflammatory responses by activating NFκB and activator protein 1 (AP-1) while a high level of ROS results in apoptosis or necrosis (Gliore *et al.*, 2006). Another example of how ROS act as signalling molecules is the treatment of tracheal myocytes with exogenous H_2O_2. This caused the activation of extracellular signal-related kinases (ERK) via successive activation of PKC, Raf-1 and MAPK-kinase 1 (Hoidal, 2001).

The mitochondria of cells produce cellular energy and act as signalling organelles, playing a pivotal role in cell physiology. Mitochondria are the central organelles in cell bioenergetics (Carreras and Poderoso, 2007). ROS are produced by aerobic cells as a by-product during mitochondrial electron transport, or by several oxidoreductases and metal-catalysed oxidation of metabolites. Several studies have indicated that ROS are required participants in normal physiologic signalling in many cells (Thannickal and Fanburg, 2000; Forman and Torres, 2002).

During activation, neutrophils increase their oxygen consumption unrelated to mitochondrial respiration. This is referred to as a respiratory burst because of the

transient consumption of oxygen. This is performed by a multicomponent NADPH reduced oxidase and is critical for a phagocyte's bacteriocidal action (Forman and Torres, 2002). Oxygen is used as an electron acceptor by NADPH oxidase (NOX). The reduced oxygen species which are formed (superoxide and hydrogen peroxide) can kill microbes when combined with the neutrophil granule enzymes. The signalling pathway which leads to NOX activity is thought to involve tyrosine phosphorylation events through Src-like kinases, the activation of small GTP-binding proteins and activation of phospholipase D (Serrander *et al.*, 1999).

O_2^- enhances monocytic adhesion and migration across an *in vitro* model for the blood-brain barrier. However, H_2O_2 and $OH^\bullet$ did not affect either adhesion or migration. ROS have been shown to be one of the signal transduction pathways involved in enhanced migration of monocytes after O_2^- treatment (Van der Goes *et al.*, 2001). When phagocytes are recruited to inflammatory sites, they undergo several physiological changes, including increased adhesiveness, production of ROS and augmentation in phagocytosis (Hermann *et al.*, 1999).

3.1.3.2 Nitric oxide

Nitric oxide is important in the regulation of immune, cardiovascular and nervous systems. Reactive oxygen and nitrogen species are known to play roles in mediating cytotoxicity through altering the protein, lipid and nucleic acid structure and function, resulting in the disruption of cellular homeostatic mechanisms. Subtle changes in the rate of production of reactive species may initiate signalling cascades (Tarpey *et al.*, 2004).

Significant effects of nitric oxide on mitochondrial respiration are evident by its high-affinity binding to cytochrome oxidase, the final electron acceptor. The synthesis of NO from L-arginine and oxygen is catalysed by NO synthases (NOS), of which there are three isoforms; neuronal (NOSI or nNOS), inducible (NOSII or iNOS) and endothelial (NOSIII or eNOS). A significant number of spliced and post-translationally modified variants also exist. NOSI and III are expressed in different tissues constitutively and when interacting with various proteins can have different effects. They can increase or decrease enzyme activity, modify subcellular traffic, participate in ubiquitination and degradation (Guzik *et al.*, 2003; Aubry, *et al.*, 1997). Constitutive NOS are activated by Ca^{2+} pulses after activation of cell surface receptors. NOSI and III are characterised by fast and transient responses to facilitate neural transmission or to induce a prompt vasodilation in response to changes in blood flow. NOSII gene expression is modulated by inflammatory mediators, like TNFα, IFNγ and LPS that activate transcription factors like NF-κB or AP-1. The activities of NOS isoforms are able to sustain NO cytosolic concentrations large enough to reach mitochondria. Effects of NO and H_2O_2 are confluent on modulation of MAPKs and cyclin D1 (Guzik *et al.*, 2003; Aubry, *et al.*, 1997).

All three isoforms of NOS catalyse the same reaction, which is the conversion of L-arginine and molecular oxygen to N-hydroxy-L-arginine and further to citrulline and nitric oxide. They differ in respect of their regulation, the amplitude and duration of the production of NO and their cellular and tissue distribution. NO activity is not restricted to the site of its production as NO radicals are highly diffusible. The interaction is not restricted to a single defined receptor and can react with other organic molecules (oxygen, superoxide and transition metals), structures in DNA, prosthetic groups (eg. heme) or proteins (Bogdan, 2001). NO generation is a feature

of dendritic cells, NK cells, macrophages, microglia, Kupffer cells, eosinophils and neutrophils. NO inhibits the adhesion of platelets and leukocytes to endothelium. Endogenously produced NO and NO donors significantly impede the rolling, firm adherence and/or transmigration of leukocytes. Importantly, NO can inhibit the expression and/or function of integrins. NO influences leukocyte chemotactic response by several mechanisms, such as production of chemokines (MCP-1, MIP1α and MIP2), inhibiting the activation of chemokines (IL-8) and function as an intracellular messenger in chemokine signalling pathways (Bogdan, 2001).

The role of NO in the generation of cGMP was proposed in various models and plays an important role in vasodilation and neurotransmission (Mossalayi *et al.*, 1997). The induction of NO production through the activation of NOSII led to the generation of cGMP and nitriles, end products of the NO pathway in human monocytes/macrophages, eosinophils, myeloid leukemias and epithelial cells (Mossalayi *et al.*, 1997).

Endogenous NO is a mediator in the signalling pathway for chemotaxis induced by a chemoattractant like fMLP. Reports also show that exogenous NO released from NO donors, inhibits this chemotaxis. However, it has also been reported that NO itself shows chemotactic ability for neutrophils (Adaci *et al.*, 2000). In many *in vivo* experiments, monocyte maturation into macrophage-like cells is essential for nitrite production (Dugas *et al.*, 1995)

3.1.3.3 Cell signalling pathways

Multicellular organisms require complex networks of intracellular and extracellular signalling to allow cell to cell communication in physiological processes, such as tissue homeostasis and repair responses to injured tissue. Extracellular responses are typically initiated by growth factors, hormones, cytokines and neurotransmitters binding to specific cell surface receptors. The interaction of these ligands with receptors generates various types of intracellular signals that may involve changes in ion concentrations (ion-channel linked receptors), activation of trimeric GTP-binding regulatory proteins (G-protein-coupled receptors) and activation of receptor kinases (enzyme-linked receptors). Downstream signalling is then passed on by second messengers (cAMP, Ca^{2+} and phospholipid metabolites) and by protein phosphorylation cascades. The intracellular pathways lead to the activation of transcription factors that regulate the expression of specific sets of genes essential for diverse cellular functions (Turrens, 2003).

Transcription factors were the first signalling components to be identified as being redox sensitive. NF-κB is sequestered in the cytosol in a complex with its inhibitor IκB. ROS has been shown to induce NF-κB's activation (Forman and Torres, 2002). NFκB is essential in cellular processes such as immunity, inflammation, cell proliferation and apoptosis. It is activated by innate and immune mediators (inflammatory cytokines such as TNFα and IL-1β), toll-like receptors and antigen receptor ligation. They all signal through different receptors and adaptor proteins, but all converge to activation of IκB kinase (Gloire *et al.*, 2006).

AP-1 is a transcription factor complex formed by dimerization of members of the Jun and Fos protein families. ROS regulates AP-1 activity by several mechanisms, one of which is the c-Jun N-terminal kinase (JNK) cascade. The JNKs are part of the MAPK superfamily of serine/threonine kinases. MAPKs include more than a dozen proteins belonging to three families [extracellular signal-regulated kinases (ERKs), p38 MAPK and JNK/stress activated protein kinases (SAPKs)] (Rao, 2001). MAPKs are proline-directed serine and threonine protein kinases activated by dual specificity kinases by phosphorylation of threonine and tyrosine in a Thr-Xaa-Tyr motif in a loop near the active site. p38 MAPK is activated by MAP kinase kinase 3 or MAP kinase kinase 6 (MAPKK6). All MAPKs are activated through a phosphorylation cascade (Forman and Torres, 2002). MAPKs are activated by ROS, hormones and growth hormones (Tang *et al.* 2007). Autologous plasma modulates ROS generation by the activation of Akt/PKB signalling pathways in PBMCs. There is a functional association between Akt/PKB and PKC/NADPH oxidase system for producing ROS (Veloso *et al.*, 2008). ROS regulates cell function through redox sensitive cysteine residues, such as protein tyrosine phosphatases that control the phosphorylation state of numerous signal-transducing proteins and are therefore involved in the regulation of cell proliferation, differentiation, survival, metabolism and motility. H_2O_2 in cells leads to the activation of p38 MAPK by NADPH oxidase (Bedard and Krause, 2007). Ligand-induced activation of receptor tyrosine kinases can lead to PI3K-mediated activation of Rac which is then able to switch on ROS generation via NOX. ROS activate Src, JNKs, p38 MAPK and ERK1/2. PKC can also be activated by H_2O_2 (Novo and Parola, 2008). All three MAPK families are believed to be redox-dependent biomolecules that modulate cell proliferation, survival and apoptosis.

ROS and NO are recognised as important regulators of apoptotic pathways. NO induces the inhibition of NF-κB, decreased Bcl-2 expression and increased p53 expression by NO-mediated inhibition of proteasome degradation triggered by direct DNA damage. NO can directly induce cytochrome c release through mitochondrial membrane potential loss or by tyrosine nitration of cytochrome c. NO donors or endogenous NO induces apoptotic cell death with activation of JNK/SAPK, p38 MAPK, and caspase 3 or inactivation of NF-κB. In this way, increased iNOS expression and NO production act as a negative regulating feedback modulator of NF-κB activity (Carreras and Poderoso, 2007).

Inflammatory stimuli activate four major intracellular signalling pathways, NFκB, and the three MAPK pathways. Inactivated by phosphatases, several transcription factors can be phosphorylated by p38 MAPK. MAPK and SAPKs 1 and 2 activate cAMP response element binding protein and the p65 subunit of NFκB and also phosphorylate histone H3 and high mobility group protein 14 (Saklavala, 2004). p38 MAPK stimulation in PMN has been shown to cause H_2O_2 production (Ono and Han, 2000).

Phosphoinositide 3-kinases are a subfamily of lipid kinases that catalyse the addition of a phosphate molecule to the 3-position of the inositol ring of phosphoinositides (Rameh and Cantley, 1999). PI3K is a key signalling enzyme that responds to growth factors, cytokines and environmental agents. Once activated, it can support various cell functions, such as growth, migration and survival. It can induce the phosphorylation/activation of Akt/protein kinase B (PKB) which then triggers cytoprotective events such as BAD phosphorylation and NF-κB activation (Lee *et al.*2005). ROS and PI3K act in the serum withdrawal-induced signalling pathway in

U937s. It is suggested that serum withdrawal rapidly increases cellular ROS levels which then induces PI3K activation, which in turn promotes the process leading to the accumulation of more ROS. This mutual interaction was shown to amplify signals needed to activate death mediator SAPK. ROS and PI3K may also mediate the serum withdrawal-induced NF-κB activation and therefore the NF-κB-mediated survival pathway (Lee *et al.*, 2005). PI3K stimulates ROS production. ROS regulates Akt1 and p38 MAPK activation for survival (Wang *et al.*, 2007).

Uncoupling protein 2 (UCP2) is ubiquitously expressed in various tissues and by monocytes and macrophages. It is from the mitochondrial proton carrier family and is located in the inner membrane of the mitochondrion. This protein uncouples chemotaxis by dissipating the electrochemical gradient that builds up across the mitochondrial membrane and causes reduced ATP synthesis, increased heat generation and less intracellular ROS. It may therefore influence the genes involved in monocyte recruitment. Its overexpression decreases H_2O_2 production, reduces intracellular calcium mobilization, reduces β_2 integrin expression and β_2 mediated firm adhesion (Ryu *et al.*, 2004). A decrease in UCP2 promotes an increase in ROS (Emre *et al.*, 2007).

Src-family kinases (SFK) are rapidly activated following integrin-ligand interactions (Harburger and Calderwood, 2009). Src family protein tyrosine kinases team up with integrin adhesive receptors to transmit ‘outside-in’ signals. SFKs are activated downstream of integrins and downstream of other receptors and are essential for integrin signalling. SFKs interact with focal adhesion kinase (FAK) downstream of integrins. C-Src and other SFKs form complexes with FAK in adherent cells as a response to ligand-induced integrin clustering. The c-Src-FAK complex propagates

integrin signals, because it promotes SFK-dependent phosphorylation of additional tyrosine residues in FAK that serve as docking sites for proteins involved in outside-in signalling. Tyrosine phosphorylation of several SFK substrates occurs within seconds of integrin ligation. SFKs regulate multiple pathways downstream of integrins, including PI3K, MAPKs and Rho GTPases (Shattil, 2005). Ligand binding and receptor clustering leads to phosphorylation of tyrosine on immunoreceptor tyrosine-based activation motifs (ITAMs) by SFKs. The phospho-ITAM then recruits the Syk on related zeta-chain-associated protein kinase (ZAP70) tyrosine kinase by their dual phosphotyrosine-binding SH2 domains, leading to their phosphorylation and activation, which then initiates downstream signalling. β_2 integrins also signal by an ITAM-based immunoreceptor-type mechanism in several primary cell types. Syk (a central component of immunoreceptor signalling) activation by β_2 integrin-mediated activation in human monocytic cell lines and human neutrophils appears independent of FAK activation, therefore suggesting a novel integrin signal transduction pathway. Studies showed that Syk is required for β_2-integrin mediated spreading and ERK activation in macrophages, as well as various integrin-mediated functional and signalling responses of neutrophils. Syk appears downstream of SFKs during integrin signal transduction. Integrins can also interact with Syk in an ITAM-independent manner. β_2 integrin chains and ZAP70 can interact with the N-terminal SH2 domain of Syk. However, this does not rule out the ITAM mediated signalling, rather, most likely that recruitment and activation of Syk downstream of integrins is mediated by two parallel, non-exclusive pathways, giving a more delicate control of receptor proximal signalling events in integrin-mediated adhesion (Jakus *et al.*, 2007).

Ras/Rho family GTPases act upstream and downstream of integrin activation. Integrin receptors are able to affect activation and translocation of Rac and Cdc42

GTPases to the cell membrane and thereby regulate GTPase function. Small GTPases also function upstream to regulate integrin adhesion and motility eg. Rap1 (Lemons and Cadic, 2008). NADPH oxidase is stimulated by integrin signalling, growth factors, cytokines/hormones, immunological stimuli, hypoxia and Ras. Rac also stimulates ROS production (Novo and Parola, 2008).

3.1.4 Cell lines used in this study

As previously mentioned, CD11b/CD18 and CD11c/CD18 are expressed mainly on neutrophils, monocyte and macrophage cells (Ho and Springer, 1983; Ingalls and Golenblock, 1995; Rezzonico *et al.*, 2000). It was therefore decided to use the THP1, HL60 and U937 premonocytic cell lines for this study.

The THP1 cell line was derived from a patient with acute monocytic leukemia. HL60 cells were isolated from a patient with acute promyelocytic leukemia while U937 cells were isolated from the pleural fluid of a patient with diffuse histiocytic lymphoma. HL60 cells are promyelocytic cells while U937 and THP1 cells are monocytoid (Koeffler, 1983; Harris and Ralph, 1985; Schwende *et al.*, 1996).

HL60 cells are known to have the ability to weakly phagocytose latex or yeast particles. They possess few Fc- and C3b-receptors and have receptors for the chemotactic tripeptide fMLP and insulin. HL60 cells stain positive for myeloperoxidase but do not have alkaline phosphatase and have only small quantities of acid phosphatase. They have low β-glucuronidase, lysozyme and glucose-6-phosphate dehydrogenase (G6PD) in their granules and have a low capacity to degranulate. However, there is evidence that these enzymes are stored within

granules and are released in an active form upon stimulation. HL60 cells have a marginal capacity to produce H_2O_2 and O_2^- and their ability to kill *Staphylococcus* and other microbes is muted. When differentiated, HL60 cells become monocytoid in character and their production of lysozyme, acid phosphatase, β-glucuronidase and oxidative burst increases (Harris and Ralph, 1985).

U937 cells show a weak presence of acid and alkaline phosphatase but are shown to release lysozyme into the cell culture medium. They have few Fc-, C3- and chemotactic peptide receptors on their cell surface when compared to normal monocytes. A small percentage of cells are phagocytic and H_2O_2 and O_2^- are only weakly produced. U937 cells show an increase in alkaline and acid phosphatase and β-glucuronidase production on differentiation and their ability to produce ROS increases. The phagocytic ability of U937 and HL60 cell lines is induced by vitamin D_3 (Harris and Ralph, 1985).

These cell lines can also be differentiated into more than one lineage by several differentiating agents, such as retinoic acid, PMA, interferons, vitamin D_3, dimethyl sulphoxide (DMSO) and butyric acid. HL60 cells can be differentiated into granulocytes (DMSO, retinoic acid), monocytes (vitamin D_3), macrophage-like (PMA) and eosinophil cells (butyric acid) (Collins, 1987). The U937 cell line has many characteristics of an immature monocyte and has become a valuable tool for studying mononuclear phagocytes and the functional properties of monocytes, such as phagocytosis, chemotaxis and cytotoxicity. The expression of many of these functions depends on stimulation with differentiating agents (Sheth *et al.*, 1988).

Several differentiation agents have been tested for their ability to differentiate cells and upregulate CD11b cell surface expression. We decided that vitamin D_3 was the most useful differentiation agent for this study as it differentiates cells into a monocyte lineage and is able to upregulate CD11b and CD11c on the cell surface of these cells (Weber *et al.*, 1995). HL60 cells showed an increased expression of CD11b, a lesser increase in expression of CD11c and a decreased expression of CD11a when induced to differentiate with vitamin D_3 (Miller *et al*, 1986). Literature also shows that 10^{-6} M vitamin D_3 differentiated approximately 85% of U937 and HL60 cells into a monocyte lineage (Koeffler, 1983). Vitamin D_3 increases the phagocytic ability of THP1 cells and allows them the ability to release O_2^- upon stimulation with PMA (Schwende *et al.*, 1996).

The primary function of vitamin D_3 is the regulation of calcium and phosphorus metabolism. Vitamin D_3 has been shown to increase the production of TNFα by macrophages and to decrease IL-6, IL-1α, and IL-8 in monocytes (Gurlek *et al*, 2002). Vitamin D_3 signalling to myeloid differentiation involves PI3-kinase activation and signal complex formation with the vitamin D_3 receptor (Hmama *et al.*, 1999). Vitamin D3 stimulates the upregulation of CD89 (Fc-receptor for IgA) but downregulates CD64, CD32 (both FcγRs), and CD23 and diminishes the capacity to phagocytose IgE-sensitised erythrocytes in U937s and THP1s (Spittler *et al.*, 1997). Vitamin D3 enhanced the mRNA levels of IL-1, TNFα and IL-6 in U937 cells, but on stimulation with LPS, these levels increased and significant amounts of these monokines were released by the cells. This was not found to be the case in HL-60 or THP1 cells where zymosan-induced oxidative burst was enhanced with vitamin D_3 (Taimi *et al.*, 1993). CD23 gene expression decreases with vitamin D_3 (Bottling *et al.*, 1996).

3.2 Methods

3.2.1 Materials

HEPES, PMA, retinoic acid (RA), vitamin D_3, EDTA, fMLP, fibrinogen, HBSS, 2'7'-dichlorofluorescin diacetate (DCF-DA), wortmannin, 4,5,-diaminofluorescein-diacetate (DAF-DA), and penicillin/streptomycin were from Sigma Aldrich (St. Louis, Missouri, USA); Gibco heat-inactivated fetal bovine serum (HI-FBS) and the Vybrant Phagocytosis Assay kit were from Invitrogen (California, USA); RPMI 1640 medium was from Lonza (Basel, Switzerland); $CD14^+$ Microbead kit and magnetic cell sorting (MACS) separator columns were from Miltenyi Biotec (Bergisch Gladbach, Germany); Intraprep Permeabilization kit, CD11b-fluorescein 5'-isothiocyanate (FITC), CD11c-phycoerythrin (PE), CD14-PC5 and the relative isotype controls were from Beckman Coulter (Fullerton, California, USA); anti-human myeloperoxidase (MPO)-FITC, Falcon tubes and Vacutainer tubes were from Becton Dickinson (San Jose, California, USA); Chemicon QCM Migration Assay kit was from Millipore (Billerica, Massachusetts, USA); BSA was from Roche (Mannheim, Germany); wedelolactone and 4-amino-5-(4-chlorophenyl)-7-(*t*-butyl) pyrazolo[3,4-*d*]pyrimidine (PP2) were from Calbiochem (Darmstadt, Germany); IL-1β, IL-6 and TNF-α ELISA kits were from eBiosciences (San Diego, USA); cell culture inserts, cell culture flasks and 96-well Maxisorp plates were from Nunc (Roskilde, Denmark); MycoProbe™ Mycoplasma Detection Kit was from R&D Systems (Minneapolis, USA) and anti-human phospho-NF-κB p65 (Ser536)(93H1) rabbit mAb (Alexa Fluor®488 Conjugate) was from Cell Signaling Technology (Beverly, Massachusetts, USA).

3.2.2 Routine Cell Culture

Cell lines were routinely maintained in RPMI1640 cell culture medium, containing 25 mM HEPES and 2 mM L-glutamine, supplemented with 1% (v/v) each of penicillin and streptomycin. U937 and THP1 cells were also supplemented with 10% HI-FBS while HL-60 cells were supplemented with 20% HI-FBS. Cells were cultured at 37 ºC in a humidified atmosphere with 5% CO_2 and 95% air. The cell lines were maintained between 1 x 10^5 and 1 x 10^8 cells per mL and were cultured in 75 cm^2 flasks. The medium was removed every three days by centrifuging the cells in sterile 50 mL Falcon tubes at 1000 x g for 5 minutes using an Eppendorf 5810 centrifuge and fresh medium was added. All cell lines were tested for Mycoplasma contamination prior to use in experiments using the MycoProbe™ Mycoplasma Detection Kit.

3.2.3 Cell counts

Cell counts were performed using a Neubauer counting chamber (Superior). Cells were diluted 1:1 with trypan blue stain (0.4% trypan blue in PBS). When cells have died, the loss in integrity of the membrane structure allows this stain to enter the cells, where live cells exclude the stain. This allows for the counting of clear, live cells and dark blue, dead cells. Each large square of the Neubauer counting chamber represents 0.1 mm^3 and 1 cm^3 is approximately 1 mL. Therefore the total number of cells was determined using the equation:

Cells/mL = average cell count per square x dilution factor x 10^4

3.2.4 Cell differentiation

As mentioned previously, the three cell lines used are able to differentiate into monocytic, macrophage or neutrophil-like cells. The upregulation of CD11b on these cells is a widely-used marker for differentiation. PMA (20, 50 and 100 ng/ml), retinoic acid (100 nM) and vitamin D_3 (1 μM) were used to differentiate the cells. Cells were seeded at 1-3 x 10^5 cells per mL and incubated for 24 hours. Differentiating agents were added and cells were analysed for CD11b upregulation after three days.

3.2.5 Isolation of $CD14^+$ peripheral blood mononuclear cells

Most cell separation techniques take advantage of the differences in the physical or biological properties of cells. Mononuclear cells have a lower density than granulocytes and lymphocytes. Therefore, we are able to separate blood cells into two fractions by layering the blood over a separation fluid of intermediate density. Following centrifugation, the mononuclear cells can be found above the separation fluid, while the granulocytes and lymphocytes sediment to the bottom of the tube. By isolating mononuclear cells using density gradient centrifugation, the average purity of the cells is between 60-90% (lymphocytes being the main contaminant). This purity can be improved to 95-98% by using a hyperosmotic density gradient medium (usually Ficoll).

MACS has become a widely used tool for the isolation of many cell types from any complex cell mixture, such as peripheral blood, hematopoietic tissue or cultured cells. Magnetic cell sorting technology makes use of small super-paramagnetic particles and

high gradient magnetic fields to isolate cells. A cell suspension is specifically immunomagnetically labelled using small super-paramagnetic microbeads which are covalently conjugated to a monoclonal antibody or to a ligand specific for a certain cell type. After labelling, the cells are passed through a separation column which is placed in the external magnetic field of a strong permanent magnet. This magnetisable column matrix serves to create a high gradient magnetic field which acts as a specific magnetic cell filter. The magnetic cells remain on the column, while the unlabelled cells flow through. When the column is removed from the magnetic field, the matrix is demagnetised and the previously magnetised cells can be eluted from the column. MACS magnetic particles are made up of dextran and iron oxide and are between 20 and 100 nm in diameter. The core of these molecules is a cluster of iron oxide crystals which are too small to have a defined magnetic orientation, meaning they do not retain any residual magnetism when removed from the magnetic field (they are therefore paramagnetic) (Miltenyi and Schmitz, 2000).

The mononuclear cells were isolated by isopaque-Ficoll density gradient centrifugation by drawing blood from the individual directly into VacuTainer cell preparation tubes (Boyum, 1984). The tubes were gently inverted eight times directly after taking the blood. Within half an hour, the tubes were centrifuged at 400 x g for 25 minutes using a Beckman J-6 centrifuge. The PBMCs in the tube were mixed with the serum and transferred to a sterile 15 mL Falcon tube. This tube was centrifuged at 1650 x g for 10 minutes (using an Eppendorf 5804R centrifuge), before aspirating the supernatant. Each tube was grated against the underside of a 96-well microtiter plate to loosen the pellet. The Falcon tubes were filled with RPMI 1640 medium containing 10% HI-FBS and 1% (v/v) each of penicillin and streptomycin, before centrifugation at 1650 x g for 10 minutes. The supernatant was aspirated and the cell

pellet loosened as before. The PBMCs were counted using trypan blue to determine the total cell number. $CD14^+$ monocytes were then isolated from the PBMCs using a Miltenyi CD14 microbead kit. PBMCs were resuspended in 80 µl MACS buffer (PBS, 0.5% BSA and 2 mM EDTA, pH 7.2) per 10^7 total cells. CD14 microbeads were then added (20 µl of beads per 10^7 total cells) and incubated for 15 minutes on ice. Cells were washed with 1-2 mL of MACS buffer per 10^7 cells and centrifuged at 300 x g for 10 minutes. The MACS buffer was aspirated and cells were resuspended at 10^8 cells per 500 µl of MACS buffer. MS magnetic columns were placed in the magnetic field of a MACS separator. The columns were rinsed with 500 µl of MACS buffer before the cell suspension was added (500 µl per column). The unlabelled cells that passed through the column were collected, and the columns were washed three times with 500 µl of buffer. The columns were removed from the separator and placed in a suitable collection tube (a 15 mL Falcon tube). One ml of MACS buffer was added to the column and a column plunger was firmly pushed into the column to flush out the magnetically labelled cells. These $CD14^+$ cells were centrifuged at 1000 x g to remove the MACS buffer and resuspended in RPMI medium containing 10% HI-FBS and 1% (v/v) penicillin/streptomycin. Cells were incubated at 37 ºC in a humidified atmosphere with 5% CO_2 and 95% air for 24 hours before being used in experiments.

3.2.6 Flow cytometric determination of cell surface markers

After the isolation or differentiation of cells, it was necessary to stain for various cell surface markers to ensure the correct cells had been isolated, or that the desired cell surface markers had been upregulated. This was done by centrifuging an aliquot of the cells for 5 minutes at 1000 x g, before resuspending the cells in blocking buffer

(1% HI-FBS and 1% BSA in PBS, pH 7.4) for 30 minutes at room temperature. Cells were centrifuged as before and resuspended at 1 x 10^6 cells per mL, and stained with 20 µl of antibody to the cell surface marker in question. Samples were incubated for 30 minutes at room temperature in the dark. Cells were centrifuged as before and washed twice with PBS before analysis on the flow cytometer. At the same time, a sample was stained with an appropriate isotype control to ensure there was no non-specific binding of the antibody to the cells. Cell surface markers detected in this study were CD11b (using a CD11b-FITC antibody), CD11c (using a CD11c-PE antibody) and CD14 (using a CD14-PC5 antibody).

3.2.7 Flow cytometry

A Beckman Coulter FC500 was used for all flow cytometry analysis. During each experiment, it was ensured that a consistent number of cells was used during each experiment and a minimum of 10 000 events was counted per sample. The mean fluorescence intensity or the population median was used to compare samples. Histograms showing and example of the control cells and positive controls for ROS, phagocytosis and MPO assays are shown in the (Figure A.7 to A.9)

3.2.8 Chemotaxis

Migration of differentiated cells was tested using a Chemicon QCM^{TM} Chemotaxis 96-well Cell migration assay (3 µm pore size for U937 and HL-60 cells and 5 µm pore size for THP1 cells). Differentiated cells were serum starved for between 18 and 24 hours before treatment with recombinant CD23 proteins. All plates and reagents

were brought to room temperature before use. Cells were centrifuged at 1000 x g for 5 minutes and washed twice with PBS. Cells were then resuspended in serum-free medium at $2x10^6$ cells per mL. Figure 3.1 shows the plate setup of the Chemicon Migration assay.

The lid and migration plate of the migration chamber were removed and 150 µl of medium was added to the feeder tray (Figure 3.1). This medium was made up of serum-free RPMI1640 and 10 µg/ml fMLP in all the test conditions except for the positive control, where RPMI1640 with 10% FBS was added. The migration plate was replaced and 50 µl of serum-free medium containing either 200 ng/ml of fibrinogen or recombinant CD23 proteins was added, or in the case of the positive and negative control, just serum-free medium was added. The differentiated cells were then added to each well (50 µl giving $1x10^5$ cells/well and 100 ng/ml of fibrinogen or CD23 protein) and the plate incubated for 24 hours as per normal cell culture conditions.

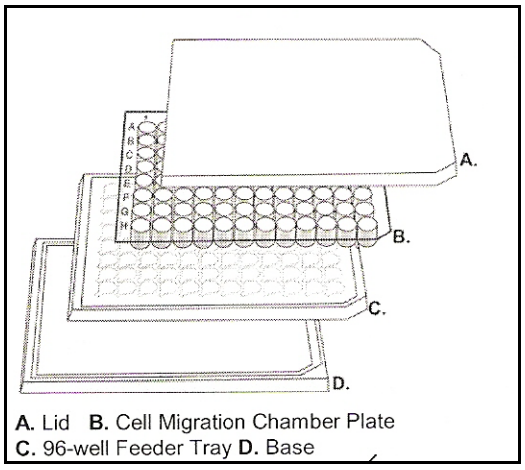

Figure 3.1: Chemicon Migration kit plate setup.

Following incubation, the migration plate is removed and the medium and cells are gently discarded from the top side by flipping out the remaining cell suspension. This migration plate is then placed in a new 96-well feeder tray, containing 150 µl of prewarmed Cell Detachment solution as provided in the kit. The plate is incubated for 30 minutes at 37 ºC. The cells are dislodged from the underside of this migration tray by gently tilting the tray back and forth several times during the incubation. Seventy five µl of this cell detachment solution is then transferred to a new plate together with 75 µl from the corresponding well from the migration feeder plate. A lysis buffer/dye solution was prepared by mixing CyQuant GR dye 1:75 with 4x lysis buffer. Fifty µl of this was added to the combined solution containing the migratory cells and incubated for 15 minutes at room temperature in the dark. The new mixture (150 µl per sample) is added to a new black 96-well plate (Nunc) and read with a Fluorescan Ascent FL fluorimeter using a 480/520 nm filter set.

Prior to the use of this kit, Nunc cell culture inserts were used to optimise the positive control and cell migration towards several chemoattractants (serum, fMLP, MCP-1 and IL-8). Based on the results of these experiments (data not shown), it was decided to use serum as a positive control for chemotaxis and fMLP as the chemoattractant in the experiments.

3.2.9 Phagocytosis

The Vybrant Phagocytosis Assay kit was modified for use on a flow cytometer to observe phagocytosis in cells. Differentiated cells were washed and resuspended in fresh medium at $1x10^6$ cells/ml. Fibrinogen and the recombinant CD23 proteins were made up to 200 ng/ml in fresh RPMI160 medium with 10% serum and 200 µl was

aliquotted into Beckman Coulter flow cytometry tubes, along with a control tube where no protein was added. An equal volume of evenly resuspended cells was added to each tube and incubated for one hour at 37 ºC (final protein concentration of 100 ng/mL). Fluorescein-labelled *E. coli* K-12 bioparticles were prepared by thawing a vial of fluorescent particles and a vial of concentrated Hanks buffered saline solution (HBSS). The HBSS was pipetted into the fluorescent vial and sonicated briefly. The sonicated bioparticles were then transferred to a sterile glass McCartney containing 4.5 mL of ddH_2O. After the differentiated cells had been incubated with the test proteins for one hour, 50 µl of the fluorescent bioparticle suspension was added to each tube, gently mixed and incubated at 37 ºC for 1 hour. Tubes were centrifuged at 1000 x g for 5 minutes using an Eppendorf 5804 centrifuge before aspirating the supernatant. During this time, a vial of trypan blue is thawed and transferred to a McCartney containing 4 ml of ddH_2O. This trypan blue is used to quench the fluorescence of any extracellular fluorescent bioparticles that have not been engulfed, by adding 100 µl to the cells and incubating for 1 minute before adding 500 µl of PBS and centrifuging as before. The trypan blue was aspirated and samples were washed twice with PBS. Samples were resuspended in 500 µl of PBS and measured using the 488 nm laser on a Beckman Coulter FC500 flow cytometer on FL1.

3.2.10 Reactive Oxygen Species

To measure ROS, the dye DCF-DA can be used. It is freely permeable and incorporates into the hydrophobic lipid regions of the cell. The acetate moieties are cleaved, leaving a non-fluorescent 2'7'-dichlorofluorescin. This is oxidised by hydrogen peroxide and peroxidases into dichlorofluorescein which is fluorescent (Robinson *et al.*, 1994).

Differentiated cells were centrifuged and resuspended in PBS at $1x10^6$ cells/ml and stained with 2.5 μM DCF-DA for 30 minutes at 37 ºC in the dark. Cells were centrifuged at 1000 x g and washed three times with PBS to remove any remaining stain and the cells are resuspended in RPMI1640 medium with 10% FCS. Flow cytometry tubes were labelled and aliquots of 200 μl of test sample or medium control are added to each tube, before adding an equal volume of the cell suspension and mixing gently. This was incubated at 37 ºC in the dark for 30 minutes, 1 hour and 24 hours. CD23 proteins were tested at a final concentration of 100 ng/ml and 100 ng/ml PMA was used as a positive control. After the incubation period, EDTA is added to a final concentration of 50 mM to stop the reaction, before reading sample fluorescence on a Beckman Coulter FC500 flow cytometer.

Results were analysed using the mean fluorescence intensity of samples in triplicate. Because the cells are loaded with the dye prior to the experiment, it is difficult to get the same level of fluorescence in cells throughout all experiments. Therefore the mean fluorescence intensity of each sample was normalised as a percentage of the average of the control samples for that particular experiment, and the experimental control set at 100 percent.

3.2.11 Signalling pathway inhibition

To investigate which signal transduction pathway is involved with sCD23 and CD11 interactions leading to ROS production, five different inhibitors were chosen. Adenine 9-β-arabinofuranoside (ara) has been used to characterise the role of AMP-kinase (AMPK) in cells (Derave *et al.*, 2000). Wedelolactone is an inhibitor of IκB kinase

(IKK), which is essential for the phosphorylation and degradation of IκBα that allows NF-κB activation to occur (Kobori *et al.,* 2004). PD169316 is a selective inhibitor of p38 MAPK which has an inhibitory effect on p38 MAPK at an IC50 of 89 nM and an inhibitory effect on ERK at an IC50 100-fold higher than this (Kim *et al.* 2006; Gallagher *et al.,* 1997; Fu *et al.* 2003). PP2 is a potent selective inhibitor of Src kinases (Hanke *et al.,* 1996; Lee *et al.*, 2004). Wortmannin is a potent inhibitor of the enzymatic activation of PI3K. Interestingly, it has also been shown that wortmannin inhibits the activation of NF-κB and AP-1 by LPS and PMA, but not their activation by TNF, ceramide or H_2O_2 (Manna and Aggarwal, 2000).

Differentiated cells were centrifuged and resuspended in PBS at $1x10^6$ cells/ml and stained with 2.5 μM DCF-DA for 30 minutes at 37 ºC in the dark. Cells were centrifuged at 1000 x g and washed three times with PBS to remove any remaining stain and the cells resuspended in RPMI1640 medium with 10% FCS. Flow cytometry tubes were labelled and aliquots of 100 μl of pathway inhibitor or medium control added to each tube, before adding an equal volume of the cell suspension and mixing gently. Concentrations of inhibitors used were ara (1mM), PD169316 (20 μM), PP2 (10 μM), wedelolactone (100 μM) and wortmannin (100 nM). Samples were then incubated for 30 minutes at 37 ºC before adding 200 μl of the test protein and mixing gently. A further 60 minute incubation followed before the reaction was stopped by adding EDTA to a final concentration of 50 mM. Samples were then analysed with a Beckman Coulter FC500 flow cytometer as previously mentioned. Due to the difficulty of handling such a large number of samples for this experiment, a large batch of cells would be stained and the experiment was staggered over three hours. A control panel would be analysed first, made up of control cells with and without each different inhibitor. Thirty minutes later a panel would be set up from the

same batch of stained cells for derCD23, with a medium only control tube and the tubes with all the inhibitors added. After thirty minutes, the derCD23 protein was added to the positive control tube and the tubes containing the inhibitors. This was repeated for the other two CD23 proteins. The results were analysed in the same way as the ROS experiments in Section 3.2.10. Where the inhibitors are added to cells without protein, the control used was cells with no inhibitor. However, in the experiments where the CD23 proteins were added after the inhibitors, the control used was the cells incubated with the relevant protein.

3.2.12 NF-κB

NF-κB is a ubiquitous transcription factor found in an inactive form in the cytoplasm by its association with a class of inhibitory IκB proteins. NF-κB's activation is brought about by the phosphorylation of IκB by IKK. This causes IκB to degrade and NF-κB can translocate into the nucleus where it binds to DNA elements and positively regulates the transcription of genes involved in immune and inflammatory responses, cell growth and apoptosis. It controls the transcription of TNFα, IL-2, IL-6, IL-8, lymphotoxin, GM-CSF, β-interferon and adhesion molecules. In neutrophil-induced tissue destruction, the release of inflammatory mediators is mediated by β_2 integrins. It has also been reported that monocyte β_2 integrin-mediated cytokine production is due to NF-κB activation (Kim *et al.*, 2004). CD11b aggregation induces IKK activation, subsequent NF-κB activation and proinflammatory cytokine activation (Kim *et al.*, 2004).

The production of NF-κB by differentiated cells was investigated using flow cytometry. Differentiated cells were centrifuged and resuspended in fresh medium as

above. They were then exposed to control medium, wedelolactone inhibitor (100 μM) and the three CD23 proteins (100 ng/ml), for 15 or 30 minutes before being centrifuged and washed with PBS. Cells were fixed and permeablised using Intraprep Permeabilization reagent. Reagent 1 consists of 5.5 % formaldehyde and 100 μl was added to 5 x 10^5 cells, vortexed vigorously and incubated at room temperature for 15 minutes. PBS was then added to make up 4 ml and the samples were centrifuged at 300 x g for 5 minutes. The supernatant was aspirated and 100 μl of reagent 2 was added (a saponin-based permeabilising and lysing medium). The samples were incubated for 5 minutes at room temperature before gently agitating for 2 seconds. The samples were centrifuged and washed before resuspending in 90 μl incubation buffer (0.5 % BSA in PBS) and incubating for 30 minutes at room temperature. Ten μl of anti-human phospho-NF-κB p65 (Ser536)(93H1) rabbit mAb (Alexa Fluor®488 Conjugate) was added and incubated in the dark at room temperature for 1 hour. Samples were centrifuged and washed twice before resuspending in 500 μl of PBS and analysed using the 488 nm laser on a Beckman Coulter FC500 flow cytometer on FL1.

3.2.13 Nitric Oxide

The level of nitric oxide produced by cells under the influence of recombinant sCD23 proteins was investigated using the dye, DAF-DA. This is a membrane permeable dye, which, once it has entered the cells, reacts with NO in the presence of oxygen to form the highly fluorescent triazolofluorescein (DAF-2T). DAF2 gives nanomolar detection of NO (Bartoz, 2006).

Cells were washed and resuspended at 1 x 10^6 cells/ml. DAF-DA was added to a concentration of 1 μg/ml (2.2 μM) for 30 minutes at 37ºC. Cells were centrifuged at 100 x g and resuspended in fresh RPMI1640 medium with 10% FBS and incubated for a further 30 minutes at 37 ºC to allow complete de-esterification of the intracellular diacetates. Cells were centrifuged as before and resuspended in fresh medium at 1 x 10^6 cells/ml and aliquoted into 24-well plates (200 μl) with an equal volume of control or CD23 proteins (final concentration of 100 ng/ml). Cells were incubated for 24 hours at 37 ºC. After the incubation time, cells were transferred into flow cytometry tubes and analysed using the 488 nm laser on a Beckman Coulter FC500 flow cytometer on FL1.

3.2.14 Myeloperoxidase

MPO is an abundant enzyme released by activated neutrophils, monocytes and macrophages. MPO can amplify the oxidising potential of H_2O_2 by using it as a co-substrate to generate a variety of oxidants, including diffusible radical species, reactive halogens, aldehydes and nitrating agents. MPO can use H_2O_2 and nitrite to generate reactive intermediates that are able to nitrate aromatic compounds and tyrosine residues. HOCl can also react with NO_2^- to form a nitrating and chlorinating intermediate (Chrisholm *et al.*, 1999).

The production of MPO by differentiated cells was investigated using flow cytometry. Differentiated cells were centrifuged and resuspended in fresh medium as above. They were then exposed to control medium and the three CD23 proteins (100 ng/ml) for 24 hours before being centrifuged and washed with PBS. Cells were fixed and permeablised using Intraprep Permeabilization reagent as described in Section 3.2.12.

Twenty µl of a 5x dilution of 12.5 µg/ml stock of anti-human MPO conjugated to FITC was added and incubated in the dark at room temperature for 30 minutes. Samples were centrifuged and washed twice before resuspending in 500 µl of PBS and analysing using the 488 nm laser on a Beckman Coulter FC500 on FL1.

3.2.15 Cytokines

The secretion of IL-6, IL-1β and TNF-α by cells treated with recombinant CD23 proteins was investigated by ELISA. Cells (500 µl of a 1 x 10^6 cells/ml suspension) were aliquoted into 24-well plates (Nunc) with an equal volume of medium containing recombinant proteins (to a final concentration of 100 ng/ml) or LPS and incubating at 37 ºC for 24 hours. The supernatants were removed into sterile Eppendorfs and frozen at -80 ºC until analysis. All three cytokines were analysed using kits from eBioscience according to manufacturer's instructions. Briefly, 100 µl of capture antibody, diluted in coating buffer, was added per well of a Nunc Maxisorp 96-well ELISA plate. The plate was sealed with parafilm and incubated overnight at 4 ºC. Wells were aspirated and washed 5 times with 200µl /well wash buffer (0.05% Tween-20 in PBS). Wells were blocked by adding 200 µl/well of assay diluent and incubated at room temperature for 1 hour. Plates were aspirated and washed as previously described. A standard curve was constructed by diluting the kit standard in assay diluent and making two-fold dilutions of this standard. The standard and samples were added to the plate (100 µl/well), covered and incubated overnight at 4 ºC for maximal sensitivity. The plates were aspirated and washed as previously described before adding 100 µl/well of detection antibody diluted in assay diluent and incubating for 1 hour at room temperature. The plates were aspirated and washed as previously described. Avidin-horseradish peroxidase (HRP), diluted in assay diluent,

was added to each well (100 µl) and incubated at room temperature for 30 minutes. The plates were aspirated and washed with 200 µl of wash buffer seven times, before adding 100 µl of substrate solution and incubating at room temperature. After a blue colour had developed, the reaction was stopped by adding 50 µl of stop solution (2N H_2SO_4) and reading the plates at 450 nm on a Powerwave XS multiplate reader (Biotek). A reference wavelength of 570 nm was also read and subtracted from the 450 nm values.

3.2.16 Data analysis

Statistical analysis was performed using Graphpad Prism 5 software. Data were analysed using a 1 way ANOVA with Tukeys Multiple Comparison post-test.

3.3 Results

3.3.1 Cell Differentiation

Various differentiating agents were compared for their ability to differentiate three cell lines into a monocytic lineage. This was done by incubating the cells with the differentiation agents for three days before testing for cell surface upregulation of CD11b. In Figure 3.2, we can see that all the differentiation agents were able to upregulate CD11b on the cell surface and therefore cause differentiation of cells. Figure 3.2 (A) shows the effect of differentiating agents on HL60 cells. PMA and retinoic acid show similar upregulation, but vitamin D_3 shows much higher upregulation of CD11b. The upregulation of CD11b on THP1 cells is not as high as in the HL60 or U937 cells [Figure 3.2 (B)]. Retinoic acid showed the lowest level of

upregulation while vitamin D_3 and PMA showed a much higher upregulation of CD11b. Upregulation of CD11b on U937 cells is similar to the upregulation seen in HL60 cells [Figure 3.2 (C)]. Again, PMA and retinoic acid caused similar upregulation, while vitamin D_3 showed a much higher upregulation of CD11b.

However, this differentiation was at the cost of cell viability with regard to PMA and retinoic acid. It was noted that PMA and retinoic acid caused substantial cell death in all cell lines after three days of differentiation, while the addition of vitamin D_3 as a differentiation agent did not appear to have any adverse effect on cell viability (data not shown). For the purpose of this study, it was important to choose a differentiation agent that caused a substantial increase in cell surface expression of CD11b and CD11c. It was therefore decided to use vitamin D_3 as a differentiation agent for all experiments.

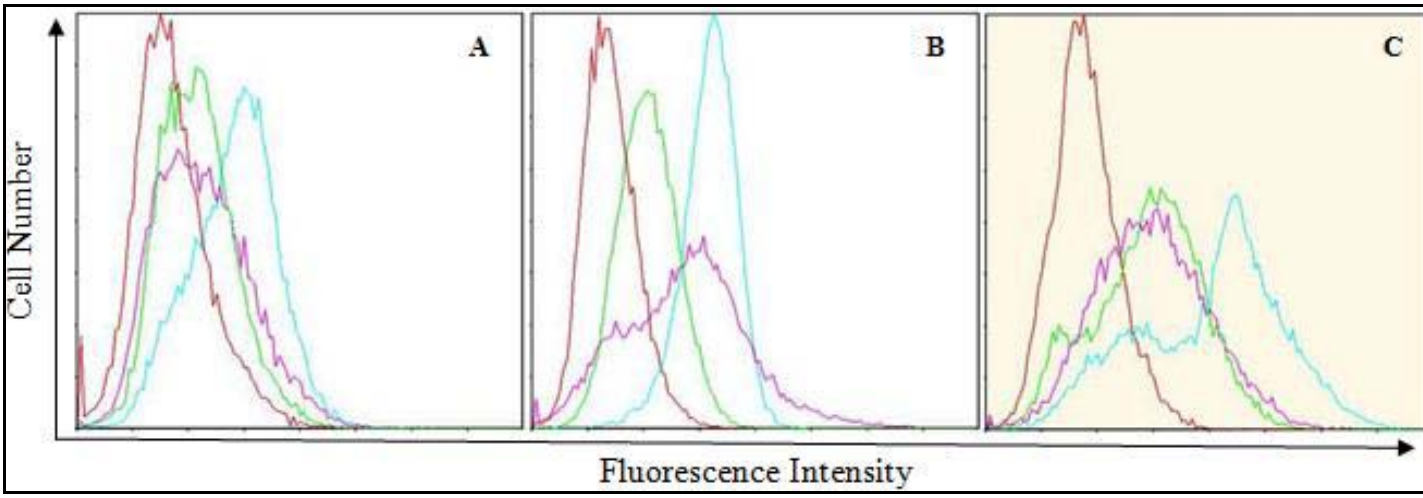

Figure 3.2: Histogram overlays comparing CD11b upregulation by differentiation agents in A) HL60, B) THP1 and C) U937 cells. $1x10^6$ cells were exposed to medium (red line) 100 ng/mL PMA (pink line), 100 nM RA (green line) and 1 μM vitamin D_3 (blue line) for 72 hours before being stained for CD11b and analysed with a flow cytometer.

Figure 3.3 shows the cell surface expression of CD11b and CD11c for both vitamin D_3 differentiated and undifferentiated cells used for experimentation. The overlays demonstrate that although undifferentiated cells do express a low level of CD11b and CD11c, the differentiated cells express a much higher level of these proteins.

Figure 3.3 (A and B) shows the expression of CD11b and CD11c in undifferentiated and differentiated HL60 cells, respectively. The undifferentiated cells show the presence of CD11b and CD11c in comparison to the negative isotype control, which indicates a low basal level of CD11b and CD11c on the cell surface of undifferentiated cells. The differentiated cells show a large shift in expression of both the integrins, although the expression of CD11b shows a much more significant upregulation of this integrin. This was expected as previous literature shows that CD11c is not upregulated to the same degree as CD11b in these cells (Miller *et al.*, 1986).

THP1 cells show a different pattern of upregulation of integrins (Figure 3.3 C and D). It appears that these cells show more cell surface expression of CD11c than CD11b in undifferentiated cells. In the same way, the upregulation of the two cell surface markers after differentiation shows that the shift in upregulation of CD11c is greater than the shift seen in CD11b upregulation.

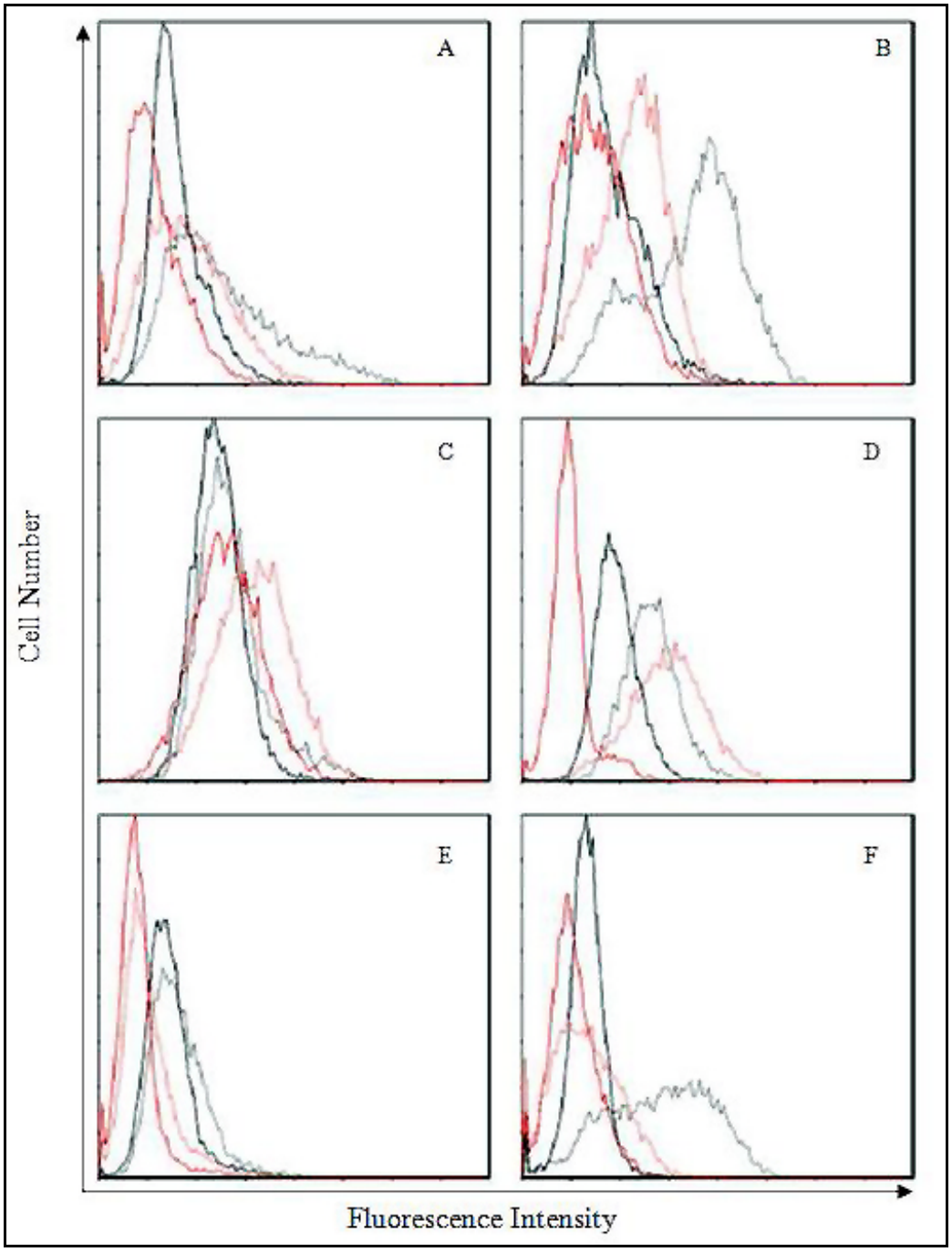

Figure 3.3: Expression of CD11b and CD11c on undifferentiated and vitamin D_3 differentiated cell lines. (A) HL60 undifferentiated, (B) differentiated HL60, (C) THP1 undifferentiated, (D) differentiated THP1, (E) U937 undifferentiated and (F) differentiated U937. In (A), (C) and (E) CD11 expression is relative to an isotype control; while in (B), (D) and (F) CD11 expression is relative to undifferentiated cells. Solid black line represents CD11b control expression while the dotted black line indicates CD11b experimental culture expression. Solid red line represents CD11c control expression while the dotted red line indicates CD11c experimental culture expression.

Figure 3.3 (E and F) shows the cell surface expression of CD11b and CD11c on undifferentiated and differentiated U937 cells, respectively. Again, the presence of the two integrins in undifferentiated cells can be seen in low amounts, while the addition of vitamin D_3 increases the cell surface expression of these β_2 integrins. The U937 cells show a similar expression profile to the HL60 cells, with CD11b being upregulated to a larger extent than CD11c.

The upregulation of CD11b was analysed before every experiment carried out, to ensure differentiation of the cell culture prior to use.

3.3.2 $CD14^+$ PBMC isolation

Monocytes were isolated from PBMCs using MACS technology. CD14 was used as an isolation antibody, as this is a cell surface marker found mainly on monocytes. CD11b could have been used to isolate monocytes from the PBMCs, however there is then the risk that the magnetic antibody will block any subsequent interactions between sCD23 and CD11b on the cell surface. Figure 3.4 shows the CD14 staining of PBMCs prior to MACS isolation and after isolation. The purity of the isolated cells was estimated to be approximately 95%.

The isolated cells were then used to investigate their response to sCD23 proteins with regard to their chemotactic, phagocytic and oxidative burst.

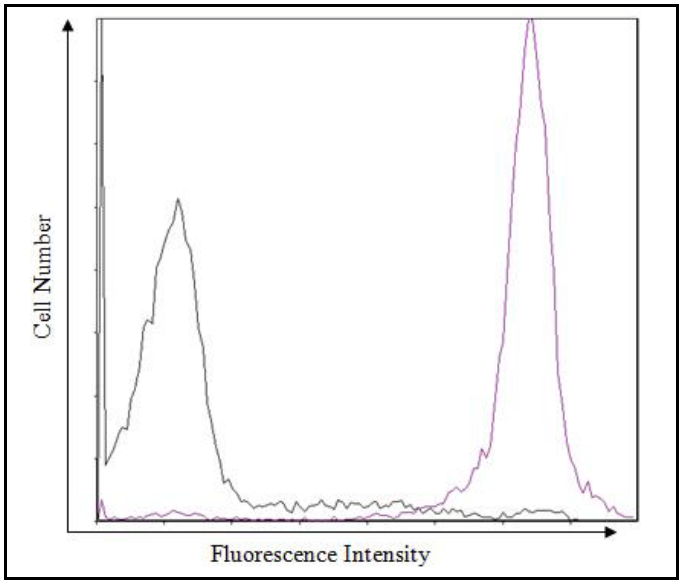

Figure 3.4: Overlay plot of CD14 staining in MACS isolated $CD14^+$ cells from PBMCs. The black line represents CD14 staining of the original PBMC population, while the purple line represents the histogram of CD14 staining in MACS isolated cells.

3.3.3 Chemotaxis

The β_2 integrins are believed to play a very important role in the chemotactic response of leukocytes. This chemotactic ability was tested using a Cell Migration Assay from Chemicon International. Due to the expense of the kits, these experiments were only conducted on differentiated cells.

Figure 3.5 (A) shows the percentage of chemotaxis of HL60 cells compared to control cells that only had the chemoattractant added to the bottom well, where the control is set at 100%. As we can see from the graph, the positive control (10% serum in medium) produced a significantly positive result, which was expected since the cells were serum starved for at least 18 hours prior to experimentation. The figure also shows that although the percentage of chemotaxis is lowered slightly with fibrinogen

and the sCD23 proteins, only derCD23 is able to significantly lower the chemotactic ability of the cells in response to fMLP.

Figure 3.5 (B) shows the percentage of chemotaxis of differentiated THP1 cells compared to control cells. Again, the positive control is significantly positive while the fibrinogen and recombinant CD23 proteins show a slight decrease in chemotaxis. Only the fibrinogen and CD23M150 are able to elicit a significant decrease in chemotaxis.

The effect of sCD23 proteins on the differentiated U937 cell line can be seen in Figure 3.5 (C). As demonstrated by the previous two cell lines, the positive control for this cell line is significantly positive. This cell line showed an increase in chemotaxis with the CD23M79 protein, although this increase was not significant in either of the experiments. Fibrinogen and CD23M150 also showed a decrease in chemotaxis, although this was not significant. The derCD23 protein, however, showed a significant decrease in chemotaxis, similar to the HL60 cell line.

Figure 3.5 (D) shows the chemotaxis of $CD14^{+}$ cells isolated from PBMCs. The positive control in this experiment was higher than the control, but due to large variation in the experiment this increase in chemotaxis was not significant. The CD23M150 and CD23M79 proteins also showed an increase in chemotaxis, but also showed a large variation in values, resulting in them not being significantly different to the control response. The fibrinogen and derCD23 showed a decrease in chemotaxis, with the derCD23 being significantly lower than the control.

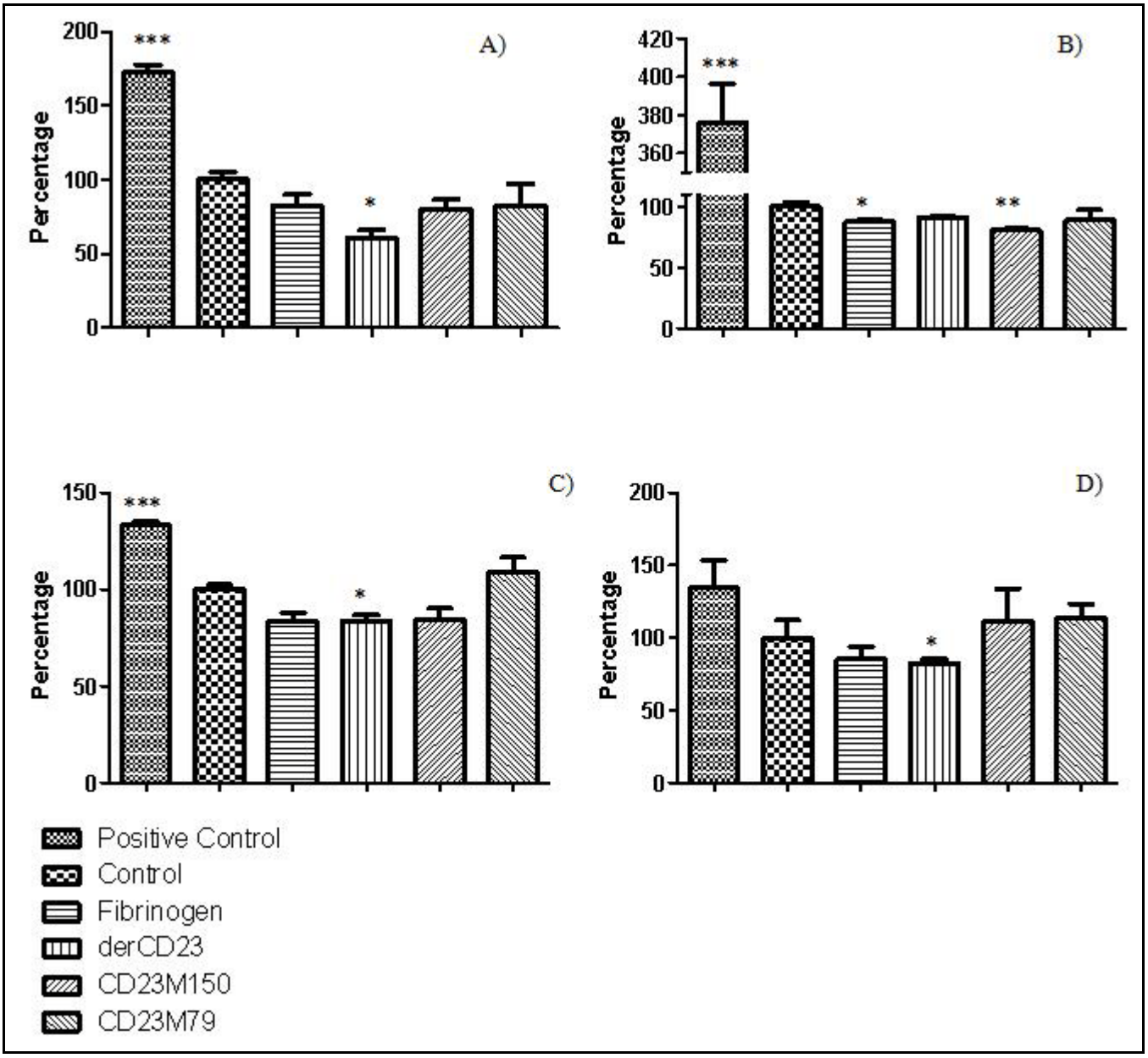

Figure 3.5: Chemotaxis of (A) HL60, (B) THP1, (C) U937 and (D) $CD14^+$ cells. Differentiated cells were incubated with medium as the control, 10% serum as the positive control and 100 ng/ml of fibrinogen or CD23 proteins for 24 hours and allowed to migrate using fMLP as a chemoattractant. Error bars represent SEM of an experiment done in triplicate. This figure represents one of two experiments in triplicate, where the results were similar in both experiments, except for the $CD14^+$ cells where only one experiment in triplicate was performed. Asterisks represent significant differences compared to control where (***) is equivalent to $P<0.0005$, (**) is equivalent to $P< 0.005$ and (*) is equivalent to $P< 0.05$.

The chemotaxis experiments showed that there was little change in the response of cells to the chemoattractant fMLP in the presence of sCD23 proteins and fibrinogen. derCD23, however, showed a small but significant decrease in chemotaxis in the HL60 and U937 cell lines, as well as the $CD14^{+}$ isolated PBMCs. CD23M79 and fibrinogen were able to significantly decrease the chemotactic ability of cells in THP1 cells.

3.3.4 Phagocytosis

The β_2 integrins are involved in the ability of neutrophils, macrophages and monocytes to phagocytose foreign particles. This phagocytic ability is activated by the binding of ligands to β_2 integrins. This experiment, therefore, tested the phagocytic response of cells exposed to sCD23 proteins, as ligands of CD11b and CD11c.

Figure 3.6 (A) shows the percentage of phagocytosis in differentiated HL60 cells compared to control cells which were differentiated, but treated with PBS instead of protein. The positive control, PMA, showed a significant increase in phagocytosis as expected. The CD23M79 protein showed an increase in phagocytosis by cells, although this was not significant. Fibrinogen, derCD23 and CD23M150 all showed a decrease in phagocytosis, although this decrease was only significant in the case of fibrinogen and derCD23.

Figure 3.6 (B) shows the same experiment in THP1 differentiated cells. In this cell line, no significant changes in phagocytic ability were observed. The positive control of PMA, which increased the phagocytic ability of the HL60 and U937 cells, had no significant effect on the cells, even causing a decrease in phagocytosis in this cell line.

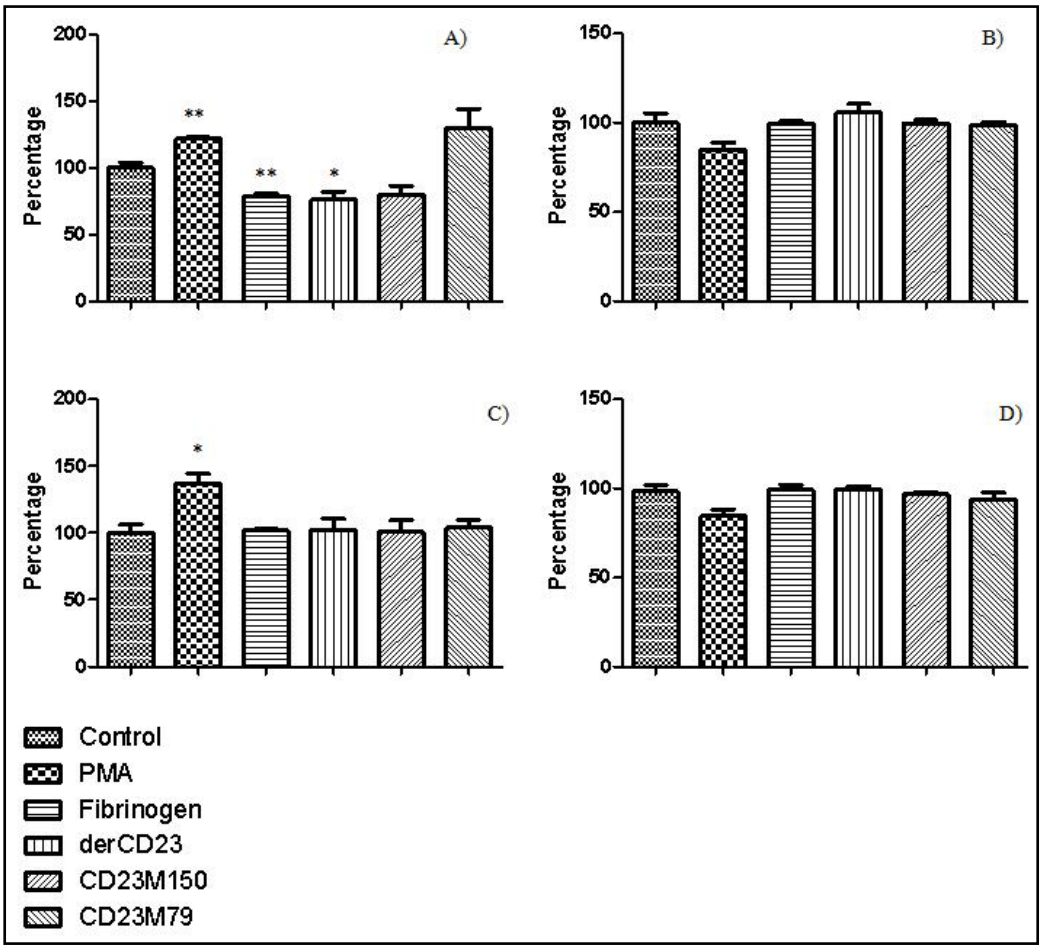

Figure 3.6: Phagocytosis of *E. coli* K12 cells by differentiated (A) HL60, (B) THP1, (C) U937 and (D) $CD14^+$ cells. Cells were preincubated with PBS (control), PMA (positive control), fibrinogen and CD23 proteins for 1 hour prior to adding *E. coli* K12 cells. Cells were incubated for a further hour before being washed and analysed for phagocytosis. Error bars represent SEM of an experiment done in triplicate. This graph represents one of three experiments, showing similar results for all experiments, except for the $CD14^+$ experiment which was only done once. Asterisks represent significant differences compared to control where (**) is equivalent to $P< 0.005$ and (*) is equivalent to $P<0.05$.

The U937 cell line also showed little effect on phagocytosis when treated with recombinant sCD23 proteins and fibrinogen [Figure 3.6 (C)]. The PMA positive control showed a significant increase in phagocytic ability of the cells, as expected.

The $CD14^+$ PBMCs responded in the same way as the differentiated THP1 cells when the effect of sCD23 proteins on phagocytic ability was investigated [Figure 3.6 (D)]. As with the THP1 cells, a decrease in phagocytosis was seen with PMA, while the recombinant sCD23 proteins and fibrinogen showed no change in phagocytic ability.

The same experimental design was then used to investigate whether the sCD23 proteins would have any effect on the undifferentiated cell lines. The HL60 cell line showed again that PMA is a good positive control due to the significantly higher phagocytic ability of the cells [Figure 3.7 (A)]. The fibrinogen and sCD23 proteins proved to have little effect on the phagocytic ability of the cells, with CD23M79 showing a slight decrease in phagocytic ability, but this was not significant.

Similarly, Figure 3.7 (B) shows that the phagocytic ability of undifferentiated THP1 cells is unaffected by the addition of sCD23 proteins or fibrinogen. The positive control shows a significant increase in the phagocytosis by the cells, as expected.

Undifferentiated U937 cells showed an increase in phagocytosis in response to fibrinogen and all three sCD23 proteins; however these differences were not significant (Figure 3.7 (C)). The PMA control showed a large significant increase in phagocytosis.

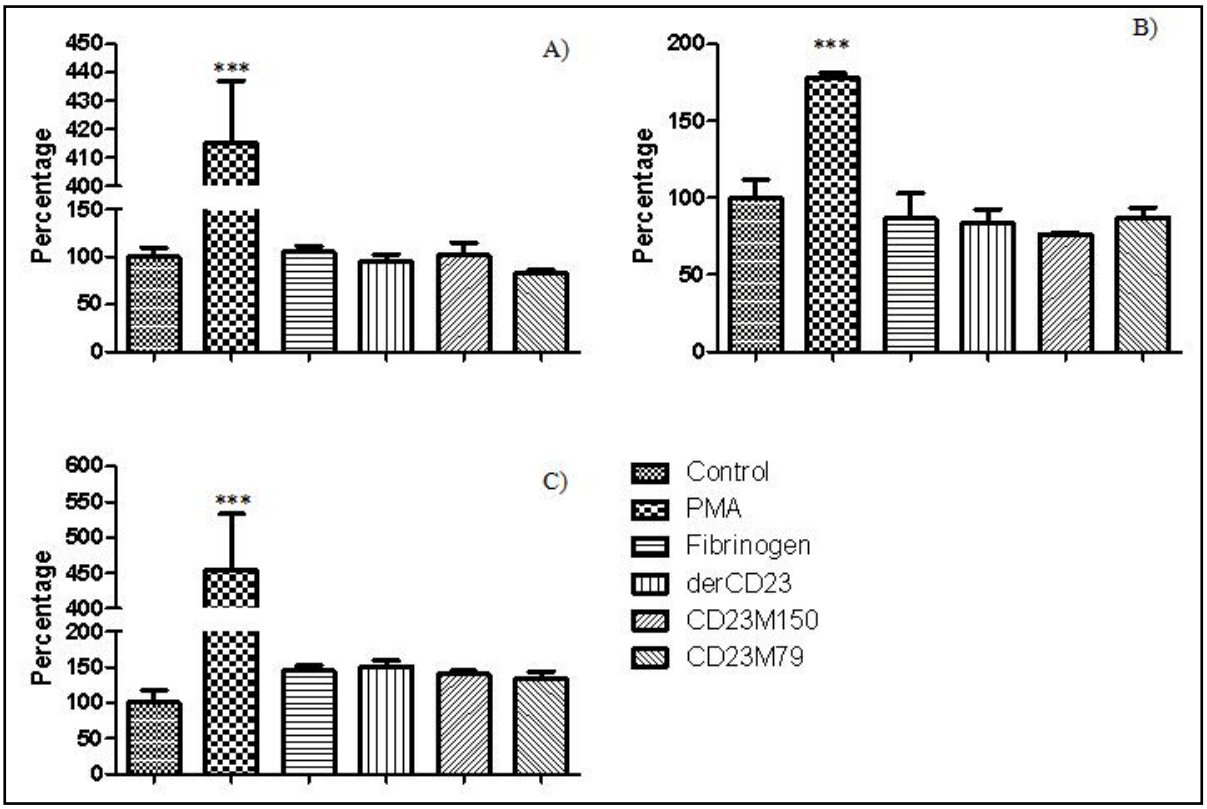

Figure 3.7: Phagocytosis of *E. coli* K12 cells by undifferentiated (A) HL60, (B) THP1 and (C) U937 cell lines. Cells were preincubated with PBS (control), PMA (positive control), fibrinogen and CD23 proteins for 1 hour prior to adding *E. coli* K12 cells. Cells were incubated for a further hour before being washed and analysed for phagocytosis. Error bars represent SEM of an experiment done in triplicate. This graph represents one of three experiments, which gave similar results. Asterisks represent significant differences compared to control where (***) is equivalent to P< 0.0005.

In general, the recombinant sCD23 proteins showed no effect on phagocytosis. derCD23 was able to significantly decrease phagocytosis in differentiated HL60 cells, but this was the only change in the ability of the cells to phagocytose *E. coli* bioparticles, apart from the positive control in each experiment.

3.3.5 Reactive Oxygen Species

ROS are very important in the regulation of signalling pathways in mononuclear phagocytes. Therefore the effect of soluble CD23 proteins on the production of ROS

in these cells was investigated. The experiment was conducted at different time points to ascertain what the best time point was to compare ROS production. ROS was initially tested at 30 minutes, 60 minutes, 120 minutes and 24 hours. However, the effects seen at 30 and 60 minutes had dissipated by 120 minutes and 24 hours. Therefore the results are shown only for the 30 and 60 minute experiments.

After thirty minutes of incubation, HL60 cells showed little change in ROS except for the positive control, which showed a significant increase in ROS, and CD23M79, which showed a small, yet significant, decrease in ROS production compared to the control cells [Figure 3.8 (A)]. After a further thirty minute incubation, the differentiated HL60 cells show a significant increase in the production of ROS by the positive control, fibrinogen, derCD23 and CD23M150 [Figure 3.8 (B)]. Again, the CD23M79 shows a slight decrease in ROS production, but this reduction is no longer significant after 60 minutes.

The THP1 differentiated cell line showed a significant increase in ROS by PMA as expected [Figure 3.8 (C)]. derCD23 demonstrated a small, but significant, increase in ROS production, while all other proteins showed no significant difference from the control cells after 30 minutes. Figure 3.8 (D) shows that the production of ROS increases significantly 60 minutes after the addition of PMA, fibrinogen, derCD23 and CD23M150. CD23M79 again shows no significant upregulation of ROS production.

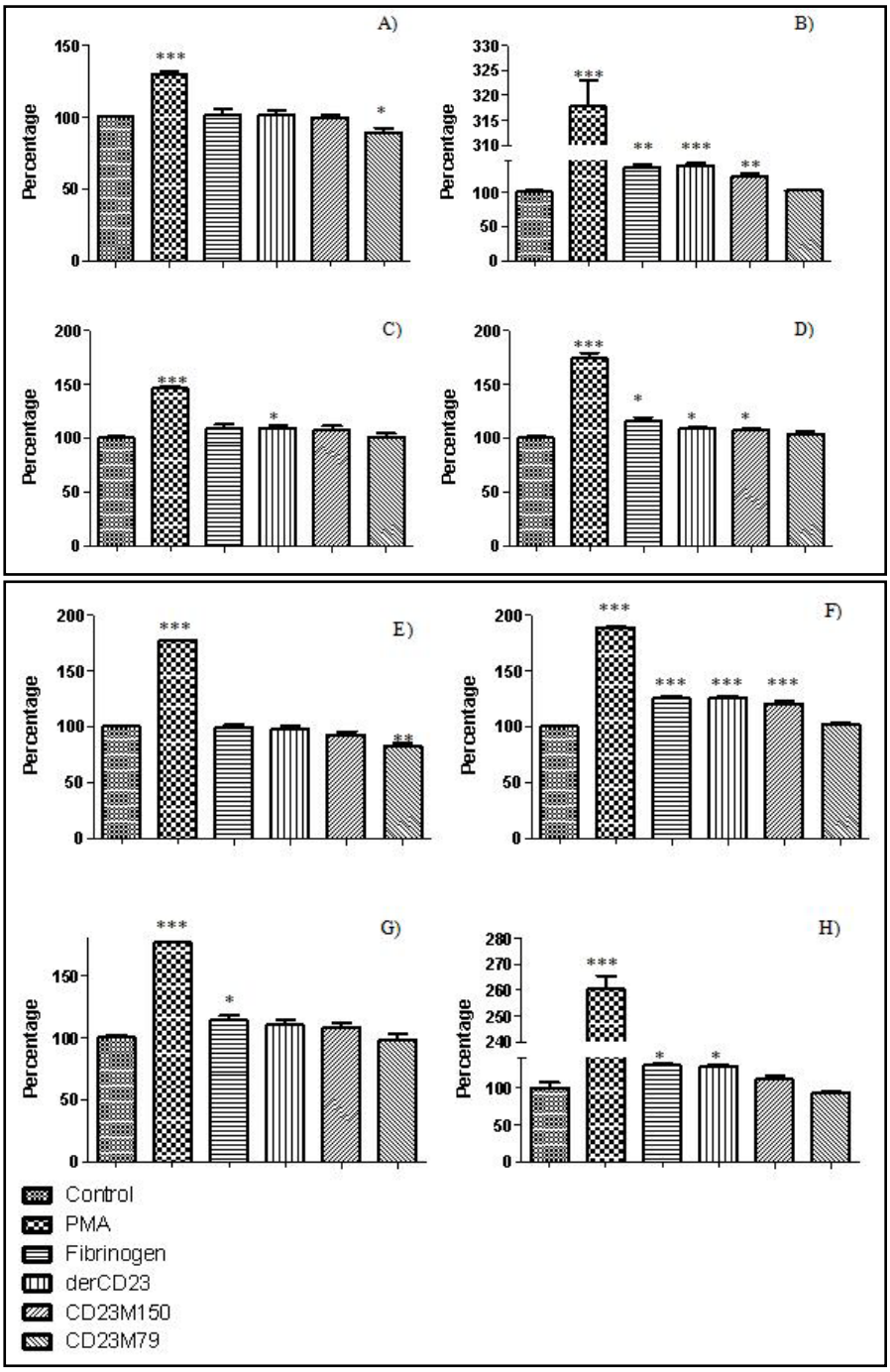

Figure 3.8: ROS production by differentiated HL60, THP1, U937 and $CD14^+$ cells. HL60 (A;B); THP1 (C;D); U937 (E;F); $CD14^+$ cells (G;H) were treated for 30 minutes (A;C;E;G) and 60 minutes (B;D;F;H) with PBS (control), PMA (positive control), fibrinogen or CD23 proteins. Error bars represent SEM of an experiment done in triplicate. This graph represents one of four experiments, all showing similar results, except in the case of CD14+ cells, where it represents one experiment. Asterisks represent a significant difference compared to control where (***) is equivalent to $P<0.0005$, (**) represents $P<0.005$ and (*) represents $P<0.05$.

The U937 cell line produced similar results as the HL60 and THP1 cell line for ROS production after 30 minutes [Figure 3.8 (E)]. The production of ROS was significantly increased by PMA, while the ROS production was decreased significantly by CD23M79. The addition of fibrinogen, derCD23 and CD23M150 did not significantly influence the production of ROS by the U937 cells after 30 minutes. The decrease in ROS caused by CD23M79 appears to have stabilised after 60 minutes and is no longer significantly lower than the control [Figure 3.8 (F)]. The production of ROS is significantly increased after 60 minutes with PMA, fibrinogen, derCD23 and CD23M150. This again shows similar trends in the stimulation of ROS production by the derCD23 and CD23M150 as the HL60 and THP1 cell lines.

The same experiment was carried out using the $CD14^+$ PBMCs [Figures 3.8 (G) and (H)]. The PMA positive control increased the production of ROS significantly after both 30 and 60 minutes. Fibrinogen showed a small but significant increase in ROS production after 30 minutes and 60 minutes. The CD23M150 and CD23M79 showed little effect on the production of ROS after both 30 and 60 minutes. derCD23, however, showed little effect after 30 minutes, but showed a significant increase in ROS production after 60 minutes.

The same experiments were then carried out using undifferentiated cells from the three cell lines. HL60 cells show little effect on ROS after 30 minutes [Figure 3.9 (A)], with only the positive control showing a significant difference. The production of ROS in HL60 cells is significantly upregulated by PMA, fibrinogen, and all three sCD23 proteins after 60 minutes [Figure 3.9 (B)]. It is important to note, however, that the upregulation of ROS by CD23M79 is not as substantial an upregulation and is not as significant a result as the other two CD23 proteins.

Undifferentiated THP1 cells show little effect on ROS production after 30 minutes [Figure 3.9 (C)]. The PMA positive control shows a significant increase in ROS production as expected. The PMA positive control continues to stimulate ROS production by undifferentiated THP1 cells after 60 minutes [Figure 3.9 (D)]. Fibrinogen is also able to stimulate a significant increase in ROS production while derCD23 and CD23M150 show little effect above the control samples. Again, CD23M79 produces different ROS production to the shorter sCD23 proteins, and shows a significant decrease in ROS production by undifferentiated THP1 cells.

Figure 3.9 (E) shows the effect of soluble CD23 proteins on undifferentiated U937 cells after 30 minutes. There is an increase in ROS production in all samples, except for CD23M79, where there is a decrease. However, the only significant change in ROS production is seen with the PMA positive control. Figure 3.9 (F) shows the production of ROS by undifferentiated U937 cells after 60 minutes. As was seen in the same experiments with HL60 and THP1 cells, there was a significant increase in the production of ROS with PMA, fibrinogen, derCD23, and CD23M150. However, it must again be noted that the CD23M79 protein is producing no increase in ROS production.

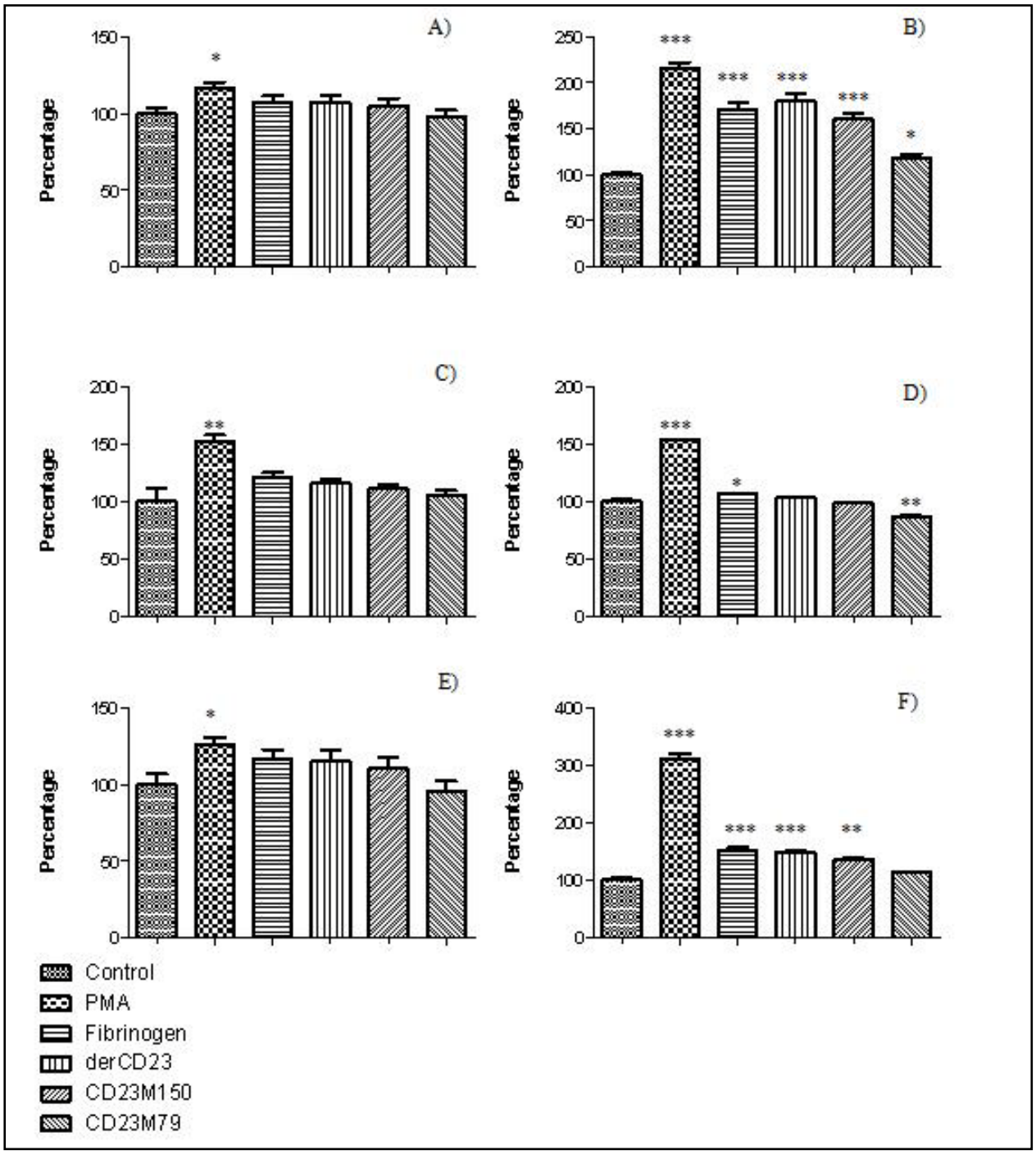

Figure 3.9: ROS production by undifferentiated HL60, THP1 and U937 cell lines. HL60 (A;B); THP1 (C;D); U937 (E;F) were treated for 30 minutes (A;C;E) and 60 minutes (B;D;F) with PBS (control), PMA (positive control), fibrinogen or CD23 proteins. Error bars represent SEM of an experiment done in triplicate. This graph represents one of two experiments, all showing similar results. Asterisks represent a significant difference compared to control where (***) is equivalent to $P<0.0005$, (**) represents $P<0.005$ and (*) represents $P<0.05$.

Several general trends are noticed in these experiments. The effect of the recombinant proteins on ROS is most significant after 60 minutes. If we examine this time point for the cell lines, we see that in differentiated cells, fibrinogen consistently causes an increase in ROS production in all cell lines and the primary cells. In the same way, derCD23 also shows a consistently significant increase in ROS production by all differentiated cell lines and the primary cells at 60 minutes. CD23M150 is also able to significantly increase the production of ROS in all the cell lines, but not in the primary isolated cells. The CD23M79 protein shows no effect on the production of ROS.

The undifferentiated cells show different trends in ROS production to the differentiated cells. Again, fibrinogen is able to increase ROS production significantly. However, derCD23 is only able to significantly increase ROS production in HL60 and U937 cells. In the same way, CD23M150 is also able to significantly increase ROS production in HL60 and U937 cells. However, CD23M79 shows a significant increase in ROS production in HL60 but decrease in THP1 cells.

3.3.6 Pathway inhibition

Due to the effects that the recombinant CD23 proteins had on the production of ROS by cells, it was decided to investigate what effect there would be on the production of ROS in the cell lines if inhibitors to signalling pathways were added to the cells prior to the proteins being added. These pathway inhibition experiments were also conducted on undifferentiated cells to determine what the effects of differentiation of the cell lines are.

It is important to note what effect these inhibitors have on untreated cells to enable effective comparison to the cells treated with proteins. Figure 3.10 (A) shows the effect of inhibitors on differentiated, untreated HL60 cells. The graph shows that the inhibitors had little effect on the production of ROS by the cells, except for ara, which showed that the blocking of AMPK significantly increases the production of ROS in differentiated HL60 cells. The addition of derCD23 to differentiated HL60 cells appeared to cause no significant increase in the production of ROS above the control in differentiated HL60 cells where AMPK, p38 MAPK, Src kinase, and PI3K had been inhibited [Figure 3.10 (B)]. There was however a significant increase in the production of ROS when IKK was inhibited. The CD23M150 protein showed no significant increase in ROS production in differentiated HL60 cells after the addition of pathway inhibitors [Figure 3.10 (C)]. The inhibitors for PI3K and IKK appeared to show a decrease in ROS production, however, these decreases were not statistically significant. In the same way as CD23M150, the CD23M79 protein appears to show no increase in ROS production in the HL60 differentiated cells with the addition of pathway inhibitors [Figure 3.10 (D)]. As with the CD23M150 protein, a decrease in ROS production is seen with the PI3K inhibitor, although this was not significant.

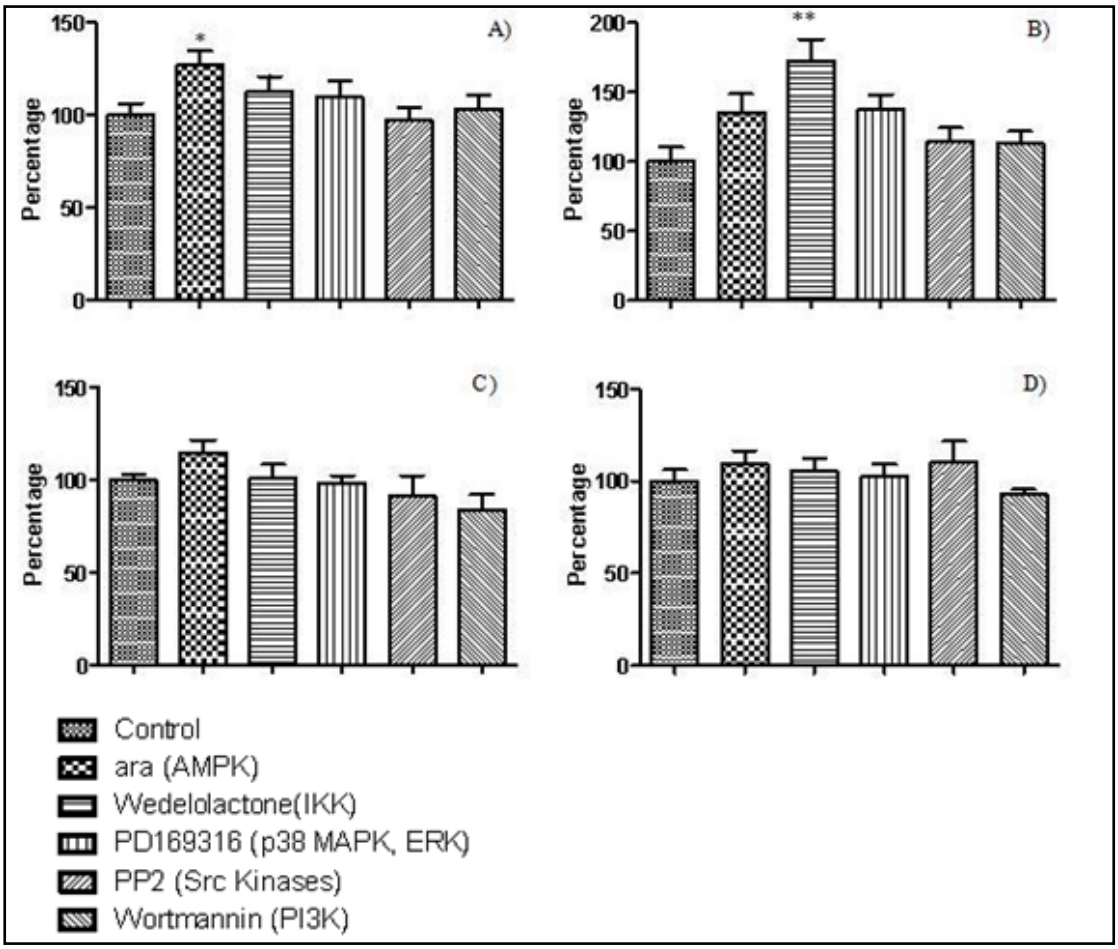

Figure 3.10: ROS production by differentiated HL60 cells preincubated with signal pathway inhibitors and CD23 proteins. (A) Control differentiated cells (no protein added); (B) HL60 cells preincubated with derCD23 and pathway inhibitors; (C) HL60 cells preincubated with CD23M150 and pathway inhibitors; (D) HL60 cells preincubated with CD23M79 and pathway inhibitors. DCF-DA prestained cells were preincubated with pathway inhibitors for 30 minutes before adding the relevant protein or control and incubating for a further 60 minutes before analysis on a flow cytometer. Error bars represent SEM of an experiment done in triplicate. This graph represents one of two experiments, both showing similar results. Asterisks represent significant differences compared to control where (**) is equivalent to $P < 0.005$ and (*) is equivalent to $P < 0.05$.

Figure 3.11 shows the production of ROS caused by the addition of pathway inhibitors to undifferentiated HL60 cells. As can be seen from Figure 3.11 (A), the ROS production by control cells was not significantly affected by the addition of the pathway inhibitors, although the inhibition of AMPK did show more of an increase in

ROS production than other inhibitors. This trend was also noted with the differentiated HL60 cells. The other inhibitors, except for PI3K inhibitor, also caused a slight insignificant increase in ROS. The addition of derCD23 together with pathway inhibitors did not cause any significant increase in ROS production [Figure 3.11 (B)]. The CD23M150 protein appeared to have the same effect on ROS production together with pathway inhibitors in the HL60 cells as the derCD23 showed [Figure 3.11 (C)]. No significant increase in the production of ROS was seen with this protein. However, a significant decrease in ROS production can be seen with the PI3K inhibitor. Figure 3.11 (D) shows the effect of CD23M79 on ROS production with the addition of pathway inhibitors in undifferentiated HL60 cells. The graph shows an increase in ROS with the AMPK inhibitor and the Src kinase inhibitor, but these increases are not significant.

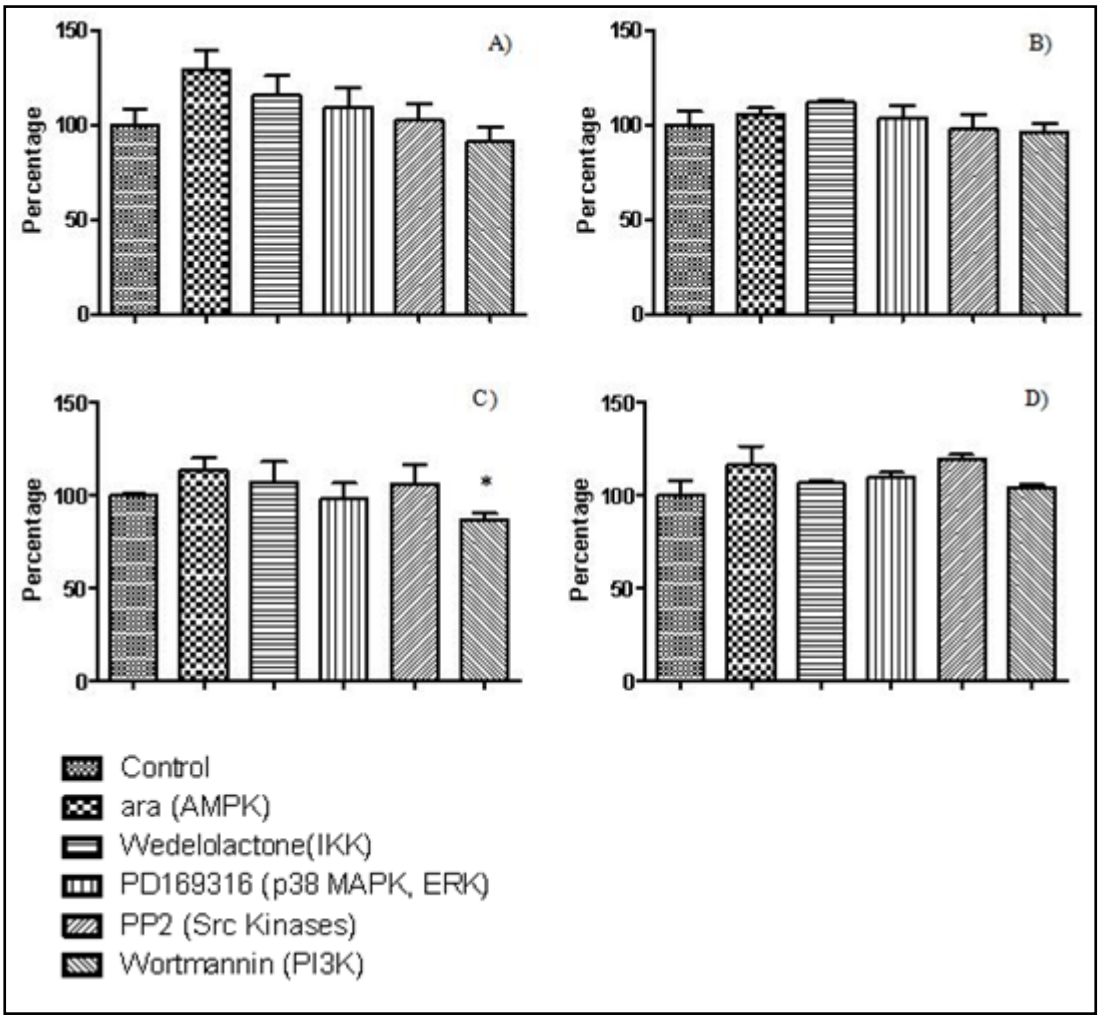

Figure 3.11: ROS production by undifferentiated HL60 cells preincubated with signal pathway inhibitors and CD23 proteins. (A) Control undifferentiated cells (no protein added); (B) HL60 cells preincubated with derCD23 and pathway inhibitors; (C) HL60 cells preincubated with CD23M150 and pathway inhibitors; (D) HL60 cells preincubated with CD23M79 and pathway inhibitors. DCF-DA prestained cells were preincubated with pathway inhibitors for 30 minutes before adding the relevant protein or control and incubating for a further 60 minutes before analysis on a flow cytometer. Error bars represent SEM of an experiment done in triplicate. This graph represents one of two experiments, both showing similar results. Asterisk represents significant difference compared to control where (*) is equivalent to $P< 0.05$.

The THP1 differentiated cell line showed little effect in the production of ROS by pathway inhibitors [Figure 3.12 (A)]. However, the IKK inhibitor showed a significant decrease in ROS production by these cells. Figure 3.12 (B) shows the

effect of pathway inhibitors on differentiated THP1 ROS production to which derCD23 has been added. The graph shows a significant increase in ROS production with AMPK, IKK and p38 MAPK/ERK inhibitors, while no change in ROS is seen with Src kinase and PI3K inhibitors. The inhibition of AMPK prior to the addition of CD23M150 showed a significant increase in ROS production by THP1 cells [Figure 3.12 (C)].

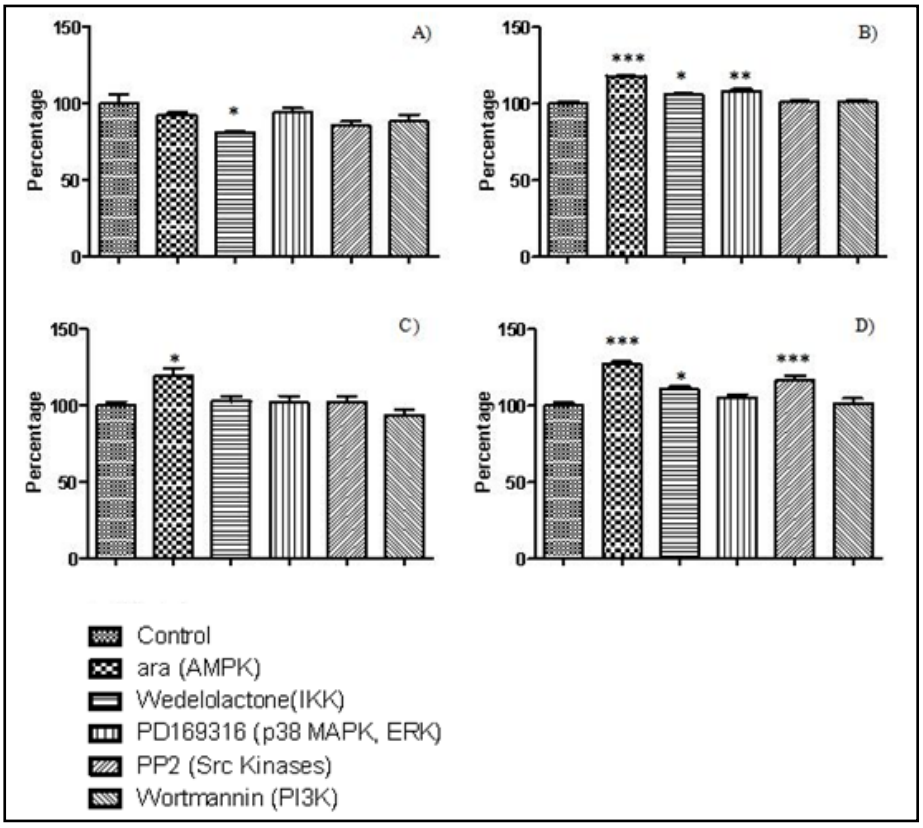

Figure 3.12: ROS production by differentiated THP1 cells preincubated with signal pathway inhibitors and CD23 proteins. (A) Control differentiated cells (no protein added); (B) THP1 cells preincubated with derCD23 and pathway inhibitors; (C) THP1 cells preincubated with CD23M150 and pathway inhibitors; (D) THP1 cells preincubated with CD23M79 and pathway inhibitors. DCF-DA prestained cells were preincubated with pathway inhibitors for 30 minutes before adding the relevant protein or control and incubating for a further 60 minutes before analysis on a flow cytometer. Error bars represent SEM of an experiment done in triplicate. This graph represents one of two experiments, both showing similar results. Asterisks represent significant differences compared to control where (***) is equivalent to $P<0.0005$, (**) is equivalent to $P< 0.005$ and (*) is equivalent to $P< 0.05$.

All the other inhibitors appeared to have little effect on ROS production, except for the PI3K inhibitor which showed a slight decrease in ROS production which was not significant. CD23M79 demonstrated a significant increase in ROS production when cells were preincubated with the AMPK, Src kinase and IKK inhibitors [Figure 3.12 (D)]. The p38 MAPK and PI3K inhibitors showed no significant change in ROS production by the protein.

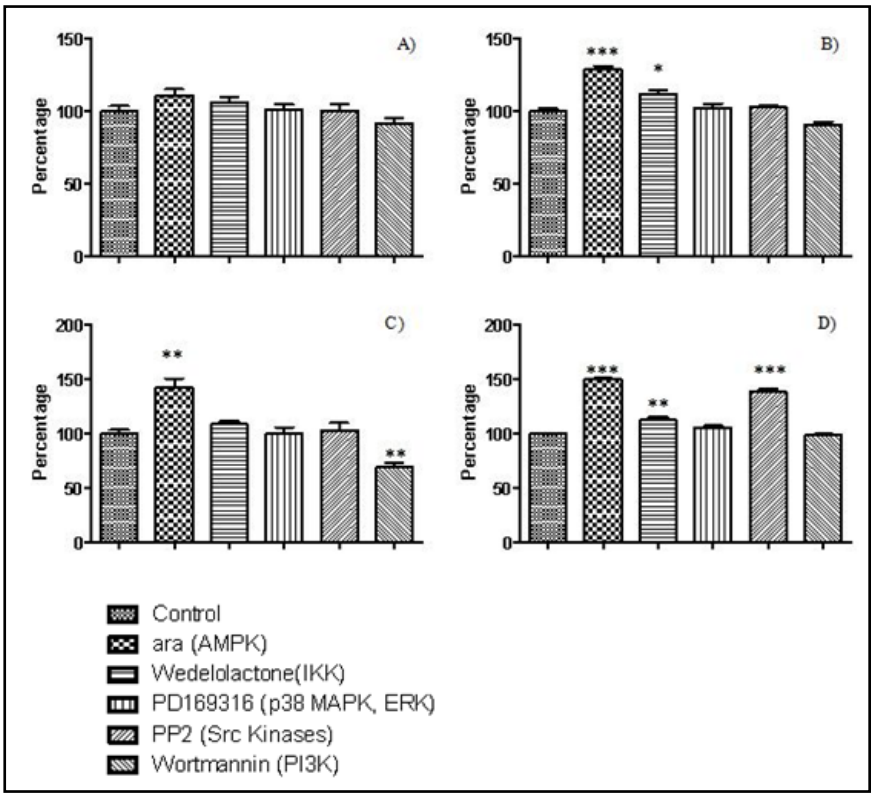

Figure 3.13: ROS production by undifferentiated THP1 cells preincubated with signal pathway inhibitors and CD23 proteins. (A) Control undifferentiated cells (no protein added); (B) THP1 cells preincubated with derCD23 and pathway inhibitors; (C) THP1 cells preincubated with CD23M150 and pathway inhibitors; (D) THP1 cells preincubated with CD23M79 and pathway inhibitors. DCF-DA prestained cells were preincubated with pathway inhibitors for 30 minutes before adding the relevant protein or control and incubating for a further 60 minutes before analysis on a flow cytometer. Error bars represent SEM of an experiment done in triplicate. This graph represents one of two experiments,

both showing similar results. Asterisks represent significant differences compared to control where (***) is equivalent to P<0.0005, (**) is equivalent to P< 0.005 and (*) is equivalent to P< 0.05.

Naïve THP1 cells showed no significant increase in the production of ROS with pathway inhibitors [Figure 3.13 (A)]. The significant decrease in ROS by the IKK inhibitor on differentiated cells has disappeared.

Undifferentiated THP1 cells show a slight increase in ROS with the addition of derCD23 and all pathway inhibitors, although the increase is only significant in the case of the AMPK and the IKK inhibitors [Figure 3.13 (B)]. The AMPK pathway inhibitor encourages a significant increase in ROS production when in the presence of CD23M150, while the PI3K pathway inhibitor decreases ROS significantly [Figure 3.13 (C)]. Figure 3.13 (D) shows the significant increase in ROS production by the addition of AMPK, IKK and Src kinase inhibitors and CD23M79 in THP1 cells.

Untreated U937 cells showed a significant increase in the production of ROS when their AMPK, IKK and p38 MAPK/ERK pathways were inhibited [Figure 3.14 (A)]. The addition of Src kinase and PI3K inhibitors alone appeared to have no effect on the production of ROS. derCD23 showed a significant increase in ROS production by differentiated U937 cells by all of the inhibitors added [Figure 3.14 (B)]. In the same way, the blocking of pathways prior to the addition of CD23M150 to U937 cells showed a significant increase in ROS production with all inhibitors, except the PI3K inhibitor [Figure 3.14 (C)]. With this inhibitor, cells showed a slight, but insignificant, increase in ROS. Figure 3.14 (D) shows that the significant increase in production of ROS by U937 cells in response to CD23M79 is the same as with

derCD23. All inhibitors showed a significant increase in ROS production with this recombinant protein.

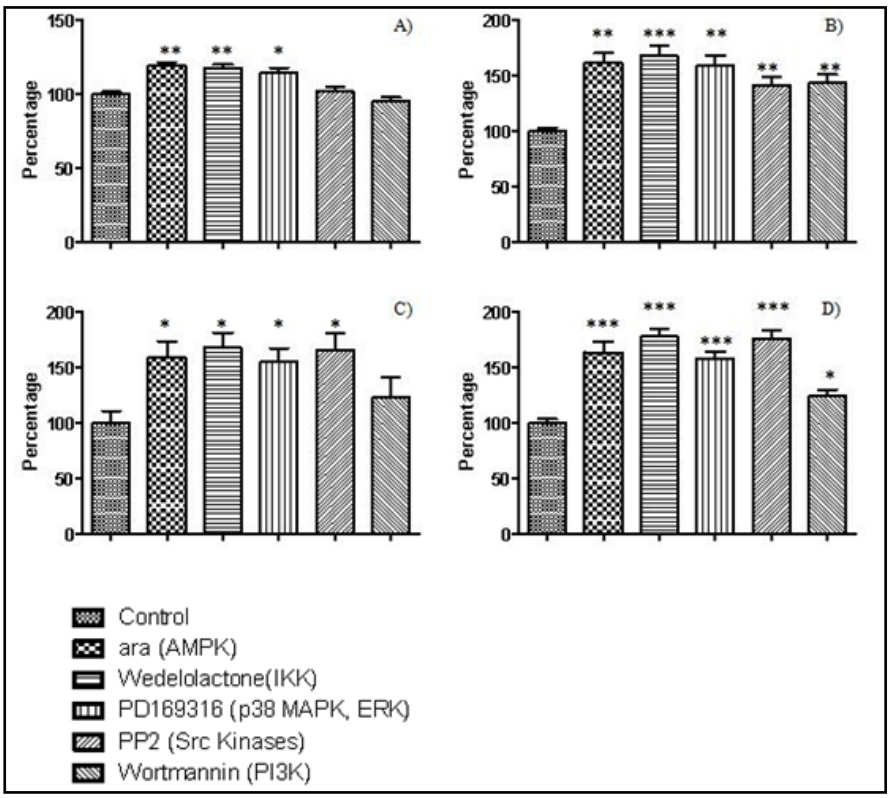

Figure 3.14: ROS production by differentiated U937 cells preincubated with signal pathway inhibitors and CD23 proteins. (A) Control differentiated cells (no protein added); (B) U937 cells preincubated with derCD23 and pathway inhibitors; (C) U937 cells preincubated with CD23M150 and pathway inhibitors; (D) U937 cells preincubated with CD23M79 and pathway inhibitors. DCF-DA prestained cells were preincubated with pathway inhibitors for 30 minutes before adding the relevant protein or control and incubating for a further 60 minutes before analysis on a flow cytometer. Error bars represent SEM of an experiment done in triplicate. This graph represents one of two experiments, both showing similar results. Asterisks represent significant differences compared to control where (***) is equivalent to $P<0.0005$, (**) is equivalent to $P< 0.005$ and (*) is equivalent to $P< 0.05$.

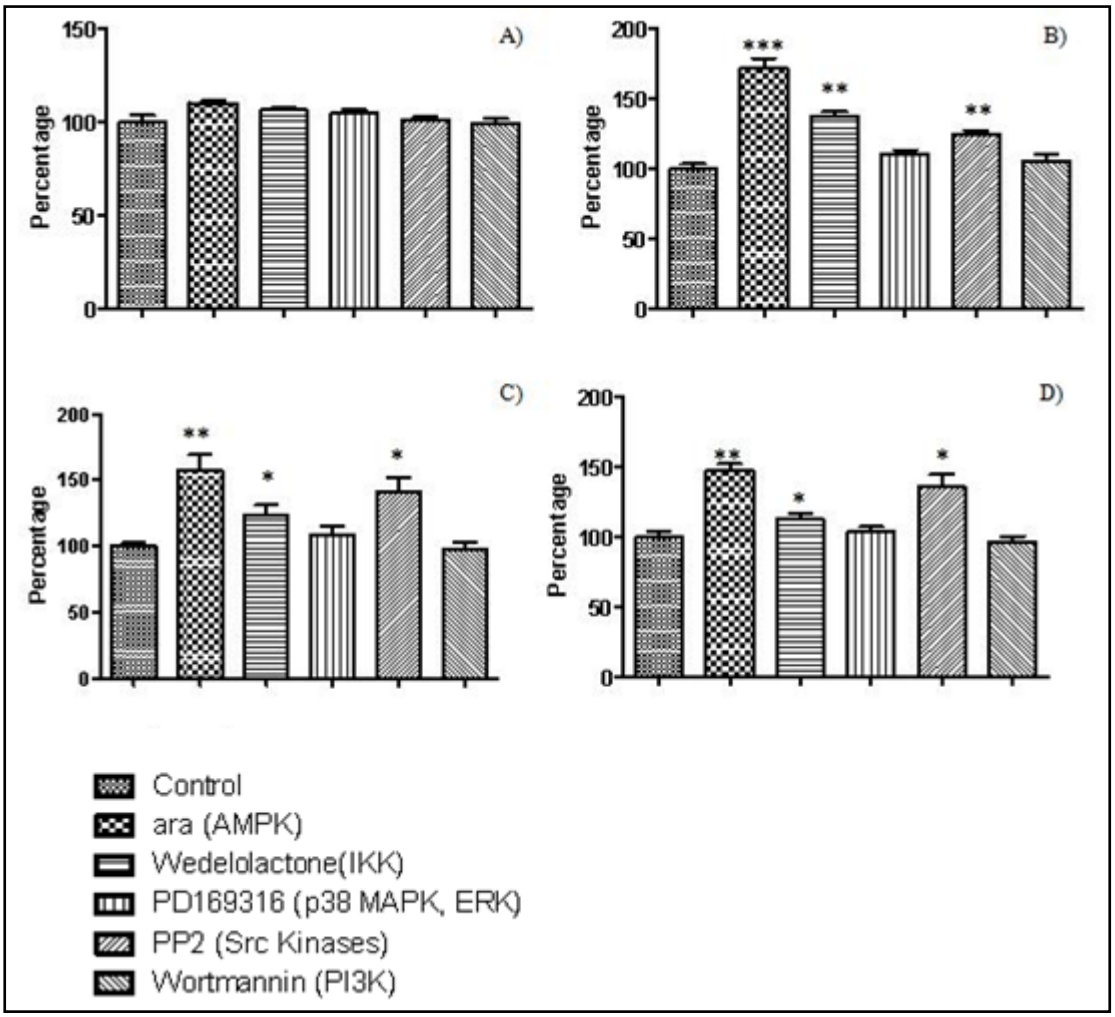

Figure 3.15: ROS production by undifferentiated U937 cells preincubated with signal pathway inhibitors and CD23 proteins. (A) Control undifferentiated cells (no protein added); (B) U937 cells preincubated with derCD23 and pathway inhibitors; (C) U937 cells preincubated with CD23M150 and pathway inhibitors; (D) U937 cells preincubated with CD23M79 and pathway inhibitors. DCF-DA prestained cells were preincubated with pathway inhibitors for 30 minutes before adding the relevant protein or control and incubating for a further 60 minutes before analysis on a flow cytometer. Error bars represent SEM of an experiment done in triplicate. This graph represents one of two experiments, both showing similar results. Asterisks represent significant differences compared to control where (***) is equivalent to $P<0.0005$, (**) is equivalent to $P< 0.005$ and (*) is equivalent to $P< 0.05$.

Naïve U937 cells show little increase in the production of ROS on the addition of pathway inhibitors [Figure 3.15 (A)]. In contrast to that, the addition of AMPK, IKK and Src kinase inhibitors together with derCD23 significantly increases the production

of ROS by these cells [Figure 3.15 (B)]. p38 MAPK/ERK inhibitor and PI3K inhibitor show no significant effect on these cells. Similarly, Figure 3.15 (C) shows the same trend with the addition of these pathway inhibitors together with CD23M150. In this case, the PI3K inhibitor shows a slight, but insignificant, decrease in ROS production. The same trend is again noted in the pathway inhibition experiment conducted with CD23M79 [Figure 3.15 (D)]. A significant increase is seen with the AMPK, IKK and Src kinase inhibitors, but no significant change with p38 MAPK and a slight (but insignificant) change with PI3K inhibitor.

Due to the nature in which these cells are stained for ROS (using a cell permeable dye which then changes to a fluorescent product when oxidised by ROS), it is difficult to say for sure whether a pathway inhibitor had an effect on the inhibition of ROS production. The dye will only effectively show an increase in ROS production by the cell, since the cells are loaded with dye prior to adding the inhibitors and proteins.

There are some trends that can be drawn from these pathway inhibition experiments (Table 3.1). These trends should be compared to the effect that the inhibitor alone had on the cell lines (i.e. the 'None' column). In differentiated HL60 cells, only ara (AMPK inhibitor) showed an increase in ROS production. However, when incubated with derCD23 and CD23M150, this increase in ROS production by ara is no longer significant. derCD23 protein showed no increase in ROS production except with wedelolactone (IKK inhibitor). This is interesting, since in differentiated HL60 cells, derCD23 has been shown to significantly increase ROS production.

Table 3.1: Table showing summary of ROS inhibitor experiments. (+) indicates a non-significant increase, + indicates an increase ($p<0.05$), ++ indicates an increase ($p<0.005$), +++ indicates an increase ($p<0.0005$) and – indicates a significant decrease.

Inhibitor		**None**	**AMPK**	**IKK**	**p38 MAPK/ERK**	**Src kinase**	**PI3K**
HL60	Untreated		+				
Differentiated	derCD23	+++	(+)	++	(+)		
	CD23M150	++	(+)				
	CD23M79						
HL60	Untreated						
Naïve	derCD23	+++					
	CD23M150	+++					-
	CD23M79	+					
THP1	Untreated			-			
Differentiated	derCD23	+	+++	+	++		
	CD23M150	+	+				
	CD23M79		+++	+		+++	
THP1	Untreated						
Naïve	derCD23		+++	+			
	CD23M150		++				-
	CD23M79	-	+++	++		+++	
U937	Untreated		++	++	+		
Differentiated	derCD23	+++	++	+++	++	++	++
	CD23M150	+++	+	+	+	+	(+)
	CD23M79		+++	+++	+++	+++	+
U937	Untreated						
Naïve	derCD23	+++	+++	++		++	
	CD23M150	++	++	+		+	
	CD23M79		++	+		+	

HL60 undifferentiated cells only show an increase in ROS production with ara (AMPK inhibitor), although this increase is not significant. It is also interesting to note that in undifferentiated HL60 cells, all three of the sCD23 proteins have been shown to significantly increase ROS production, although this trend is not seen when incubated with any of the pathway inhibitors.

The pathway inhibitors appeared to have no significant effect on the production of ROS in untreated differentiated THP1 cells. derCD23 shows a significant increase in the production of ROS with the ara (AMPK), wedelolactone (IKK) and PD 169316 (p38 MAPK/ERK) inhibitors. This protein has been shown to increase ROS production in differentiated THP1 cells previously. The CD23M150 protein has also been shown to increase ROS production, however, only cells incubated with the ara inhibitor showed a significant increase in ROS production when this protein is added. The CD23M79 protein showed little effect on the production of ROS in differentiated THP1 cells previously. However, when incubated with ara (AMPK), wedelolactone (IKK) and PP2 (Src kinase) inhibitors prior to addition of the protein, a significant increase in ROS production is seen.

The pathway inhibitors also appeared to have no significant effect on the production of ROS in undifferentiated THP1 cells. derCD23 shows a significant increase in the production of ROS with the ara (AMPK) and wedelolactone (IKK) inhibitors. This protein has shown no significant increase in ROS production in undifferentiated THP1 cells previously. The CD23M150 protein has also been shown to have little effect on ROS production in undifferentiated THP1 cells, and similarly only cells incubated with the ara inhibitor showed a significant increase in ROS production when this protein is added. The CD23M79 protein showed a significant decrease in

the production of ROS in undifferentiated THP1 cells previously. However, when incubated with ara (AMPK), wedelolactone (IKK) and PP2 (Src kinase) inhibitors prior to addition of the protein, a significant increase in ROS production is seen.

U937 differentiated cells showed an increase in ROS production when exposed to ara (AMPK), wedelolactone (IKK) and PD 169316 (p38 MAPK/ERK) inhibitors. The derCD23 and CD23M150 proteins have previously shown their ability to significantly increase ROS production in differentiated U937 cells. This production of ROS is also significant when the cells are pre-exposed to ara (AMPK), wedelolactone (IKK), PD169316 (p38 MAPK/ERK), PP2 (Src kinase) and wortmannin (PI3K) inhibitors, although in the case of CD23M150 treated cells, wortmannin's increase in ROS is not significant. The CD23M79 protein showed no significant increase in ROS production in differentiated U937 cells, but again the production of ROS was significant when the cells are pre-exposed to all the inhibitors.

The pathway inhibitors appeared to have no significant effect on the production of ROS in undifferentiated U937 cells. The derCD23 and CD23M150 proteins have previously shown their ability to significantly increase ROS production in undifferentiated U937 cells. This production of ROS is also significant when the cells are pre-exposed to ara (AMPK), wedelolactone (IKK) and PP2 (Src kinase) inhibitors. The CD23M79 protein showed no significant increase in ROS production in undifferentiated U937 cells, but again the production of ROS was significant when the cells are pre-exposed to ara(AMPK), wedelolactone (IKK) and PP2 (Src kinase) inhibitors.

3.3.7 NF-κB

NF-κB is an important signalling molecule in many cell functions. It has been previously demonstrated that NF-κB is involved in CD23 signalling pathways (Mossalayi *et al.*, 1997; Ten *et al.*,1999a). This was investigated at 15 and 30 minutes exposure to the recombinant sCD23 proteins. The best response was seen after 15 minutes and overlays of the histograms from the different cell lines are shown.

Figure 3.16 (A) shows the histogram overlays of the control HL60 cells compared to the cells incubated with the IKK inhibitor and HL60 cells incubated with LPS as a positive control. This figure also shows the histogram overlays of the control HL60 cells with the three sCD23 proteins (figure 3.16 B). It can be seen in (A) the inhibitor causes the population to shift to the left indicating less staining for NF-κB, while LPS shows no effect on NF-κB staining. In (B) the CD23 proteins cause a very slight shift to the left of the population compared to control cells, with no significant difference in the NF-κB produced by the three proteins.

Figure 3.16 (C and D) shows histogram overlays of the identical experiment conducted with THP1 cells. It can be seen in (C) that the inhibitor causes the population to shift substantially to the left indicating less staining for NF-κB, while LPS shows little effect on NF-κB staining. In (D) the CD23 proteins cause a shift of the population when compared to control cells, with derCD23 showing only a slight shift compared to CD23M150 and CD23M79 which show a larger shift to the left and therefore less NF-κB production.

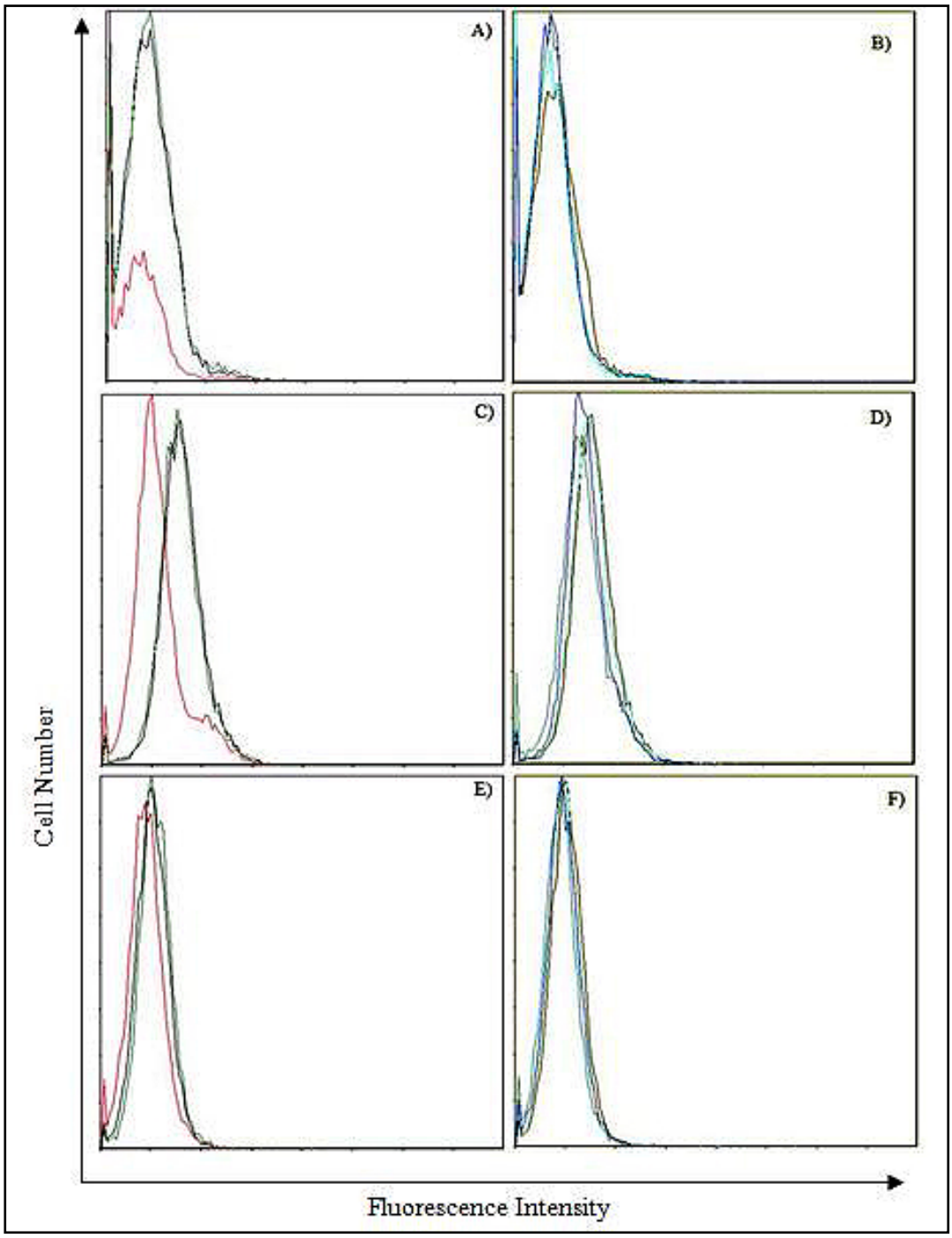

Figure 3.16: Histogram overlays of NF-κB activation in HL60 (A;B), THP1 (C;D) and U937 (E;F) cells. Cells are incubated with the CD23 protein or control for 15 minutes before being stained for NF-κB. (A;C;E) Overlays of control cells (black), cells incubated with PP2 inhibitor (red) and LPS (green); (B;D;F)) Overlays of control cells (black), derCD23 (cyan), CD23M150 (aquamarine) and CD23M79 (dark blue).

The effect on NF-κB production in U937 cells is shown in Figure 3.16 (E and F). It can be seen in (E) that the inhibitor causes the population to shift to the left indicating less staining for NF-κB, while LPS shows a slight shift to the right on NF-κB staining, indicating a slight increase in NF-κB. In (F) the CD23 proteins cause a shift of the population to the left of the control cells, with derCD23 and CD23M79 showing only a slight shift and CD23M150 showing marginally more of a shift to the left.

Although the histograms of these results show that the shift in NF-κB production is very small, one has to remember that these histograms use a logarithmic scale to express fluorescence. The mean fluorescence intensity of these histograms was analysed in the same way as the ROS experiments, and although there was no significant changes seen with the HL60 cells, a significant decrease was seen with CD23M150 and CD23M79 ($p<0.05$) in THP1 cells while U937 cells showed a significant decrease with the CD23M150 protein ($p<0.05$) (data not shown).

3.3.8 Nitric Oxide

The production of nitric oxide was measured using DAF-DA dye. However, no significant changes were observed with any of the cell lines on treatment with recombinant sCD23 proteins (data not shown). This could be because the detection method was not sensitive enough to detect any changes. Aubry *et al.*, (1997) showed that NOS mRNA took up to 24 hours to be upregulated when sCD23 is crosslinked to cells; however no production of NO was observed during the experiments conducted for this study. In many *in vivo* experiments, maturation into macrophage-like cells from monocytes is essential for nitrite production (Dugas *et al.*, 1995). This could explain the lack of nitric oxide production by the cells.

3.3.9 Myeloperoxidase

The HL60 cell line showed an increase with MPO on the addition of PMA, derCD23 and CD23M79 [Figure 3.17 (A)]. The increase observed was a small percentage, although it was statistically significant in all three cases. The THP1 cell line showed no change in MPO after 24 hours, even with the PMA control [Figure 3.17 (B)]. The U937 cell line showed the same trend in MPO production as was seen with the HL60 cell line [Figure 3.17 (C)]. A marginal increase in MPO production was induced with PMA, derCD23 and CD23M79; however, only the increase seen in derCD23 was statistically significant.

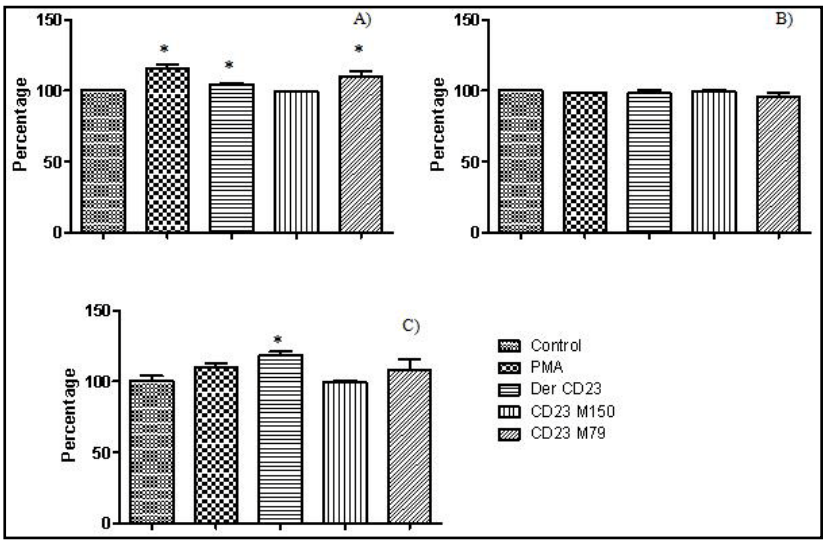

Figure 3.17: MPO expressed above control in (A) HL60, (B) THP1 and (C) U937 differentiated cells treated with control (PMA) and CD23 proteins. Error bars represent SEM of triplicate values. Asterisks represent statistical significance where (*) is equivalent to $P<0.05$. This graph represents one of two experiments with similar results.

3.3.10 Cytokines

The production of IL-1β, IL-6 and TNFα were investigated using ELISA kits. The absolute levels of cytokines produced by the experiments were not always consistent, although the trends seen in the production were. It was therefore decided to express the cytokine data as a percentage of the control of each experiment, so that the trends could be compared. One set of experiments from each cell line were compared to a LPS positive control, which did not seem very effective in upregulating the production of the cytokines being investigated, therefore the repeat experiments were compared to a PMA positive control. Standard curves for these experiments can be seen in Figures A.10-A.12 in Appendix A.

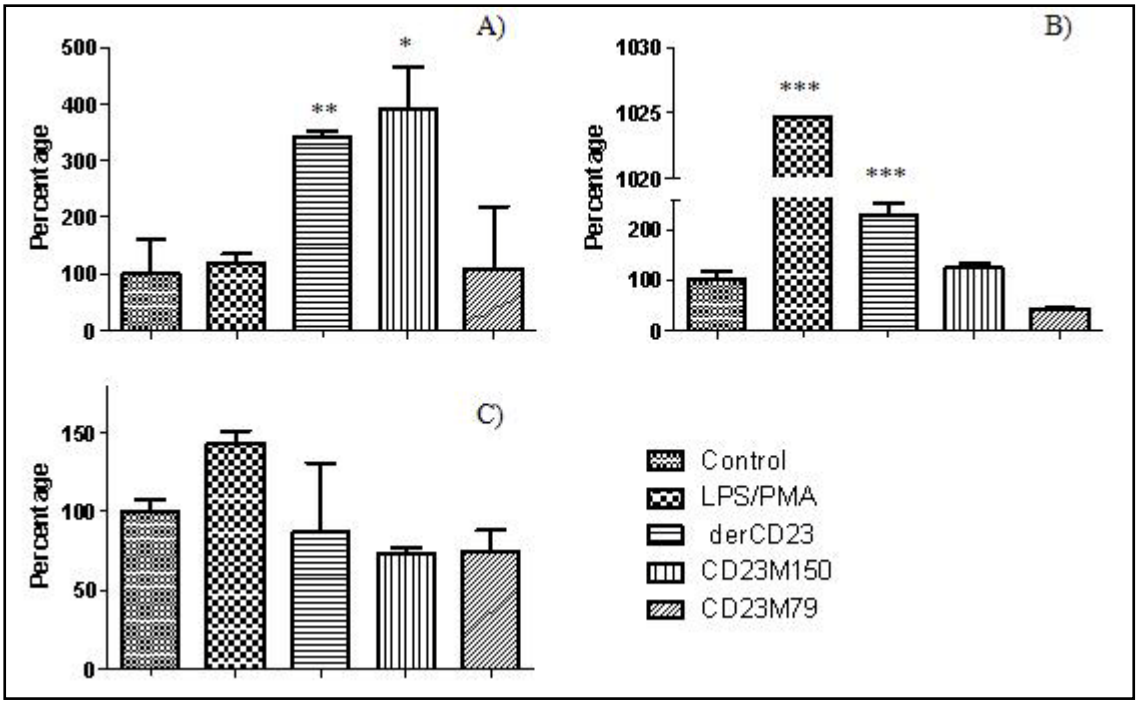

Figure 3.18: Production of IL-1β by differentiated (A) HL60; (B) THP1; (C) U937 cells after 24 hour incubation with sCD23 proteins and a positive control (LPS/PMA). Results are expressed as percentage of control (medium) cytokine production. Error bars represent SEM of triplicate values.

Asterisks represent a statistical significance compared to control where (*) represents P<0.05, (**) represents P<0.005 and (***) represents P<0.0005. This figure is representative of one of two experiments conducted. Similar trends were observed in the two experiments.

Figure 3.18 (A) shows the production of IL-1β by HL60 cells in response to sCD23 proteins. A significant increase in the production of IL-1β by derCD23 and CD23M150 is shown. Figure 3.18 (B) shows the production of IL-1β by THP1 cells in response to sCD23 proteins. The production of the cytokine is greatly increased by the positive control (PMA) and derCD23, while there is a slight (insignificant) increase by CD23M150. The production of IL-1β by U937 cells in response to sCD23 proteins is shown in Figure 3.18 (C). This figure shows an increase in cytokine production by the positive control (although not significant), but no increase in production by the recombinant proteins.

HL60 cells significantly increase IL-6 production with positive control (LPS/PMA) and derCD23 exposure, with no response seen with the CD23M150 and CD23M79 proteins [Figure 3.19 (A)]. THP1 differentiated cells showed a similar trend to the HL60 cells, with a significant increase in IL-6 production by both the positive control and derCD23 [Figure 3.19 (B)]. While an increase is seen in the stimulation of these cells to produce IL-6 by CD23M150, this increased cytokine production is not significant due to the large differences between the control samples. In contrast to the other two cell lines, the U937 cell line shows a decrease in production of IL-6 by recombinant sCD23 proteins [Figure 3.19 (C)]. This decrease is significant in the case of derCD23 and CD23M150.

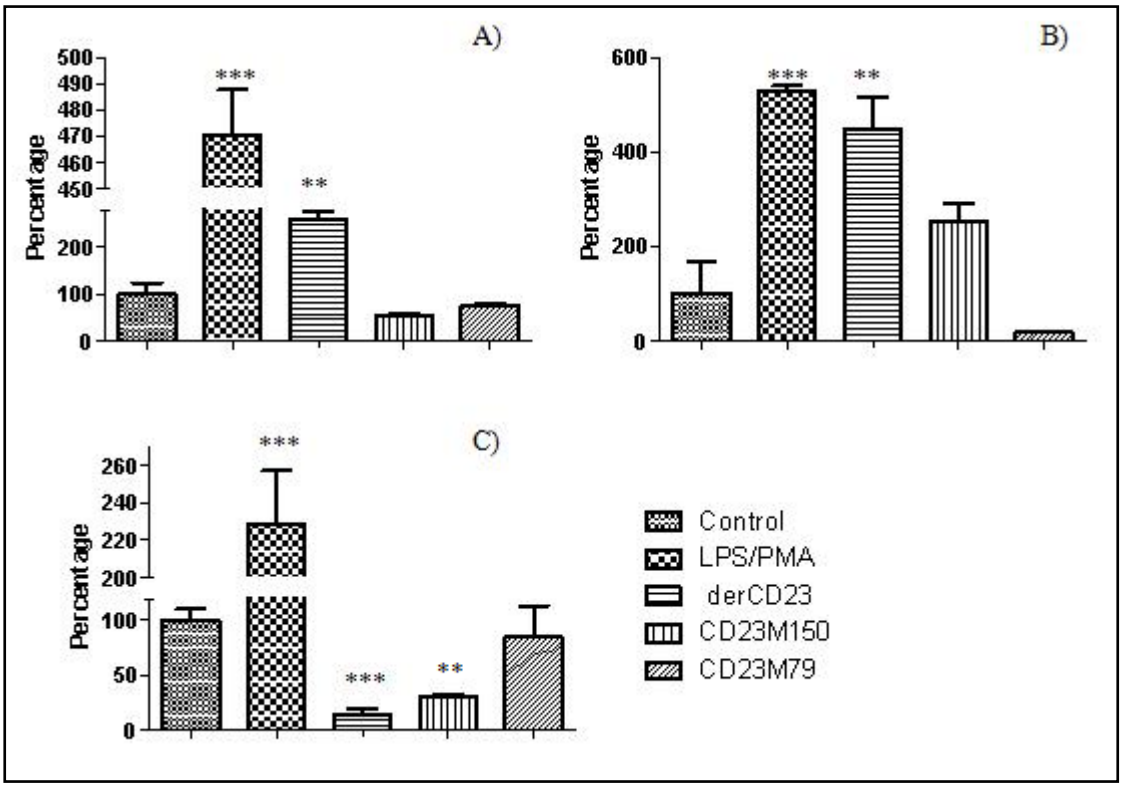

Figure 3.19: Production of IL-6 by differentiated (A) HL60; (B) THP1; (C) U937 cells after 24 hour incubation with sCD23 proteins and a positive control (LPS/PMA). Results are expressed as percentage of control (medium) cytokine production. Error bars represent SEM of triplicate values. Asterisks represent a statistical significance compared to control where (*) represents P<0.05, (**) represents P<0.005, and (***) represents P<0.0005. This figure is representative of one of two experiments conducted. Similar trends were observed in the two experiments.

TNFα production by HL60 cells was significantly increased by the positive control and by derCD23 [Figure 3.20 (A)]. In the same way as IL-1β, the CD23M150 and CD23M79 proteins did not have an effect on TNFα production. TNFα production by THP1 cells exposed to sCD23 proteins shows a significant increase in production by the positive control and an increase by CD23M150, although not significant [Figure 3.20 (B)]. TNFα production by recombinant sCD23 proteins by U937 cells shows a decrease in production of TNFα by the proteins and the positive control [Figure 3.20 (C)]. However, this decrease is only significant for CD23M150 and CD23M79. Since

these results only represent one experiment for U937 cells due to a problem with one of the TNFα kits, they cannot be used with confidence.

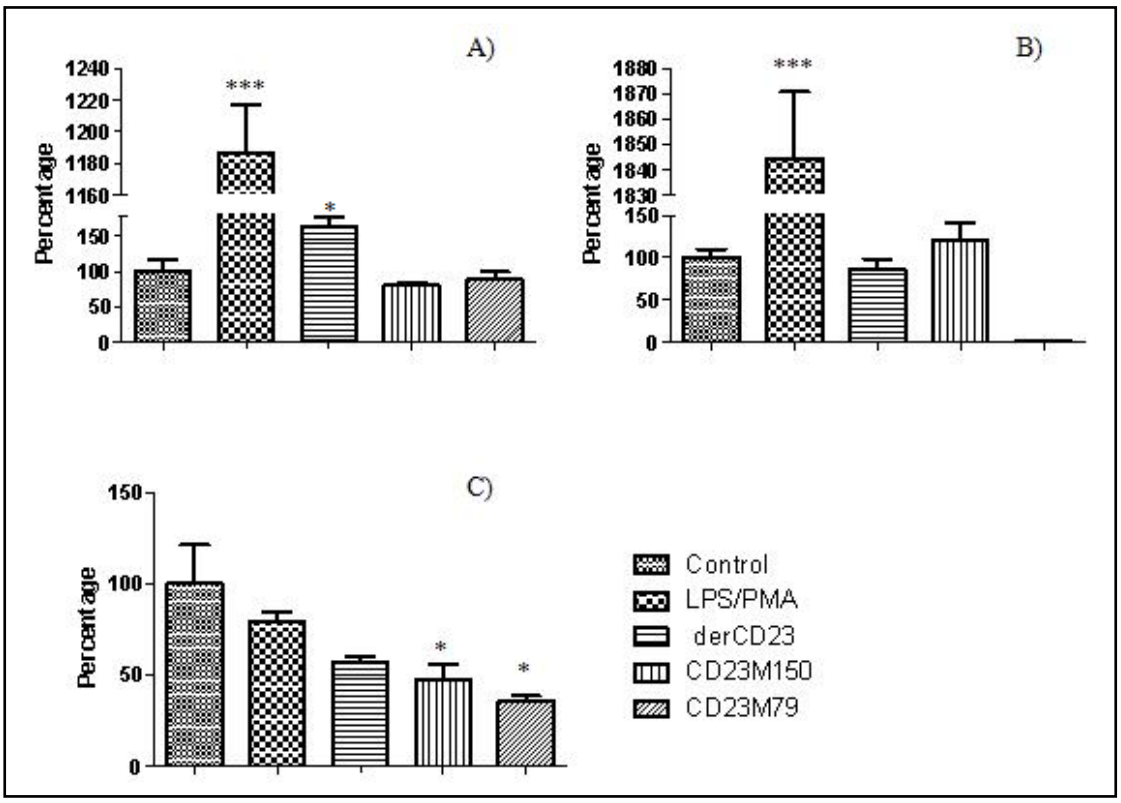

Figure 3.20: Production of TNF-α by differentiated (A) HL60; (B) THP1; (C) U937 cells after 24 hour incubation with sCD23 proteins and a positive control (LPS/PMA). Results are expressed as percentage of control (medium) cytokine production. Error bars represent SEM of triplicate values. Asterisks represent a statistical significance compared to control where (*) represents $P<0.05$, (**) represents $P<0.005$, and (***) represents $P<0.0005$. This figure is representative of one of two experiments conducted for HL60 and THP1 and a single experiment for U937. Similar trends were observed in the two experiments.

The CD23M79 protein seemed unable to upregulate the production of any of the cytokines regardless of which cell line was used.

3.4 Discussion

The cell signalling pathways in cells are a complex and intricate network and more research into these pathways is constantly taking place. The aim of this project was to try to identify what effects the binding of sCD23 proteins have on their CD11b and CD11c ligands. In Chapter 2, we proved that the CD11b and CD11c αI domains bind to the recombinant sCD23 proteins produced for this work.

We also successfully differentiated three premonocytic cell lines into monocytic cells, with the main aim being to upregulate CD11b and CD11c on their cell surface. Vitamin D_3 proved an excellent differentiating agent for this task.

The differentiated cells were then exposed to the recombinant proteins to investigate what effect the proteins would have on the normal β_2 integrin functions of the cell, namely chemotaxis and phagocytosis. There appeared to be no effect on chemotaxis with the CD23M79 protein in all the cell lines tested. The CD23M150 protein was able to significantly decrease chemotaxis in THP1 cells, but not in the other two cell lines. The derCD23 protein, on the other hand was able to cause a significant decrease in chemotaxis in all three cell lines as well as in monocytes isolated from PBMCs. Fibrinogen was also able to decrease chemotaxis in all three cell lines, although this was not always significant. Both HL60 and U937 cells have been shown to have receptors for the chemotactic tripeptide fMLP (Harris and Ralph, 1985), therefore the inadequate choice in chemotactic agent can be ruled out as an explanation for the lack of chemotaxis in these cell lines.

Phagocytosis was tested in differentiated and undifferentiated cell lines. The phagocytic results showed little or no effect on the ability of the cells to phagocytose *E. coli*, both in differentiated and undifferentiated cells. Only two treatments caused a significant change in the phagocytic ability of cells; derCD23 and fibrinogen were able to significantly decrease phagocytosis in differentiated HL60 cells. This trend was also seen with primary $CD14^+$ isolated monocytes, which supports the idea that the sCD23 proteins do not influence CD11b and CD11c's role in phagocytosis.

The phagocytosis results for undifferentiated cells were as expected, since HL60 cells are known to be able to phagocytose some bioparticles weakly, and their phagocytic potential is only upregulated when differentiated (Harris and Ralph, 1985). In the same way, only a small percentage of undifferentiated U937 cells have been found to be able to phagocytose (Harris and Ralph, 1985). However, a greater change in phagocytic potential was expected with differentiated cells. Schwende *et al.* (1996) have shown the upregulation of phagocytic ability of THP1 cells when differentiated with vitamin D_3. However, the recombinant proteins were not able to influence this ability to phagocytose *E. coli* K12 bioparticles. Perhaps the results may have been different had a different bioparticle been chosen for phagocytosis, however CD11b phagocytosis has been shown to be mediated by gram negative bacteria with the ligand mainly used being LPS (Greenberg and Grinstein, 2002). It has been previously shown that with β_2 integrin-dependent phagocytosis, the binding of a particle is sometimes not enough to stimulate phagocytosis, but that receptor activation is also required simultaneously for phagocytosis to occur (Ehlers, 2000). CD11b has also been shown to be able to perform phagocytosis of non-opsonised or complement opsonised particles through distinct mechanisms. This indicates that it is able to trigger different signalling pathways, as it has been shown to do in neutrophils.

It was found that the zymosan and opsonised zymosan bound CD11b in two different sites, possibly resulting in different conformations and leading to the activation of distinct pathways (Le Cabeq *et al.*, 2002). It is also thought that a second phagocytic receptor may be required for phagocytosis to occur via β_2 integrins (Ehlers, 2000). CD11b has been shown to require extracellular signals (such as cytokines and bacterial products) to perform phagocytosis (Dupuy and Caron, 2008). It could therefore be possible that the phagocytosis of *E. coli* is not being upregulated or downregulated by the sCD23 proteins due to their binding either interfering with the binding of the *E. coli* or due to the binding of sCD23 proteins not activating the CD11 integrins, or requiring another ligand or cytokine to be effective. Since these proteins do demonstrate the ability to increase the respiratory burst of the cell lines, it is possible that sCD23 proteins favour the upregulation of antibody mediated phagocytosis, such as that seen with FcγRIII (Taborda and Casadevall, 2002). CD11b has been shown to interact with glycosylphosphatidylinositol (GPI)-linked membrane proteins using a *cis* interaction. An example of this interaction is the binding of CD11b to FcγRIII which promotes antibody-dependent phagocytosis (Porter and Hogg, 1998). Another explanation could be that CD23 proteins are able to stimulate the ability of monocytes to attach to foreign particles, but that they do not enhance the cells ability to internalise those particles. It could be that in addition to the CD23 proteins enhancing the activation of the cells and their binding to foreign particles, other surface molecules need to be activated or the affinity of the integrin was not enough to allow for internalization of the foreign particle (Serrander *et al.* 1999). Since any external fluorescence was quenched before analysis, this binding of the *E. coli* K12 particles could not have been seen unless the *E. coli* was internalised by the cells.

The production of ROS in cells is very important in cell signalling and plays a role in signal transduction cascades, protein phosphorylation, gene transcription, transcription factor activation and disease, among others (Hoidal, 2001). PI3K, MAPK and NF-κB are regulated by ROS to name a few. It is interesting to note the differences in ROS production by cells exposed to the different sCD23 proteins. However, there are several very complex pathways involved, as can be seen from Figure 3.21. The derCD23 protein increased the production of ROS by differentiated HL60, U937, THP1 and $CD14^+$ cells (significantly in HL60, U937 and $CD14^+$ cells). It was also able to increase the ROS produced in undifferentiated HL60s and U937s. This is unexpected as undifferentiated HL60 and U937 cells are known to have a very low capacity to produce ROS. However, this can be explained by the fact that the cell lines showed a good basal level of CD11b and CD11c on the cell surface before differentiation and it could be the binding to these lower levels of integrins that result in the ROS production (Figure 3.3). In the same way, CD23M150 was also able to increase ROS production in all three differentiated cell lines (significantly in HL60 and U937 cell lines), as well as significantly in undifferentiated HL60 and U937 cells. The CD23M79 protein showed no significant increase in ROS in any of the differentiated cell lines. It did show a significant increase in ROS in undifferentiated THP1 cells. These data show that the derCD23 and the CD23M150 are able to activate ROS, and therefore possibly several signalling pathways, much more efficiently than the CD23M79 protein. The activation of these cells to produce ROS, yet their inability to affect phagocytosis or increase chemotaxis might cause confusion. However, Van der Goes *et al.* (2001) found that although O_2^- enhanced monocytic adhesion and migration across the blood-brain barrier, H_2O_2 and OH^- did not show an effect. It is therefore possible that the ROS being produced by the cells is H_2O_2 or OH^- and therefore not having an effect on the cell migration. It has also been

shown that in some cases of CD11b-dependent phagocytosis, respiratory burst is absent (Ehlers, 2000). This could indicate that if cells are stimulated to produce ROS by the binding of sCD23 proteins to CD11b/CD11c, they are no longer able to perform CD11b-dependent phagocytosis.

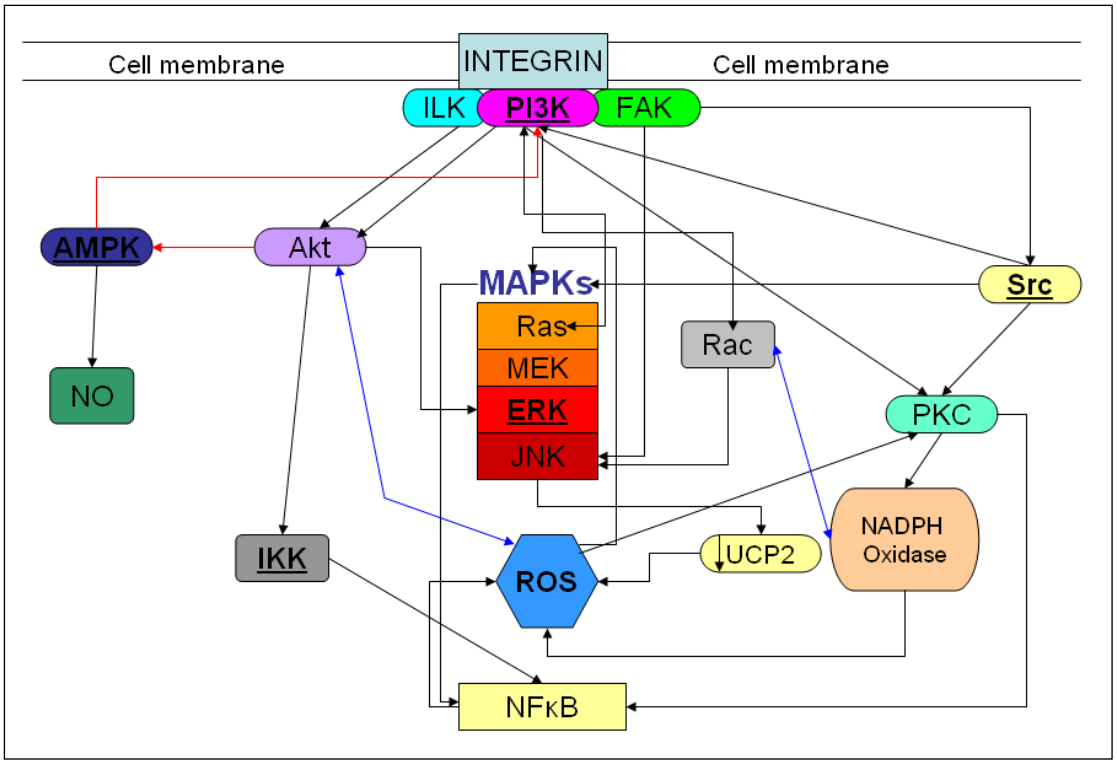

Figure 3.21: The intricate networks possibly involved in ROS signalling by integrins. Blue arrows represent reversible reactions, red arrows represent inhibitory reactions. ILK; Integrin linking kinase.

Due to the intricate network of signalling pathways involved in β_2 and CD23 signalling, it was attempted to determine which signalling pathways affect or are affected by this increase in ROS produced by the proteins. We know that CD11b and CD11c are possibly involved in PI3K, NF-κB and MAPK signalling pathways, CD23 is involved in MAPK, PI3K, NF-κB and AMP kinase pathways, while Src kinases are thought to be involved in NADPH oxidase signalling which leads to ROS production.

derCD23 showed a significant increase in ROS production with differentiated HL60 cells. However, the pathway inhibitor studies show that this increase in ROS is still significant and even exacerbated when a IKK inhibitor is pre-incubated with the cells and the increase in ROS is no longer seen with AMPK, p38 MAPK/ERK, Src kinase and PI3K inhibitors. These data could indicate that derCD23 is able to act through more than one of these pathways simultaneously. derCD23 was also able to show an increase in ROS in differentiated THP1 cells. The pathway inhibitor studies showed that this increase seen in ROS production is lower when Src kinase and PI3K inhibitors are pre-incubated with the cells. The addition of AMPK, IKK and p38 MAPK/ERK inhibitors also exacerbated the increase in ROS by derCD23. The decrease in ROS production by derCD23 with the Src kinase and PI3K inhibitors could indicate that these pathways are used for derCD23 stimulation of oxidative burst. Differentiated U937 cells showed a significant increase in the production of ROS with derCD23. This production of ROS with derCD23 in differentiated U937 cells remained significant with all five inhibitors. However, it must be noted that a significant increase in ROS was seen in differentiated U937 cells on the addition of AMPK, IKK and p38 MAPK/ERK inhibitors alone. The ability of the Src kinase and PI3K inhibitors to decrease this oxidative burst could indicate that the derCD23 is acting through these pathways, but goes unnoticed due to the basal effect of the inhibitors on the cells.

derCD23 was also able to significantly increase the production of ROS by undifferentiated HL60 and U937 cells. This increase in ROS was not seen in undifferentiated HL60 cells with all five of the inhibitors, showing that they may all in some way affect the ability of derCD23 to cause ROS production. In undifferentiated U937 cells, only the AMPK, IKK and Src kinase inhibitors caused

this significant increase in ROS to be exacerbated, while the p38 MAPK/ERK and PI3K inhibitors removed this oxidative burst seen, indicating that they could be involved in the signalling pathway of derCD23 in undifferentiated U937 cells. The THP1 undifferentiated cells did not show a significant increase in ROS production with derCD23, however, a significant increase in ROS production in undifferentiated THP1 cells is seen with the addition of AMPK and IKK inhibitors with derCD23. Since AMPK usually acts by blocking PI3K, it is possible that by blocking this kinase, you enable PI3K to signal and therefore produce ROS. It is also possible that by blocking IKK, it causes an increase in Akt, which can lead to an increase in ROS formation.

The CD23M150 protein showed a significant increase in ROS production in all three differentiated cell lines. The differentiated HL60 cell line showed no increase in ROS production with the addition of the inhibitors, indicating that they may all, in some way, be involved in ROS production by CD23M150. THP1 differentiated cells showed an increase in ROS production by all inhibitors except the AMPK inhibitor, showing another wide range of signalling pathway possibilities with this protein. The differentiated U937 cells show a significant increase in ROS production with CD23M150 when all inhibitors except the PI3K inhibitor are pre-incubated. This indicates that CD23M150 ROS production may be blocked if PI3K activity is removed.

CD23M150 was also able to significantly increase the production of ROS by undifferentiated HL60 and U937 cells. The same increase in ROS was not seen in undifferentiated HL60 cells with all five of the inhibitors, showing that they may all in some way block the ability of CD23M150 to produce ROS. In undifferentiated

U937 cells, only the AMPK, IKK and Src kinase inhibitors caused this significant increase in ROS to increase further, indicating that by blocking the p38 MAPK/ERK and PI3K pathways, the ability to increase ROS production is lost. The THP1 undifferentiated cells did not show a significant increase in ROS production with CD23M150, however, a significant increase in ROS production in undifferentiated THP1 cells is seen with the addition of AMPK inhibitor with CD23M150. Again, by blocking AMPK we may be removing a kinase that blocks PI3K activity, and therefore enables the cells to produce ROS freely, therefore showing the significant increase in ROS production.

The CD23M79 protein did not have a significant effect on the ROS production by any of the three cell lines. The differentiated HL60 cells also showed no significant increase in ROS production with the five pathway inhibitors and CD23M79. However, the differentiated THP1 cells showed a significant increase in ROS production with the AMPK, IKK and Src kinase inhibitors. The largest increase in ROS production is seen with AMPK and Src kinase inhibitors, which could indicate that these cells are then forced to use the PI3K pathway to signal with CD23M79 which results in ROS production, rather than the alternative pathway that does not produce ROS. The five pathway inhibitors caused a significant increase in ROS production by differentiated U937 cells in conjunction with CD23M79. This could be explained by the fact that by blocking certain pathways in conjunction with the CD23M79 protein, the cells are forced to use other signalling pathways that may result in ROS production.

In undifferentiated cells, the CD23M79 protein caused a significant increase in ROS production only in THP1 cells. There was also no significant increase in ROS

production by undifferentiated HL60 cells with the five inhibitors pre-incubated before adding CD23M79. A significant increase in ROS was seen in undifferentiated THP1 cells with the addition of AMPK, IKK and Src kinase inhibitors together with CD23M79. Similarly, a significant increase in ROS was seen in undifferentiated U937 cells with the addition of AMPK, IKK and Src kinase inhibitors together with CD23M79. Again, these results seem to show that the addition of these inhibitors in conjuction with the CD23M79 protein is forcing the cells to signal through a pathway that results in more ROS production.

In short, the general trends show that derCD23 ROS production is mostly decreased when Src kinase is blocked in both differentiated and undifferentiated cells, when PI3K is blocked in differentiated cells and when p38 MAPK/ERK is blocked in undifferentiated cells. CD23M150 has a reduced ability to produce ROS in some way with all the inhibitors with differentiated and undifferentiated cells. Lastly, although CD23M79 does not seem to stimulate oxidative burst, however an increase is seen with all inhibitors in HL60 cells and differentiated U937 cells, when blocking p38 MAPK/ERK and Src kinases in undifferentiated U937 cells, when blocking Src kinases and PI3K in differentiated THP1 cells and when blocking p38 MAPK/ERK and PI3K in undifferentiated THP1 cells.

Due to its ability to amplify oxidation and its use of nitrating compounds, cells were tested for the upregulation of MPO by the sCD23 proteins. derCD23 showed a small but significant increase in MPO in HL60 and U937 cells, but no change in THP1 cells. The CD23M150 protein did not show any increase in MPO production. The CD23M79 protein showed an increase in MPO production in HL60 cells. However, superoxide dismutase, catalase and MPO have been shown to be prone to inactivation

by ROS (Splettstoesser and Schuff-Werner, 2002). Despite this inactivation of the enzyme activity of MPO, it is unknown what effect ROS have in the intracellular MPO levels. Although MPO is found in monocytes, it is much more abundant on neutrophils, which could explain why such low levels of intracellular MPO were found in the monocytic cell lines. Again, the derCD23 seems to be the most stimulating of the three CD23 proteins.

The production of NF-κB by proteins was also tested. The production of NF-κB was shown to decrease to a small degree in HL60 cells. There was a very small decrease in the production of NF-κB by U937 cells. The THP1 cell line showed a decrease in the production of NF-κB, but this was more pronounced in CD23M150 and CD23M79 than in derCD23-treated cells. This decrease in the production of NF-κB could explain the lack of TNFα, IL-1β and IL-6 cytokines by the CD23M150 and CD23M79, as NF-κB is thought to control the transcription of inflammatory cytokines (Kim *et al.*, 2004). Although it is widely thought that ROS activates NF-κB, it has also recently been thought that ROS may act as inhibitors for NF-κB (Zhang and Chen, 2004). This may explain the lack of NF-κB activation in these cells.

The production of cytokines was also investigated. In these experiments only the HL60 and THP1 data were repeated and the U937 data were not reliable. It is interesting to note that derCD23 caused an increase in IL-1β, IL-6 and TNF-α in HL60 cells. It also showed an increase in IL-1β and IL-6 in THP1 cells. CD23M150 was able to upregulate IL-1β production in HL60 cells, and TNF-α production in THP1 cells. This shows that derCD23 was able to activate HL60 cells (Dale *et al.*, 2008). These data are also supported by the work of Rezzonico *et al*. (2001) who

found that sCD23 binding to β_2 integrins produced IL-1β, IL-6 and TNF-α in isolated monocytes. It has also been shown previously that CD23M150 is able to stimulate the production of IL-1β and TNF-α in PBMCs (Daniels *et al.*, 2005). The CD23M79 protein showed a complete lack of stimulation of these three cytokines. This could indicate that the CD23M79 protein does not activate these cells, which is supported by the lack of ROS production by this protein.

The THP1 cells behaved differently to the HL60 and U937 cells in most experiments. It is important to note at this point that the THP1 cell line had a much less pronounced upregulation of CD11b compared to the HL60 and U937 cell lines. It is also important to note that the CD11c upregulation for this cell line was more pronounced than that of CD11b and of that of CD11c in the other two cell lines. This could explain the differences seen in the results with this cell line. However, this cell line also showed no binding to the sCD23 proteins. This could indicate that the THP1 cell was unable to bind the sCD23 proteins, possible due to another upregulated ligand or cell surface molecule interfering with the binding.

Overall, it would seem that binding of derCD23 proteins to β_2 integrin-upregulated cells caused an increase in cell signalling through ROS, but this signalling on its own did not affect the cells ability to phagocytose and caused a decrease in chemotaxis. While CD23M150 showed a similar increase in the production of ROS as derCD23, it showed no change in phagocytic or chemotactic ability of the cells, and only produced some inflammatory cytokines and lowered NF-κB in some cell lines. The production of ROS by CD23M79 was only seen in undifferentiated cells and not in differentiated cells. The CD23M79 protein also showed no inflammatory cytokine response and showed a decrease in NF-κB in some cell lines. However, we know that this protein

definitely binds to CD11b on cells and to the αI domain of CD11b and CD11c. It appears that though this protein may bind CD11b and CD11c on cells, this binding does not have a proinflammatory effect on cells. The CD23M150 protein, also binds CD11 αI domain and CD11-upregulated cells, and it has an effect on cells, such as the production of some inflammatory cytokines and the increase in ROS. derCD23 on the other hand, seems also able to activate all cells. It causes a decrease in chemotaxis, an increase in ROS and the production of inflammatory cytokines. This difference in effect could be due to the ways in which the different CD23 proteins are able to bind the CD11 proteins. There are several binding activation states of β_2 integrins, and it is possible that the structure or size of the different CD23 proteins allow them to bind the CD11 proteins in different ways which could cause different activation states of the CD11 proteins. It is also possible that the self-association of the sCD23 proteins (specifically those with extensive stalk regions such as the CD23M79 of this study) is causing an effect on CD11 binding and activation. We know that sCD23 trimers are able to increase IgE synthesis through simultaneous CD21 and IgE binding, thereby preventing IgE binding membrane CD23 (Tsicopoulos and Joseph, 2000). McCloskey *et al.* (2007) have shown that the structure of CD23 has an effect on IgE synthesis. They found that the ability of the sCD23 to form trimers or oligomers affected the synthesis of IgE, where derCD23 was found to inhibit IgE synthesis, a sCD23 recombinant protein spanning the entire extracellular sequence showed no effect on IgE synthesis and a sCD23 spanning the extracellular sequence with an isoleucine zipper sequence on the N terminus for stabilisation of the oligomeric structure stimulated IgE synthesis. In the same way, it is possible that the derCD23 is able to activate the cell lines through its binding to CD11b/CD11c, the CD23M150 is able to partially activate the CD11 on the cell lines, while the CD23M79 protein could

possibly be forming oligomers which allow binding, but prevent activation of the CD11 proteins.

The interactions between sCD23 and CD11 could affect inflammatory disease, as well as hamper the movement of monocytes to sites of inflammation, which would be detrimental to any disease or inflammatory tissue. If there was a way to block this binding of sCD23 to CD11b and CD11c then this effect might be overcome. This could be done by blocking antibodies or small peptides, or by blocking the signalling pathways involved in the interactions of these two proteins.

Chapter 4: Conclusions and future studies

The results of this study have shown that there is much work that can still be done to investigate the interaction between sCD23 and the β_2 integrin proteins. The protein interaction studies have shown that sCD23 binds cells that have the β_2 integrin proteins upregulated on their cell surface and that this binding is significantly diminished by an anti-CD11b antibody specific for the αI domain. It was proven difficult to produce recombinant full-length CD11b and CD11c, however we were able to show that sCD23 is able to bind a recombinant αI domain of CD11b and CD11c, using ELISA. The ELISA data were further supported by SPR data which showed binding of CD11c αI domain to derCD23 and CD23M79. The binding studies have shown that sCD23 proteins bind the αI domain of CD11b and CD11c, however this does not rule out the possibility that the proteins could bind to additional sites on the β_2 integrin proteins. Other ligands for β_2 integrin proteins have been shown to bind to other sites in addition to the αI domain of integrins. For example, the αI domain is only minimally implicated in the binding of Factor X to CD11b (Zhou *et al.*, 1994). Zymosan is also able to bind CD11b through one or more lectin sites found outside of the I domain (Thornton *et al.*, 1996).

The derCD23 protein was able to decrease phagocytosis with differentiated HL60 cells. This decrease, although significant, was not very large and was not seen with the other cells. There is a possibility that the sCD23 proteins may affect the adherence of foreign particles to β_2 integrins without their internalisation, however this would need to be investigated further. It could also be that other extracellular signals are required in addition to the binding of CD23 proteins to the β_2 integrin proteins before a more significant change in phagocytic ability of the cells is seen.

The derCD23 protein was also able to significantly decrease the chemotaxis of HL60 and U937 cells. CD23M150 was also able to significantly decrease the chemotaxis in THP1 cells. An important difference that stands out between the THP1 cells compared to the HL60 and U937 cells is the difference in upregulation between the CD11b and CD11c integrins. The THP1 cell line showed a much higher expression of CD11c when differentiated, while CD11b was preferentially upregulated in the HL60 and U937 cell lines. This could possibly explain the difference seen in the chemotaxis results. It is possible that derCD23 binds preferentially to CD11b in HL60 and U937 cells, while CD23M150 binds preferentially to CD11c in THP1 cells. It could also indicate that although derCD23 is able to bind CD11c, derCD23 on its own is not sufficient to decrease chemotaxis, either due to an inability to alter the activation state of CD11c or due to another activator required to increase the affinity state of the CD11 proteins.

derCD23 was also able to significantly increase the production of MPO by HL60 and U937 cells. This effect was also seen with the CD23M79 protein in HL60 cells. Although the increase in MPO was very small, MPO is primarily an indicator of the cell's cytotoxic potential. This would indicate that the cells are being activated by these proteins, as seen with the increase in oxidative burst. The method used to detect MPO was only detects the protein level of MPO whereas a method determining MPO expression levels in correlation to the activity of MPO might be a better indicator for cytotoxic potential in future studies.

derCD23 was able to induce significant oxidative burst in all differentiated and naïve cell lines. In the same way, CD23M150 was able to significantly stimulate oxidative

burst in differentiated and naïve HL60 and U937 cells and in differentiated THP1 cells. The CD23M79 protein was unable to change the oxidative burst in any of the cell lines. These data suggest that it may be the binding to CD11b that is causing this increase in oxidative burst. Both the HL60 and U937 cells have a higher level of CD11b present on the cell surface when naïve and differentiated. The THP1 cells have a very low level of CD11b on naïve cells compared to CD11c and this level is only increased on differentiation. It is only with these CD11b-upregulated THP1 cells that we see an increase in oxidative burst. The increase in oxidative burst by cells could serve several purposes. A small increase in ROS production could indicate the activation of cell signalling pathways. CD23 has been shown to prevent apoptosis in B cells, so it is possible that this increase in ROS production plays a role in the apoptotic rescue of monocytes. The increase in ROS production could also indicate the activation of signalling pathways involved in inflammation, and be linked as a precursor for diseases such as those commonly attributed in part to CD23 (such as hyper IgE syndrome, rheumatoid arthritis and asthma). It is important to note that derCD23 showed the same decrease in phagocytosis and chemotaxis and increase in ROS production in these experiments as did fibrinogen. Fibrinogen is also able to bind CD11 proteins and is responsible for altering leukocyte function by changing their phagocytic, migration, NF-κB-mediated transcription, cytokine production and degranulation activities (Flick *et al.*, 2004). It would therefore seem that sCD23 proteins (especially derCD23) may be able to have the same effect on inflammation as fibrinogen. Since fibrinogen is considered an inflammatory 'acute phase reactant' (Flick *et al.*, 2004) and derCD23 (which is associated with house dust mite allergies) has a similar effect on monocytes, it would imply that derCD23 is the acute phase reactant in allergic inflammation.

The effect of blocking signalling pathways was also investigated. AMPK is known to inhibit PI3K. The blocking of AMPK in differentiated HL60 cells showed an increase in ROS, indicating that these cells may have a high basal activity of AMPK which inhibits PI3K and therefore ROS production. When the AMPK inhibitor is added in conjunction with derCD23, CD23M150 and CD23M79 in naïve and differentiated THP1 and U937 cells, a large increase in ROS is seen. This could again be explained by a high basal level of AMPK which then blocks PI3K. When this basal AMPK is blocked, it allows the proteins to signal freely through PI3K, causing a large increase in ROS. IKK is downstream in the signalling pathway from Akt which signals through ERK and produces ROS when IKK is blocked. ERK is a MAPK and is upstream in the signalling pathway to PI3K. Akt is also able to inhibit AMPK, which could demonstrate why a basal level of AMPK blocking PI3K is not seen with the THP1 and U937 cells as is seen in HL60 cells. The p38MAPK/ERK inhibitor shows an increase in ROS production with derCD23 in THP1 differentiated cells and with all three sCD23 proteins in differentiated U937 cells. The Src kinases are activated by FAK and activate PI3K, MAPKs and PKC. If Src kinases are blocked, FAK is forced to signal through JNK. ROS is increased in differentiated U937 cells when PI3K is blocked in conjunction with derCD23 protein and CD23M79. CD23M150 only showed increases in ROS with all cell lines with the AMPK inhibitor which results in the free use of the PI3K pathway. The results indicate that all the pathways are able to be utilised by the cells when other pathways are blocked, however, PI3K appears to be the commonly used pathway.

Although there is much work that can be done on these signalling pathways, it would seem that most of the data points to the sCD23 proteins signalling through β_2 integrin

proteins using the PI3K pathway as the major pathway. It is also possible that the MAPK, Akt and Src kinase pathways contribute to the results seen.

One of the initial events in integrin signaling is the activation of PI3K and Src kinases (Dib *et al.*, 2008). Therefore utilisation of the PI3K and MAPK signalling pathways in the binding of sCD23 proteins to CD11 proteins is no surprise. It is important to note at this stage that the activation of neutrophils and monocytes to their full chemotactic, phagocytic and adhesive abilities is dependent on the prior activation of CD11b. This is achieved via the outside-in signalling generated by either the receptor-clustering pathway or the G protein pathway. The receptor-clustering pathway has been shown to signal though PI3K. Since sCD23 proteins do not increase chemotaxis or phagocytosis, yet they activate monocytes (most likely through PI3K), it is possible that sCD23 proteins are the 'primers' for CD11 outside-in signalling activation and activate cells to enhance the effect of other ligands on their phagocytic, chemotactic, adhesive and inflammatory abilities.

It is important to note that all three sCD23 proteins have been shown to bind the αI domains of the CD11b and CD11c proteins. However, it would seem that some additional stimulation or activation of the cells or a change in affinity or avidity of the CD11c protein is required to elicit a response from the cells. In the same way, even though all three sCD23 proteins are binding to the CD11b and CD11c proteins, they are not demonstrating the same results. It could be the differences in structure between the sCD23 proteins that cause the results seen with the cells. It is possible that the CD23M79 proteins are self-associating due to having a section of the leucine zipper sequence, while the other two sCD23 proteins do not (this has been shown in another study in our laboratory, unpublished data). This oligomerisation appears not

to affect binding to CD11 proteins, but may affect the subsequent ability of the CD11 proteins to induce signalling pathways, the activation state of CD11 proteins or prevent the CD11 proteins from binding other ligands simultaneously.

These results show that it would be very valuable to further investigate the interaction surfaces between sCD23 and the αI domains of CD11b and CD11c. Surface Plasmon resonance spectroscopy was used in this study, but nonspecific interaction of CD11 with the SA chip surface greatly influenced binding data. It would be interesting to use the αI domains as ligands in future, or alternatively use dextran in the running buffer to suppress nonspecific binding. As mentioned in section 2.4, the SPR data needs to be replicated with additional controls added. It could also be useful to use full length integrin α subunits during the analysis to assess whether there is a difference in the binding to sCD23 proteins observed between the αI domain and full length α subunits.

Another method that can be used to investigate the binding of these two proteins is to use Quartz Crystal Microbalance with Dissipation Monitoring (QCM-D). With this method, cells that have the β_2 integrin proteins upregulated on their cell surface (in the same way as used in this study) could be used to investigate the binding of sCD23 proteins. This can then also be repeated with the inclusion of various β_2 integrin blocking proteins or synthetic blocking peptides. In the same way, synthetic blocking peptides designed to block sections of the sCD23 proteins could also be produced and preincubated with the sCD23 proteins before they are used in experiments. Synthetic blocking peptides to sCD23 could also be used in ELISA experiments to investigate whether binding to cells expressing β_2 integrins is decreased or completely blocked by the addition of one or a combination of peptide inhibitors.

Diamond *et al.* (1993) have previously produced α subunit chimeras for β_2 integrins which have successfully transfected COS cells. In the same way, chimeras could be produced for CD11b and CD11c α subunits for use in QCM-D experiments as well as ELISA experiments such as those carried out in this thesis.

It would also be interesting to simultaneously stain the proteins fluorescently and investigate the binding using a confocal microscope, which would possibly give a good visual interpretation on how these proteins bind. Site directed mutagenesis of both the CD23 and the CD11b/CD11c proteins would also be useful for investigating which amino acid motifs are essential for the CD23-β_2 integrin interactions. These proteins could be used for ELISA, SPR and QCM-D analyses.

The cell studies have also shown a whole range of new experiments that could be carried out. This work was conducted using monocytic cell lines and isolated $CD14^+$ monocytes. It would be interesting if the chemotaxis, phagocytosis and oxidative burst experiments were also carried out using neutrophils. Since neutrophils have shown to use different phagocytic, chemotactic and signalling pathways, it would be interesting to investigate if the sCD23 proteins showed a different effect in neutrophils on interaction with the β_2 integrin proteins. This alone is a significant amount of work and with the lack of information on the interaction between these known ligands, it is vital that these experiments are conducted in the future.

Further cell studies could also look at the upregulation of other possible CD23 ligands in the U937, HL60 and THP1 cells on stimulation with vitamin D_3. However, CD21 and IgE are both only produced by B cells, so they will not be found to be upregulated

by these cells. Flow cytometry can be used to detect the levels of vitronectin receptor present in the same way as was used to investigate the upregulation of CD11b and CD11c . It might also be useful to repeat the ELISA binding experiments as well as the oxidative burst experiments using blocking antibodies for the vitronectin receptor, to ensure that the binding of sCD23 to the vitronectin receptor is not influencing the results seen in any way.

Several experiments can still be conducted with the monocyte cells. We have shown little change in the phagocytosis of *E. coli* bioparticles by sCD23 stimulated monocytes. However, it may be that CD23 stimulates the upregulation of phagocytosis of non-bacterial particles, or only opsonised particles. It would be useful to repeat these experiments with other phagocytic particles. Confocal microscopy could also be used to assess whether the phagocytic particles are adhering to the outside of the cells and not being injested, or whether there is no adherence at all when stimulated with CD23 proteins. Since FcγRII cooperates with CD11b to stimulate respiratory burst and antibody-dependent phagocytosis (Ehlers, 2000), it may be useful to use antibody-coated particles in phagocytic experiments and look at isotype-specific phagocytosis at the same time. The oxidative burst experiments have shown that the sCD23 proteins are definitely involved in activating the cells and inducing various signalling pathways. These experiments could be repeated with other methods of detection for ROS (H_2O_2, NOS and MPO). Western blotting or flow cytometry could also be used to investigate the upregulation of several of the cell signalling pathway components and their activated forms (with phospho-specific antibodies) such as PI3K, p38 MAPK, ERK, AMPK, Akt, NF-κB and Src kinase. In the same way, it can be investigated what happens to these signalling pathways that the sCD23 stimulate when they are blocked by various inhibitors as well as various

combinations of these inhibitors. Another useful experiment to repeat would be to investigate the production of cytokines by these cells when exposed to sCD23 proteins. However, it would be most useful if a cytokine bead array is used to investigate this, as one small sample could show the upregulation or downregulation of a bigger range of cytokines (up to ten cytokines can be measured simultaneously from one sample) and it is suggested that a Th1/Th2 panel of cytokines is used to investigate these interactions. Another alternative would be to use quantitative PCR to determine the upregulation of cytokines.

The interaction between sCD23 and β_2 integrin proteins is proving to be a very interesting subject and in my opinion is going to provide years of interesting research ahead of us.

Chapter 5: References

Adachi, M., M. Fukuda and E. Nishida. 2000. Nuclear Export of MAP Kinase (ERK) Involves a MAP Kinase Kinase (MEK)-dependent Active Transport Mechanism. *The Journal of Cell Biology*, 148: 849-856.

Aitken, A. and M. Learmonth. 1996. Estimation of disulphide bonds using Ellman's reagent. The Protein Protocols Handbook, pp487-488. J.M. Walker, Ed. Humana Press, New Jersey.

Alderson, M.R., Tough, T.W., Ziegler, S.F. and Armitage, R.J. 1992. Regulation of human monocyte cell-surface and soluble CD23 (FcεRII) by granulocyte macrophage colony-stimulating factor and IL-3. *Journal of Immunology*, **149**: 1252-1257.

Anderson, D.C. and T.A. Springer. 1987. Leukocyte Adhesion Deficiency: An inherited defect in the Mac-1, LFA-1 and p150, 95 glycoproteins. *Annual Reviews in Medicine*, 38: 175-194.

Armant, M., H. Ishihara, M. Rubio, G. Delespesse and M. Sarfati. 1994. Regulation of cytokine production by soluble CD23: costimulation of interferon γ secretion and triggering of tumour necrosis factor α release. *Journal of Experimental Medicine*, **180**: 1005-1011.

Arnaout, M.A., S.K. Gupta, M. W. Pierce, and D. G. Tenen. 1988. Amino Acid Sequence of the Alpha Subunit of Human Leukocyte Adhesion Receptor Mol (Complement Receptor Type 3). *Journal of Cell Biology*, **106**: 2153-2158.

Arnau, J., C. Lauritzen, G.E. Petersen and J. Pederson. 2006. Current strategies for the use of affinity tags and tag removal for the purification of recombinant proteins. *Protein Expression and Purification*, **48**: 1-13.

Askew, S.L. 2006. Cytokine signalling functions of human soluble IgE receptors in peripheral blood mononuclear cells from normal and hyper-allergic individuals and in B-lymphoblastoid and monocytic cell lines. Masters dissertation. Department of Biochemistry and Microbiology, Nelson Mandela Metropolitan University.

Asquith, B., C. Debacq, A. Florins, N. Gillet, T. Sanchez-Alcaraz, A. Mosley and L. Willems. 2006. Quantifying lymphocyte kinetics in vivo using Carboxyfluorescein diacetate, succinimidyl ester. Proceedings of the Royal Society of Biological Sciences, 273: 1165-1171.

Aubry, J-P., N. Dugas., S. Lecoanet-Henchoz, F. Ouaaz, H. Zhou, J-F. Delfraissy, P.Graber, J-P. Kolb, B. Dugas and J-Y. Bonnefoy. 1997. The 25-kDa soluble CD23 activates type III constitutive nitric oxide-synthase activity via CD11b and CD11c expressed by human monocytes. *Journal of Immunology*, **159:** 614-622.

Aubry, J-P., S. Pochon, J-F. Gauchat, A. Nueda-Marin, V.M. Holers, P. Graber, C. Siegfried and J-J. Bonnefoy. 1994. CD23 interacts with a new functional extracytoplasmic domain involving N-linked oligosaccharides on CD21. *Journal of Immunology*, **152:** 5806-5813.

Beavil, R.L., P. Graber, N. Aubonney, J-Y. Bonnefoy and H.J. Gould. 1995. CD23/FcεRII and its soluble fragments can form oligomers on the cell surface and in solution. *Immunology*, **84:** 202-206.

Bedard, K. and K-H. Krause. 2007. The NOX family of ROS-generating NADPH oxidases: Physiology and pathophysiology. *Physiology Reviews*, **87**: 245-313.

Berton, G. and C.A. Lowell. 1999. Integrin signalling in neutrophils and macrophages. *Cell Signalling*, **11**: 621-635.

Bogdan, C. 2001. Nitric Oxide and the immune response. *Nature Immunology*, **2**: 907-916.

Borland, G., A.L. Edkins, M. Acharya, J. Matheson, L.J. White, J.M. Allen, J-Y. Bonnefoy, B.W. Ozanne and W. Cushley. 2007. αvβ5 integrin sustains growth of human pre-B cells through an RGD-independent interaction with a basic domain of the CD23 protein. *Journal of Cell Biology*, **282**: 27315-27326.

Bottling, J., F. Oberg, H. Torma, P.Tuohimaa, M. Blauer and K. Nilssen. 1996. Vitamin D3- and retinoic acid-induced monocytic differentiation: Interactions between the endogenous vitamin D3 receptor, retinoic acid receptors and retinoid x receptors in U-937 cells. *Cell Growth and Differentiation*, **7**: 1239-1249.

Boyum, A. 1984. Separation of lymphocytes, granulocytes, and monocytes from human blood using iodinated density gradient media. *Methods in Enzymology*, **108**:88-102.

Bradford, M.M. 1976. A rapid and sensitive method for the quantitation of microgram quantities of protein utilizing the principle of protein-dye binding. *Analytica Biochemistry*, **72**: 248-254.

Bullard, D.C., X. Hu, J.E. Adams, T.R. Schoeb and S.R. Barum. 2007. p150/95 (CD11c/CD18) expression is required for the development for experimental autoimmune encephalomyelitis. *American Journal of Pathology*, **170**: 2001-2008.

Carreras, M.C. and J.J. Poderoso. 2007. Mitochondrial nitric oxide in the signalling of cell integrated responses. *American Journal of Physiology*, **292**: C1569-1580.

Charrier-Hisamuddin, L., C.L. Laboisse and D. Merlin. 2008. ADAM-15: a metalloproteinase that mediates inflammation. *FASEB Journal*, **22**: 641-653.

Chen, B-H., M.A. Check, T.H. Caven, Y. Chan-Li, A. Beavil, R. Beavil, H. Gould and D.H. Conrad. 2002. Necessity of the stalk region for immunoglobulin E interaction with CD23. *Immunology*, **107**: 373-381.

Cho, S., M.A. Kilmon, E.J. Studer, H. van der Putten and D.H. Conrad. 1997. B cell activation and IgE, especially IgE production, is inhibited by high CD23 levels in vivo and in vitro. *Cellular Immunology*, **180**: 36-46.

Choi, J. and S-U. Nham. 2002. Loops within the CD11c I Domain Critical for Specific Recognition of Fibrinogen. *Biochemical and Biophysical Research Communications*, **292**, 756–760.

Choi, J., L. Leyton and S-U. Nham. 2005. Characterisation of αX I-domain binding to Thy-1. *Biochemical and Biophysical Research Communications*, **331**: 557-561.

Chrisholm III, G.M., S.L. Hazen, P.L. Fox and M.K. Cathcart. 1999. The oxidation of lipoproteins by monocytes-macrophages. *Journal of Biological Chemistry*, **274**: 25959-25962.

Clark, E, D.B. 2001. Protein refolding for industrial processes. *Current Opinion in Biotechnology*, **12**:202-207

Collins, S.J. 1987. The HL-60 promyelocytic leukemia cell line: proliferation, differentiation and cellular oncogene expression. *Blood*, **70**: 1233-1244.

Conrad, D.H. 1990. FcεRII/CD23: The low affinity receptor for IgE. *Annual Reviews of Immunology*, **8**: 623-645.

Corbi, A.L., L.J. Miller, K. O'Connor, R.S. Larson and T.A. Springer. 1987. cDNA cloning and complete primary structure of the α subunit of a leukocyte adhesion glycoprotein, p150,95. *The EMBO Journal*, **6**:4023-4028.

Corbi, A.L., T.K. Kishimoto, L.J. Miller and T.A. Springer. 1988. The Human Leukocyte Adhesion Glycoprotein Mac- 1 (Complement Receptor Type 3, CDllb) α Subunit: Cloning, primary structure and relation to the integrins, Von Willebrand factor and factor B. *Journal of Biological Chemistry*, **263**: 12403-12411.

Corry, D.B. and F. Kheradm. 1999. Induction and regulation of the IgE response. *Nature*, **402:** B18-B23.

Dale, D.C., L. Boxer and W.C. Liles. 2008. The phagocytes: neutrophils and monocytes. *Blood*, **112**: 935-945.

Daniels, B.B. 2003. The effect of human soluble FcεRII on the RPMI8866 B-lymphoblastoid and the U937 monocyte cell lines. Masters dissertation. Department of Biochemistry and Microbiology, Nelson Mandela Metropolitan University.

Daniels, B.B., S.L. Askew, M. van de Venter and V. Oosthuizen. 2005. Production of biologically active recombinant human soluble CD23 and its effect on PBMCs isolated from hyper-IgE blood. *Cellular Immunology*, **234**: 146-153.

Delves, P.J., S.J. Martin, D.R. Burton and I.M. Roitt. 2006. Roitt's Essential Immunology, 11th Ed. Blackwell Publishing Ltd.Oxford.

Derave, W., H. Ai, J. Ihlemann, L.A. Witters, S. Kristiansen, E.A. Richter and T. Ploug. 2000. Dissociation of AMP-activated protein kinase activation and glucose transport in contracting slow-twitch muscle. *Diabetes*, 49: 1281-1287.

Dessaint, J.P., M. Capron and A. Capron. 1990. Immunoglubulin E-stimulated release of mediators from mononuclear phagocytes, eosinophils, and platelets, In: H. Metzger (Ed.) *Fc Receptors and the action of antibodies*, pp 260-280. ASM, Washington.

Diamond, M.S. and T.A. Springer. 1993. A subpopulation of mac-1 (CD11b/CD18) molecules mediates neutrophil adhesion to ICAM-1 and fibrinogen. *Journal of Cell Biology*, **120:** 545-556.

Diamond, M.S., J. Garcia-Aguilar, J.K. Bickford, A.L. Corbi and T.A. Springer. 1993. The I domain is a major recognition site on the leukocyte integrin Mac-1 (CD11b/CD18) for four distinct adhesion ligands. *Journal of Cell Biology*, **120**: 1031-1043.

Diamond, M.S., Staunton, D.E., Marlin, S.D., and T.A. Springer. 1991. Binding of the integrin Mac-1 CD11b/CD18 to the third Ig-like domain of ICAM-1 CD54 and its regulation by glycosylation. *Cell*, **65**: 961-971.

Dib, K., L. Axelsson and T. Andersson. 2008. β_2 integrins target Rap GTPases to the plasma membrane by means of degranulation. *Biochemical and Biophysical Research Communications*, **376**: 642-646.

Dugas, B., M.D. Mossalayi, C. Damais and J-P. Kolb. 1995. Nitric oxide production by human monocytes: evidence for a role of CD23. *Immunology Today*, **16**: 574-579.

Dupuy, A. and E. Caron. 2008. Integrin-dependent phagocytosis – spreading from microadhesion to new concepts. *Journal of Cell Science*, **121**: 1773-1783.

Ehlers, M.R.W. 2000. CR3: a general purpose adhesion-recognition receptor essential for innate immunity. *Microbes and Infection*, **2**: 289-294.

Ellman, G.L. 1959. Tissue sulfhydryl groups. *Archives of Biochemistry and Biophysics*, **82**:70-77.

Emre, Y., C. Hurtaud, T. Nubel, F. Criscuolo, D. Ricquier and A-M. Cassard-Doulcier. 2007. Mitochondria contribute to LPS-induced MAPK activation via uncoupling protein UCP2 in macrophages. *Biochemical Journal*, **402**: 271-278.

Flick, M.J., X. Du and J.L. Degen. 2004. Fibrin(ogen)-αMβ2 interactions regulate leukocyte function and innate immunity *in vivo*. *Experimental Biology and Medicine*, **229**: 1105-1110.

Forman, H.J. and M. Torres. 2002. Reactive oxygen species and cell signalling. Respiratory burst in macrophage signalling. *American Journal of Respiratory and Critical Care Medicine*, **166**: 54-58.

Fourie, A.M., F. Coles, V. Moreno and L. Karlsson. 2003. Catalytic activity of ADAM18, ADAM15 and MDC-L (ADAM28) on synthetic peptide substrates and in ectodomain cleavage of CD23. *Journal of Biological Chemistry*, **278**: 30469-30477.

Fremeaux-Bacchi, V., J-P. Aubry, J-Y. Bonnefoy, M.D. Kazatchkine, J-P Kolb and E.M. Fischer. 1998. Soluble CD21 induces activation and differentiation of human monocytes through binding to membrane CD23. *European Journal of Immunology*, **28**: 4268–4274.

Fu Y, O'Connor LM, Shepherd TG, and M.W. Nachtigal. 2003. The p38 MAPK inhibitor, PD169316, inhibits transforming growth factor beta-induced Smad signalling in human ovarian cancer. *Biochemical and Biophysical Research Communications*, **310**:391-7.

Gahmberg, C.C. 1997. Leukocyte adhesion: CD11/CD18 integrins and intercellular adhesion molecules. *Current Opinion in Cell Biology*, **9**:643-650.

Gahmberg, C.G., L. Valmu, S. Fagerholm, P. Kotovuori, E. Ihanus, L.Tian and T. Pessa-Morikawa. 1998. Leukocyte integrins and inflammation. *Cellular and Molecular Life Sciences*, **54**: 549-555.

Gahmberg, C.G., S.C. Fagerholm, S.M. Nurmi, T. Chavakis, S. Marchesan and M. Grönholm. 2009. Regulation of integrin activity and signalling. *Biochimica et Biophysica Acta*, **1790:** 41-444.

Gallagher T.F., Seibel G.L., Kassis S., Laydon J.T., Blumenthal M.J., Lee J.C., Lee D., Boehm J.C., Fier-Thompson S.M., Abt, J.W., Soreson M.E., Smietana J.M., Hall R.F., Garigipati R.S., Bender P.E., Erhard K.F., Krog A.J., Hofmann G.A., Sheldrake P.L., McDonnell P.C., Kumar S., Young P.R., Adams J.L. 1997.

Regulation of stress-induced cytokine production by pyridinylimidazoles; inhibition of CSBP kinase. *Bioorganic and Medicinal Chemistry*, **51**:49-64.

Georgakopoulos, T., S.T. Moss and V. Kanagasundaram. 2008. Integrin CD11c contributes to monocyte adhesion with CD11b in a differential manner and requires Src family kinase activity. *Molecular Immunology*, **45**: 3671-3681.

Ginsberg, M.H., A. Partridge and S.J. Shattil. 2005. Integrin regulation. *Current Opinion in Cell Biology*, **17**: 509-516.

Gliore, G., S. Legrand-Poels and J. Piette. 2006. NFκB activation by reactive oxygen species: fifteen years later. *Biochemical Pharmacology*, **72**: 1493-1505.

Gould, H.J. and B.J. Sutton. 2008. IgE in allergy and asthma today. *Nature Reviews Immunology*, **8**: 205-217.

Gould, H.J., Sutton, B.J., Beavil, A.J., Beavil, R.L., McCloskey, N., Coker, H.A., Fear, D. and Smuthwaite, L. 2003. The biology of IgE and the basis of allergic disease. *Annual Reviews in Immunology*, **21**: 579-628.

Greenberg, S. and S. Grinstein. 2002. Phagocytosis and innate immunity. *Current Opinion in Immunology*, **14:** 136-145.

Gu, B., L.J. Bendall and J.S. Wiley. 1998. Adenosine triphosphate-induced shedding of CD23 and L-selectin (CD62L) from lymphocytes is mediated by the same receptor but different metalloproteases. *Blood*, **92**: 946-951.

Gurlek, A., M.R. Pittelkow and R. Kumar. 2002. Modulation of growth factor/cytokine synthesis and signalling by 1α,25-dihydroxyvitamin D_3: implications in cell growth and differentiation. *Endocrine Reviews*, **23**: 763-786.

Guzik, T.J., R. Korbut and T. Adamek-Guzik. 2003. Nitric oxide and superoxide in inflammation and immune regulation. *Journal of Physiology and Pharmacology*, **54:** 469-487.

Haishima, Y., C. Hasegawa, T. Yagami, T. Tsuchiya, R. Matsuda and Y. Hayashi. 2003. Estimation of uncertainty in kinetic-colourimetric assay of bacterial toxins. *Journal of Pharmaceutical and Biomedical Analysis*, **32**: 495-503.

Hamelmann, E., C. Rolinck-Werninghaus and U. Wahn. 2002. From IgE to anti-IgE: Where do we stand? *Allergy*, **57**: 983-994.

Hanke, J.H., J.P. Gardner, R.L. Dow, P.S. Changelian, W.H. Brissette, E.J. Weringer, B.A. Pollok and P.A. Connelly. 1996. Discovery of a Novel, Potent, and Src Family-selective Tyrosine Kinase Inhibitor: Study of Lck-and Fyn- dependent T cell activation. *Journal of Biological Chemistry*, 271: 695–701.

Harburger, D.S. and D.A Calderwood. 2009. Integrin signalling at a glance. *Journal of Cell Science*, **122**: 159-163.

Harris, P. and P. Ralph. 1985. Human leukemic models of myelomonocytic development: A review of the HL60 and U937 cell lines. *Journal of Leukocyte Biology*, **37**: 407-422.

Harris, E.S., T.M. McIntyre, S.M. Prescott and G.A. Zimmerman. 2000. The leukocyte integrins. *Journal of Biological Chemistry*, **275**: 23409-23412

Hermann, P., M. Armant, E. Brown, M. Rubio, H. Ishihara, D. Ulrich, R.G. Caspary, F.P. Lindberg, R. Armitage, C. Maliszewski, G. Delespesse and M. Sarfati. 1999. The vitronectin receptor and its associated CD47 molecule mediates proinflammatory cytokine synthesis in human monocytes by interaction with soluble CD23. *Journal of cell Biology,* **144:** 767-775.

Heyman, B. 2000. Regulation of antibody responses via antibodies, complement and Fc receptors. *Annual Reviews of Immunology*, **18**: 709-737.

Hibbert, R.G., P. Teriete, G.J. Grundy, R.L. Beavil, R. Reljic, V.M. Holers, J.P. Hannan, B.J. Sutton, H.J. Gould and J.M. McDonnell. 2005. The structure of human CD23 and its interactions with IgE and CD21. *Journal of Experimental Medicine,* **202**: 751-760.

Hmama, Z., D. Nandon, L. Sly, K.L. Knutsun, P. Herrera-Velit and N. E. Reiner. 1999. 1α, 25-dihydroxyvitamin D_3-induced myeloid cell differentiation is regulated by a vitamin D receptor-phosphatydylinositol 3-kinase signalling complex. *Journal of Experimental Medicine*, **11**: 1583-1594.

Ho, M-K. and T.A. Springer. 1983. Biosynthesis and Assembly of the α and β Subunits of Mac-1, a Macrophage Glycoprotein Associated with Complement Receptor Function. *The Journal of Biological Chemistry*, **258**: 2766-2769.

Hoidal, J.R. 2001. Reactive oxygen species and cell signalling. *American Journal of Respiratory Cell and Molecular Biology*, **25**: 661-663.

Hunt, I. 2005. From gene to protein: a review of new and enabling technologies for multi-parallel protein expression. *Protein Expression and Purification*, **40**: 1-22.

Ihanas, E., L. Uotila, A. Toivanen, M. Stefanidakis, P. Bailly, J-P. Cartron and C.G. Gahmberg. 2003. Characterization of ICAM-4 binding to the I domains of the CD11a/CD18 and CD11b/CD18 leukocyte integrins. *European Journal of Biochemistry*, **270:** 1710-1723.

Ingalls, R.R. and D.T. Golenbock. 1995. CD11c/CD18, A transmembrane Signalling Receptor for Lipopolysaccharide. *Journal of Experimental Medicine*, **181**:1473-1479.

Jakus, Z., S. Fodor, C.L. Abram, C.A. Lowell and A. Mocsai. 2007. Immunoreceptor-like signalling by β_2 and β_3 integrins. *TRENDS in Cell Biology*, **17**: 493-501.

Janeway, P. Travers, M. Walport and M. Sholmchik. 2001. *Immunobiology vol. 5*, Garland Press.

Jenei, V., R.K. Deevi, C.A. Adams, L. Axelsson, D.G. Hirst, T. Andersson and K. Dib. 2006. Nitric oxide produced in response to engagement of β_2 integrins on human neutrophils activates the monomeric GTPases Rap1 and Rap2 and promotes adhesion. *Journal of Biological Chemistry*, **281**: 35008-35020.

Karagiannis, S.N., J.K. Warrack, K.H. Jennings, P.R. Murdock, G. Christie, K. Moulder, B.J. Sutton and H.J. Gould. 2001. Endocytosis and recycling of the complex between CD23 and HLA-DR in human B cells. *Immunology*, **103**: 319-331.

Kaufmanpaterson, R.L., R. Or, J. M. Domenico, G. Delespesse and E.W. Gelfand. 1994. Regulation of CD23 expression by IL-4 and corticosteroid in human B lymphocytes. Altered response after EBV Infection. *Journal of Immunology*, **152**:2139.

Kijimoto-Ochiai, S. 2002. CD23 (the low-affinity IgE receptor) as a C-type lectin: a multidomain and multifunctional molecule. *Cellular and Molecular Life Sciences*, **59:** 648-664.

Kikutani, H., S. Inui, R. Sato, E.L. Barsumian, H. Owaki, K. Yamasaki, T. Kaisho, N. Uchibayashi, R.R. Hardy, T. Hirano, S. Tsunasawa, F. Sakiyama, M. Suemura and T. Kishimoto. 1986. Molecular structure of human lymphocyte receptor for immunoglobulin E. *Cell*, **47**: 657-665.

Kim M, Carman CV and Springer TA. 2003. Bidirectional transmembrane signalling by cytoplasmic domain separation in integrins. *Science*, **301**: 1720-1725.

Kim, C.H., K-H. Lee, C-T. Lee, Y.W. Kim, S.K. Han, Y-S. Shim and C-G. Yoo. 2004. Aggregation of β_2 integrins activates human neutrophils through the IκB/NF-κB pathway. *Journal of Leukocyte Biology*, **75**: 286-292.

Kim, J.S., V. Saengsirisuwan, J.A. Sloniger, M.K. Teachey and E.J. Henriksen. 2006. Oxidant stress and skeletal muscle glucose transport: Roles of insulin signalling and p38 MAPK. *Free Radical Biology and Medicine*, **41**: 818-824.

Kishimoto, T.K., N. Hollander, T.M. Roberts, D.C. Anderson and T.A. Springer. 1987. Heterogenous mutations in the β subunit common to the LFA-1, Mac-1 and p150,95 glycoproteins cause leukocyte adhesion deficiency. *Cell*, **50**: 193-202.

Klugewitz, K., K. Lei, D. Schuppan, R. Nuck, P. Gaehtgens and B. Walzog. 1997. Activation of the β_2 integrin Mac-1 (CD11b/CD18) by an endogenous lipid mediator of human neutrophils and HL60 cells. *Journal of Cell Science*, **110**: 985-990.

Kobori, M., Z. Yang, D. Gong, V. Heissmeyer, H. Zhu, Y-K. Jung, M. Angelica M Gakidis, A. Rao, T. Sekine, F. Ikegami, C. Yuan and J. Yuan. 2004. Wedelolactone suppresses LPS-induced caspase-11 expression by directly inhibiting the IKK Complex. *Cell Death and Differentiation*, **11**: 123–130.

Koeffler, H.P. 1983. Induction of differentiation of human acute myelogenous leukemia cells: Therapeutic implications. *Blood*, **62**: 709-721.

Kolb, J-P., A. Abadie, A. Proschnicka-Chalufour, A. de Gramont and J. Poggioli. 1994. CD23-mediated cell signalling. *Journal of Lipid Mediators and Cell Signalling*, **9**: 27-35.

Kolb, J-P., A. Abadie, N. Paul-Eugene, M. Capron, M. Sarfati, B. Dugas and G. Delespesse. 1993. Ligation of CD23 triggers cyclic AMP generation in human B lymphocytes. *Journal of Immunology*, **150**: 4798-489.

Kruger, N.J. 1996. The Bradford Method for Protein Quantitation. *Methods in Molecular Biology*, **32**: 9-15.

Laemmli, U.K. 1970. Cleavage of structural proteins during the assembly of the head of bacteriophage T4. *Nature*, **227**: 680-685.

Larson, R.S., M.L. Hibbs and T.A. Springer. 1990. The leukocyte integrin LFA-1 reconstituted by cDNA transfection in a nonhematopoietic cell line is functionally active and not transiently regulated. *Cell Regulation*, **1**: 359-367.

Le Cabeq, V., S. Carreno, A. Moisand, C. Bordier and I. Maridonneau-Parini. 2002. Complement receptor 3 (CD11b/CD18) mediates type II and type II phagocytosis during non-opsonic and opsonic phagocytosis, respectively. *Journal of Immunology*, **169**: 2003-2009.

Lecoanet-Henchoz, S., J-F. Gauchat, J-P. Aubry, P. Graber, P. Life, N. Paul-Eugene, B. Ferrua, A.L. Corbi, B. Dugas, C. Plater Zyberk and J-Y. Bonnefoy.

1995. CD23 regulates monocyte activation through a novel interaction with the adhesion molecules CD11b-CD18 and CD11c-CD18. *Immunity*, **3**: 119-125.

Lee, M., J-Y. Kim and W.B. Anderson. 2004. Src Tyrosine Kinase Inhibitor PP2 Markedly Enhances Ras-independent Activation of Raf-1 Protein Kinase by Phorbol Myristate Acetate and H_2O_2. *Journal of Biological Chemistry*, **279**: 48692–48701.

Lee, S.B., S.H. Hong, H. Kim and H.D. Um. 2005. Co-induction of cell death and survival pathways by phosphoinositide 3-kinase. *Life Sciences*, **78**: 91-98.

Lemieux, G.A., F. Blumenkron, N. Yeung, P. Zhou, J. Williams, A.C. Grammer, R. Petrovich, P.E. Lipsky, M.L. Moss and Z. Werb. 2007. The low affinity IgE receptor (CD23) is cleaved by the metalloproteinase ADAM10. *Journal of Biological Chemistry*, **282**: 14836-14844.

Lemons, M.L. and M.L. Cadic. 2008. Integrin signalling is integral to regeneration. *Experimental Neurology*, **29**: 343-352.

Li, R. and M.A. Arnaout. 1999. Functional analysis of the beta 2 integrins. *Methods in molecular biology*, **129:105**-24.

Lilie, H., E. Schwarz and R. Rudolph. 1998. Advances in refolding of proteins produced in *E. coli*. *Current Opinion in Biotechnology*, **9**: 497-501.

Loomis, K.H., K.W. Yaeger, M.M. Batenjany, M.M. Mehler, A.C. Grabski, S.C. Wong and R.E. Novy. 2005. InsectDirect™ System: rapid, high-level protein

expression and purification from insect cells. *Journal of Structural and Functional Genomics*, **6**: 189–194.

Ludin, C., H. Hofstetter, M. Sarfati, C. A. Levy, U. Suter, D. Alaimo, E. Kilchherr, H. Frost and G. Delespesse. 1987. Cloning and expression of the cDNA coding for a human lymphocyte IgE receptor. *The EMBO Journal*, **6**: 109-114.

Lyons, A.B. and C.R. Parish. 1994. Determination of lymphocyte division by flow cytometry. *Journal of Immunological Methods*, **171**: 131-137.

Manna, S.K. and B.B. Aggarwal. 2000. Wortmannin inhibits activation of nuclear transcription factors NF-κB and activated protein-1 induced by lipopolysaccharide and phorbol ester. *FEBS Letters*, **473:113-118.**

Marshall, L.A., M.J. Hansburg, B.J. Bolognese, R.J. Gum, P.R. Young and R.J. Mayer. 1998. Inhibitors of p38 mitogen-activated kinase modulate IL-4 induction of low-affinity IgE receptor (CD23) in human monocytes. *Journal of Immunology*, **161**: 6005-6013.

Matsui, M., R. Nunez, Y. Sachi, R.G. Lynch and J. Yodoi. 1993. Alternative transcripts of the human CD23/ FcεRII. A possible novel mechanism of generating a soluble isoform in the type-II cell surface receptor. *FEBS*, **335**: 51-56.

Mayadas, T.N. and X. Cullere. 2005. Neutrophil β_2 integrins: moderators of life or death decisions. *Trends in Immunology*, **26**: 388-395.

Mazzone, A. and G. Ricevuti. 1995. Leukocyte CD11b/CD18 integrins: biological and clinical relevance. *Hematologica*, **80**: 161-175.

Mazzone, A. and G. Ricevuti. 1995. Leukocyte CD11/CD18 Integrins: Biological and clinical relevance. *Haematologica*, **80**:161-175.

McCloskey, N. J. Hunt, R.L. Beavil, M.R. Jutton, G.J. Grundy, E. Girardi, S.M. Fabiane, D.J. Fear, D.H. Conrad, B.J. Sutton1 and H.J. Gould. 2007. Soluble CD23 monomers inhibit and oligomers stimulate IgE synthesis in human B cells. *Journal of Biological Chemistry*, **282**: 24083 – 24091.

Middleton, A.J.P. 2002. Preparative protein refolding. *TRENDS in Biotechnology*, **20:** 437-443.

Miller, L.J., R. Schwarting and T.A. Springer. 1986. Regulated expression of the mac-1, LFA-1, p150,95 glycoprotein family during leukocyte differentiation. *Journal of Immunology*, **137**: 2891-2900.

Miltenyi, S. and J. Schmitz. 2000. High gradient magnetic cell sorting. *Flow Cytometry and Cell Sorting*, *2nd ed.*, Springer-Verlag, Berlin. Pp218-247.

Misawa, S. and I. Kumagai. 1999. Refolding of therapeutic proteins produced in *Escherichia coli* as inclusion bodies. *Biopolymers (Peptide Science)*, **51**: 297-307.

Mossalayi, M.D., M. Arock and P. Debre. 1997. CD23/FcεRII: Signalling and clinical implication. *International Reviews in Immunology*, **16**: 129-146.

Nissim, A., S. Schwarzbaum, R. Siraganian and Z. Eshhar. 1993. Fine specificity of the IgE interaction with the low and high affinity Fc receptor. *Journal of Immunology,* **150:** 1365-1374.

Noti, J.D. and B. C. Reinemann. 1995. The Leukocyte integrin gene CD1lc is translationally regulated during monocyte differentiation. *Molecular Immunology*, **32**: 361-369.

Novo, E. and M. Parola. 2008. Redox mechanisms in hepatic chronic wound healing and fibrogenesis. *Fibrogenesis and Tissue Repair*, **1**: 5-63.

Old, R.W. and S.B. Primrose. 1994. *Principles of gene manipulation, 5th Ed*, p178. Blackwell Science Ltd., London.

Ono, K. and J. Han. 2000. The p38 signal transduction pathway activation and function. *Cellular Signalling*, **12**: 1-13.

Oxvig, C., C. Lu and T.A. Springer. 1999. Conformational changes in tertiary structure near the ligand binding site of an integrin I domain. *Proceedings of the National Academy of Sciences*, **96:** 2215-2220.

Paul-Eugene, N., J-P. Kolb, A. Abadie, J. Gordon, G. Delespesse, M. Sarfati, J-M. Mencia-Huerta, D. Braquet and B. Dugas. 1992. Ligation of CD23 triggers cAMP generation and release of inflammatory mediators in human monocytes. *Journal of Immunology*, **149**: 3066-3071.

Petsch, D., W-D. Decker and F.B. Anspach. 1998. Proteinase K digestion of proteins improves detection of bacterial endotoxins by the *Limulus* amebocyte lysate assay: application for endotoxin removal from cationic proteins. *Analytical Biochemistry*, **259**: 42-47.

Pollock, K.G.J., K.S. McNeil, J.C. Mottram, R.E. Lyons, J.M. Brewer, P. Scott, G.H. Coombs and J. Alexander. 2003. The *Leishmania mexicana* cysteine protease, CPB2.8, induces potent Th2 responses. *Journal of Immunology*, **170**: 1749-1753.

Porter, J.C. and N. Hogg. 1998. Integrins take partners: cross-talk between integrins and other membrane receptors. *Trends in Cell Biology*, **8:** 390-396.

Prescott, L.M., J.P. Harley and D.A. Klein. 1996. Microbiology, 3rd Ed., pp 586-600 Wm. C. Brown Publishers, U.S.A.

Pullen, S.S. and P.D. Friesen. 1995. Early transcription of the ie-1 transregulator gene of Autographa californica nuclear polyhedrosis virus is regulated by DNA sequences within its 5'noncoding leader region. *Journal of Virology*, **69**: 156-165.

Rameh, L.E. and L.C. Cantley. 1999. The role of phosphoinositide 3-kinase lipid products in cell function. *Journal of Biological Chemistry*, **274**: 8347-8350.

Rao, K.M.K. 2001. MAP kinase activation in macrophages. *Journal of Leukocyte Biology*, **69**: 3-10.

Rezzonico, R., R. Chicheportiche, V. Imbert and J-M. Dayer. 2000. Engagement of CD11b and CD11c β_2 integrin by soluble CD23 induced IL-1β production on primary human monocytes through mitogen-activated protein-kinase-dependent pathways. *Blood*, **95**: 3868-3875.

Rezzonico, R., V. Imbert, R. Chicheportiche and J-M. Dayer. 2001. Ligation of CD11b and CD11c β_2 integrins by antibodies or soluble CD23 induces macrophage inflammatory protein 1α (MIP-1α) and MIP-1β production in primary human monocytes through a pathway dependent on nuclear factor–κB. *Blood*, **97**: 2932-2940.

Richards, M.L. and D.H. Katz. 1991. Biology and chemistry of the low affinity IgE receptor (FcεRII/CD23). *Critical Reviews in Immunology*, **11**: 65-86.

Robinson, J.P., W.O. Carter and P.K. Narayanan. 1994. Oxidative product formation analysis by flow cytometry. *Methods in Cell Biology*, **41**: 437-447.

Rodem, S.U. and P.D. Friesen. 1993. The hr5 transcriptional enhancer stimulates early expression from the Autographa californica nuclear polyhedrosis virus genome but is not required for virus replication. *Journal of Virology*, **67**: 5776-5785.

Ryu, J-W., K.H. Maeng, J-B. Kim, J. Ko, J.Y. Park, K-U. Lee, M.K. Yong, S.W. Park, Y.H. Kim and K.H. Han. 2004. Overexpression of uncoupling protein 2 in THP1 monocytes inhibits β_2 integrin-mediated firm adhesion and endothelial migration. *Arteriosclerosis, Thrombosis and Vascular Biology*, **24**: 864-870.

Saklavala, J. 2004. The p38 MAP kinase pathway as a therapeutic target in inflammatory disease. *Current Opinions in Pharmacology*, **4**: 372-377.

Sambrook, J., E.F. Fritsch and T. Maniatis. 1989. Molecular Cloning: A laboratory manual. 2nd ed., pp 1.53-1.72, 14.5-14.20. Cold Spring Harbour Laboratory Press, U.S.A.

Sancho, D., Santis, A.G., Alonso-Lebrero, J.L., Viedma, F., Tejedor, R and Sanchez-Madrid, F. 2000. Functional analysis of ligand-binding and signal transduction domains of CD69 and CD23 C-type lectin leukocyte receptors. *Journal of Immunology*, **156**: 3868:3875.

Sarfati, M., B. Bettler, M. Letellier, S. Fournier, M. Rubio-Trujillo, H. Hofstetter and G. Delespesse. 1992. Native and recombinant soluble CD23 fragments with IgE suppressive activity. *Immunology*, **76**: 662-667.

Sato, T., A. Konishi, S. Yasuno, J. Arai, M. Kamei, M. Bitoh, Takashi Yamaguchi. 1997. A new method for studying the binding of human IgE to CD23 and the inhibition of this binding. *Journal of Immunological Methods*, **209**:59–66.

Sayers, I., J.E.M. Housden, A.C. Spivey and B.A. Helm. 2004. The importance of Lys-352 of the human immunoglobulin E in FcεRII (CD23) recognition. *Journal of Biological Chemistry*, **279**: 35320-35325.

Schulz, O., B.J. Sutton, R.L. Beavil, J. Shi, H.F. Sewell, H.J. Gould, P. Laing and F. Shakib. 1997. Cleavage of the low-affinity receptor for human IgE (CD23) by a mite cysteine protease: Nature of the cleaved fragment in relation to the structure and function of CD23. *European Journal of Immunology*, **27**: 584-588.

Schwende, H., E. Fitzke, P. Ambs and P.Dieter. 1996. Differences in the state of differentiation of THP-1 cells induced by phorbol ester and 1,25-dihydroxyvitamin D_3. *Journal of Leukocyte Biology*, **59**: 555-561.

Serrander, L., J. Larsson, H. Lundquist, M. Lindmark, M. Falman, C. Dahlgren and O. Stendahl. 1999. Particles binding β_2-integrins mediate intracellular production of oxidative metabolites in human neutrophils independently of phagocytosis. *Biochemica et Biophysica Acta*, **1452**: 133-144.

Shattil, S.J. 2005. Integrins and Src: dynamic duo of adhesion signalling. *TRENDS in Cell Biology*, **15**: 399-403.

Sheth, B., I. Dransfield, L.J. Partridge, M.D. Barker and D.R. Burton. 1988. Dibutyryl cyclic AMP stimulation of a monocyte-like cell line, U937: A model for monocyte chemotaxis and Fc receptor-related functions. *Immunology*, **63**: 483-490.

Shi, J., R. Ghirlando, R.L. Beavil, A.J. Beavil, M.B. Keown, R.J. Young, R.J. Owens, B.J. Sutton and H.J. Gould. 1997. Interaction of the low-affinity CD23/FcεRII lectin domain with the Fcε3-4 fragment of human immunoglobulin E. *Biochemistry*, **36:** 2112-2122.

Shimaoka, M. and T.A. Springer. 2004. Therapeutic agonists and the conformational regulation of the β_2 integrins. *Current Topics in Medicinal Chemistry*, **4**: 1485-1495.

Smith, D.B. and K.S. Johnson. 1988. Single-step purification of polypeptides expressed in *Escherichia coli* as fusions with glutathione *S*-transferase. *Gene*, **67:** 31-40.

Soussi, A.G., B. Lamkhioued, M. Masao, D. Aldebert, M. Sarfati, A. Capron and M. Capron. 1998. Molecular characterization of the low-affinity IgE receptor FcεRII/CD23 expressed by human eosinophils. *International Immunology*, **10**: 395-404.

Spittler, A., M. Willheim, F. Leutmezer, R. Ohler, W. Krugluger, C. Reissner, T.Lucas, T. Brodowicz, E. Roth and G. Boltz-Nitulescu. 1997. Effects of 1,25-dihydroxyvitamin D_3 and cytokines on the expression of MHC antigens, complement receptors and other antigens on human blood monocytes and U937 cells: role in cell differentiation, activation and phagocytosis. *Immunity*, **90**: 286-293.

Splettstoesser, W.D. and P. Schuff-Werner. 2002. Oxidative stress in phagocytes – 'The enemy within'. *Microscopy Research and Technique*, **57**: 441-455.

Sutton, B.J. and H.J. Gould. 1993. The human IgE network. *Nature*, **366**: 421-428.

Sutton, B.J., R.L. Beavil and A.J. Beavil. 2000. Inhibition of IgE-receptor interactions. *British Medical Bulletin*, **56**: 1004-1018.

Taborda, C.P. and A. Casadevall. 2002. CR3 (CD11b/CD18) and CR4 (CD11c/CD18) Are Involved in Complement-Independent Antibody-Mediated Phagocytosis of Cryptococcus neoformans. *Immunity*, **16**:791–802.

Taimi, M., H. Defacque, T. Commes, J. Favero, E. Caron, J. Marti and J. Dornand. 1993. Effect of retinoic acid and Vitamin D on the expression of interleukin-1β, tumour necrosis factor-α and interleukin-6 in the human monocytic cell line U937. *Immunology*, **79**:229-235.

Tang, D., Y. Shi, R. Kang, T. Li, W. Xiao, H. Wang and X. Xiao. 2007. Hydrogen peroxide stimulates macrophages and monocytes to actively release HMGB1. *Journal of Leukocyte Biology*, **81**: 741-747.

Ten, R.M., M.J. McKinstry, G.D. Bren and C.V. Paya. 1999a. Signal transduction pathways triggered by the FcεRIIb receptor (CD23) in human monocytes lead to nuclear factor-κB activation. *Journal of Allergy and Clinical Immunology*, **104:**376-387.

Ten, R.M., M.J. McKinstry, S.A. Trushin, S. Asin and C.V. Paya. 1999b. The signal transduction pathway of CD23 (FcεRIIb) targets IκB kinase. *Journal of Immunology*, **155**: 3851-3857.

Terpe, K. 2003. Overview of tag protein fusions: from molecular and biochemical fundamentals to commercial systems. *Applied Microbiology and Biotechnol*ogy, **60**: 523-533.

Texido, G., H. Eibel, G. Le Gros and H. Van der Putten. 1994. Transgene CD23 expression on lymphoid cells modulates IgE and IgG1 responses. *Journal of Immunology*, **153**: 3028-3042.

Thannickal, V.J. and B.L. Fanburg. 2000. Reactive oxygen species in cell signalling. *American Journal of Physiology - Lung Cellular and Molecular Physiology*, **276**: 1005-1028.

Thornton, B.P., V. Vetvicka, M. Pitman, R.C. Goldman and G.D. Ross. 1996. Analysis of the sugar specificity and molecular location of the beta- glucan-binding lectin site of complement receptor type 3 (CD11b/CD18). Journal of Immunology, ***156:*** *1235-1246.*

Todar, K. 2008. Todar's online textbook of bacteriology. http//:www.textbookofbacteriology.net

Tsicopoulos, A. and M. Joseph. 2000. The role of CD23 in allergic disease. *Clinical and Experimental Allergy*, **30**:602-605.

Turrens, J.F. 2003. Mitochondrial formation of reactive oxygen species. *Journal of Physiology*, **552**: 335-344.

Van der Goes, A., D. Wouters, S.M.A. van der Pol, R. Huizinga, E. Ronken, P. Adamson, J. Greenwood, C.D. Dijkstra and H.E. De Vries. 2001. Reactive oxygen species enhance the migration of monocytes across the blood-brain barrier *in vitro. FASEB Journal*, **15**: 1852-1854.

Veloso, C.A., C.A., Insoni, E.A. Borges, R.T. Mattos, M.R. Calsolari, J.S. Reis, A.A. Bosco, M.M. Chaves and J.A. Nogueira-Machado. 2008. The inhibition of ROS production in peripheral blood mononuclear cells from type 2 diabetic patients by autologous plasma depends on the Akt/PKB signalling pathway. *Clinica Chimica Acta*, **394**: 77-80.

Vorup-Jensen, T., C. Ostermeier, M. Shimaoka, U. Hommel and T.A. Springer. 2003. Structure and allosteric regulation of the $\alpha x \beta_2$ integrin I domain. *Proceedings of the National Academy of Sciences*, **100**: 1873-1878.

Walters, S.E., R.H. Tang, M. Cheng, S.M. Tan and S.K. Alex Law. 2005. Differential activation of LFA-1 and Mac-1 ligand binding domains. *Biochemical and Biophysical Research Communications*, **337**:142-148.

Wang, Y., M.M. Ziegler, G.K. Lam, M.G. Hunter, T.D. Eubank, V.V. Khramtsov, S. Triandapani, C.K. Sen and C.B. Marsh. 2007. The role of NADPH oxidase complex, p38 MAPK and Akt in regulating human monocyte/macrophage survival. *American Journal of Respiratory Cell and Molecular Biology*, **36**: 68-77.

Webb, J.R., A. Campos-Neto, P.J. Ovendale, T.I. Martin, E.J. Stromberg, R. Badaro and S.G. Reed. 1998. Human and murine immune responses to a novel *Leishmania major* recombinant protein encoded by members of a multicopy gene family. *Infection and Immunity*, **66**: 3279-3289.

Weber, C., J.C. Calzada-Wack, M. Goretzki, A. Pietsch, J.P. Johnson and H.W.L. Ziegler-Heitbrock. 1995. Retanoic acid inhibits basal and interferon-γ-induced expression of intracellular adhesion molecule 1 in monocytic cells. *Journal of Leukocyte Biology*, **57**: 401-406.

White, L.J., B.W. Bradford, P. Graber, J-P. Aubry, J-Y. Bonnefoy and W. Cushley. 1997. Inhibition of apoptosis in a human pre-B cell line by CD23 is mediated via a novel receptor. *Blood,* **90**: 234-243.

Wright, S.D., S.M. Levin, M.T.C. Jong, Z. Chad and L.G. Kabbashi. 1989. CR3 (CD11b/CD18) expresses one binding site for Arg-Gly-Asp-containing peptides and a second site for bacterial lipopolysaccharide. *Journal of Experimental Medicine*, **169**: 175-183.

Wurzburg, B.A., Tarchevskaya, S.S. & Jardetzky, T. 2006. Structural changes in the lectin domain of CD23, the low-affinity IgE receptor, upon calcium binding. *Structure,* **14**: 1049 – 1058.

Yamaguchi, T., M. Suzuki, H. Kimura and M. Kato. 2006. Role of Protein Kinase C in Eosinophil Function. *Allergology International*, **55**: 245-252.

Zen, K., M. Utech, Y. Liu, I. Soto, A. Nusrat and C.A. Parkos. 2004. Association of BAP31 with CD11b/CD18. The *Journal of Biological Chemistry*, **279**: 44924–44930.

Zhang, Y. and F. Chen. 2004. Reactive Oxygen Species (ROS), Troublemakers between Nuclear Factor-κB (NF- κB) and c-Jun NH_2-terminal Kinase (JNK). *Cancer Research,* **64:** 1902-1905.

Zhou, L., D.H.S. Lee, J. Plescia, C.Y. Lau, D.C. Altier. 1994. Differential ligand binding specificities of recombinant CD11b/CD18 integrin I domain. *Journal of Biological Chemistry*, **269**: 17075-17079.

Appendix A

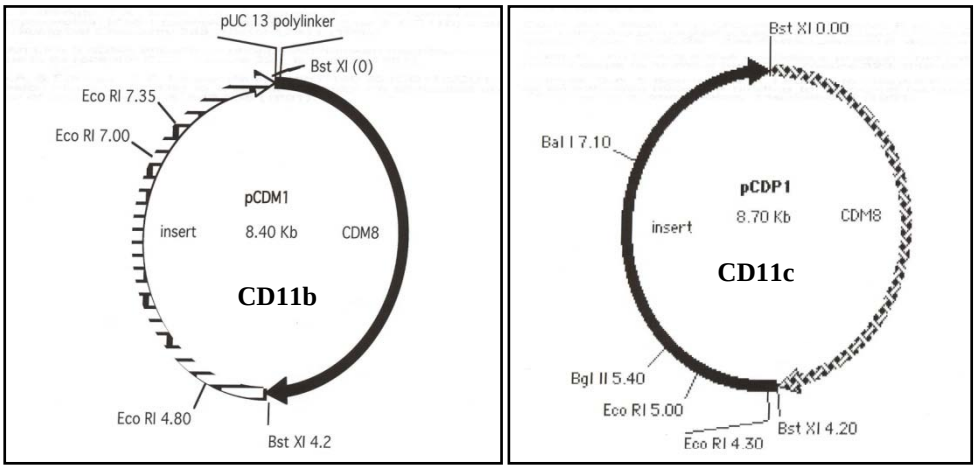

Figure A.1: Vector maps of pCDM1 (CD11b) and pCDP1 (CD11c) showing plasmid sizes and restriction sites. http://www.addgene.org.

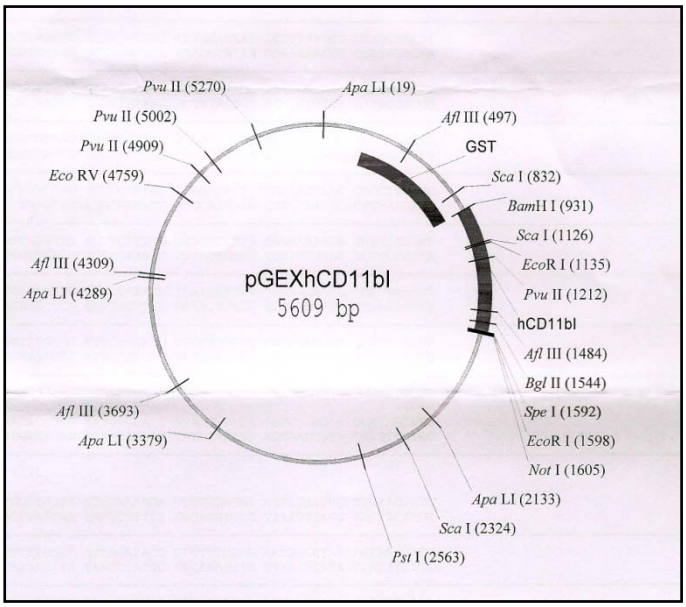

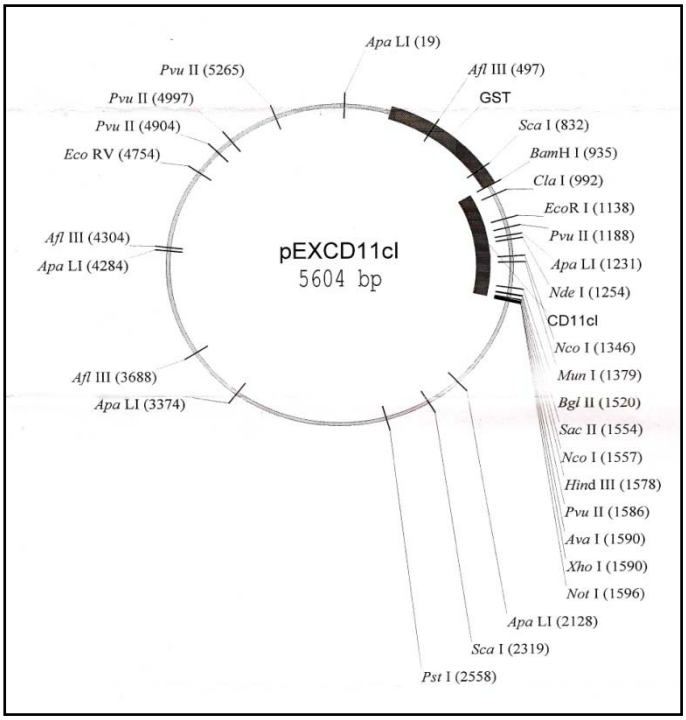

Figure A.2: Vector map of CD11b I domain and CD11c I domain-encoding plasmids, showing vector sizes, restriction sites and inserted DNA**.**

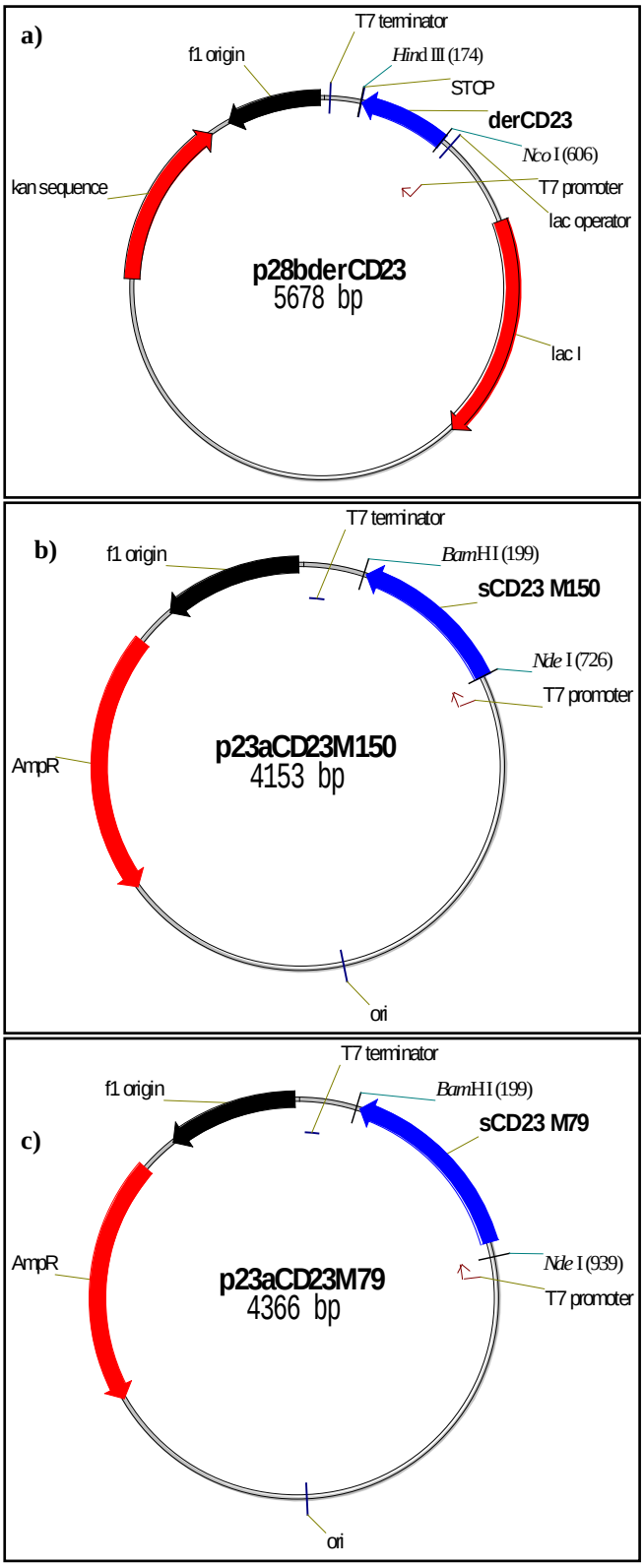

Figure A.3: Vector maps of recombinant plasmids used to express human CD23 protein. a) Vector map of pET28b(+) containing the coding region for soluble derCD23. This encodes M156 – E298, the soluble 16 kDa protein; b) Vector map of pET23a(+) containing the coding region for soluble CD23 clone M150. This encodes M150 – S321, the soluble 25 kDa protein; c) Vector map of pET23a(+)

containing the coding region for soluble CD23 clone M79. This encodes M79 – S321, the soluble 33 kDa protein.

```
hCD23           MEEGQYSEIEELPRRRCCRRGTQIVLLGLVTAALWAGLLTLLLLWHWDTTQSLKQLEERA 60
M79CD23         ------------------------------------------------------------
M150CD23        ------------------------------------------------------------
derCD23         ------------------------------------------------------------

hCD23           ARNVSQVSKNLESHHGDQMAQKSQSTQISQELEELRAEQQRLKSQDLELSWNLNGLQADL 120
M79CD23         ------------------MAQKSQSTQISQELEELRAEQQRLKSQDLELSWNLNGLQADL 42
M150CD23        ------------------------------------------------------------
derCD23         ------------------------------------------------------------

hCD23           SSFKSQELNERNEASDLLERLREEVTKLRMELQVSSGFVCNTCPEKWINFQRKCYYFGKG 180
M79CD23         SSFKSQELNERNEASDLLERLREEVTKLRMELQVSSGFVCNTCPEKWINFQRKCYYFGKG 102
M150CD23        ----------------------------MELQVSSGFVCNTCPEKWINFQRKCYYFGKG 31
derCD23         ---------------------------------SGFVCNTCPEKWINFQRKCYYFGKG 25
                                                ************************

hCD23           TKQWVHARYACDDMEGQLVSIHSPEEQDFLTKHASHTGSWIGLRNLDLKGEFIWVDGSHV 240
M79CD23         TKQWVHARYACDDMEGQLVSIHSPEEQDFLTKHASHTGSWIGLRNLDLKGEFIWVDGSHV 162
M150CD23        TKQWVHARYACDDMEGQLVSIHSPEEQDFLTKHASHTGSWIGLRNLDLKGEFIWVDGSHV 91
derCD23         TKQWVHARYACDDMEGQLVSIHSPEEQDFLTKHASHTGSWIGLRNLDLKGEFIWVDGSHV 85
                ************************************************************

hCD23           DYSNWAPGEPTSRSQGEDCVMMRGSGRWNDAFCDRKLGAWVCDRLATCTPPASEGSAESM 300
M79CD23         DYSNWAPGEPTSRSQGEDCVMMRGSGRWNDAFCDRKLGAWVCDRLATCTPPASEGSAESM 222
M150CD23        DYSNWAPGEPTSRSQGEDCVMMRGSGRWNDAFCDRKLGAWVCDRLATCTPPASEGSAESM 151
derCD23         DYSNWAPGEPTSRSQGEDCVMMRGSGRWNDAFCDRKLGAWVCDRLATCTPPASEGSAE-- 143
                ************************************************************

hCD23           GPDSRPDPDGRLPTPSAPLHS 321
M79CD23         GPDSRPDPDGRLPTPSAPLHS 243
M150CD23        GPDSRPDPDGRLPTPSAPLHS 172
derCD23         ---------------------
```

Figure A.4: CD23 Protein variants aligned to human CD23. Amino acid numbers are provided on the right of the figure for each variant. The CD23 variants encode M79CD23$^{79-321}$, M150CD23$^{150-321}$ and derCD23$^{156-298}$.

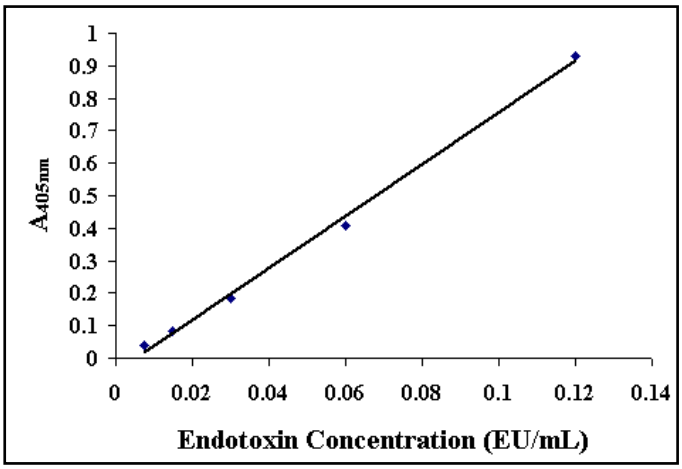

Figure A.5: Endotoxin standard curve generated with the LAL test kit. y= 7.9633x - 0.041; R^2 = 0.9972.

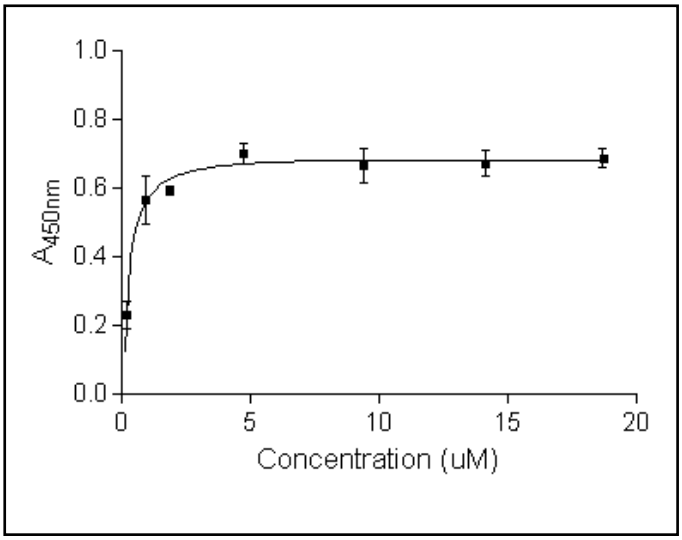

Figure A.6: Example of a binding curve between sCD23 and CD11b αI domain proteins.

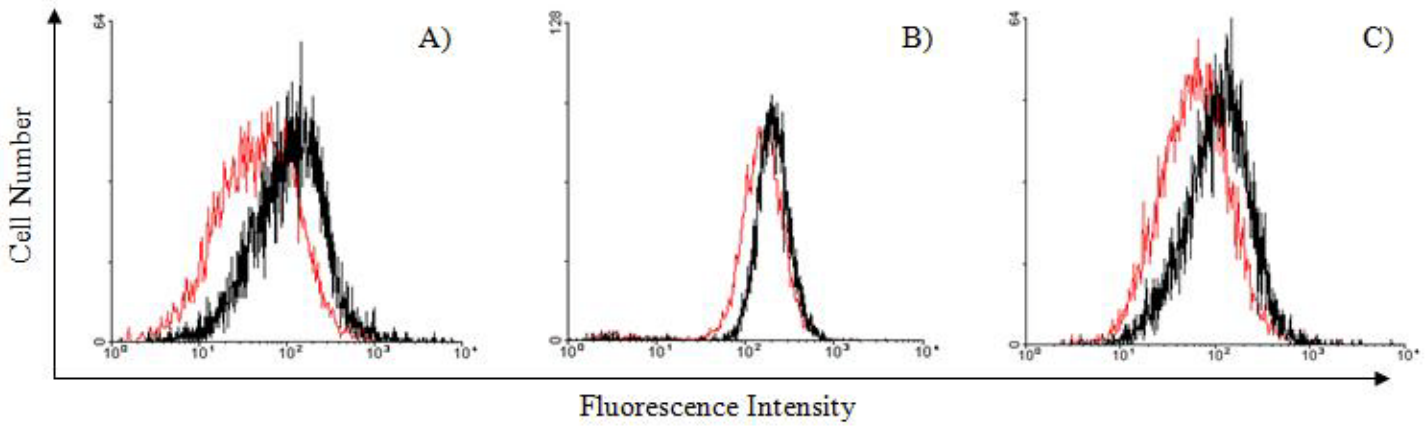

Figure A.7: Histogram overlays of ROS production in HL60 (A), THP1 (B) and U937 (C) cells**.** Cells are incubated with the PMA positive control for 60 minutes before analysed. Control cells are shown in red and PMA-exposed cells are shown in black.

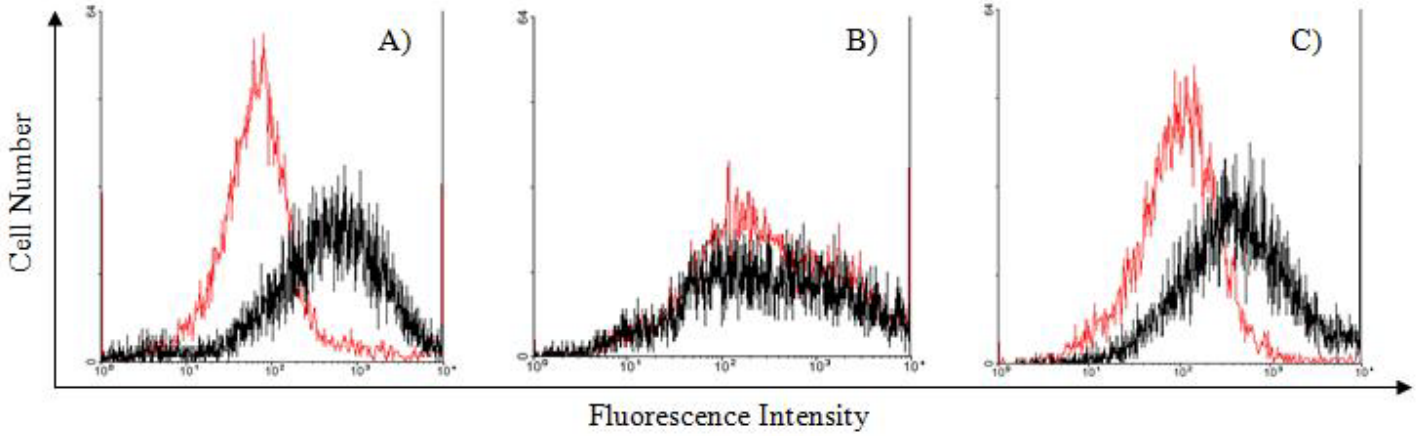

Figure A.8: Histogram overlays of phagocytosis of E. coli K12 bacteria in HL60 (A), THP1 (B) and U937 (C) cells. Cells are incubated with the PMA positive control for 60 minutes before analysed. Control cells are shown in red and PMA-exposed cells are shown in black.

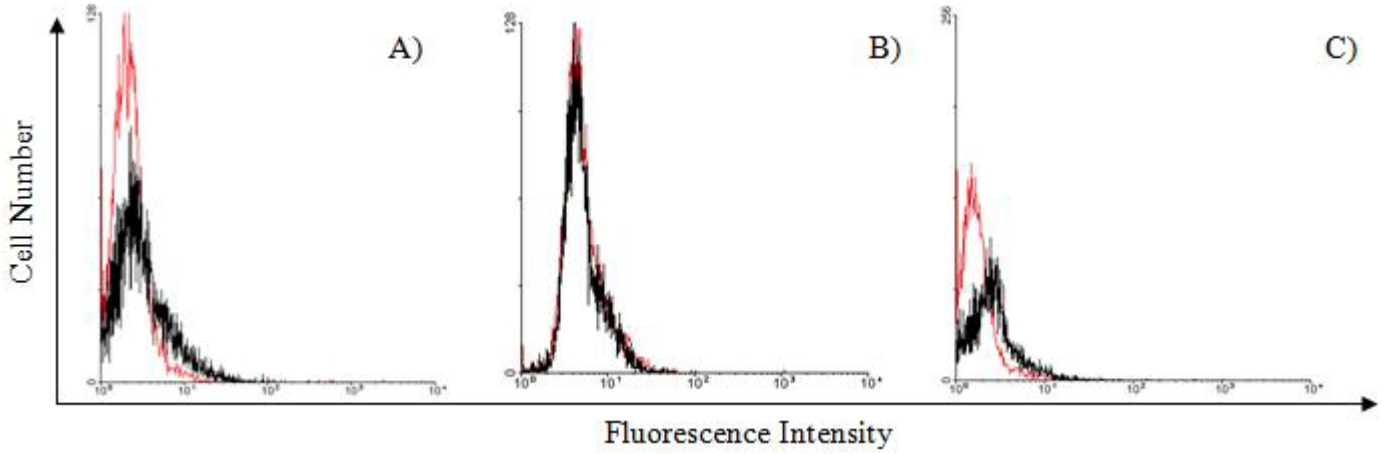

Figure A.9: Histogram overlays of MPO presence in HL60 (A), THP1 (B) and U937 (C) cells. Cells are incubated with PMA for 24 hours before being stained for MPO. Control cells are shown in red and PMA-exposed cells are shown in black.

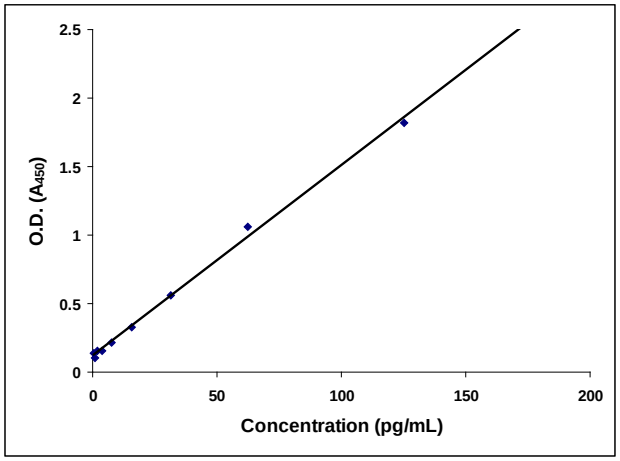

Figure A.10: Cytokine standard curve used for the quantification of IL-1β. The equation obtained from linear regression was y = 0.0139x + 0.1198 and the R^2 value was 0.9969.

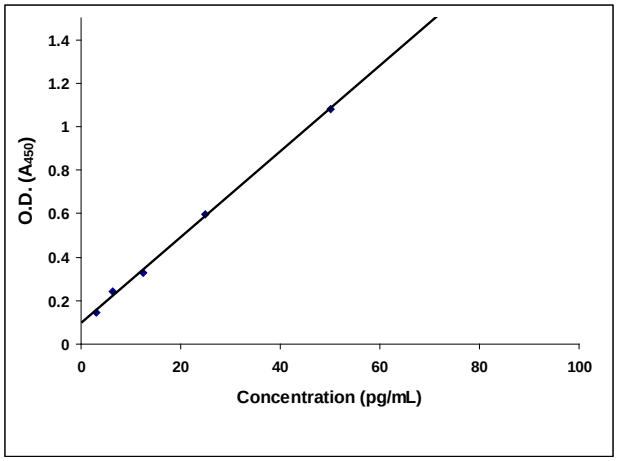

Figure A.11: Cytokine standard curve used for the quantification of IL-6. The equation obtained from linear regression was y = 0.0197x + 0.0973 and the R^2 value was 0.9982.

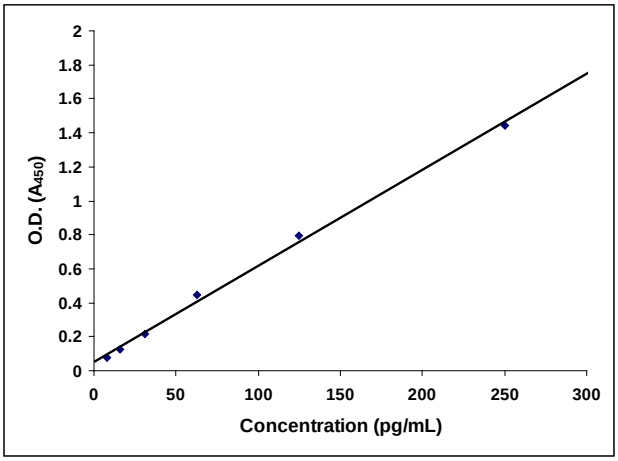

Figure A.12: Cytokine standard curve used for the quantification of TNFα. The equation obtained from linear regression was $y = 0.0057x + 0.0542$ and the R^2 value was 0.9971.

Publications submitted from the current study

Human soluble CD23 binds the β_2 integrins CD11b/CD18 and CD11c/CD18 at their αI domains

Brodie Daniels[1], Maryna van de Venter[1], Sang-Uk Nham[2] and Vaughan Oosthuizen[1,3.]

[1] Department of Biochemistry & Microbiology

Nelson Mandela Metropolitan University

PO Box 77000

Port Elizabeth, 6031, South Africa

[2] Sang-Uk Nham

Div. Science Education

Kangwon National University

Chuncheon, Kangwon, 200-701, South Korea

[3] Corresponding author:

Tel: +2741 504 2435

Fax: +2741 504 2814

Email: vaughan.oosthuizen@nmmu.ac.za

Abstract

β_2 integrins are important in a variety of cell-adhesion reactions during immune-inflammatory mechanisms and the binding of their natural ligands generates outside-in cellular signalling, leading to cell activation. The binding of CD23 to β_2 integrins contributes to this signalling in monocytes but the interaction site for CD23 is unknown. Differentiated HL60 and U937 monocytic cells were used to demonstrate the binding of three recombinant CD23 constructs (corresponding to 16, 25 and 33 kDa human soluble CD23) to upregulated CD11b/CD18 and CD11c/CD18. This binding was partially blocked with the addition of a blocking antibody specific for the CD11b/CD18 αI domain, demonstrating that the αI domains are involved in binding to CD23. Recombinant αI domain proteins of CD11b and CD11c bound the three CD23 proteins with equilibrium dissociation constants of approximately 0.3 μM as determined by ELISA. These dissociation constants for β_2 integrin are comparable to other integrin ligands. This study has shown that CD23 interacts directly with the αI domains of β_2 integrins and that the interaction surface likely spans the lectin domain as well as either the stalk or C-terminal tail of CD23.

1. Introduction

The integrin family of proteins are heterodimeric membrane-bound glycoproteins that mediate homotypic and heterotypic cell-to-cell adhesion and cell-matrix interactions in a broad range of biologic functions [1]. Integrins are functionally important in a variety of cell-adhesion reactions during immune-inflammatory mechanisms. The engagement of β_2 integrins by natural ligands and certain monoclonal antibodies (mAbs) also generates outside-in cellular signalling, leading to leukocyte activation.

Integrins have been organized into 8 distinct subfamilies based on their β subunit associations. The β_2 subfamily includes cell surface glycoproteins that have four distinct α subunits (CD11a, b, c and d) which associate with the β_2 (CD18) subunit [2]. The α subunit has a long extracellular domain and a short cytoplasmic domain. The α subunit of integrins contain a β propeller structure formed by 7 repeating elements. Nine of the 18 α subunits, including the four that combine to form β_2 integrins contain an I-domain inserted between the second and third blades of the β propeller. The α subunit β-propeller domain and the β-subunit I-like domain form the integrin head, a ligand-binding structure in the headpiece. The I domain is located at the top of the integrin head. α subunit I domains and β subunit I-like domains form an α/β fold with a metal-ion dependent adhesion site (MIDAS) on the "top" of the domain, while C and N terminal connections are on the distal "bottom" face [3]. Two conformations of the I domain have been found; open and closed. Only an open conformation can allow ligand binding [4]. There are 5 exposed loops surrounding the MIDAS, which undergo conformational changes to bind ligands [5].

The majority of integrins are fairly promiscuous receptors and most recognize the RGD (arginine-glycine-aspartic acid) sequence found in several adhesive proteins [2].

For CD11b/CD18 more than thirty protein and non-protein molecules are reported to be ligands, including intracellular adhesion molecule 1, complement C3 fragment iC3b, fibrinogen, heparin, neutrophil elastase, neutrophil inhibitory factor, complement factor H, extracellular matrix proteins (laminin, collagens, vitronectin) and CD23 [6]. CD11c/CD18 also binds several of these ligands, but not all of them [7].

The low affinity immunoglobulin E (IgE) receptor, CD23, is an interesting ligand for CD11b and CD11c. It is found on a variety of cell types, including B cells, monocytes, eosinophils and Langerhans cells [8]. CD23 is a type II transmembrane protein and a member of the C-type lectin family. It consists of a carboxy-terminal lectin domain, a stalk region and a short N-terminal cytoplasmic tail. Distal to the lectin domain of human CD23 is a C-terminal tail region containing an inverted RGD sequence [9].

CD23 is a labile protein in that soluble CD23 fragments (sCD23) are released from the cell in human and murine systems. The human CD23 is initially cleaved by the ADAM-10 protease [10] and subsequent cleavage results in soluble forms of approximately 25, 27-29, 33 and 37 kDa in size [11]. These sCD23 occur in normal subjects, but elevated levels are associated with inflammatory and lymphoproliferative diseases [12], while the allergenicity of dust mites may be linked to cleavage of CD23 to a 16 kDa lectin fragment lacking the C-terminal tail [13]. sCD23 plays a role in inflammatory mechanisms by inducing IL-1β production by macrophages via interaction with CD11b and CD11c [1; 14], as well as causing NO production and IL-1β, IL-6 and TNF-α secretion by monocytes. Engagement of CD11b or CD11c by antibodies induces nuclear translocation of NF-κB in monocytes

[15]. NF-κB can then in turn induce the transcription of several genes, such as the genes for chemokines, cytokines, inflammatory mediators, growth factors and adhesion molecules [16].

The interaction between CD23 and the $\alpha_V\beta_5$-integrin promotes growth of pre-B cells, indicating a role in rescue of germinal centre B lymphocytes [17]. These authors mapped the interaction with $\alpha_V\beta_5$-integrin to an Arg-Lys-Cys motif on an exposed loop of CD23, and also found that recognition on the integrin occurs at a site distinct from the normal RGD sequence binding site of integrins. However, there does not seem to be any data mapping the binding of β_2 integrins to CD23. In this study we show that the αI domain of CD11/CD18 is the site for interaction with CD23.

2. Methods

2.1 Production of recombinant CD23 proteins

Coding regions for three recombinant human CD23 proteins were amplified by polymerase chain reaction (PCR) from a λ-phage complementary DNA library, prepared from buffy coat, and ligated into prokaryotic expression vectors (pET 23a for CD23M79 and CD23M150 and pET 28b in the case of derCD23) (Novagen, Madison, USA). derCD23 corresponds to the 16 kDa sCD23 (S^{156} – E^{298}), CD23M150 corresponds to the 25 kDa sCD23 (M^{150} – S^{321}) and CD23M79 corresponds to the 33 kDa sCD23 (M^{79} – S^{321}) (Figure 1b). Recombinant CD23 proteins were expressed and purified as previously described [18].

2.2 Production of CD11b and CD11c I domains

Vectors containing the coding regions of human CD11b and CD11c αI domains were kindly donated by Dr Sang-Uk Nham (Kangwon National University, Korea). αI domain proteins were isolated as previously described [19]. Briefly, *E. coli* BL21 (DE3) cells were induced to express CD11b or CD11c expression with 1 mM IPTG for four hours. Harvested cells were resuspended in αI domain isolation buffer (20 mM Tris/HCl pH 7.5, 10 mM EDTA) and lysed by sonication. Supernatant was filtered with a 0.45 micron filter and applied to GSTrap columns (Amersham Biosciences) for purification. The GST-tagged αI domain proteins were eluted with 15 mM reduced glutathione in 20 mM Tris/HCl, pH 8.0 and dialised against two changes of PBS for at least 12 hours to remove glutathione.

2.3 Cell culture

U937 and HL60 promonocytic cell lines were routinely maintained in RPMI1640 cell culture medium (Bio-Whittaker) containing 25 mM HEPES and 2 mM L-glutamine, supplemented with 1 % (v/v) each of penicillin and streptomycin (Sigma). U937 cells were also supplemented with 10 % heat-inactivated fetal bovine serum (HI-FBS) (Gibco) while HL-60 cells were supplemented with 20 % HI-FBS. Cells were cultured at 37 ºC in a humidified atmosphere with 5 % CO_2 and 95 % air. The cell lines were maintained between 1 x 10^5 and 1 x 10^8 cells per mL and were cultured in 75 cm^2 flasks (Nunc). All cell lines were tested for Mycoplasma contamination prior to use in experiments.

2.4 Cell surface upregulation of CD11b/CD18 and CD11c/CD18

Vitamin D_3 (1 μM) was used to differentiate the cells, thereby causing cell surface upregulation of CD11b and CD11c. Cells were seeded at 1-3 x 10^5 cells per mL and incubated for 24 hours before adding vitamin D_3. Cells were then incubated for three days before being analysed for CD11b and CD11c upregulation. Cells were harvested and resuspended in blocking buffer (1% HI-FBS and 1% BSA in PBS, pH 7.4) for 30 minutes at room temperature. Cells were resuspended at 1 x 10^6 cells per mL, and stained with 20 μl of either CD11b-FITC (IM0530) or CD11c-PE (IM1760) (Beckman Coulter) for 30 minutes at room temperature in the dark. Cells were washed twice with PBS before analysis on a Beckman Coulter FC500 flow cytometer. Cells were stained with an appropriate isotype control to ensure no non-specific binding of the antibody to the cells occurred.

2.5 Cell-binding assay

For the binding assay, 1 μg/mL of each recombinant CD23 protein in PBS as well as the same concentration of fibrinogen as control, was used to coat a black 96-well plate overnight at 4 ºC. Plates were washed three times with PBS and blocked for 1 hour at room temperature with 2 % BSA in PBS. Differentiated cells were stained with carboxyfluorescein diacetate, succinimidyl ester (CFSE) (Molecular Probes) according to manufacturers instructions. Briefly, cells were resuspended in PBS/0.1% BSA at 1x10^6 cells per mL. CFSE was added to a 10 μM final concentration and cells were incubated in the dark for 10 minutes at 37 ºC before the reaction was stopped by adding 5 volumes of ice cold cell culture medium to the cells. Cells were washed with PBS and resuspended in HBSS binding buffer (10 mM HEPES, 1 mM $CaCl_2$, pH 7.3) and 100 μl aliquoted into each well of a 96-well plate incubated in the dark for one hour. The cells were gently removed and the plate washed twice with PBS to

remove any unbound cells. One hundred µl of PBS was then added to each well and fluorescence measured using a Fluoroscan Ascent FL microtiter plate reader (Thermo Labsystems) with the excitation wavelength set at 488 nm and the emission wavelength set at 518 nm.

2.6 Antibody blocking of cell binding

To investigate whether the binding of differentiated cells to sCD23 was due to CD11/CD18 integrins, a blocking antibody, CBRM1/5 (eBioscience), was preincubated with differentiated cells for 30 minutes at 37 ºC at a concentration of 5 µg/mL before being washed and used in the cell binding assay. CBRM1/5 monoclonal antibody reacts with an activation specific epitope of human CD11b. The epitope recognised by this mAb resides on the αI domain of CD11b.

2.7 Binding of CD11 αI domains to recombinant human soluble CD23

The ability of CD11b and CD11c αI domains to bind CD23 was tested using an enzyme linked immunosorbent assay (ELISA). Fibrinogen was used as control, since it binds CD11b and CD11c αI domains [20; 21]. CD23 and fibrinogen were coated on a 96-well plate at 20 µg/mL in PBS overnight at 4 ºC. Plates were washed three times with PBS-0.05 % Tween 20 (PBS-T) before being blocked with 100 µl 1% salmon testis DNA (Fluka) in PBS for one hour at room temperature. Plates were washed and CD11b αI domain or CD11c αI domain (0-1000 µg/mL) were added in 50 µl aliquots in binding buffer and incubated for one hour at room temperature. PBS-T was used to wash the plates before adding 100 µl of a 1:10 000 dilution of a polyclonal goat anti-schistosomal GST antibody (GE Healthsciences) diluted in PBS-

T. The plate was incubated for 1 hour before washing three times with PBS-T. An anti-goat secondary antibody conjugated to peroxidase (Sigma) was used to detect the primary antibody at a concentration of 1:20 000 in PBS-T for one hour at room temperature before adding 100 µl of 3,3',5,5'-tetramethylbenzidine (TMB) substrate (Sigma). The reaction was stopped using 50 µl of a 1 N solution of sulphuric acid before reading at 450 nm using a Multiscan MS microplate reader (Labsystems).

2.8 Statistics

GraphPad Prism version 5 for Windows was used for all statistical analysis. One way ANOVA's were used to analyse cell binding data, while the protein binding used a non-linear one site binding curve with specific binding.

3. Results

3.1 Production of recombinant proteins

Three different recombinant soluble CD23 proteins were purified from the inclusion bodies of *E. coli* BL21(DE3) cells, after induction of expression with IPTG. The protein was renatured in 72 hours using rapid dilution and purified with a single chromatographic step, using Superdex 75 gel chromatography. Purified protein (Figure 1a) was tested for LPS levels before being filter-sterilized and stored. This method yielded between 0.75 and 3 mg of pure sCD23 per liter of culture. CD11b and CD11c αI domains were purified from *E. coli* lysates as GST fusion proteins using glutathione-agarose affinity chromatography (Figure 2).

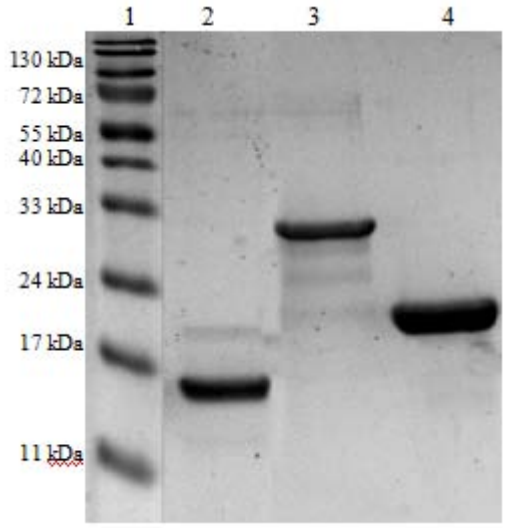

Figure 1: (A) SDS-PAGE pattern of purified recombinant sCD23 proteins. Lane 1, LMW marker; Lane 2, purified derCD23; Lane 3, purified CD23M79; Lane 4, purified CD23M150. (B) Schematic of CD23 protein variants. The CD23 variants encode exCD23$^{48-321}$, M150CD23$^{150-321}$, derCD23$^{156-298}$. CT, N-terminal cytoplasmic domain; TM, transmembrane domain; Stalk, α-helical coiled coil; CTLD, C-type lectin-like domain; Tail, C-terminal tail region .

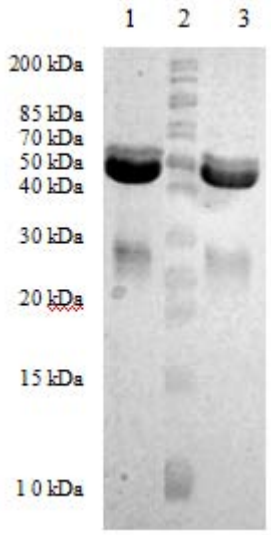

Figure 2: SDS-PAGE pattern of purified CD11 αI domains . Lane 1, purified CD11b I domain; Lane 2, LMW marker; Lane 3, purified CD11c I domain.

3.2 Cell-binding assay

Vitamin D_3 has been used in several studies for the differentiation of leukocytes and subsequent upregulation of CD11b and CD11c on the cell surface [22; 23; 24]. Figure 3 shows the upregulation of these two surface markers on the HL60 and U937 cell lines, respectively. We observed that the upregulation of CD11c on both cell lines is not as substantial as that of CD11b. The same trend has been observed in previous studies with HL60 cells [25]. However, it is interesting to note that the upregulation of CD11c is greater on HL60 cells than U937 cells. To investigate CD23 binding to these cell surface markers we used CD23-coated plates to which differentiated and fluorescently stained HL60 and U937 monocytes were added (Figure 4).

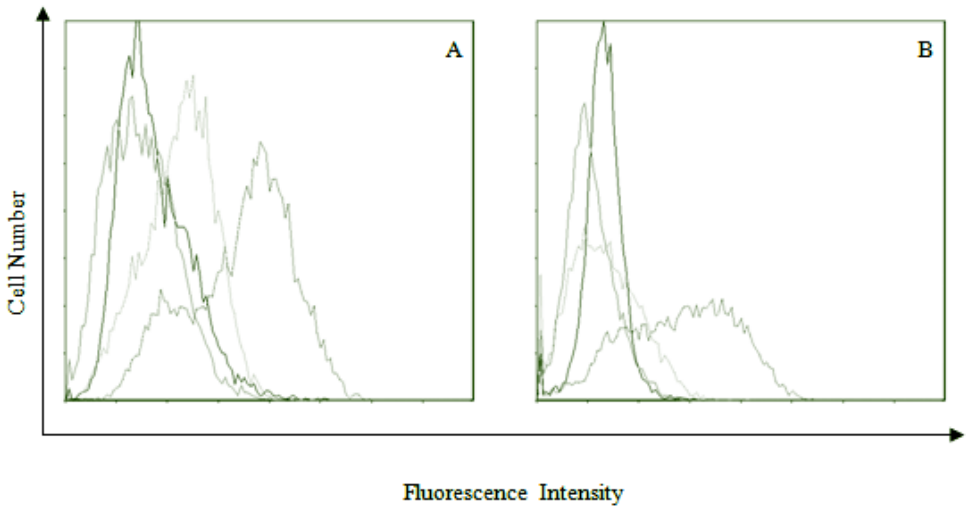

Figure 3: The expression of CD11b and CD11c upon differentiation of HL60 and U937 cells with vitamin D_3. HL60 upregulation of CD11b and CD11c are shown in panel A and B repectively, while U937 upregulation of CD11b and CD11c are shown in panel C and D respectively. The shaded area represents control (untreated) expression while the unshaded black line indicates the expression of either CD11b or CD11c on vitamin D3 treated cells.

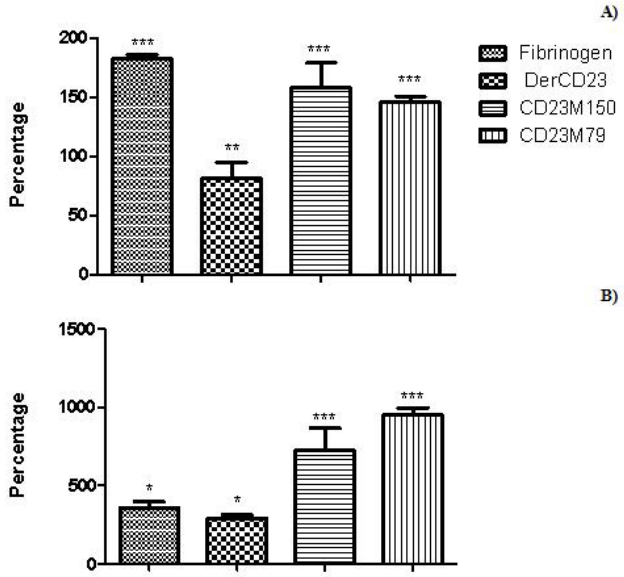

Figure 4: Binding of differentiated HL60 (A) and U937 (B) cells to soluble CD23. Fluorescently labeled cells were incubated with immobilized proteins. Each figure is representative of three experiments done in triplicate. Error bars represent SEM values. Asterisks represent significant difference compared to BSA where (*) represents $P<0.05$, (**) $P<0.005$ and (***) $P<0.0005$.

HL60 cells bound preferentially to plates coated with CD23 and fibrinogen, as compared to the control BSA-coated plates (Figure 4A). Furthermore, binding to CD23M79 and CD23M150 was comparable to fibrinogen, but less to derCD23. The differentiated U937 cells also demonstrate that they are able to bind immobilized sCD23 proteins and fibrinogen in a statistically significant way (Figure 4B). Again, U937 cells bound better to CD23M150 and CD23M79 than derCD23, but these cells preferentially bound sCD23 when compared to fibrinogen.

3.3 Antibody blocking of cell binding

The cell binding studies were repeated in the presence of a blocking antibody to prove that differentiated cells bound recombinant sCD23 proteins through interaction with the CD11b αI domain. CBRM1/5 blocks CD11b-dependent adhesion to fibrinogen and ICAM1 [26; 27]. Similarly, we show that the antibody is able to block the binding

of HL60 cells to fibrinogen and sCD23 proteins (Figure 5A). The differentiated U937 cells also show a decrease in binding to fibrinogen and sCD23 proteins when pre-incubated with blocking antibody CBRM1/5 (Figure 5B). The blocking was significant for CD23M150 and CD23M79 in the case of U937 cells. Since CBRM1/5 recognizes an epitope on the CD11b αI domain, we conclude that sCD23 binds CD11b/CD18 and possibly also CD11c/CD18 through the αI domain.

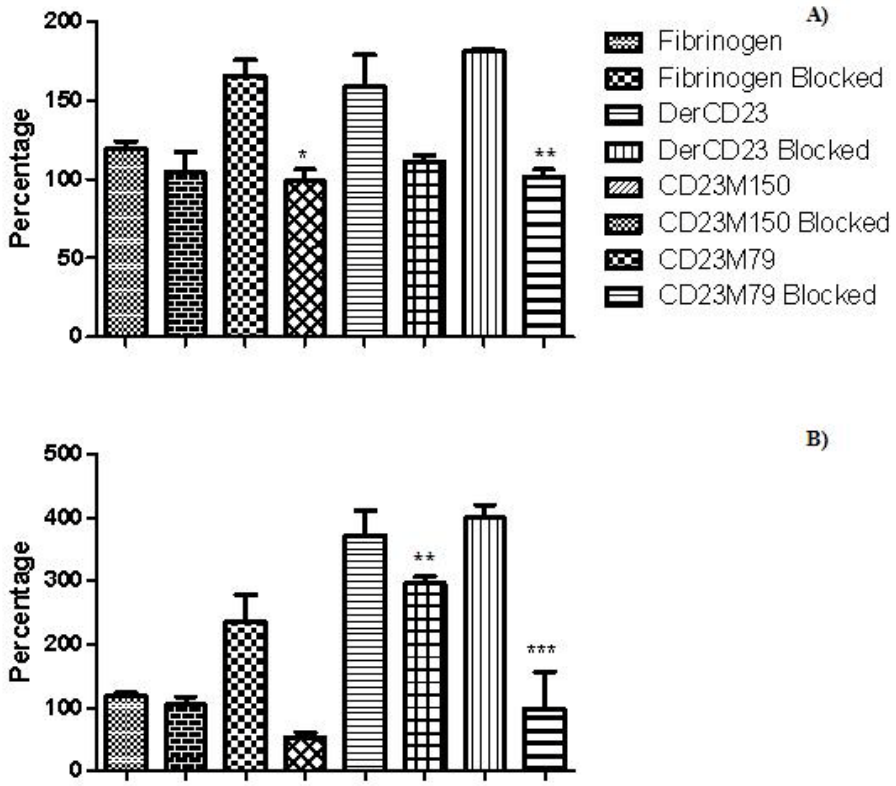

Figure 5: Inhibition of binding of differentiated HL60 (A) and U937 (B) cells to CD23. Each figure is representative of two experiments done in triplicate. Error bars represent SEM values. Asterisks represent significance compared to unblocked control cells where (*) represents $P<0.05$, (**)$P<0.005$ and (***)$P<0.0005$.

3.4 Binding of CD11 αI domains to recombinant human soluble CD23

We measured the affinity of the CD23 interaction with the αI domain by using purified CD11b and CD11c αI domain-GST fusion proteins in an ELISA (Table 1). These data confirm the cell data that interaction between CD23 and CD11b/CD11c

occurs through the αI domain of the integrins. The CD11b αI domain appeared to have very little difference in its affinity for the CD23 proteins (K_D of 0.27 ± 0.07 μM for derCD23, 0.32 ± 0.06 μM for CD23M150 and 0.25 ± 0.06 μM for CD23M79), although these affinities seemed slightly higher than what was seen by fibrinogen (K_D 0.44 ± 0.13 μM). The affinity of CD11c αI domain for CD23M150 and CD23M79 were very similar (K_D of 0.28 ± 0.08 μM and 0.29 ± 0.07 μM, respectively), while the affinity for derCD23 was lower (K_D 0.46 ± 0.13 μM). Fibrinogen had a dissociation constant of 0.33 ± 0.09 μM for CD11c αI domain.

Table 1: Equilibrium dissociation constants for CD11b/c αI domain interaction with CD23 and fibrinogen. K_D (in μM) is determined from three experiments done in triplicate for CD11b and two experiments done in triplicate for CD11c.

Protein	CD11b αI domain	CD11c αI domain
Fibrinogen	0.44 ± 0.13	0.33 ± 0.09
derCD23	0.27 ± 0.07	0.46 ± 0.13
CD23M150	0.32 ± 0.06	0.28 ± 0.08
CD23M79	0.25 ± 0.06	0.29 ± 0.07

4. Discussion

CD11b and CD11c were upregulated to the cell surface of HL60 and U937 cells when treated with vitamin D_3. These cells were shown to bind sCD23 proteins and the fibrinogen control. Their binding was also blocked using an antibody directed against the CD11b αI domain. This indicates that the binding to CD23 proteins was at least partly due to their interaction with the αI domain of CD11b. We interpret the residual binding that was not blocked by the antibody as being possibly caused by the interaction of CD23 with the αI domain of CD11c. There is also the possibility, however, that CD23 interacted with other ligands on the cells, such as the vitronectin

receptor. We also noted that the 25 kDa and 33 kDa proteins had very similar levels of binding to the two αI domains. The 16 kDa derCD23, although still showing significant binding to the cells, demonstrated a lower level of binding. This could be explained by its shorter length compared to the other two CD23 proteins. This could indicate that the lectin domain of CD23 is involved in binding to the αI domains of integrins, but that the larger proteins may have another section of CD23, either in the stalk or C-terminal tail that is involved in binding these αI domains, in addition to the lectin domain.

The binding of the sCD23 proteins to the αI domains of CD11b and CD11c are further proven by the *in vitro* ELISA data. The affinity of CD11b and CD11c αI domains for several ligands is known. Thy-1 is a membrane protein involved in cell adhesion and signalling regulation in neurons and T-cells and binds CD11b and CD11c. Thy-1 binds the CD11c αI domain with a K_D of 1.16 ± 0.14 μM, which is an approximately 2-fold higher affinity than its binding to CD11b αI domain of 2.4 ± 0.46 μM [28]. CD11b binds iC3b with a K_D of 12.5 nM and the αI domain binds at 300 nM [29]. The hookworm-derived neutrophil inhibitory factor (NIF) binds to the αI domain with a K_D of 1 nM and this binding has been shown to be activation independent [30]. CD11b has also been shown to bind fibrinogen with a K_D of 0.22 ± 0.06 μM [31] while CD11c has been shown to bind plasminogen with a K_D of 1.9 μM [32].

The binding of the integrin αI domains to fibrinogen in our experiments is similar to that seen in published data [31] as well as having similar affinities as other ligands of these αI domains. It is interesting to note that all three of the CD23 proteins produced have the RKC motif shown to be the site of CD23 binding for the integrin, $\alpha_v\beta_5$ [17]. It is therefore possible to speculate that this motif is also a possible binding site for the

CD11b and CD11c αI domains. However, the cell binding data shows that the binding of derCD23 to the αI domains is much weaker than the other two CD23 proteins, indicating further interaction sites in either the stalk or C-terminal tail. Surface Plasmon resonance spectroscopy of the interaction between these proteins would yield more sensitive binding analysis data to further elucidate their interaction sites. Nonetheless, this is the first time that it has been shown that sCD23 proteins bind CD11b and CD11c through their αI domains.

5. References

[1] Rezzonico R, Chicheportiche R, Imbert V, Dayer J-M**.** Engagement of CD11b and CD11c β2 integrin by soluble CD23 induced IL-1β production on primary human monocytes through mitogen-activated protein-kinase-dependent pathways. Blood 2000; 95: 3868-3875.

[2] Mazzone A, Ricevuti G. Leukocyte CD11/CD18 Integrins: Biological and clinical relevance. Haematologica 1995; 80:161-175.

[3] Shimaoka M, Springer TA. Therapeutic agonists and the conformational regulation of the β_2 integrins. Cur Top Med Chem 2004; 4: 1485-1495.

[4] Walters SE, Tang RH, Cheng M, Tan SM, Law SKA. Differential activation of LFA-1 and Mac-1 ligand binding domains. Biochem Biophys Res Commun 2005; 337:142-148.

[5] Choi J, Nham S-U. Loops within the CD11c I Domain Critical for Specific Recognition of Fibrinogen. Biochem Biophys Res Commun 2002; 292: 756–760.

[6] Zen K, Utech M, Liu Y, Soto I, Nusrat A and Parkos CA. Association of BAP31 with CD11b/CD18. J Biol Chem 2004; 279: 44924–44930.

[7] Sadhu C, Ting HJ, Lipsky B, Hensley K, Garcia-Martinez LF, Simon SI *et al.*. CD11c/CD18: novel ligands and a role in delayed-type hypersensitivity. J Leukoc Biol 2007; 81: 1395-1403.

[8] Conrad DH, Ford JW, Sturgill JL, Gibb DR. CD23: an overlooked regulator of allergic disease. Curr Allergy Asthma Rep 2008; 7: 331-337.

[9] Kijimoto-Ochiai, S. CD23 (the low-affinity IgE receptor) as a C-type lectin: a multidomain and multifunctional molecule. Cell Mol Life Sci, 59: 648-664.

[10] Weskamp G, Ford JW, Sturgill J, Martin S, Docherty AJP, Swendeman S, *et al.* ADAM10 is a principal 'sheddase' of the low-affinity immunoglobulin E receptor CD23. Nat Immunol 2006; 7: 1293-8

[11] Gould HJ, Sutton BJ. IgE in allergy and asthma today. Nat Immunol 2008; 8: 205-217.

[12] Hibbert RG, Tierete P, Grundy GJ, Beavil RL, Reljic R, Holers VM, *et al* . The structure of human CD23 and its interactions with IgE and CD21. J Exp Med 2005; 202: 751-760.

[13] Schulz O, Sutton BJ, Beavil RL, Shi J, Sewell HF, Gould HJ, *et al.*. Cleavage of the low-affinity receptor for human IgE (CD23) by a mite cysteine protease: Nature of the cleaved fragment in relation to the structure and function of CD23. Eur J Immunol 1997; 27: 584-588

[14] Sato T, Konishi A, Yasuno S, Arai J, Kamei M, Bitoh M, *et al.* A new method for studying the binding of human IgE to CD23 and the inhibition of this binding. J Immunol Methods 1997; 209:59–66.

[15] Rezzonico R, Imbert V, Chicheportiche R, Dayer J-M. Ligation of CD11b and CD11c β2 integrins by antibodies or soluble CD23 induces macrophage inflammatory protein 1α (MIP-1α) and MIP-1β production in primary human monocytes through a pathway dependent on nuclear factor–κB. Blood 2001; 97: 2932-2940.

[16] Finkel T, Gutkind JS. Signal transduction and human disease. New York: John Wiley and Sons, 2003.

[17] Borland G, Edkins AL, Acharya M, Matheson J, White LJ, Allen JM, *et al*. αvβ5 Integrin sustains growth of human pre-B cells through an RGD-independent interaction with a basic domain of the CD23 protein. J Biol Chem 2007; 282: 27315-27326.

[18] Daniels BB, Askew SL, van de Venter M, Oosthuizen V. Production of biologically active recombinant human soluble CD23 and its effect on PBMCs isolated from hyper-IgE blood. Cell Immunol 2005; 234: 146-153.

[19] Nham, S-U. Characteristics of fibrinogen binding to the domain of CD11c, an α subunit of p150,95. Biochemical and Biophysical Research Communications 1999; 264: 630-634.

[20] Flick MJ, Du X, Degen JL. Fibrin(ogen)-αMβ2 interactions regulate leukocyte function and innate immunity in vivo. Exp Biol Med 2004; 229: 1105-1110.

[21] Georgakopoulos T, Moss ST, Kanagasundaram V. Integrin CD11c contributes to monocyte adhesion with CD11b in a differential manner and requires Src family kinase activity. Mol Immunol 2008; 45: 3671-3681.

[23] Dodd RC, Cohen MS, Newman SL and Gray TK. Vitamin D metabolites change the phenotype of monoblastic U937 cells. Proc Natl Acad Sci USA 1983; 80:7538-7541.

[23] Koeffler HP. Induction of differentiation of human acute myelogenous leukemia cells: Therapeutic implications. Blood 1983; 62: 709-721.

[24] Taimi M, Defacque H, Commes T, Favero J, Caron E, Marti J, *et al.* Effect of retinoic acid and vitamin D on the expression of interleukin-lβ, tumour necrosis factor-α and interleukin-6 in the human monocytic cell line U937. Immunology 1993; 79:229-235.

[25] Miller LJ, Schwarting R, Springer TA. Regulated expression of the Mac-1, LFA-1, p150,95 glycoprotein family during leukocyte differentiation. J Immunol 1986; 137: 2891-2900.

[26] Diamond MS, Springer TA. A subpopulation of mac-1 (CD11b/CD18) molecules mediates neutrophil adhesion to ICAM-1 and fibrinogen. J Cell Biol 1993; 120: 545-556.

[27] Oxvig C, Lu C, Springer TA. Conformational changes in tertiary structure near the ligand binding site of an integrin I domain. Proc Natl Acad Sci USA 1999; 96: 2215-2220.

[28] Choi J, Leytona L, Nham S-U. Characterisation of αX I-domain binding to Thy-1. Biochem Biophys Res Commun 2005; 331: 557-561.

[29] Li R, Arnaout MA. Integrin Protocols. Methods Mol Biol 1999; 129: 105-124.

[30] Rieu P, Ueda T, Haruta I, Sharma CP, Arnaout M A. The A-domain of beta 2 integrin CR3 (CD11b/CD18) is a receptor for the hookworm-derived neutrophil adhesion inhibitor NIF. J Cell Biol 1994; 127: 2081-2091.

[31] Zhou L, Lee DH, Plescia J, Lau CY and Altieri DC. Differential ligand binding specificities of recombinant CD11b/CD18 integrin I-domain. J Biol Chem 1994; 269: 17075-17079.

[32] Gang J, Choi J, Lee JH and Nham S-U. Identification of critical residues for plasminogen binding by the αX I domain of the β2 integrin, αX β2. Mol Cells 2007; 24: 240-246.